



NATIONAL INSTITUTE FOR **NUCLEAR PHYSICS** AND **HIGH-ENERGY PHYSICS**

---

# ANNUAL REPORT

## 1999

Kruislaan 409, 1098 SJ Amsterdam  
P.O. Box 41882, 1009 DB Amsterdam

# Colofon

## Publication edited for NIKHEF:

Address: Postbus 41882, 1009 DB Amsterdam  
Kruislaan 409, 1098 SJ Amsterdam

Phone: +31 20 592 2000

Fax: +31 20 592 5155

E-mail: [directie@nikhef.nl](mailto:directie@nikhef.nl)

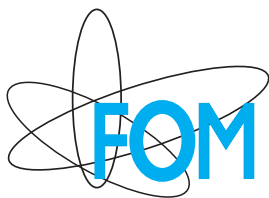
Editors: Eddy Jans, Peter Kluit

Layout & art-work: Kees Huysen

Organisation: Anja van Dulmen

Cover Photograph: An impression of the probationation (Photo: NIKHEF)

URL: <http://www.nikhef.nl>



The National Institute for Nuclear Physics and High-Energy Physics (NIKHEF) is a joint venture of the Stichting voor Fundamenteel Onderzoek der Materie (FOM), the Universiteit van Amsterdam (UVA), the Katholieke Universiteit Nijmegen (KUN), the Vrije Universiteit Amsterdam (VUA) and the Universiteit Utrecht (UU). The NIKHEF laboratory with its accelerator facility (AmPS) is located at the Science Research Centre Watergraafsmeer (WCW) in Amsterdam.

The activities in experimental subatomic physics are coordinated and supported by NIKHEF with locations at Amsterdam, Nijmegen and Utrecht. The scientific programme is carried out by FOM, UVA, KUN, VUA and UU staff. Experiments are done at the European accelerator centre CERN in Geneva, where NIKHEF participates in two LEP experiments (L3 and DELPHI), in a neutrino experiment (CHORUS) and in SPS heavy ion experiments (NA57 and NA49). NIKHEF recently joined the Tevatron experiment D0 at Fermilab, Chicago. At DESY in Hamburg NIKHEF participates in the ZEUS, HERMES and HERA-B experiments. Research and development activities are in progress for the future experiments ATLAS, ALICE and LHCb with the Large Hadron Collider (LHC) at CERN.

The subatomic physics programme with intermediate energy electromagnetic probes has been concluded with the in-house electron accelerator.

NIKHEF is closely cooperating with the University of Twente. Training and education of students are vital elements in the research climate of the laboratory.

# Contents

<b>Preface</b>	<b>1</b>
<b>A Ongoing Experiments</b>	<b>3</b>
<b>1 AmPS Physics</b>	<b>3</b>
1.1 Introduction	3
1.2 Internal Target Program	3
1.3 EMIN	9
1.4 Experiments abroad	12
<b>2 HERMES</b>	<b>14</b>
2.1 Introduction	14
2.2 Data taking	14
2.3 Physics analysis	14
2.4 The silicon detector project	17
2.5 The long-range plan	18
<b>3 ZEUS</b>	<b>19</b>
3.1 Introduction	19
3.2 Physics Results	19
3.3 Microvertex Project	21
<b>4 CHORUS</b>	<b>24</b>
4.1 Introduction	24
4.2 Specific NIKHEF activities	25
<b>5 DELPHI</b>	<b>27</b>
5.1 Data taking and detector status	27
5.2 Selected research topics	27

<b>6</b>	<b>L3</b>	<b>32</b>
6.1	Introduction	32
6.2	W and $\tau$ Physics	32
6.3	Particle Correlations and Cosmics	33
6.4	Two-photon Physics	34
6.5	Some additional highlights	36
<b>7</b>	<b>Heavy Ion Physics</b>	<b>38</b>
7.1	Introduction	38
7.2	WA98	38
7.3	NA57	41
<b>B</b>	<b>MEA/AmPS facility</b>	<b>42</b>
<b>1</b>	<b>MEA/AmPS decommissioning</b>	<b>42</b>
1.1	Introduction	42
1.2	Preparations	42
1.3	JINR dismantling	43
1.4	Other dismantling activities	44
<b>C</b>	<b>Experiments in preparation</b>	<b>45</b>
<b>1</b>	<b>ALICE</b>	<b>45</b>
<b>2</b>	<b>Antares: A cosmic neutrino telescope</b>	<b>47</b>
<b>3</b>	<b>ATLAS</b>	<b>48</b>
3.1	Introduction	48
3.2	ATLAS Experiment	48
3.2.1	End Cap Toroids	48
3.2.2	Muon Spectrometer	48
3.2.3	Semi Conductor Tracker	50
3.2.4	Data Acquisition, Trigger System and Detector Control System	50
3.3	D0 Experiment	51
3.4	R&D activities: MediPix	51
<b>4</b>	<b>B Physics</b>	<b>53</b>
4.1	Introduction	53

4.2	HERA-B	53
4.3	LHCb	53
<b>D</b>	<b>Theoretical Physics</b>	<b>57</b>
<b>1</b>	<b>Theoretical Physics Group</b>	<b>57</b>
1.1	Particles, fields and symmetries	57
1.2	Research program	57
<b>2</b>	<b>CHEAF</b>	<b>59</b>
2.1	Introduction	59
2.2	Connection between Gamma ray Bursts and Supernovae: birth events of black holes?	59
2.3	First redshifts and polarisation of Gamma Ray Bursts measured with ESO's Very Large Telescope	60
2.4	Record number of CHEAF Ph.D. degrees awarded	60
<b>E</b>	<b>Technical Departments</b>	<b>61</b>
<b>1</b>	<b>Computer Technology</b>	<b>61</b>
1.1	Computer- and network infrastructure	61
1.2	SARA	61
1.3	AMS-IX	62
1.4	Computer strategy 2000-2001	62
1.5	Software for experiments	62
<b>2</b>	<b>Electronic Department</b>	<b>64</b>
2.1	Introduction	64
2.2	Projects	64
2.3	New Projects	68
2.4	Special projects	70
<b>3</b>	<b>Mechanical Technology</b>	<b>71</b>
3.1	Introduction	71
3.2	Projects in exploitation	71
3.3	Projects for third parties	73
3.4	Developments within the Mechanical Technology group	74

<b>F</b>	<b>Publications, Theses and Seminars</b>	<b>75</b>
<b>1</b>	<b>Publications</b>	<b>75</b>
1.1	Ph.D. Theses	81
1.2	Invited Talks	82
1.3	Seminars at NIKHEF	86
1.4	NIKHEF Annual Scientific Meeting, December 16-17, 1999, Utrecht	88
<b>G</b>	<b>Resources and Personnel</b>	<b>89</b>
<b>1</b>	<b>Resources</b>	<b>89</b>
<b>2</b>	<b>Membership of Councils and Committees during 1999</b>	<b>90</b>
<b>3</b>	<b>Personnel as of December 31, 1999</b>	<b>91</b>

# Preface

In 1999, again a sudden death shocked the NIKHEF community; dr. Werner Ruckstuhl, leader of the NIKHEF B Physics team, died on July 8<sup>th</sup>. We remember him as an excellent physicist with drive and witticism.

On the other side of the scale there was the collective joy about the Nobel prize awards to Gerard 't Hooft and Tini Veltman. This well-deserved honour stimulates even further the enthusiasm about our field, especially amongst the young generation.

The past year was the first without an in-house experimental facility. The analysis of AmPS data taken in earlier years, however, is still going on. Specific subjects include the effects of short-range correlations and occupancies of shell-model orbitals. The –mostly– polarized beam and target experiments performed in 1998 are presently being analysed. The data on the knock out of protons and neutrons from deuterium has lead to a value for the electric form factor of the neutron.

The accelerator and ring have been dismantled almost completely by our Russian colleagues of the Joint Institute for Nuclear Research at Dubna. More than half of the equipment was shipped to Dubna before Christmas. The action will be completed by the summer of 2000. Most of the detectors and ancillary equipment found their way to sister institutes abroad.

From our experiments at DESY it is worth noting that the HERMES collaboration saw the first –not yet conclusive– evidence of gluon polarisation in polarized protons. Also, a –possibly nuclear– effect was observed at small  $x$  and  $Q^2$  in the ratio of longitudinal and transverse photon absorption cross sections. The ZEUS collaboration reported that charged and neutral current deep-inelastic cross sections at large  $x$  and  $Q^2$  no longer show enhancements over expectations, especially in a next-to-leading order QCD description with 'state-of-the-art' parton distributions.

At CERN, with an excellently performing LEP collider, the efforts of the four experiments including L3 and DELPHI in which NIKHEF is involved, are joined to find the first glimpse of the Higgs. In the year 1999 nothing was found as yet. At present LEP is running at an energy well beyond 200 GeV. The CHORUS collabo-

ration is continuing its analysis of emulsions and hence improving the limits on possible neutrino oscillations.

NIKHEF physicists have contributed to the efforts to obtain 'circumstantial' evidence for the existence of a quark gluon plasma, notably in strangeness enhancement (NA57).

The preparation of forthcoming experiments at the LHC makes good progress. For the ATLAS detector the Dutch in kind contribution within the common fund consists of important parts of the end cap toroidal magnets: the huge vacuum vessels and the cold masses, in particular the winding of the superconducting coils. These components are being constructed by two Dutch companies under the supervision of NIKHEF and Rutherford Appleton Laboratory, the latter being responsible for the design. In 1999, also the clean room for the construction of the 'Barrel Outer Large' (BOL) muon detectors, including a large marble table, became operational.

Two alternatives for the honeycomb chambers for the HERA-B detector are presently being studied for the construction of the outer tracker of the LHCb detector for which NIKHEF has the responsibility. An interim Memorandum of Understanding for the construction of the detector has been signed.

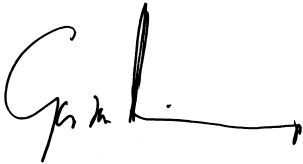
The ALICE group within NIKHEF makes good progress with prototype silicon strip detectors and the assembly method for two longers of the inner tracking system.

After ample discussions within the Institute, it was decided to put forward a proposal to join the French initiative for the construction of a cosmic neutrino detector. Phase 1 of the detector called ANTARES will be set up in the Mediteranean Sea (near Toulon) at the depth of 2.5 km. If this proposal is granted, NIKHEF will contribute about 20% of the phase 1 construction. NIKHEF especially aims at bringing 'all data to shore' in order to enhance the scientific discovery potential for the ultimate 1 km<sup>3</sup> detector.

Finally, it is worth mentioning that a number of 'internet-related' activities took place. NIKHEF houses since long a large part of the Amsterdam Internet Exchange (AMS-IX), one of the three major European nodes. The number of its participants has in-

creased during 1999 by some 50%. A British Company, TeleCity, has rented most of the accelerator building to install additional services. A large project supported by the Science Department of the University of Amsterdam, the Institutes of the Dutch Research Organisation NWO situated on site and a number of Dutch companies, aided by a significant sum of additional investment money from the Dutch Government, has been set up. Its goal is to advance the use of internet and computer technology for both scientific and economic activities. In its framework NIKHEF will set up a virtual laboratory based on particle included X-ray emission with a micro beam of protons and  $\alpha$ -particles. This PIXE facility, presently housed at the Free University at Amsterdam, will be moved shortly to the NIKHEF site.

With all this progress in mind, as well as with the prospects sketched above we entered the new millennium with confidence.

A handwritten signature in black ink, appearing to read 'Ger van Middelkoop'. The signature is stylized, with a large 'G' and 'M' and a long horizontal stroke at the end.

Ger van Middelkoop

# A Ongoing Experiments

## 1 AmPS Physics

### 1.1 Introduction

The major part of the beam time in 1998, the last year of operation of the AmPS accelerator, was devoted to experiments 94-05 and 97-01 of the polarized internal target physics program. In these, the spin structure of few-body systems, the proton, deuteron, and  $^3\text{He}$  nuclei, are studied. The collection of data finished in December 1998 with the closing of the AmPS facility. The following section discusses the activities employed in 1999 to analyze these data and to start finalizing the polarized internal target program. Results from the EMIN end station and from electron scattering experiments abroad are reviewed on pages 9 and 12, respectively.

### 1.2 Internal Target Program

The AmPS internal target facility allowed the study of hadronic structure from polarized internal targets with a polarized electron beam. At energies suitable for research of nuclear structure (below about 10 GeV) a polarized electron beam needs to be injected, since self polarization via the Sokolov-Ternov effect takes too long to be useful. Since AmPS was the first facility where experiments could be realized in which a polarized electron beam was injected, stored and scattered from polarized internal targets, several technical issues, like the usage of a partial Siberian Snake, were studied and reported. Furthermore, we studied an alternative mechanism to obtain self-polarization of lepton beams. In this mechanism, longitudinal polarization is built up in a storage ring in the presence of a strong longitudinal magnetic field. It leads to high beam polarization in a shorter time than the transverse polarization obtained with the Sokolov-Ternov effect and could be applied for instance to obtain polarized positron beams at a few GeV. Momentarily, we are refining the theoretical model that describes this self polarization for the AmPS ring.

The data taken with AmPS were further analyzed. For the polarized pion-production data in the  $\Delta$ -resonance region a code is being developed to calculate spin-dependent radiative corrections. Also, for electron scattering from hydrogen various theoretical models are studied and compared to the data. This analysis is still in progress. On deuterium, the analysis of the quasi-elastic proton and neutron knock-out data has been

completed. From these data we deduced and published a value for the charge form factor of the neutron. Furthermore, we studied the spin-dependent nuclear structure of deuterium; results are discussed below. The analysis of the data on quasi-elastic scattering off  $^3\text{He}$  in the  $(e, e'p)$ ,  $(e, e'n)$  and  $(e, e'd)$  channel is almost finalized. A preliminary result for the extraction of the neutron charge form factor from scattering off  $^3\text{He}$  is discussed. A Monte-Carlo simulation code that can fold several theoretical models over the detector acceptance has been further developed. A collaboration with J. Golak has been set up to obtain a sufficient amount of continuum-wave Faddeev calculations covering our acceptance.

The development of the polarized targets has taken much effort and commitment of resources during the last decade. The unique equipment and expertise which was built up in order to make the polarized internal target physics program feasible has been applied in 1999. The  $^3\text{He}$  target has been used at the Vrije Universiteit Amsterdam in researching a technique with which better magnetic resonance imaging pictures of lungs can be taken. The atomic beam source that produced the polarized hydrogen and deuterium targets has been modified, shipped and successfully installed during the summer of 1999 in the Blast facility at Bates (MIT), where it will be used in new sub-atomic physics research (see Fig. 1.1).

*Quasi-free pion production on  $^4\text{He}$*   
(Prop. 91-08; with ODU and Virginia)

The reactions  $^4\text{He}(e, e'p^3\text{H})\pi^0$  and  $^4\text{He}(e, e'p^3\text{He})\pi^-$  have been studied at invariant energies ranging from the pion production threshold to the delta resonance region. Comparison of the cross sections with those of pion production on the proton will provide information on  $\Delta N$  and  $\pi N$  dynamics inside the nucleus  $^4\text{He}$ .

The triple coincidence measurements were carried out at the Internal Target Facility at NIKHEF with a 670 MeV electron beam and a  $^4\text{He}$  open-ended storage cell target. The scattered electrons were detected in the BigBite large-acceptance magnetic spectrometer and the knocked out protons in the HADRON4 large-acceptance plastic scintillator array. Simultaneous measurements of both reaction channels was achieved by detecting the recoiling nuclei in the VUA Recoil

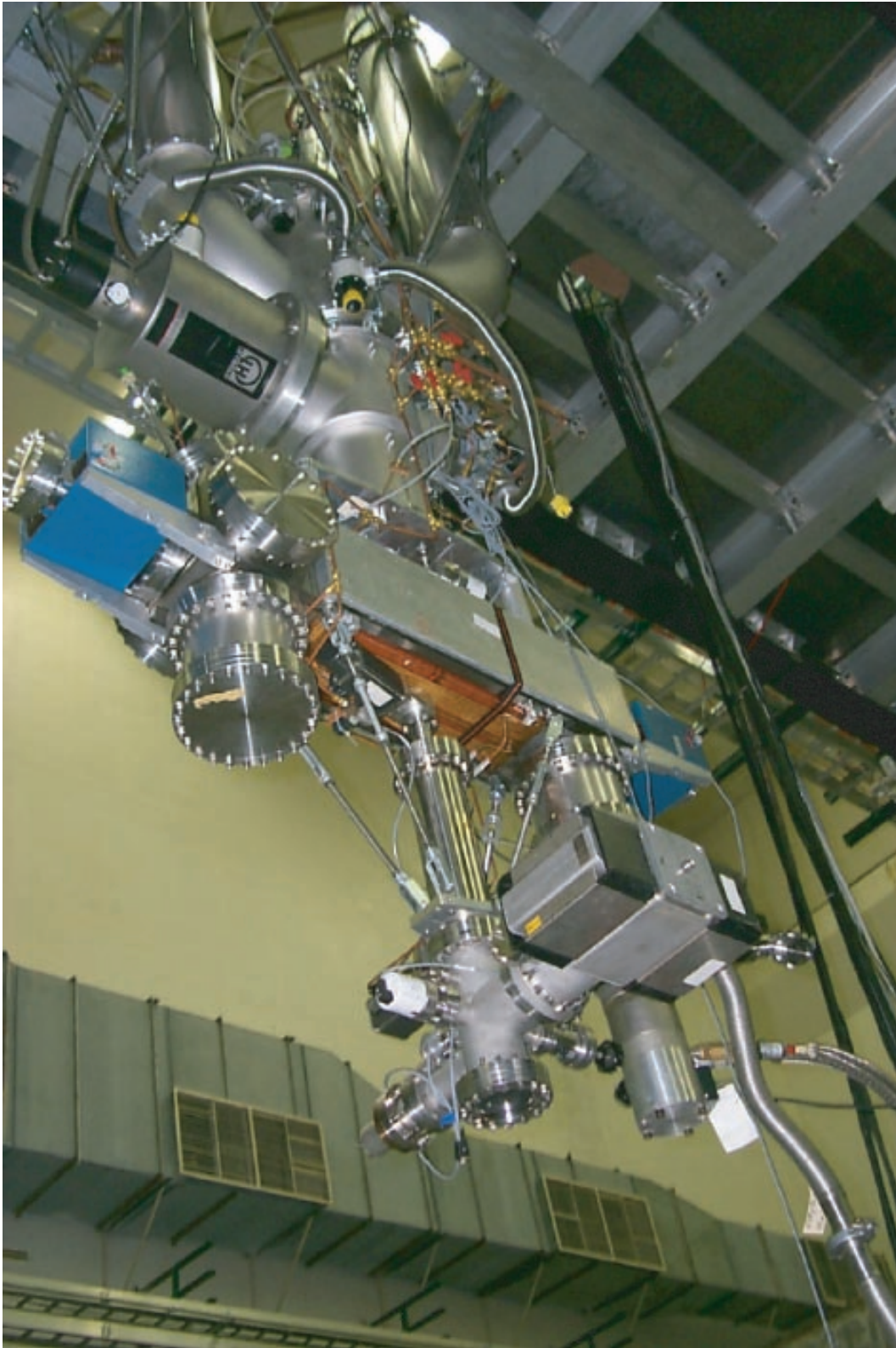


Figure 1.1: *Installation of the atomic beam source in the BLAST detector at Bates.*

Detector positioned opposite to the three-momentum transfer. In this way the detection of the neutral pion was avoided.

The integrated luminosity, determined from the  ${}^4\text{He}(e, e'){}^4\text{He}$  reaction, for which the cross section is accurately known, was  $3.5 \cdot 10^8 \mu\text{b}^{-1}$ .

In case of pion production the missing energy  $E_m$  and missing momentum  $P_m$  are equal to the energy and momentum of the emitted pion. In the  $(E_m, P_m)$  scatter plot, shown in Fig. 1.2, the bands corresponding to the pions are clearly visible. The figure also shows the missing mass spectra deduced from the  $(E_m, P_m)$  distributions. About 700  $\pi^0$  and 1200  $\pi^-$  events were identified.

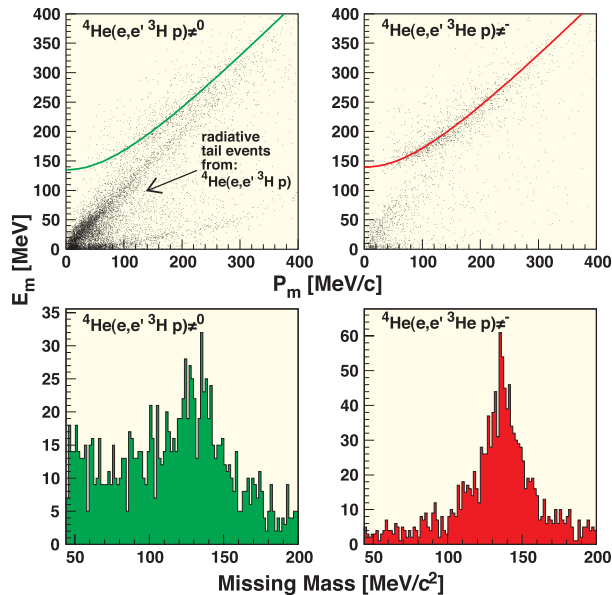


Figure 1.2: Missing energy versus missing momentum for  ${}^4\text{He}(e, e' p {}^3\text{H})\pi^0$  (top left) and  ${}^4\text{He}(e, e' p {}^3\text{He})\pi^-$  (top right). The solid lines indicate the bands corresponding to quasi-free pion production. The missing mass distributions for both channels are shown in the bottom frames.

Events stemming from radiative processes in the reaction  ${}^4\text{He}(e, e' p {}^3\text{H})$  (radiative tail) partly overlap with those from pion production. A large fraction of the radiative tail was eliminated by rejecting those events for which the missing momentum was collinear with either the electron beam or the scattered electron. The measured  ${}^4\text{He}(e, e' p {}^3\text{H})$  coincidences serve as an independent normalization and provide additional information on possible systematic errors.

The determination of the cross sections as a function of the invariant mass of the pion-nucleon system and the pion angle with respect to the transferred 3-momentum, is in progress.

*Spin correlation parameters from the reaction  $D(\vec{e}, e' p)n$*   
(Prop. 97-01; with ETH, Virginia, Arizona, TJNAF, MIT, Hampton, Novosibirsk)

The deuteron has been used extensively in the past as a testing ground for nuclear models. As it is the simplest nucleus, only consisting of a proton and neutron, accurate microscopic calculations can be made and data can be interpreted without much model dependence. The ground state wave function is dominated by a central interaction, due to the fact that the proton and neutron are mainly in a relative  $S$ -wave. A small tensor force in the nucleon-nucleon interaction induces a  $D$ -state component in the wave function. The  $S$ - and  $D$ -state components depend on the relative momentum of the proton ( $p$ ) and neutron ( $-p$ ) inside the deuteron. The wave function has been investigated with elastic electron-deuteron scattering, where one measures the two elastic form factors of the deuteron,  $A$  and  $B$ . The electromagnetic properties of a deuteron cannot be described completely with these two form factors, because for a spin-1 particle at least three observables are required. The tensor analyzing power  $T_{20}$  in elastic scattering has been measured as a third observable, to get a better understanding of the electromagnetic and spin structure of the deuteron. The ITH facility has been used for high precision measurements of  $T_{20}$  in the past [M. Ferro-Luzzi *et al.*, Phys. Rev. Lett. **77** (1996) 2630, M. Bouwhuis *et al.*, Phys. Rev. Lett. **82** (1999) 3755].

Another way to get more insight in the deuteron structure is via quasi-elastic electron-deuteron scattering. In plane wave impulse approximation (PWIA), the neutron is a spectator during the scattering process, and the missing momentum  $p_m = p$ . Therefore, a measurement as a function of  $p_m$  gives direct insight in the momentum distribution of nucleons inside the deuteron.

To enhance the sensitivity to the  $D$ -state component, one can investigate spin dependent observables in quasi-elastic scattering. The polarization of a proton inside a vector polarized deuteron depends on whether the proton and neutron are in a relative  $S$ - or  $D$ -state. In an  $S$ -state configuration the proton and neutron spins are aligned with the deuteron spin, while in a  $D$ -state the orbital angular momentum contributes

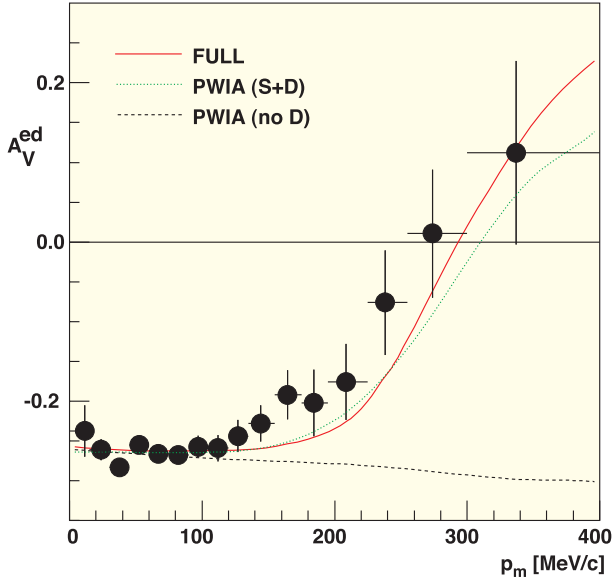


Figure 1.3: Spin correlation parameter for the reaction  $\vec{D}(\vec{e}, e'p)n$ . The data are obtained in experiment 97-01. The dotted (dashed) curve represent PWIA prediction with (without) including the effect from the  $D$ -wave, while the solid curve represents a prediction from a model by H. Arenhövel that includes contributions from reaction mechanism effects.

to the total angular momentum, and the proton and neutron spin can also be anti-aligned.

The data from the proton channel of the 97-01 experiment with vector polarized deuterium and polarized electrons have been used to determine the asymmetry in quasi-elastic electron-deuteron scattering. The results are shown in Fig. 1.3. This figure clearly shows the sensitivity to the  $D$ -wave component of the wave function. The figure also shows results of calculations by H. Arenhövel that include reaction mechanism effects. It can be seen that the result of this full model calculation does not agree with the data for  $p_m > 150$  MeV/ $c$ . This might be due to an underestimation of the  $D$ -wave effects.

Another observable that is sensitive to the deformation of the deuteron is its quadrupole moment  $Q_d$ , which has been measured with high precision. Nucleon-nucleon potentials can be used to calculate the deuteron wave function and from the wave function the quadrupole moment can be calculated. All NN-potentials underestimate this static property of the deuteron by 2-5%. In an attempt to clarify the relation between  $A_V^{ed}$  and  $Q_d$ ,

we have artificially increased the  $D$ -state probability of the deuteron such that  $Q_d$  is predicted correctly. The modified wave function has been used to calculate the spin correlation parameter and the results are shown in Fig. 1.4. Although the adjusted wave function does not give a complete description of the data either, the adjustment clearly improves the quality.

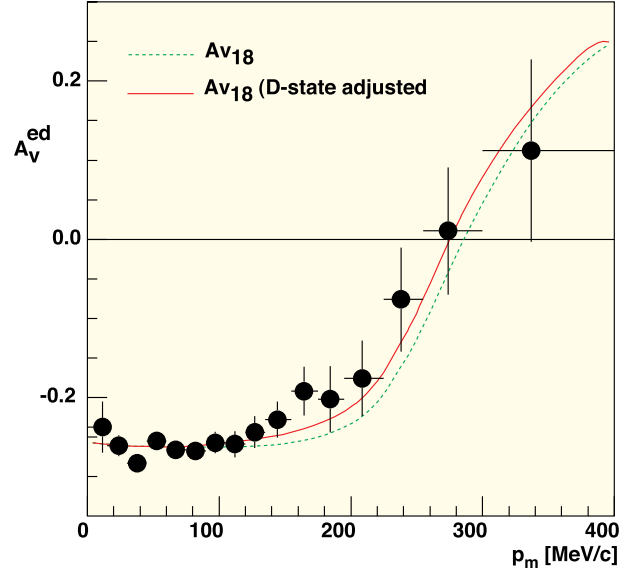


Figure 1.4: Results on the spin correlation parameter of experiment 97-01, compared to the prediction with a complete model based on the Argonne  $v_{18}$  potential (dashed curve). The solid curve represents the results of a naive calculation where the  $D$ -wave has been increased artificially (see text).

The method we have used to adjust the wave-function is too crude to give reliable results. However, it does show that the discrepancy between the data and the predictions of both the spin correlation parameter and the deuteron quadrupole moment could be reduced, if the NN-potentials were modified to allow for more orbital angular momentum. Whether it is possible to modify the NN-potentials such that the quality of the description of the nucleon-nucleon scattering data is maintained, while at the same time the  $D$ -state component of the deuteron wave function is increased, needs to be investigated.

$^3\vec{H}e(\vec{e}, e'n)$  and  $G_E^n$

(Prop. 94-05; with ETH, Virginia, Arizona, TJNAF, MIT, Hampton, Novosibirsk)

First results of the  ${}^3\vec{\text{H}}\text{e}(\vec{e}, e'X)$  experiment have become available. In the experiment asymmetries were measured in the yield of various reaction channels with the target polarization in specific orientations. Elastic scattering measurements, in which the Recoil Detector was used, provided a systematic check of the luminosity and of the beam and target polarizations.

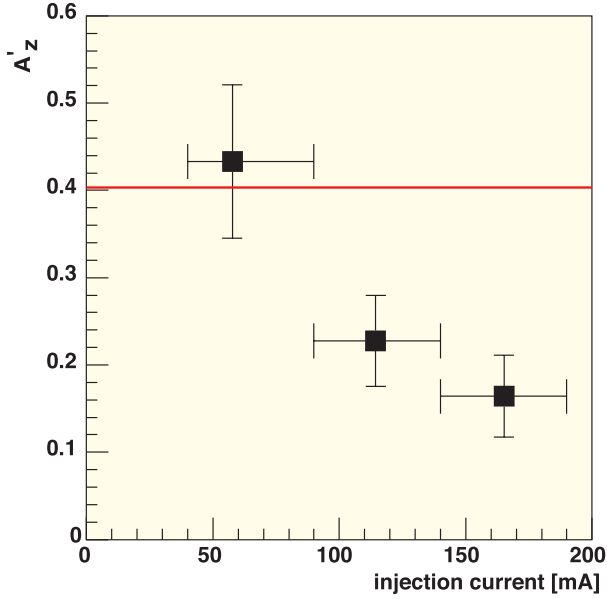


Figure 1.5: The dependence of the  $A'_z$  spin-spin correlation function on the injected current. The solid line indicates the value predicted by Nagorny. The decrease at higher current is assumed to be caused by (partial) depolarization of the electron beam.

For  ${}^3\vec{\text{H}}\text{e}(\vec{e}, e'n)$  the large  $A'_z$  asymmetry (with the target polarization along the momentum transfer  $\vec{q}$ ) is to first order independent of any structure function and only determined by kinematics. The small  $A'_x$  asymmetry (with the target polarization perpendicular to  $\vec{q}$  in the scattering plane) is sensitive to the charge form factor of the neutron,  $G_E^n$ .

The extraction of  $G_E^n$  at  $Q^2 = 0.2 \text{ GeV}^2/c^2$  was complicated by the unexpected but apparent depolarization of the electron beam in those runs where more than 100 mA of electron current was stored in AmPS. The electron polarization could not be monitored during data taking but was measured separately at very low beam currents. The results were in agreement with the data for elastic scattering also measured at currents below 100 mA. However, the result for  $A'_z$  showed a dependency on the injected current as displayed in

Fig. 1.5. The rates for random background were on the few percent level and hence could not explain the effect.

A curve was fitted to  $A'_z$  as a function of the injected current, which provided a correction factor for the  $A'_x$  data. The uncertainty of the fit introduces a significant systematic uncertainty in the final result.

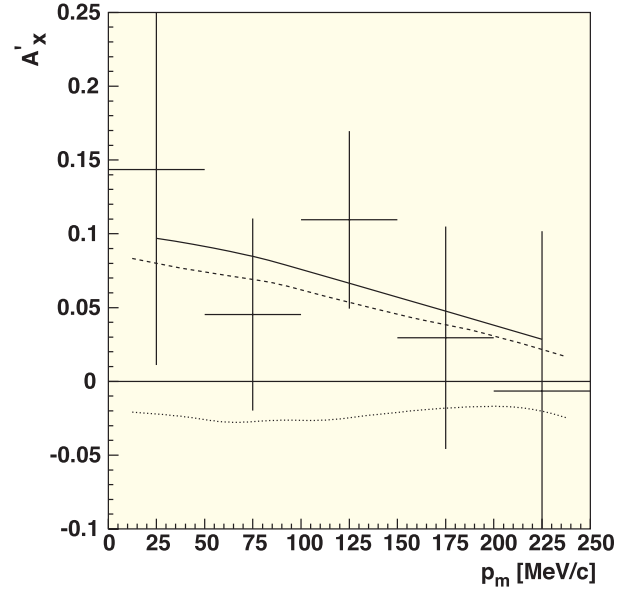


Figure 1.6: Spin-spin correlation function  $A'_x$  versus missing momentum, corrected for electron depolarization employing a linear fit to the data of Fig. 1.5. The curves are predictions by Nagorny with the assumption  $G_E^n = 0$  (dotted) and  $G_E^n = 0.05$ . Our analysis yields  $G_E^n(Q^2 = 0.2 \text{ GeV}^2/c^2) = 0.058 \pm 0.022(\text{stat}) \pm 0.025(\text{sys})$ .

To first order (plane wave impulse approximation)  $A'_x$  is proportional to  $G_E^n$ . Final state interactions and small components of the  ${}^3\text{He}$  ground state wave function complicate the picture. Figure 1.6 displays our data for  $A'_x$ , compared to the results of Monte Carlo calculations based on the relativistic formalism of Nagorny. In this analysis the resulting value for  $G_E^n$  is  $0.058 \pm 0.022(\text{stat}) \pm 0.025(\text{sys})$ . The comparison will also be made to (still ongoing) calculations based on the solutions of a non-relativistic Faddeev equation by Golak *et al.*

*Spin correlation effects in the  $\Delta$  region for the  ${}^{1,2}\vec{\text{H}}\text{e}(\vec{e}, e')$  reaction*

(Prop. 97-01; with ETH, Virginia, Arizona, TJNAF, MIT, Hampton, Novosibirsk)

A topic of interest in particle physics concerns the spin content of the nucleon, in particular the contribution of orbital angular momentum, of which little is known. This issue can be experimentally addressed by measuring double-polarization observables from electron-nucleon scattering in the  $\Delta$  region. Especially, the quadrupole transition form factors (C2 and E2) of the  $N$ - $\Delta$  excitation, are sensitive to a possible  $D$ -state admixture in the nucleon and  $\Delta$  wave functions. At the end of 1998 we have measured the longitudinal ( $A_T$ ) and sideways ( $A_{TL}$ ) spin correlation parameters in the  $\Delta$  region for the  $^1\bar{H}(\vec{e}, e')$  reaction at an average  $Q^2$  of  $0.11 \text{ GeV}/c^2$ . The  $N$ - $\Delta$  quadrupole form factor E2 (C2) enters  $A_T$ , ( $A_{TL}$ ) via an interference with the dominant magnetic ("spin-flip") dipole form factor M1. During experiments on deuterium, aiming at measuring the charge form factor of the neutron, data have been accumulated in the  $\Delta$  region as well. The ( $^2\bar{H}(\vec{e}, e')$ ) experiment was performed using a 720 MeV polarized electron beam in AmPS and an upgraded internal gas target (target thickness up to  $1.2 \times 10^{14}$  atoms/cm<sup>2</sup> and polarization up to 0.7). Scattered electrons were detected in the large acceptance magnetic spectrometer BigBite, the ejected hadrons in a time-of-flight scintillator array (see Fig. 1.7). The product of beam and target polarization was determined from the known  $e'p$  (quasi) elastic asymmetry (see Fig. 1.8). Although our main focus is on the inclusive data the exclusive channels can be studied with additional information of the TOF-detector. For a proper analysis we are currently working on Monte Carlo simulations and on corrections for contributions of radiative processes.

*Coherent  $\pi^0$  electroproduction on  $^4\text{He}$  in the  $\Delta$  region* (Prop. 94-06; with Old Dominion University and University of Virginia)

Coherent  $\pi^0$  electroproduction on a composite nucleus is an excellent testing ground for theories of resonance propagation in the nuclear medium. At energy transfers of 200-400 MeV the properties of the  $\Delta(1232)$  resonance are expected to be effectively modified by interactions with the nucleons. Coherent  $\pi^0$  electroproduction was studied on  $^4\text{He}$  by scattering electrons of 677 MeV from  $^4\text{He}$  in the Internal target setup of AmPS. Angular distributions for  $\pi^0$  over the full angular range were obtained from threshold to well over the delta-peak at two values of  $Q^2$ . The shape of the angular distributions is fairly well described by DWIA calculations and calculations including the delta explicitly, but the  $Q^2$  dependence seems to be off. A thesis was written on the results and publications are being prepared.

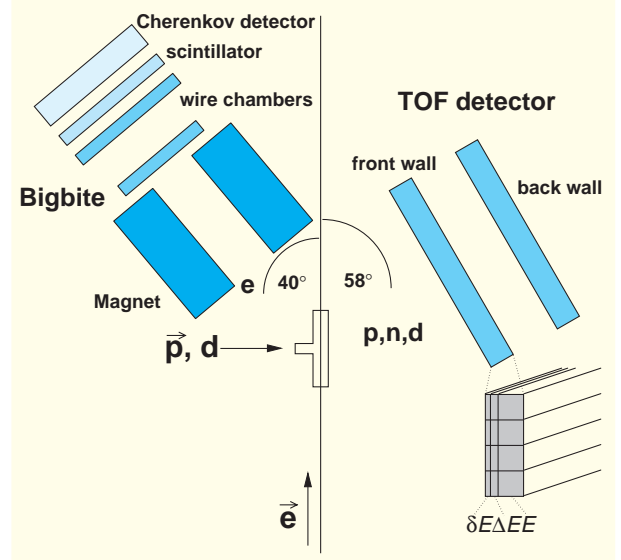


Figure 1.7: Schematic outline of the detector set-up.

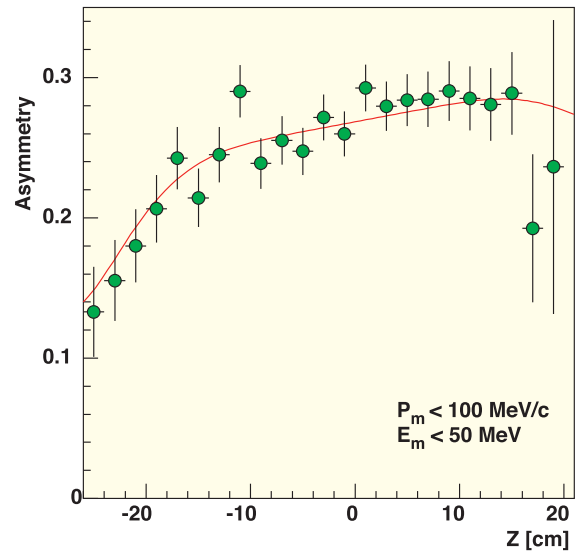


Figure 1.8: Quasielastic asymmetry for  $^2\bar{H}(\vec{e}, e'p)$  plotted versus the reconstructed vertex ( $Z$ ); the data points agree with the results of a MC-simulation (solid curve).

### 1.3 EMIN

#### *Correlations and Currents in $^3\text{He}$ Studied with the $(e, e'pp)$ Reaction*

(Prop. 97-02; with Bochum, Cracow, Glasgow, INFN-Rome, INFN-Bari, INFN-Lecce, ODU, Regina)

The availability of exact calculations of the  $^3\text{He}(e, e'pp)$  cross section makes the tri-nucleon system especially suited for unravelling the tightly connected properties of the  $NN$  interaction, short-range correlations, two-body currents and final-state interactions.

Data were collected at an energy transfer  $\omega$  of 220 MeV at three-momentum transfers  $q$  of 305, 375 and 445 MeV/c. At  $q=375$  MeV/c the  $\omega$ -dependence of the cross section was investigated between 170 and 290 MeV. In Fig. 1.9 the cross section is plotted as a function of the energy transfer for final state neutron momenta ( $p_m$ ) between 50 and 100 MeV/c.

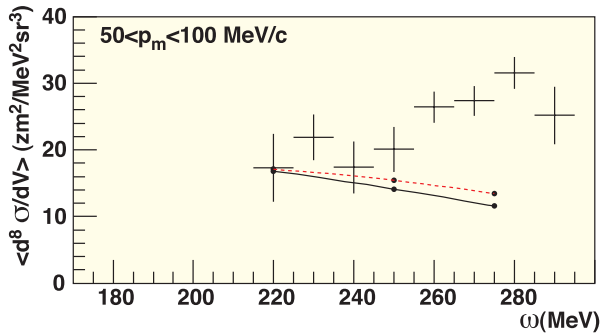


Figure 1.9: Average cross section for  $50 \leq p_m \leq 100$  MeV/c as a function of the energy transfer  $\omega$  at  $q=375$  MeV/c. The solid curve represents continuum Faddeev calculations using the Bonn-B potential and a one-body current only. The dashed curve also includes contributions from meson-exchange currents.

As a function of  $\omega$  an increasing discrepancy is observed between the data and the continuum Faddeev calculation by Golak et al., with a one-body current operator only. The effect of including meson-exchange currents (MECs) is minor. The excess strength at higher values of  $\omega$  is probably due to intermediate  $\Delta$ -excitation, a process that is not yet accounted for in the calculations.

If the  $(e, e'pp)$  reaction is driven by coupling of the virtual photon to one proton, it is directly sensitive to the initial-state wave function. As shown in Fig. 1.9, the  $^3\text{He}(e, e'pp)$  data appear to fulfil this condition at low  $p_m$  and  $\omega \leq 240$  MeV. In Fig. 1.10, the cross section is

shown for slices in  $p_m$  of 20 MeV/c wide, as a function of the variable  $p_{\text{diff},1}$ , which is related to the relative momentum of the protons in the initial state.

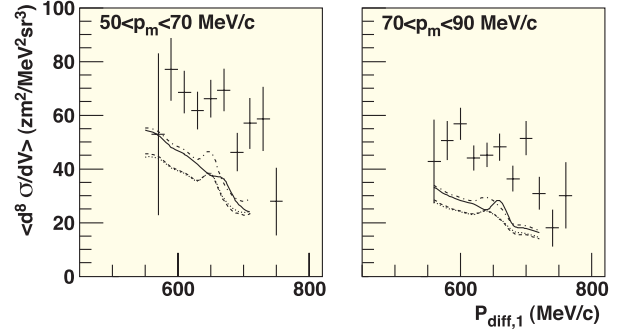


Figure 1.10: Average cross section as a function of  $p_{\text{diff},1}$  for two slices in  $p_m$  of 20 MeV/c wide. The data are compared to calculations, based on one-body currents only, using various potential models: solid curve: Bonn-B, dotted: Argonne  $v_{18}$ , dashed: CD-Bonn, dot-dashed: Nijmegen-93. The wiggles in the calculated cross section are due to small variations in the parts of the detection volume that contribute in the different kinematic configurations.

An overall discrepancy of 30 % between the data and the theoretical predictions is observed. The variations for various models of the  $NN$  interaction are of the same order of magnitude as the effects of MECs, which were only calculated for the Bonn-B potential. Since the trends of data and calculations as a function of the relative momentum are similar, the  $(e, e'pp)$  reaction can be considered in this kinematic domain as a suitable tool to probe the initial-state wave function.

$Q^2$  dependence of deduced spectroscopic strength in the reaction  $^{12}\text{C}(e, e'p)$

(with Tel Aviv, St. Petersburg, Pennsylvania State)

A comparative study was performed of the spectroscopic strength derived from  $^{12}\text{C}(e, e'p)$  data measured at low and high momentum transfer. In Fig. 1.11 we plot the summed spectroscopic factors  $S_{1p} + S_{1s}$  for  $1p$  and  $1s$  knockout as a function of  $Q^2$  in the range between 0.1 and 10  $(\text{GeV}/c)^2$ . All low  $Q^2$  results, which were obtained with an optical-model treatment of the final-state interaction, are mutually consistent and lead to a total strength  $S_{1p} + S_{1s} = 3.45 \pm 0.13$ . At higher  $Q^2$  the spectroscopic factors were deduced from a comparison of experimental cross sections with calculations employing a Glauber approach for the final-state interaction. These data exhibit a modest  $Q^2$  dependence,

which is already interesting in itself. More importantly, they do not seem to join smoothly to the low  $Q^2$  data.

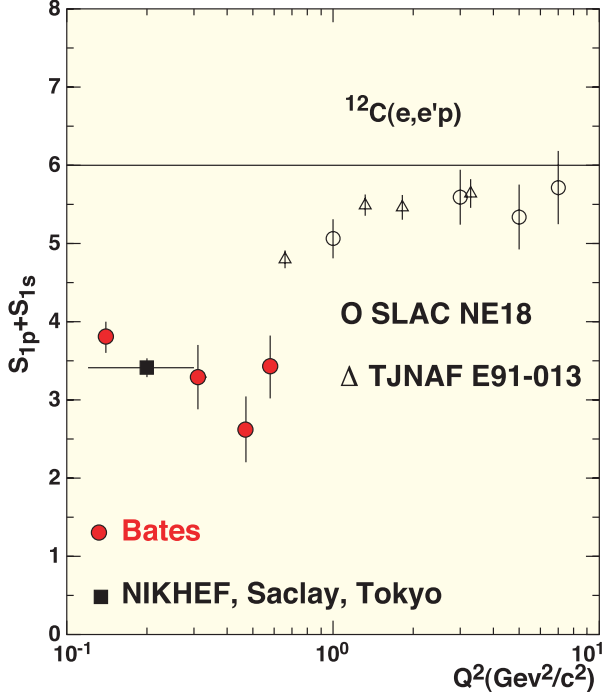


Figure 1.11:  $Q^2$  dependence of the summed spectroscopic strength  $S_{1p} + S_{1s}$  for 1p and 1s proton knockout in the reaction  $^{12}\text{C}(e, e'p)$ . The square indicates the result from a combined analysis of NIKHEF, Saclay and Tokyo data, where the horizontal bar denotes the  $Q^2$  range of these data. Other symbols represent the results from the indicated experiments at Bates, SLAC and TJNAF.

In conventional nuclear-structure models the spectroscopic strength is independent of  $Q^2$ . Hence, the question arises what the origin of the observed discontinuity around  $Q^2=0.6$  (GeV/c) $^2$  can be. The two main differences in the analysis of the low and the high  $Q^2$  data are a different treatment of the final-state interaction (FSI) and the use of a different current operator. Kelly has calculated the FSI in the  $Q^2$  range 0.2-1.2 (GeV/c) $^2$  using an optical model with empirical effective interactions. When compared to the results of a Glauber calculation, differences of up to 10% are found, which is insufficient to explain the observed discontinuity.

The current operator used in the analysis of the low  $Q^2$  data is non-relativistic, whereas in the Glauber calculations a relativistic current operator is employed. Comparisons of relativistic and non-relativistic analyses of

( $e, e'p$ ) data at low  $Q^2$  may lead to differences of up to 15%, which is not enough to explain the discrepancy observed above.

It should also be noted that only one-body currents are included in the analyses described above. Since two-body currents (meson exchange, intermediate delta excitation) markedly differ in their  $Q^2$  dependence from the one-body current, these may also be at the origin of the observed  $Q^2$  dependence of the extracted strength. Further calculations, involving one-body and two-body currents in the operator, a consistent treatment of the FSI and the current operator are needed to quantify these effects.

Instead of a reaction-mechanism effect a possible modification of the quasi-particle concept, which underlies the description at low  $Q^2$ , could also be at the origin of the observed  $Q^2$  dependence. At low energies the typical interaction time scale  $\tau_{int} \approx \hbar/\omega$  is comparable to the time specific for bound-nucleon motion in the nuclear mean-field potential. Therefore the reaction is sensitive to long-range NN correlations, which can be evaluated by treating the nucleons as quasi-particles. However, at high energies  $\tau_{int}$  becomes much smaller and the reaction is therefore less sensitive to the rearrangement processes in the residual nucleus. As a result, the effect of long-range correlations is reduced, giving rise to an increase of the spectroscopic factors. At present, quantitative calculations of this effect are not yet available.

*The semi-exclusive  $^{16}\text{O}(e, e'p)$  reaction*  
(Prop. 91-20; with INFN-Rome, INFN-Lecce, University of Bari)

The yield of the ( $e, e'p$ ) reaction at large values of the missing energy is mainly determined by multi-nucleon knockout processes. The driving mechanisms are short-range correlations (SRC), excitation and subsequent decay of the  $\Delta$ -resonance and meson-exchange currents (MEC).

The contributions from these processes were studied for the  $^{16}\text{O}(e, e'p)$  reaction in the dip region, *i.e.*, at values of the energy transfer that correspond to the kinematic region between the quasi-elastic peak and the  $\Delta$ -resonance region.

The scattered electrons and the knocked out protons were detected in the QDQ spectrometer and the segmented scintillator detector HADRON3, respectively. Measurements have been carried out in parallel kinematics at beam energies of 576 and 380 MeV. This allows for the separation of the longitudinal and trans-

verse response functions, at fixed  $(\omega, q) = (210 \text{ MeV}, 300 \text{ MeV}/c)$ . The longitudinal part of the response is largely determined by the contribution from SRC, whereas the transverse component is dominated by  $\Delta$ -excitation and MEC.

Additional measurements that were performed at  $q = 300$  and  $400 \text{ MeV}/c$  allow for the investigation of the dependence of the  $(e, e'p)$  cross section on the proton emission angle. Preliminary results have been obtained for the yield of the  $q = 400 \text{ MeV}/c$  data, measured at various angular settings of the HADRON3 detector. As the angle  $\theta_{pq}$  between the knocked out proton and the transferred three-momentum increases, the peaks due to proton knockout from the valence shells are found to decrease considerably, whereas the relative strength in the continuum rises sharply. Microscopic calculations are under way for comparison with the final data.

*Evidence for short-range correlations in  $^{16}\text{O}$*   
(Prop. 94-01; with Gent, Pavia, Georgia, INFN-Rome, INFN-Lecce, INFN-Bari, ODU, St.Louis)

The reaction  $^{16}\text{O}(e, e'pp)^{14}\text{C}$  has been investigated at three values of the transferred energy  $\omega$ , *i.e.*, 180, 210 and 240 MeV. The differential cross sections were determined as a function of the missing energy and the missing momentum.

In Fig. 1.12 the missing momentum distributions, measured for the transition to the ground state of  $^{14}\text{C}$ , are compared with the results of two calculations, which were performed with the microscopic models developed by the Pavia-group and Gent-group, respectively. Both models treat the dynamics of the proton pair in the initial state, the medium effects of the  $\Delta$ , and the final-state interaction of the ejectiles in a somewhat different way. By comparing the experimental cross sections with two independent calculations we aim at minimizing the model dependence in the interpretation of the data.

The theoretical cross sections, presented in Fig. 1.12, agree well with the data at all three values of  $\omega$ . The curves, representing the contributions of the one- and two-body currents to the ground-state transition, indicate that at  $\omega=180$  and 210 MeV the reaction is dominated by one-body currents, and that the contribution of two-body currents increases with increasing energy transfer. Hence, the agreement between the theoretical results and the data obtained independently with the two models, and the prediction of both models that the largest contribution to the cross section stems from one-body hadronic currents driven by short-range corre-

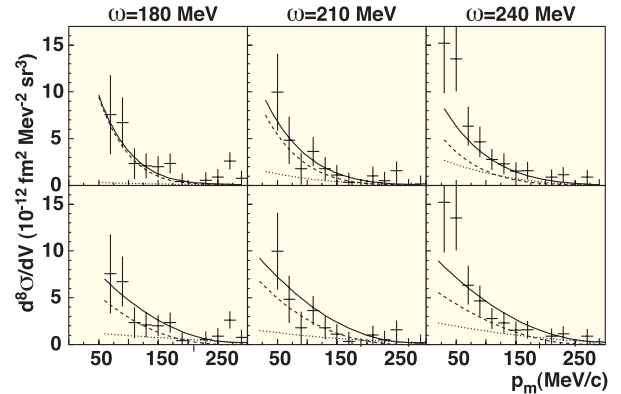


Figure 1.12: Cross sections for the transition to the ground state in  $^{14}\text{C}$  ( $-4 \leq E_x \leq 4 \text{ MeV}$ ) as a function of the missing momentum, measured for the reaction  $^{16}\text{O}(e, e'pp)^{14}\text{C}$  at three values of  $\omega$ . The curves are obtained from calculations with the Pavia-model (top) and Gent-model (bottom). The solid curves represent the full cross sections; the dashed and dotted curves correspond to the contributions of the one and two-body hadronic currents, respectively.

lations, justifies the conclusion that evidence is obtained for short-range correlations in the nucleus  $^{16}\text{O}$ .

*Depletion of the Fermi sea in  $^{208}\text{Pb}$*   
(Prop. 94-13; with Glasgow, Saclay, INFN-Rome, INFN-Lecce)

The analysis of the cross sections for the reaction  $^{208}\text{Pb}(e, e'p)$  in the missing-energy ( $E_m$ ) and momentum ( $p_m$ ) domain (0-110 MeV, 30-260 MeV/c) has proceeded in a different way than originally anticipated. Since the cross sections were measured at two different beam energies ( $E_0=461, 674 \text{ MeV}$ ) in parallel kinematics, while keeping the momentum transfer and the proton energy  $T_p=161 \text{ MeV}$  constant, the experiment would in principle allow for a longitudinal/transverse separation of the cross section. This has indeed been done experimentally (see Ann. Rep. 1998). However, the interpretation of such separated responses then becomes far from straightforward, as manifested from the results of the same procedure applied to theoretical cross sections. Both for non-relativistic and relativistic calculations by J.M. Udias (Madrid) we find that the thus extracted longitudinal and transverse responses are not equal for the low and the high beam energy. The origin of the inequality lies in heavy Coulomb-distortion effects in the electron waves, which mix the longitudinal and transverse responses. Hence, the cross sec-

tions are no longer bilinear functions of longitudinal and transverse parts that are independent of the electron kinematics. An attempt to represent the (scaled) data and calculations as a function of effective momenta was of no avail, since the scaling and the shift in momentum depend both on  $p_m$  and on the orbital quantum numbers ( $nlj$ ). Such an approach would render the whole separation procedure and subsequent interpretation heavily model dependent.

We therefore decided to analyse the high-energy and low-energy data separately, by extracting (distorted) spectral functions  $S^D(E_m, p_m)$  from the measured cross sections by dividing out the elementary electron-proton cross section. The quantity  $S^D$  is then described by a sum over all proton orbits (from the deeply bound  $1s_{1/2}$  to the  $3s_{1/2}$  valence state) of calculated distorted momentum distributions multiplied by energy distributions. The latter are delta functions of  $E_m$  for the first five valence transitions, and Lorentzians with an energy-dependent width for the deeper bound states. Each orbit has its own normalization that represents its quasi-hole strength  $Z_{nlj}$ . Parameters for the bound-state wave functions that enter the momentum-distribution calculation were taken from an earlier measurement at NIKHEF and from a variational moment approach (VMA) by Mahaux and Sartor. The final-state interaction was calculated by employing an optical-model potential that fits 160 MeV proton scattering on  $^{208}\text{Pb}$ .

In Fig. 1.13 we present the preliminary results of a multi-parameter fit to the data obtained at  $E_0=674$  MeV. The deduced quasi-hole strengths are compared to two theoretical calculations. The first is the VMA calculation for  $^{208}\text{Pb}$  by Mahaux and Sartor. The second is a calculation for correlated infinite nuclear matter (NM) to which surface correlations of the RPA type had to be added (NM+RPA) in order to justify the comparison with data for the finite nucleus  $^{208}\text{Pb}$ . Neither theory describes the data satisfactorily.

The experimental values for  $Z_{nlj}$ , shown in Fig. 1.13 exhibit relatively large, but strongly correlated, error bars since the broad energy distributions of the deep lying orbitals strongly overlap. However, their weighted sum  $Z_F = \sum Z_{nlj}(2j+1)$  is remarkably constant and accurate for a wide variation of the energy distribution parameters. The obtained value  $Z_F/82 = 0.78 \pm 0.04$  shows that about 20-25% of the protons reside outside the Fermi sea ( $E_m < 60$  MeV,  $p_m < 260$  MeV/c), in agreement with calculations for correlated nuclear matter.

Final analysis of the low-energy data, and a comparison with relativistic calculations is in progress.

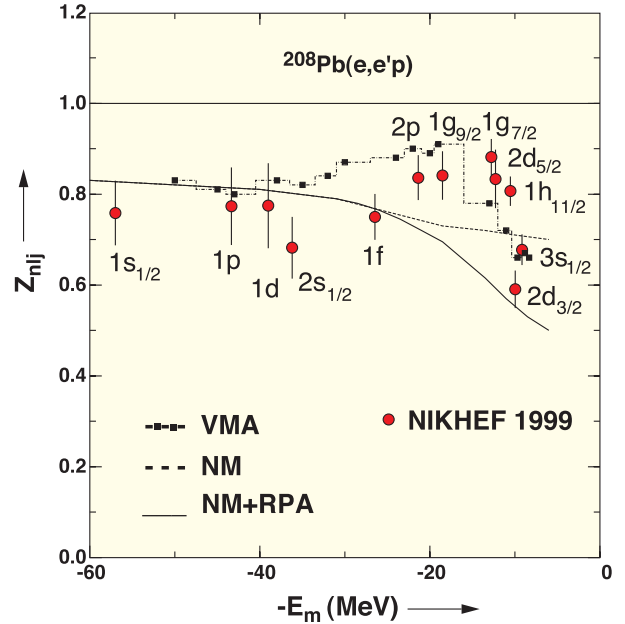


Figure 1.13: Quasi-hole strength  $Z_{nlj}$ , as deduced for the indicated orbitals in  $^{208}\text{Pb}$ , as a function of the mean removal energy in each orbit. The curves represent a calculation for correlated infinite nuclear matter (NM) to which RPA surface correlations have been added, and a calculation via a variational moment approach (VMA).

## 1.4 Experiments abroad

### Study of the $^3\text{He}(e,e'pn)$ Reaction

(Prop. A1/4-98; with the Universities of Mainz, Tübingen, Glasgow and Edinburgh)

A  $^3\text{He}(e,e'pn)$  experiment will be performed at MAMI in Mainz which is expected to yield results that are complementary to those obtained at AmPS for the  $^3\text{He}(e,e'pp)$  reaction. Since the coupling of the virtual photon depends sensitively on the spin-isospin of the nucleon pair, marked differences between the cross sections for the pp and the pn channel are expected. In this way the interplay between NN-correlations and meson-exchange and isobar currents will be investigated in the three-nucleon system. The scattered electrons will be detected in a magnetic spectrometer, while the segmented scintillator detector HADRON3 will be used for proton detection. The neutrons, emitted in the backward direction, will be detected in a 16 cm thick scintillator wall with a surface of  $14.4 \text{ m}^2$ .

For the preparation of this experiment the HADRON3

detector and its support structure as well as the accompanying VME electronics and data acquisition system, have been made operational in the A1 hall at MAMI. A first test with beam from the microtron revealed a very good response of the detector upto a luminosity of  $4400 \mu\text{A}\cdot\text{mg}\cdot\text{cm}^{-2}$ . Real electron-proton coincidences between the electron spectrometer and HADRON3 were easily identified. Modification of the data format and incorporation of the datastream of HADRON3 into the data-acquisition system of A1 is in progress. The first run of the experiment is expected to take place in spring 2000.

*Study of the Charged Pion Form Factor*  
(with the TJNAF E93-021/E96-007 collaboration)

The charge form factor of the pion is studied by scattering electrons from a virtual pion in the proton. Pion electroproduction data on  $^1\text{H}$  as well as  $^2\text{H}$ , plus extensive calibration data for the optics of the Short Orbit Spectrometer and the new small angle tune of the High Momentum Spectrometer were taken in Hall C at TJNAF in the fall of 1997. The analysis of the optics data and the pion production data on  $^1\text{H}$  are completed, along with systematic studies of detector and tracking efficiencies.

Unseparated and L/T separated cross sections are obtained by comparing the experimental yields with those generated in a Monte Carlo simulation. The optimization of the simulation is almost completed. Because of correlations between the relevant variables  $W$ ,  $Q^2$ ,  $t$  and  $\theta$  within the experimental acceptance, the cross section used in the MC simulation had to be modelled carefully. Preliminary separated cross sections for the  $^1\text{H}(e, e'\pi^+)n$  reaction were obtained for all four  $Q^2$  points between 0.6 and  $1.6 (\text{GeV}/c)^2$ . In each case, the longitudinal cross section clearly shows a  $t$ -pole behaviour, which does not factorize into  $Q^2$  and  $t$  dependent parts, contrary to what was suggested by older, less accurate data. The transverse cross section shows a clear  $Q^2$  dependence.

Isoscalar background contributions have been studied in the ratio between  $\pi^-$  and  $\pi^+$  production on deuterium. The preliminary ratio of the separated longitudinal structure functions is consistent with unity, indicating that the coupling is to the pion charge, not to the individual quarks. The ratio of the separated transverse structure functions is of the order of 0.5 at low  $-t$ , decreasing at larger  $-t$ . The results will be compared to predictions from Regge- and Born-term type models, thus determining the pion charge form factor.

## 2 HERMES

### 2.1 Introduction

The year 1999 was a successful year for the HERMES experiment at DESY, with a large amount of data collected on both polarized and unpolarized targets. The analysis of data collected in previous years yielded several important results, including a first measure of the gluon polarization in the proton. Moreover, an anomaly in the ratio of longitudinal and transverse cross sections was discovered when studying the influence of the nuclear medium on lepton-quark scattering. The NIKHEF/VUA group played a leading role in this discovery.

In 1999 the HERMES spectrometer was improved in several ways. The new Ring-Imaging Cherenkov (RICH) detector was made fully operational, enabling the identification of pions, kaons and protons over most of the momentum range accepted by the spectrometer. Furthermore, the infrastructure and first detector module of the new wheel-shaped silicon detector array (the 'Lambda Wheels') was installed. These (and other) upgrades increase the acceptance of the HERMES spectrometer for the production of particles containing charm or strange quarks.

Prior to the HERA luminosity upgrade, which is scheduled to begin in the second half of the year 2000, the HERMES collaboration prepared a long-range plan. In this report the physics programme of the experiment is described for the period 2001 to 2006. The report was approved by the DESY directorate in December 1999.

### 2.2 Data taking

In 1999 about 2.4 million deep-inelastic scattering (DIS) events have been collected on a polarized  $^2\text{H}$  target. Together with the results obtained in previous years on polarized  $^1\text{H}$  and  $^2\text{H}$  targets, these data will make it possible to perform an accurate determination of the polarization carried by up, down and sea quarks.

During a few days of dedicated data taking at high luminosity also about 0.9 million DIS events have been collected on an unpolarized Krypton target. These data will be used to study the density dependence of the new quark effect that was discovered using a Nitrogen target.

Near the end of 1999 the luminosity of the experiment for polarized deep-inelastic scattering was improved by a factor of two. The storage cell containing the polarized target was replaced by one with a smaller diameter,

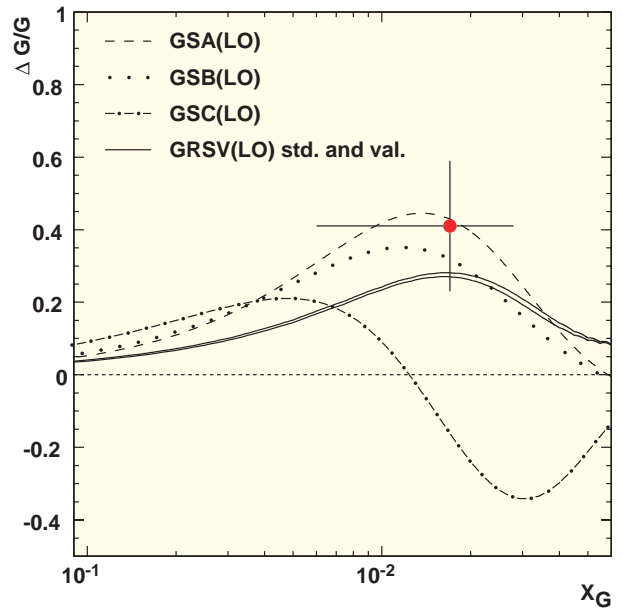


Figure 2.1: Relative polarization of the gluons in the proton as a function of the fractional momentum  $x_G$  carried by the gluons. The error includes the statistical and systematic uncertainties, but contains no contribution due to a possible model dependence of the analysis. The leading order QCD fits have been taken from T. Gehrmann and W.J. Stirling, *Phys. Rev.* **D53** (1996) 6100 and M. Glück, E. Reya, M. Stratmann and W. Vogelsang, *Phys. Rev.* **D53** (1996) 4775. The horizontal error bar identifies the  $x_G$ -range covered by the data.

resulting in an increase of the effective target density by 50 %. At the same time the positron currents reached values of 44 mA on injection, while maintaining lepton polarization levels as high as 60 %.

In general, the HERMES spectrometer operated very well during the entire year. However, the vertex chambers (VC), a set of multi-strip gas chambers (MSGC) built by NIKHEF, suffered from radiation damage due to beam losses in the vicinity of the detector, leading to a significant loss of efficiency. For that reason the VC was shipped back to Amsterdam, where the APC readout chips were replaced. The chambers were ready for testing near the end of the year.

### 2.3 Physics analysis

#### Gluon polarization

From polarized deep-inelastic lepton-nucleon scattering

experiments, it has been inferred that the quark spins account for only a fraction of the nucleon spin. One possible explanation is a significant polarization of the gluons in the nucleon. Direct measurements of the gluon polarization  $\Delta G(x_G)$ , where  $x_G$  is the fraction of the nucleon momentum carried by the gluon, have not been reported so far. The relative gluon polarization  $\Delta G/G$  in the proton has now been measured for the first time by the HERMES experiment at DESY.

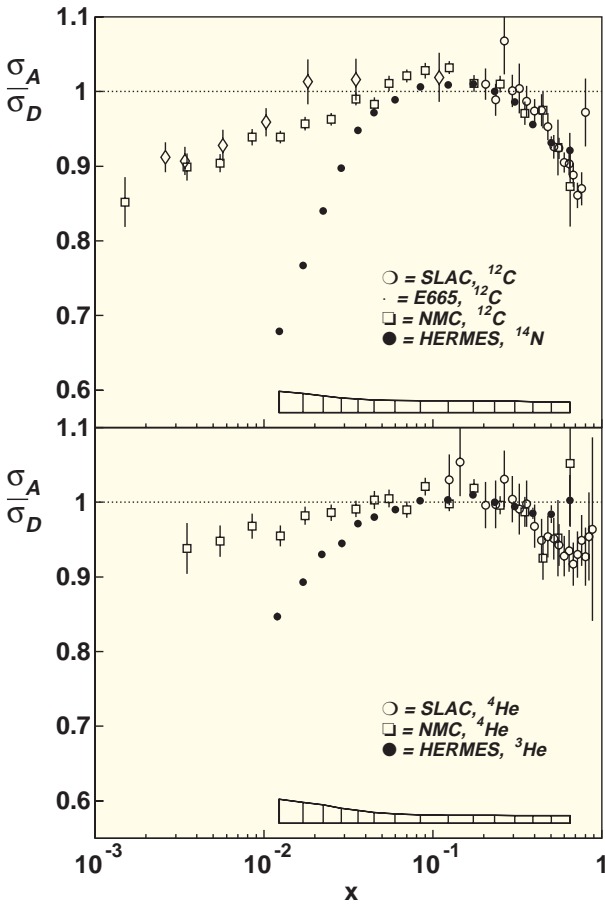


Figure 2.2: Ratio of cross sections of inclusive deep-inelastic lepton scattering from nucleus  $A$  and  $D$  versus  $x$ . The error bars of the HERMES measurements represent the statistical uncertainties, the systematic uncertainty of the HERMES data is given by the error band. The error bars of the NMC, E665, and SLAC data are given by the quadratic sum of the statistical and systematic uncertainties.

The interaction of an incident electron (or positron) with a gluon can be identified by observing two oppositely charged pions with high transverse momentum

$p_T$ . By carrying out such measurements on a polarized hydrogen target using a polarized positron beam, information on the gluon polarization can be obtained. The result for  $\Delta G/G$  is shown in Fig. 2.1, where it is compared to several leading-order QCD parameterizations, which are derived from the  $Q^2$ -evolution of polarized inclusive deep-inelastic lepton scattering data. The measurement indicates that the gluons have a significant positive polarization, i.e., the gluon spin is oriented parallel to that of the proton. Further measurements at HERMES are expected to lead to an improvement of the statistical precision of the data by a factor of two.

The present measurement of  $\Delta G/G$  contains a model dependence, since a correction needs to be made for contributions due to the QCD Compton process. The model dependence can be reduced by also measuring  $\Delta G/G$  through different reaction channels. Alternative methods to identify the interaction with a gluon rely on the observation of particles containing a charm quark. The upgrades of the HERMES spectrometer, which were mentioned above, are largely motivated by the need to identify  $D^0$  and  $J/\Psi$  mesons, and possibly  $\Lambda_C^+$  hyperons as tags of charm production events.

#### Nuclear Effects on $R = \sigma_L/\sigma_T$

The cross-section (per nucleon) for deep-inelastic scattering from a heavy nucleus is known to be different from that on the proton. This effect is known as the EMC effect at values of  $x$ , which represents the fraction of the proton momentum carried by the struck quark, larger than 0.1 and as shadowing at values of  $x$  smaller than 0.1. These effects are relatively small (about 10 % or less), and can be understood in terms of nucleon dynamics (at large  $x$ ) and the hadronic structure of the virtual photon (at small  $x$ ).

Hence, it came as a surprise when HERMES measured cross section ratios for deep-inelastic scattering on  $^{14}\text{N}$  (and  $^3\text{He}$ ) with respect to  $^2\text{H}$ , and found large deviations compared to previous measurements on neighbouring nuclei. These results are displayed in Fig. 2.2. By also considering the average four-momentum transfer squared  $Q^2$ , the difference between the data sets was found to occur in the domain  $x < 0.06$  and  $Q^2 < 1.5 \text{ GeV}^2$ .

As the previous experiments made use of largely different incident lepton energies (200 and 400 GeV for NMC and E665, respectively), the cross section ratios were measured at different values of the virtual photon polarization parameter  $\epsilon$ . This parameter is close to unity for most of the NMC and E665 data, while it varies be-

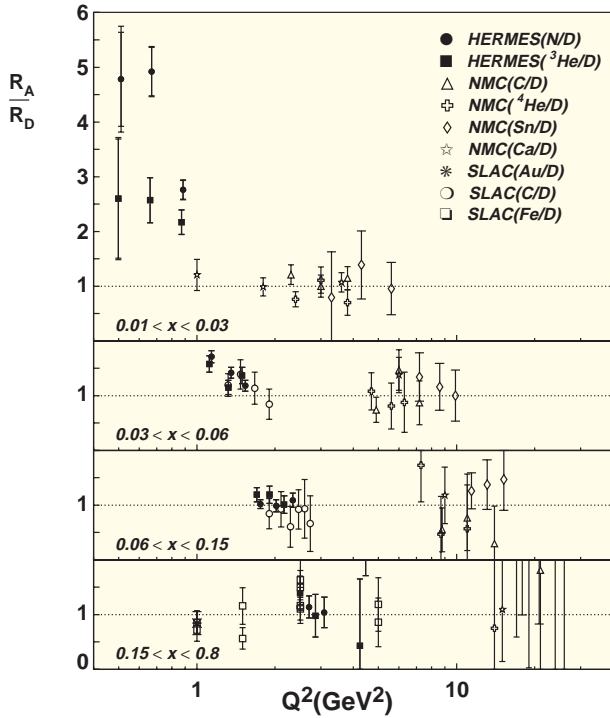


Figure 2.3: The ratio  $R_A/R_D$  for nucleus  $A$  and deuterium as a function of  $Q^2$  for four different  $x$  bins. The HERMES data on  $^{14}\text{N}$  ( $^3\text{He}$ ) are represented by the solid circles (squares). The open triangles ( $^{12}\text{C}$ ) and crosses ( $^4\text{He}$ ) have been derived from the NMC data using the same technique. The other SLAC and NMC data displayed have been derived from measurements of  $\Delta R = R_A - R_D$  taking a parameterization for  $R_D$ . The inner error bars include both the statistical uncertainty and an error representing the correlations in the fitting procedure. The outer error bars also include the systematic uncertainties.

tween 0.1 and almost 1.0 for the HERMES data. The different  $\epsilon$ -ranges probed by the experiments suggested that the anomaly shown in Fig. 2.2 can be attributed to an  $A$ -dependence of the ratio  $R = \sigma_L/\sigma_T$  of longitudinal to transverse deep-inelastic scattering cross sections at low  $x$  and low  $Q^2$ . In fact, the HERMES data could be used to derive values for the ratio  $R_A/R_D$ , which are shown in Fig. 2.3.

The rise of  $R_A/R_D$  at small values of  $x$  and  $Q^2$  can possibly be interpreted by assuming that the positron scatters from a quark-antiquark pair that is being exchanged between neighbouring nucleons. The pair carries a non-zero charge, but no net spin. Hence, the transverse component of the reaction is reduced with

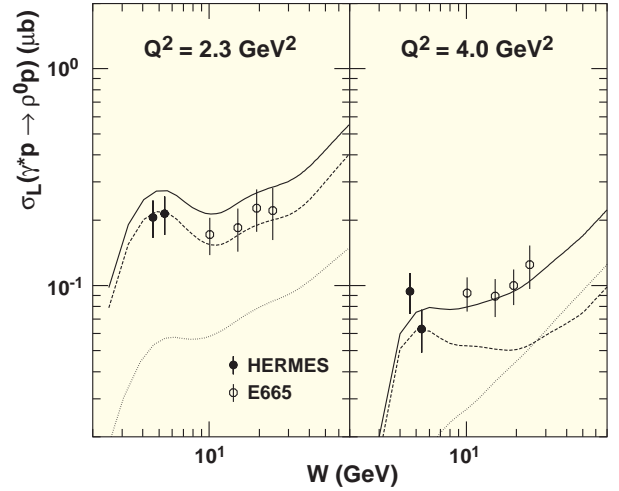


Figure 2.4: The longitudinal component of the virtual-photon production cross section for  $\rho^0$  production versus  $W$  at average  $Q^2$  values of 2.3 (left) and 4.0  $\text{GeV}^2$  (right). The solid lines represent the results of the calculations of Vanderhaeghen et al. The dashed (dotted) curves represent the quark (two-gluon) exchange contributions within these calculations.

respect to the longitudinal one, giving rise to an increase of  $R$  inside the nuclear medium.

#### $\rho^0$ vector meson production

The cross section for the production of vector mesons by real or virtual photons is closely related to other observables in lepton scattering. For example, with help of the recently introduced Off-Forward Parton Distributions (OFPDs), one can relate elastic nucleon form factors, deep-inelastic scattering structure functions, virtual Compton scattering, and vector meson production cross sections. The OFPDs represent a generalization of the parton distributions measured, for instance, in inclusive DIS experiments. According to the OFPD calculations of M. Vanderhaeghen, P.A.M. Guichon and M. Guidal (Phys. Rev. Lett. **80** (1998) 5064) the longitudinal cross sections are dominated by contributions from a quark exchange mechanism for  $W < 10$  GeV.

New data for  $\rho^0$  virtual-photon production have been obtained at HERMES. The invariant mass  $W$  of the photon-nucleon system ranges from 4.0 to 6.0 GeV, while the negative squared four-momentum transfer  $Q^2$  varies from 0.7 to 5.0  $\text{GeV}^2$ . The longitudinal component of the cross section has been derived from the total cross section  $\sigma_{tot}$  using  $\sigma_L = \frac{R}{1+\epsilon R} \sigma_{tot}$  with  $\epsilon$  the polarization of the virtual photon, and  $R$  the ratio of longitudinal and transverse cross sections  $\sigma_L/\sigma_T$ . For

A new parameterization of existing data and preliminary HERMES data was used. The results are displayed in Fig. 2.4, where they are compared to the OFPD calculations of Vanderhaeghen et al. The calculations reproduce the data fairly well, thus lending support to the predicted dominance of the quark exchange mechanism for  $W < 10$  GeV.

Most data on  $\rho^0$  production imply that s-channel helicity conservation is valid, i.e. the helicity of the produced  $\rho^0$  meson is the same as that of the virtual photon. Hence,  $\rho^0$  production should not be sensitive to the orientation of the target spin, i.e. the spin asymmetry  $A_1$  is expected to be zero.

In Fig. 2.5 the resulting values for  $A_1$  are plotted as a function of 4 different kinematic variables. The data give evidence for a positive asymmetry, which averages to  $0.30 \pm 0.11$  (stat.)  $\pm 0.04$  (syst.)  $\pm 0.05$  (model) over the entire kinematic range. The non-zero value of  $A_1$  indicates that the anticipated spin-independence of the  $\rho^0$  production cross section is violated.

## 2.4 The silicon detector project

The silicon detector project aims to develop and construct new silicon detector systems that will surround the HERMES internal target. The purpose of these detectors is to increase the acceptance of the spectrometer for  $\Lambda^0$  hyperons and  $J/\Psi$  mesons, such that the polarization of strange quarks and gluons can be measured with improved precision. Moreover, by detecting slow recoil protons, several exclusive reaction channels can be studied.

The silicon counters have to be operated under ultra-high vacuum conditions close to the high-intensity electron beam of HERA (with peak currents up to 50 mA). In order to proof the feasibility of operating silicon strip counters under such conditions, we built a so-called Silicon Test Counter (STC), which was installed below the HERMES internal target in 1998. The STC has been operated successfully for several months, thus providing a proof of principle. Moreover, it has been possible to collect some interesting data with the STC, which were (partly) analysed in 1999. In fact, the instrument could be used to measure – for the first time – the momentum distribution of recoil protons in deep inelastic scattering.

In early 1999 the STC was removed, to make place for a larger silicon detector array, the Lambda Wheels. The support structure of this wheel-shaped detector was installed, together with a prototype silicon detector module. A photograph of the prototype module is shown in

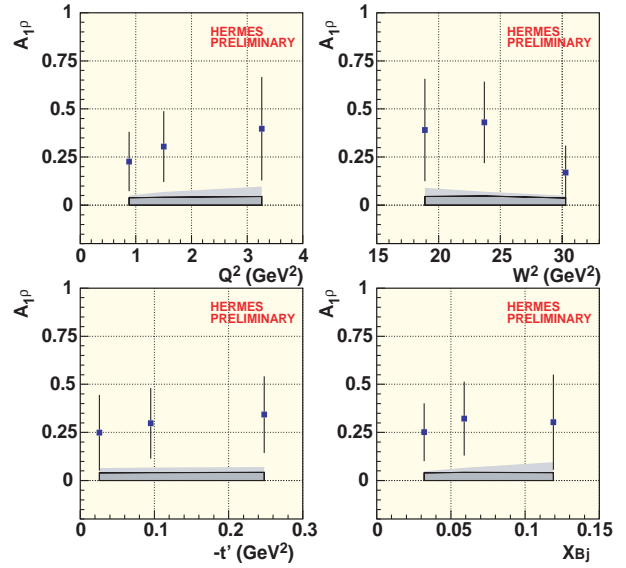


Figure 2.5: Cross-section asymmetry  $A_1$  for  $\rho^0$  electro-production on  $^1H$  with respect to the spin orientation of the target. The asymmetry is plotted versus  $Q^2$  (upper left),  $W^2$  (upper right),  $-t'$  (lower left) and  $x_{Bj}$  (lower right). The dark gray band represents the experimental systematic uncertainty, while the light gray area corresponds to the uncertainty due to the transverse contribution to the asymmetry  $A_2$ .

Fig. 2.6, while Fig. 2.7 shows a picture of the module after its installation inside the vacuum chamber.

Before installation at HERMES, the prototype module was successfully tested with cosmic rays at NIKHEF. When exposed to the HERA lepton beam, electromagnetic (EM) interference between the very intense HERA beam and the electronic trigger circuit on the carrier board of the silicon module was observed. The interference effects were strongly reduced by installing an additional EM-screen in front of the Lambda Wheels. Near the end of the year the prototype module was shown to function adequately up to the highest positron currents used by HERA in 1999, i.e., 44 mA.

The noise level of the silicon counter is increased by some 40 % due to the beam. However, even then the noise is a factor of 10 – 20 (depending on the strip length) smaller than the signal of a minimum ionizing particle. This result is in agreement with the specifications of the detector.

In 1999 preparations were made for the series production of all silicon modules needed for the Lambda Wheels. After some delay all silicon counters were delivered at the institute. The complete functionality of all



Figure 2.6: *Prototype of a silicon detector module for the Lambda Wheels. The module consists of two wedge-shaped double-sided silicon detectors. The front-end readout electronics are located on two carrier boards, which are mounted in between the two detectors. When installed the carrier boards are well outside of the acceptance of the HERMES spectrometer.*

HELIX128 chips, which are used on the carrier board of the module for the electronic readout, was tested using the new probestation at NIKHEF. The yield was high, and more than enough HELIX128 chips are now available for the construction of all modules. All other components of the detector (cooling, ADC units, power supplies, etc.) were also constructed and tested in 1999.

Following the successful commissioning of the prototype silicon detector near the end of 1999, the series production will start in early 2000. It is expected that the Lambda Wheels will be fully equipped in the course of the year 2000.

## 2.5 The long-range plan

The HERMES collaboration intends to continue recording data in the years 2001 – 2006, i.e., after the HERA luminosity upgrade, as many important (and often unique) measurements can be made concerning the (spin) structure of the nucleon and related areas. In 1999 a long-range plan has been written, in which the most prominent measurements that will be carried out in this period are described: (i) the longitudinal polar-

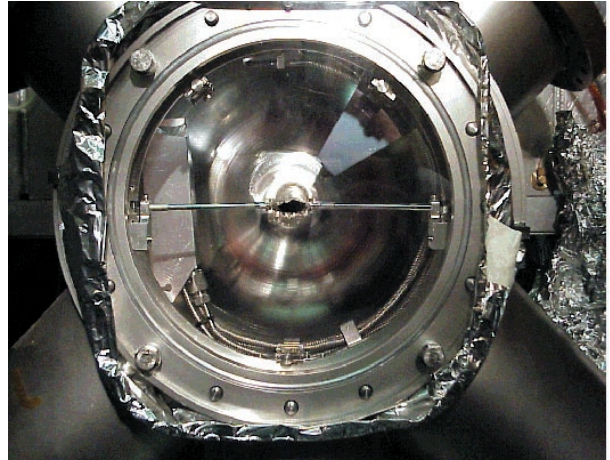


Figure 2.7: *Support structure of the Lambda Wheels after its installation in the HERMES vacuum chamber. The system will contain 12 detector modules, of which one (the prototype) can be seen in the upper right corner. The HERA lepton beam passes through the centre of the vacuum chamber, inside the (open) wakefield suppressor, of which the thin support bars are seen in the middle of the picture.*

ization of strange quarks, (ii) the longitudinal polarization of gluons, and (iii) the transverse quark polarization. Moreover, additional measurements on unpolarized heavy targets are foreseen to investigate the new nuclear effects on  $R = \sigma_L/\sigma_T$  discovered at HERMES.

Future measurements will profit from the recently realized increase of the luminosity (by a factor of 2), and various upgrades and improvements of the HERMES detector. Most of these upgrades were implemented in the last two years. They include the replacement of the threshold Cherenkov counter by a dual-radiator Ring-Imaging Cherenkov counter, an instrumented iron wall for muon identification, and the new silicon detectors described above. These improvements will make it possible to measure the gluon polarization, for instance, in three independent ways, and carry out the first measurements of the transverse spin structure of the nucleon. The latter subject is of particular interest, as the corresponding structure function  $h_1(x)$  evolves with  $Q^2$  in an unusual way, and can be used to measure the tensor charge of the nucleon.

The long-range plan was positively reviewed by the DESY PRC in the fall of 1999, and fully endorsed by the DESY directorate in December 1999.

## 3 ZEUS

### 3.1 Introduction

This year HERA provided data with both positron and electron beams. The energy of the proton beam had been increased from 820 GeV to 920 GeV in 1998.

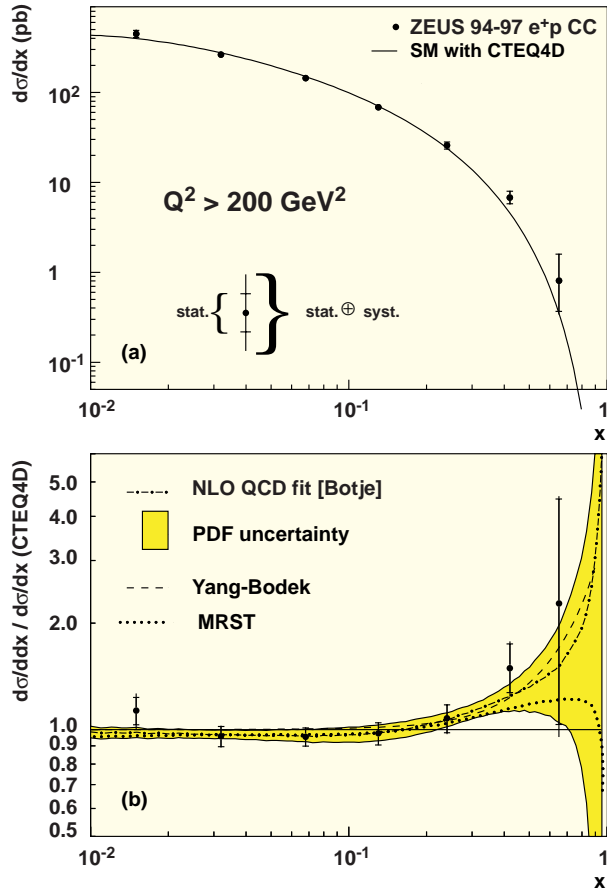


Figure 3.1: The charged current differential cross section as a function of  $x$ , together with the Standard Model predictions using the CTEQ4D parton density distributions. Below the ratio of the data to the prediction. At large  $x$  the prediction underestimates the data. The ZEUS NLO QCD fit is shown as the dot-dashed curve. Also indicated are the fits by Bodek-Yang and MRS to the data.

The integrated total luminosity obtained by ZEUS was  $16 \text{ pb}^{-1}$  for the electron running and  $70 \text{ pb}^{-1}$  for positrons. This has allowed for the first time to perform measurements at high  $Q^2$  both with electrons and positrons and so to see directly the influence of the parity violating part of the weak interaction in deep inelastic scattering. The NIKHEF group was active in

the areas of physics involving a hard scale. Two thesis defences took place during this year, one on the charged current scattering and one on the production of high  $E_T$  jets in photo-production. In the following a short summary of the most important results obtained by ZEUS is given. The microvertex project got into full swing this year and will be discussed at the end of this chapter.

### 3.2 Physics Results

In terms of the structure functions  $F_2$ ,  $F_L$  and  $xF_3$  and the usual Lorentz scalars  $x$ ,  $y$  and  $Q^2$  the neutral current double differential cross section for  $e^\pm$  is given by:

$$\frac{d^2\sigma^{NC\pm}}{dx dQ^2} = \frac{2\pi\alpha^2}{x} \frac{1}{Q^4} \times [Y_+ F_2 - y^2 F_L \mp Y_- x F_3],$$

with  $Y_\pm = 1 \pm (1-y)^2$ . In lowest order QCD the structure function  $F_2 = \sum_f A_f(Q^2) [xq_f(x, Q^2) + x\bar{q}_f(x, Q^2)]$  and  $x F_3 = \sum_f B_f(Q^2) [xq_f(x, Q^2) - x\bar{q}_f(x, Q^2)]$  where  $q_f(x, Q^2)$  and  $\bar{q}_f(x, Q^2)$  denote the momentum density of a quark and anti-quark of flavour  $f$  and  $A_f(Q^2)$  and  $B_f(Q^2)$  contain the coupling and relevant propagator terms. Charged current scattering cross sections can in the same way be parametrized in terms of the quark momentum densities as:

$$\frac{d^2\sigma^{CC}}{dx dQ^2} = \frac{G_F^2}{2\pi x} \frac{M_W^4}{(Q^2 + M_W^2)^2} \tilde{\sigma}$$

where the reduced cross section  $\tilde{\sigma}$  is given by:

$$\tilde{\sigma} = \sum_f \begin{cases} [x\bar{u}_f(x, Q^2) + (1-y)^2 x d_f(x, Q^2)] & (e^+) \\ [xu_f(x, Q^2) + (1-y)^2 x \bar{d}_f(x, Q^2)] & (e^-) \end{cases}$$

where  $G_F$  is the Fermi coupling constant and  $u_f(\bar{u}_f)$  and  $d_f(\bar{d}_f)$  are the densities of up-type and down-type (anti-)quarks.

The analysis of charged current scattering in  $e^+p$  interactions using the 1996 and 1997 data was concluded. Differential cross sections as a function of  $Q^2$  and  $x$  were determined. Also for the first time the double differential cross section  $\frac{d\sigma}{dx dQ^2}$  was extracted.

At large values of  $x$  the charged current cross section is dominated by the down-quark density in the proton. This density is not well constrained by previous measurements of deep inelastic scattering. It turned out that the predictions from previous fits performed on neutral current data underestimated the charged current cross section in the region of high  $x$ . QCD next-to-leading order fits including the ZEUS charged current

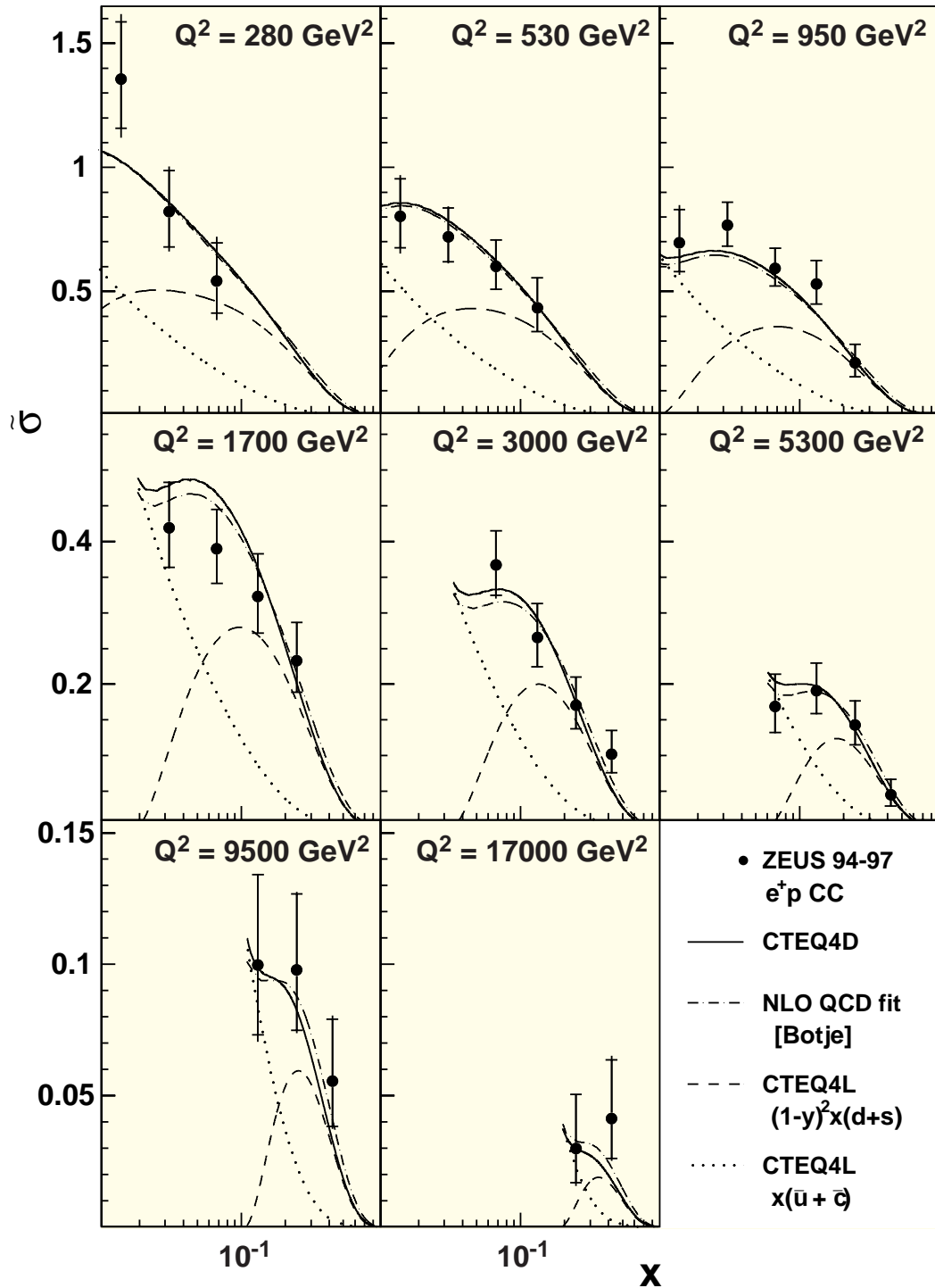


Figure 3.2: The reduced cross section for charged current scattering as a function of  $x$  for several values of  $Q^2$ . Predictions are from CTEQ4 (drawn line) and the ZEUS NLOQCD fit (dot-dashed). The decomposition from the CTEQ prediction into contributions from  $d+s$  quarks (dashed) and  $\bar{u}+\bar{c}$  (dotted) are also shown.

data were however able to describe the data satisfactorily, thus providing a significantly better constraint on the down-quark density. Figure 3.1(top) shows the differential cross section as a function of  $x$  together with the predictions of one of the successful quark density parametrisations, CTEQ4D. Figure 3.1(bottom) shows the ratio of the measured cross section and the prediction. At large  $x$  the underestimation by the model is clearly seen. The figure also shows the result of the NLO QCD fit to the data performed by the ZEUS collaboration. Figure 3.2 shows the double differential reduced cross section, together with the decomposition into quark contributions as obtained from the fit. It is clear that the  $d$ -quark density is dominant at large  $x$  but that at lower values of  $x$  also the  $\bar{u}$  and  $\bar{c}$  quarks become important.

From the shape of the differential cross section in  $Q^2$ , shown in figure 3.3, it is possible to extract a measurement of the mass of the exchanged space-like  $W$  boson.

From a completely unconstrained fit ( $G_F$  and  $M_W$  left free) the value:

$$M_W = 80.8^{+4.9}_{-4.5}(\text{stat})^{+5.0}_{-4.3}(\text{syst})^{+1.4}_{-1.3}(\text{pdf}) \text{ GeV}$$

is obtained, whereas if one uses the relation

$$G_F = \frac{\pi\alpha}{\sqrt{2}} \frac{M_Z^2}{M_W^2(M_Z^2 - M_W^2)} \frac{1}{1 - \Delta r(M_W)}$$

where  $\Delta r(M_W)$  depends on the Higgs and top quark mass, one obtains:

$$M_W = 80.50^{+0.24}_{-0.25}(\text{stat})^{+0.13}_{-0.16}(\text{syst})^{+0.30}_{-0.31}(\text{pdf})^{+0.05}_{-0.06}(M_t, M_H) \text{ GeV}$$

for  $M_H = 100 \text{ GeV}$  and  $M_t = 175 \text{ GeV}$ . This is in excellent agreement with the measurements from LEP and Fermilab of the time-like  $W$ . This provides an impressive consistency check of the description of the weak interaction provided by the Standard Model.

The significant luminosity collected by ZEUS with both electron and positron beams allowed for the first time a comparison of neutral and charged current scattering for  $e^+p$  and  $e^-p$ . Figure 3.4 shows the differential cross sections versus  $Q^2$ . At  $Q^2$  values around  $10000 \text{ GeV}^2$  the charged and neutral current cross sections become comparable. Also the effect of the  $xF_3$  structure function in the neutral current scattering is visible. This parity violating part of the cross section adds to the

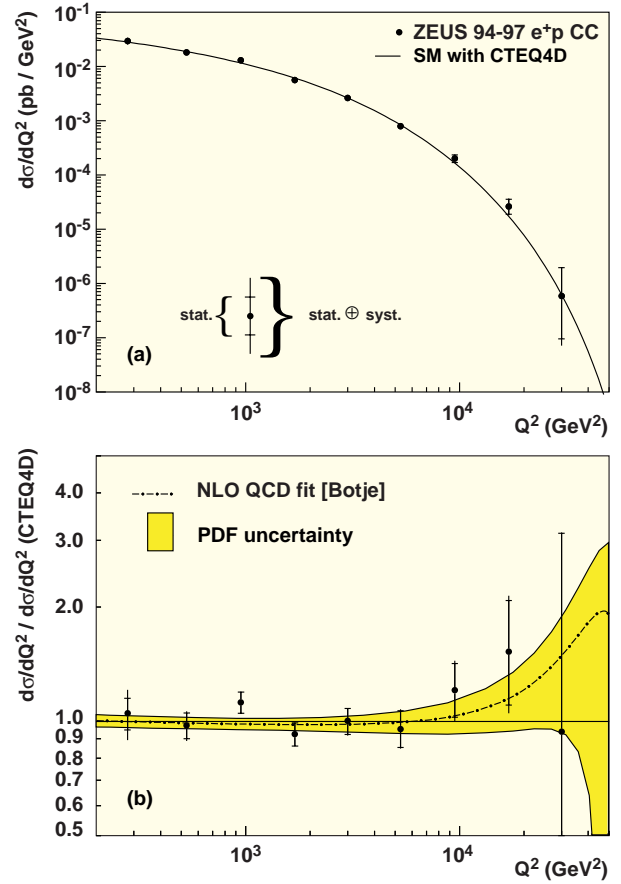


Figure 3.3: The differential charged current cross section as a function of  $Q^2$  and below the ratio to the prediction using the CTEQ parton parametrisations. The ZEUS NLO QCD fit is also shown as the dot-dashed line.

$e^-p$  and subtracts from the  $e^+p$  cross section. This is more clearly shown in Fig. 3.5 where the differential neutral current cross section for  $Q^2 > 10000 \text{ GeV}^2$  is given versus  $x$  for both  $e^-p$  and  $e^+p$  scattering. The cross section for  $e^-p$  is almost a factor of three larger than for  $e^+p$ . The full and dashed curves show the expectation using the standard model with  $M_Z = 91 \text{ GeV}$  whereas the dotted and dot-dashed curves show the prediction without  $Z$  boson exchange.

### 3.3 Microvertex Project

At the beginning of the year the design of the silicon wafer was finalized and the order was placed for all barrel wafers. These wafers have been delivered and work has proceeded on gluing two wafers into half-modules containing one wafer for  $r - \phi$  readout and one for  $z$

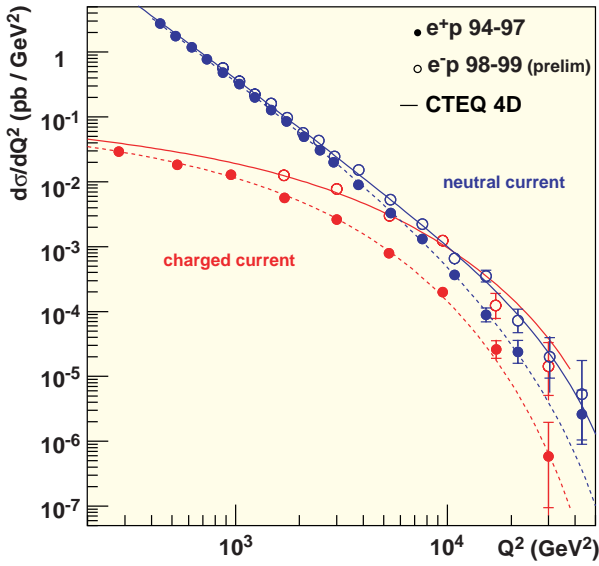


Figure 3.4: The differential cross section as a function of  $Q^2$  for charged and neutral current  $e^+p$  and  $e^-p$  scattering.

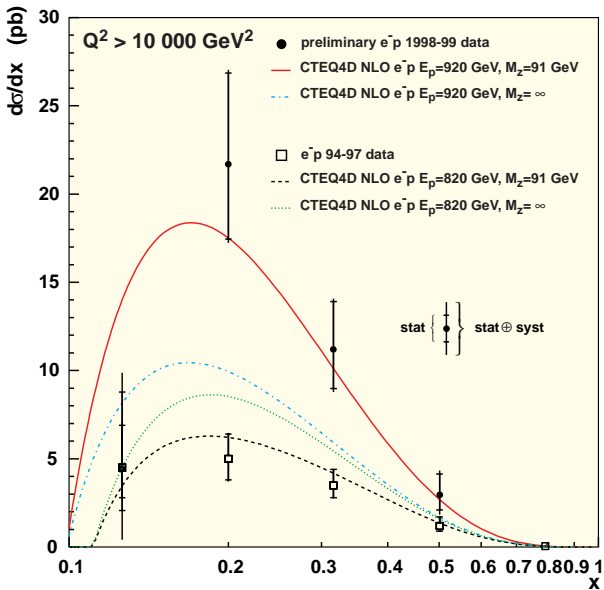


Figure 3.5: The differential cross section as a function of  $x$  for  $Q^2 > 10000 \text{ GeV}^2$  for both  $e^-p$  (dots) and  $e^-p$  (open squares) scattering. Standard model predictions for  $M_Z = 91 \text{ GeV}$  are indicated by the drawn line ( $e^-p$ ) and dashed line ( $e^+p$ ). The dotted (dot-dashed) lines indicate the cross section without  $Z$  exchange for  $e^+p$  ( $e^-p$ ).

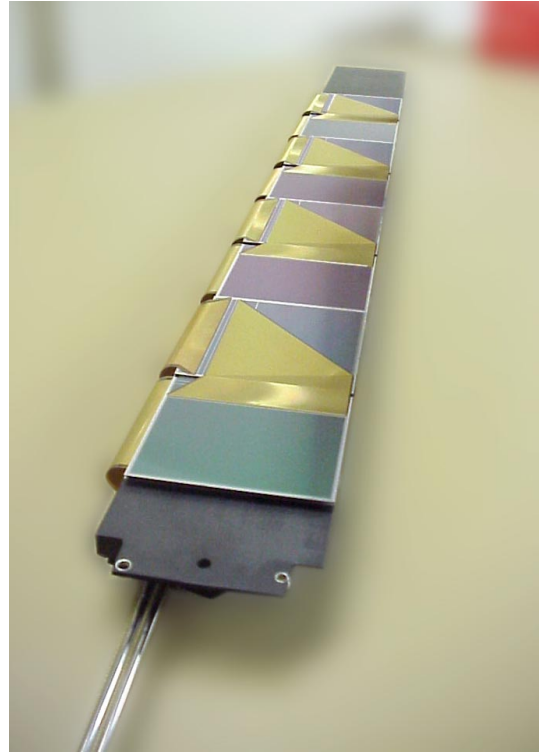


Figure 3.6: Micro vertex ladder with four modules installed.

readout. During this gluing process it was noticed that the wafers were not completely flat. All wafers had a roughly equal dome type shape, with an excursion of  $\pm 50 \mu\text{m}$  from the ideal flat plane. This significantly complicated the gluing of the wafers into half-modules. The problems were generally overcome which allowed tests of gluing of the kapton foils to proceed, followed by tests of the bonding of the strips on the wafers to the strips on the kapton foils. In the mean time the HELIX3.0 readout chips were delivered. After some initial setbacks the full set of wafers was tested at NIKHEF. The yield of chips was a pleasantly high 70 %. The production of full ladders with modules has started and is progressing steadily. (see fig 3.6).

The manufacture of the support tube, into which the full micro vertex detector will be installed, was finished ( fig. 3.7). A laser alignment system which will track deformations during the installation process has been delivered by the ZEUS Oxford group and has been installed.



Figure 3.7: *Micro vertex support tube.*

# 4 CHORUS

## 4.1 Introduction

Neutrino oscillations form a hot topic in particle physics. When firmly established experimentally, one can infer that lepton flavours mix and that not all neutrino masses are zero. This has important implications for the standard model of particle physics, astrophysics and cosmology. Strong evidence for the disappearance of atmospheric muon-neutrinos due to neutrino oscillations has been reported in 1998 by the Japan-US Super-Kamiokande (SK) Collaboration. To reconcile all current results of neutrino oscillation experiments in one theoretical frame, however, is still difficult. The results ask for independent confirmation in new experiments. The first of these, K2K, is in operation; neutrinos from a beam at KEK with an energy of a few GeV have already been observed in the SK detector, after having travelled over 250 km! Two other projects with about 700 km baselines and higher neutrino energies (MINOS at the US and CERN-Gran Sasso in Europe) are in preparation.

Since 1993 NIKHEF participates in the CHORUS (WA95) experiment at CERN, which is searching for neutrino oscillations in the  $\nu_\mu \rightarrow \nu_\tau$  appearance channel. A  $\nu_\tau$  can emerge by flavour oscillation of the  $\nu_\mu$  beam, a  $\tau$ -lepton being subsequently produced in a  $\nu_\tau$  charged-current (CC) interaction. The  $\tau$  can be recognized inside the target by its decay (kink) topology provided that its track is recorded accurately. In CHORUS this is possible through the use of a nuclear emulsion target (800 kg) together with an electronic detector. For leptonic  $\tau$ -decays a background free detection can be realised. In the emulsion, charged particles produce grains with a density of 300 per mm, which can be measured with a spatial resolution of less than a  $\mu\text{m}$ .

Charged particles created by a neutrino interaction in the emulsion target are also detected (with their momenta and charges measured) in the CHORUS electronic detector, consisting of emulsion tracker sheets, opto-electronic fibre trackers, a hexagonal magnet, a honeycomb tracker, a lead-scintillator calorimeter, and a toroidal magnetised-iron muon spectrometer.

In the off-line analysis, trajectories of charged particles through the electronic detector are reconstructed. When extrapolated in the backward direction these show the way where to look for tracks in the emulsion target. Automatic scanning microscopes use the predictions to locate the neutrino interaction vertex in-

side the emulsion. All tracks near the vertex are then extracted using 3D track searching methods. During this procedure kinks are automatically detected. In total, a sample of about 850,000  $\nu_\mu$  interactions in the emulsion plates has been found so far.

Part of the recent work is focused on the development and improvement of the automatic scanning technique. Although the major part of the scanning is performed by the Nagoya team in Japan, other institutes have joined the scanning effort. An automatic scanning facility (three microscope systems) has been set-up by CERN and NIKHEF. It is now used for background studies and pilot productions. One study deals with data from a pion test beam emulsion experiment. It is meant to analyse "white-kinks" (due to elastic pion scattering), which could occur with a very small probability and possibly produce a few events with a  $\tau$  signature, and thus provide an almost negligible background in hadronic  $\tau$  decays.

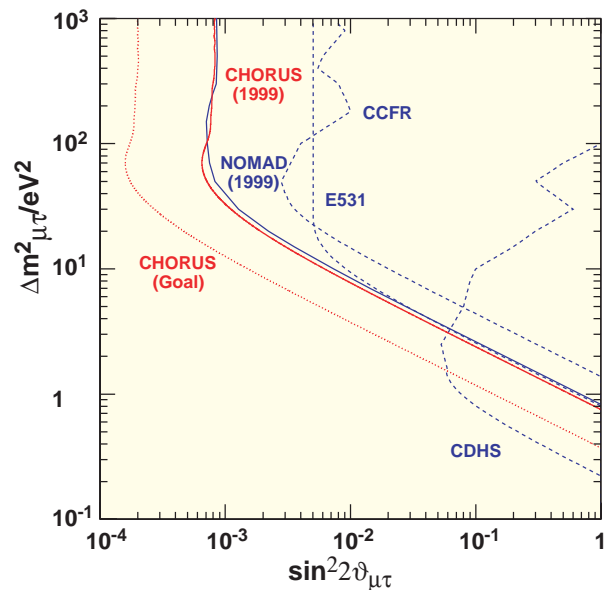


Figure 4.1: Exclusion plot (90% CL) for  $\nu_\mu \rightarrow \nu_\tau$  oscillation, state of analysis July 1999.

The first phase of the scanning and analysis has been completed during 1999. The corresponding publication is in preparation. The second phase is in start-up. To fully exploit the CHORUS potential, a major restructuring and upgrade of the analysis software, as well as

a significant improvement in the efficiency of the scanning methods has been accomplished.

With the full CHORUS data, a flavour mixing probability down to  $P(\nu_\mu \rightarrow \nu_\tau) < 10^{-4}$  at 90 % C.L in the region with  $\Delta m_{\mu\tau}^2 > 1 \text{ eV}^2$ , will be explored (see Fig. 4.1). Besides the  $\tau$  search an increasingly important part of the CHORUS programme is devoted to the study of charm production, diffractive processes, nuclear effects, and rare events.

## 4.2 Specific NIKHEF activities

The NIKHEF team is involved in the emulsion analysis for the neutrino oscillation search as well as in studies of CC  $\nu_\mu$  interactions, in the emulsion target and in the calorimeter.

An analysis of opposite sign deep-inelastic di-muon events in the calorimeter has been completed this year, and resulted in a PhD-Thesis [1]. The purpose of this work was to obtain information on the strength and shape of the strangeness distribution in the nucleon (Fig. 4.2). This analysis gives results which are in agreement with earlier data from the CDHS, CHARM-II, and CCFR collaborations. It covers data from 1995 only, less than 20% of the full data set obtained over 5 years running time.

A special opportunity arose in 1998, when  $\nu$  and  $\bar{\nu}$  beams were delivered to the NOMAD experiment. The CHORUS detector located behind the NOMAD experiment also took data and a high statistics data sample ( $5.4 \cdot 10^6 \nu$  events and  $1.2 \cdot 10^6 \bar{\nu}$  events) with the calorimeter as target was obtained. The analysis of these data [2] will lead to a measurement of the differential cross sections and the  $F_2$  and  $xF_3$  structure functions with a precision competitive with CCFR results. In addition, a four-target set-up was put in front of the calorimeter, with materials of different composition (light to heavy nuclei). The data allow in one experiment –for the first time– a measurement of the neutron-proton neutrino cross section ratio. An analysis of these data is in the start-up phase.

Concerning the emulsion work, the NIKHEF team contributes to the  $\nu_\tau$  oscillation search [3] and to charmed particle production studies [4]. Tools were produced for the running of the scanning facility under automatic as well as manual control. Algorithms for general multi-track finding and for vertex-finding with high efficiency were developed (Fig. 4.3). These are now used in all three microscopes of the CERN-NIKHEF scanning facility.

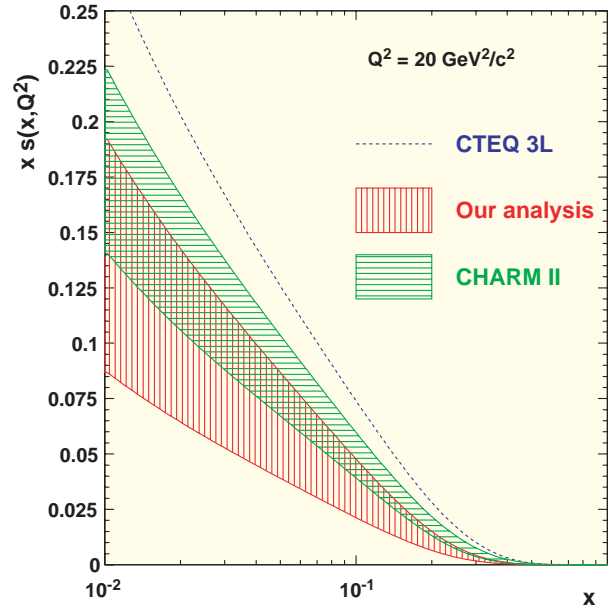


Figure 4.2: Strangeness  $x s(x, Q^2)$  distribution at  $Q^2 = 20 \text{ GeV}^2/c^2$  from CHORUS 1995 calorimeter data compared with the CHARM II result and the CTEQ 3L curve [1].

## References

- [1] C.A.F.J. van der Poel, "Neutrino induced charm production in the CHORUS calorimeter", PhD-Thesis University of Nijmegen, 15 September 1999
- [2] R. Oldeman et al., Nucl. Phys. **B79** (1999) 96
- [3] A. Eskut et al., Phys. Lett. **B424** (1998) 202 and **B434** (1998) 205; P. Annis et al., Phys. Lett. **B434** (1998) 458
- [4] O. Melzer et al. Nucl.Phys.Proc.Suppl. **75B** (1999) 112

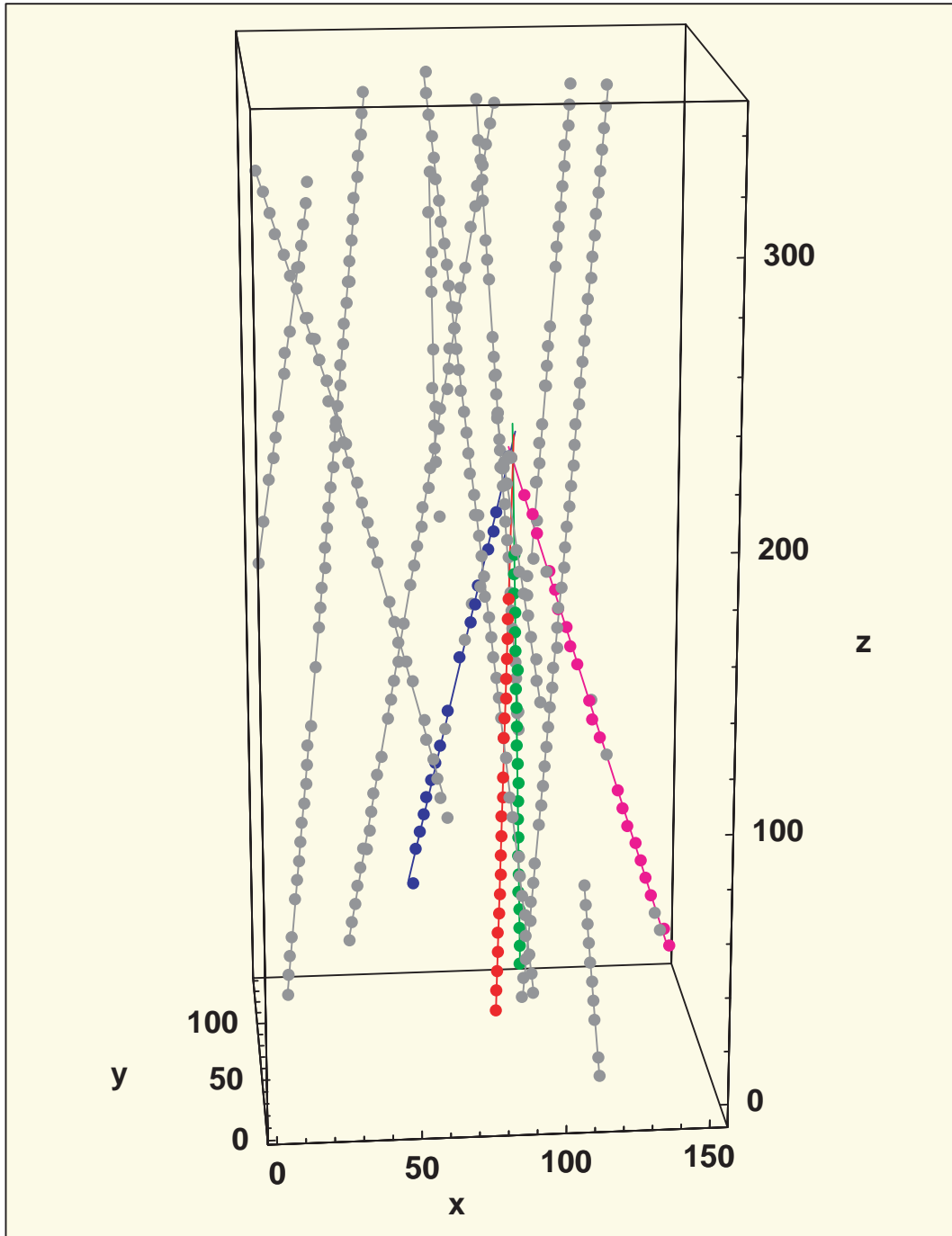


Figure 4.3: Reconstructed neutrino vertex with four emerging tracks of elementary charged particles (in colour); background tracks are shown in gray. The scale is in microns.

## 5 DELPHI

### 5.1 Data taking and detector status

The year 1999 was another very successful one for LEP and the DELPHI experiment. With a total of 288 superconducting RF cavities (+ 48 copper cavities), a maximum of 3500 MV of acceleration voltage was reached. With peak luminosities up to  $10^{32} \text{ cm}^{-2}\text{s}^{-1}$ , LEP delivered in the course of the year  $31 \text{ pb}^{-1}$  at 192 GeV total energy,  $87 \text{ pb}^{-1}$  at 196 GeV,  $89 \text{ pb}^{-1}$  at 200 GeV and  $42 \text{ pb}^{-1}$  at 202 GeV. An additional  $4 \text{ pb}^{-1}$  was delivered at the  $Z^0$  energy for detector calibration and alignment. At the end of the year a first short test run at a total energy of even 204 GeV was made. Small improvements in the RF and the cryogenics system made during the 1999/2000 winter shutdown, will possibly bring the maximum total energy of LEP in its last year of operation to 206 GeV.

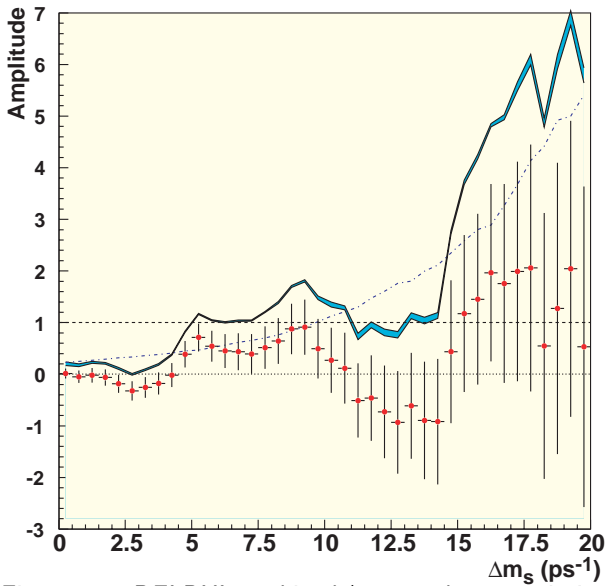


Figure 5.1: DELPHI combined  $\Delta m_s$  analyses: variation of the oscillation amplitude  $A$  as a function of  $\Delta m_s$ . The lower continuous line corresponds to  $A + 1.645 \sigma_A$  where  $\sigma_A$  includes statistical uncertainties only, while the shaded area shows the contribution from systematics. The dashed-dotted line corresponds to the sensitivity curve.

Due to the good background conditions, a significant gain in the efficiency of the DELPHI data taking was obtained. DELPHI collected a total of  $232 \text{ pb}^{-1}$  with an average efficiency of 91.7%.

No major intervention was done on the DELPHI detector during the 1998/99 winter shutdown. Also the

reconstruction software was the same as in the previous year. The final reprocessing of the 1999 data was therefore already completed in December.

### 5.2 Selected research topics

In total, 29 papers were published in physics journals by the DELPHI Collaboration in 1999, 19 of which were based on data collected at LEP II energies. Some 80 contributions were submitted to the International Europhysics Conference (HEP99) in Tampere, half of which were still on LEP I subjects. A few recent subjects, with contributions from our NIKHEF group, are discussed here.

The analysis of the  $B_s^0$  lifetime and of  $B_s^0 - \overline{B}_s^0$  oscillations from the large sample of about 3.5 million hadronic  $Z^0$  decays collected by DELPHI between 1992 and 1995 profited a lot from the full reprocessing of the event reconstruction that was done in 1996-1997. Better resolutions and much improved efficiencies for the selection of  $B_s^0$  events were obtained. The results of these analyses have been presented at the HEP99 Conference and most of the journal papers are near to completion.

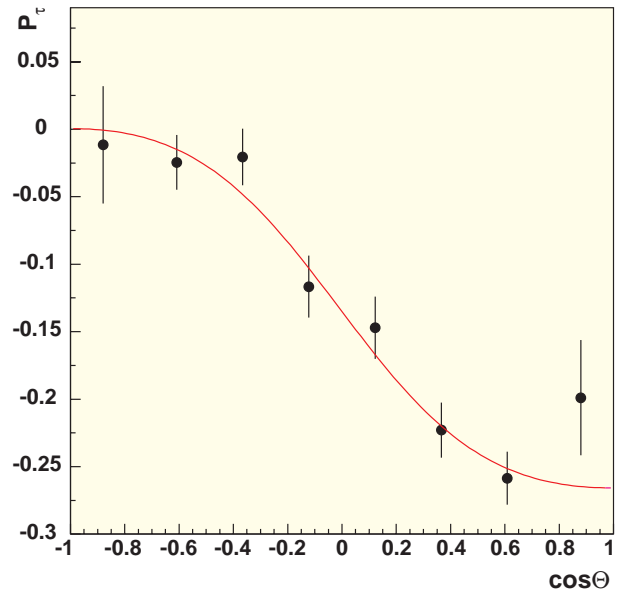


Figure 5.2:  $\tau$  polarisation as a function of the  $\tau$  production polar angle.

Oscillations of  $B_s^0$  mesons have been studied in three different analyses. One analysis uses events containing simply an identified lepton with large transverse momentum with respect to its jet axis. The proper

decay time is measured using an inclusive vertex algorithm to reconstruct the decay distance and the energy of the B meson. In the second analysis, a lepton at large transverse momentum is accompanied in the same hemisphere by an exclusively reconstructed  $D_s$  meson of opposite charge. In the third analysis, events with exclusively reconstructed  $B_s^0$  decays have been used:  $B_s^0 \rightarrow D_s^- \pi^+$  and  $B_s^0 \rightarrow D_s^- a_1^+$  with the  $D_s$  reconstructed in six different decay channels, and  $B_s^0 \rightarrow \bar{D}^0 K^- \pi^+$ ,  $B_s^0 \rightarrow \bar{D}^0 K^- a_1^+$  with the  $\bar{D}^0$  reconstructed in two decay modes. In addition, events with an exclusively reconstructed  $D_s^\pm$  meson accompanied by a large momentum hadron of opposite charge have been used.

The B hadron at the time it decays has been tagged as  $B_s^0$  or as  $\bar{B}_s^0$  via either the charge of the identified lepton or  $D_s$ , or the charge of the kaon in the other exclusive  $B_s^0$  decays. The tag at the time of production is obtained from a total of 9 discriminant variables. The  $D_s^\pm \ell^\mp$  and  $D_s^\pm h^\mp$  samples have been used to measure the  $B_s^0$  lifetime and the lifetime difference between the two physical  $B_s$  states. The combined results are  $\tau(B_s^0) = (1.46 \pm 0.11)$  ps for the lifetime and  $\Delta\Gamma_{B_s}/\Gamma_{B_s} < 0.42$  at 95% confidence level (C.L.).

No  $B_s^0$  oscillations have been observed. In a so-called "amplitude analysis" the amplitude of the oscillation is measured as a function of the assumed mass difference  $\Delta m_s$ . Combining all the three analyses the allowed interval for  $\Delta m_s$  is found to be  $\Delta m_s > 5.0$  ps $^{-1}$  at 95% C.L., where the sensitivity of the analysis is equal to 9.7 ps $^{-1}$ . These results are displayed in Figure 5.1. The combination of the results from the LEP experiments, SLD (at SLAC) and CDF (at the Tevatron, Fermilab) at present excludes mixing for  $\Delta m_s$  below 14.3 ps $^{-1}$  at 95% C.L., close to the expected experimental sensitivity of 14.5 ps $^{-1}$ .

The NIKHEF group contributed to measurements of the  $e^+e^- \rightarrow \tau^+\tau^-(\gamma)$  cross section and asymmetry at LEP II, up to centre-of-mass energies of 202 GeV. Preliminary results from data up to 196 GeV have been presented already at the HEP99 Conference in Tampere. The results from data up to 189 GeV from 1998 data are currently in the process of publication. There is still ongoing work on kaon production in  $\tau$  decays, using the high statistics Z data. The  $\tau$  polarisation measurement in  $Z \rightarrow \tau^+\tau^-$  events at LEP I has just been published and leads to one of the most precise single measurements of the weak mixing angle, with the result  $\sin^2 \theta_{eff}^{lept} = 0.23282 \pm 0.00092$ , obtained from a

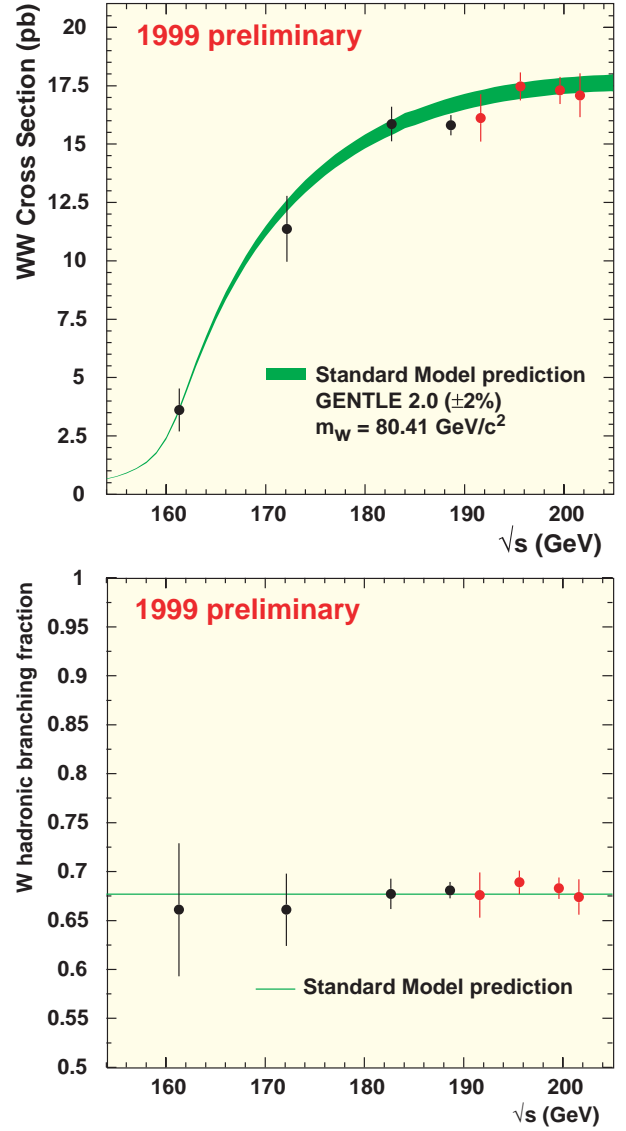


Figure 5.3:  $W^+W^-$  cross section and  $W$  hadronic branching ratio as a function of the centre-of-mass energy. The curve is the Standard Model prediction for  $m_W = 80.41$  GeV/c $^2$ . For the cross section prediction an error of 2% is assumed.

fit to the polar angle dependence of the  $\tau$  polarisation as shown in Figure 5.2.

The analysis of the W pair production cross section for the data taken in 1998 at a total energy of 189 GeV was completed at the end of the year. Based on a sample of 2392 events (1298, 911 and 183 events in the fully-hadronic, semi-leptonic and fully-leptonic final states respectively), the total cross section was measured to be  $15.83 \pm 0.38(stat) \pm 0.20(syst)$  pb. The

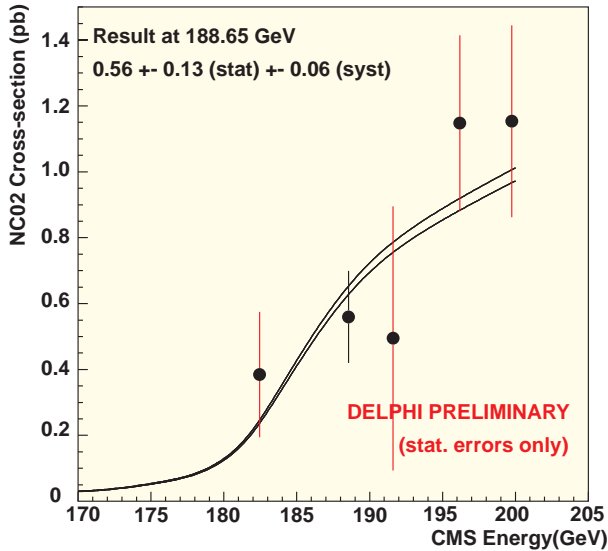


Figure 5.4:  $ZZ$  cross section as a function of the centre-of-mass energy. The curves correspond to the  $\pm 1\sigma$  band of the Standard Model prediction.

measurement of the hadronic  $W$  branching ratio yielded  $Br(W \rightarrow q\bar{q}) = 0.6803 \pm 0.0084(stat) \pm 0.0040(syst)$ . From this branching ratio one can derive the value of the CKM matrix element  $|V_{cs}| = 1.001 \pm 0.040(stat) \pm 0.020(syst)$ .

The efficient operation of both DELPHI and the LEP machine in 1999 allowed to more than double the number of collected  $WW$  events. Some 3700 events were retained for the analysis of the  $WW$  production cross section at the four different energies between 192 and 202 GeV. Very preliminary results for the hadronic branching ratio and the  $WW$  total cross section have already been presented at the November LEPC meeting at CERN, just shortly after the end of the 1999 data taking run. These preliminary results are plotted in Figure 5.3. There is good agreement with the expectation from the Standard Model.

The analysis of  $ZZ$  production continued at the new high-energy points. Our group is mainly involved in the analysis of the four jet final state. A probabilistic method is used, based on the  $b$ -tag probability of the jets, jet topological information and on the mass information using the ideogram technique (see  $W$  mass analysis in the Annual Report 1998). For the measurement of the total  $ZZ$  production cross section, also the other final states  $q\bar{q}\nu\bar{\nu}$ ,  $q\bar{q}\ell^+\ell^-$ ,  $\ell^+\ell^-\nu\bar{\nu}$  and  $\ell^+\ell^-\ell^+\ell^-$  are used. Preliminary values of the measured cross section as a function of  $\sqrt{s}$  are plotted in Figure 5.4. The

data are in good agreement with the Standard Model prediction.

Another interesting channel which is under study, is the production of a single  $W$  boson in the reaction  $e^+e^- \rightarrow We\nu$ , where the  $W$  decays either into  $q\bar{q}$  or into  $\ell\nu$ . The main diagram of interest is the one where a virtual photon is radiated off the incoming electron (or positron) and scatters with a virtual  $W$  that is radiated off the other incoming particle (the positron (or electron)), producing a  $W$  boson in the final state. The final state electron (or positron) is produced at small angle and usually remains undetected. This reaction is particularly sensitive to the anomalous trilinear gauge boson coupling constant  $\gamma WW$ . Preliminary results on the single- $W$  production cross sections and anomalous couplings at 189 GeV are shown in Figure 5.6 and presented at the HEP99 Conference. The analysis of the 1999 data is in progress.

The data collected at 189 GeV also resulted in a much improved determination of the  $W$  mass from direct reconstruction of the invariant mass of the  $W$  decay products. The analysis methods are the same as used in previous year, except that for the semi-leptonic final states, now also the  $q\bar{q}\tau\nu$  channel was included. Preliminary results were presented at the HEP99 Conference. The distributions of the reconstructed masses for the different channels are shown in Figure 5.5. The results obtained for the  $W$  mass in the  $q\bar{q}e\nu$ ,  $q\bar{q}\mu\nu$  and  $q\bar{q}\tau\nu$  channels are in agreement and the combined value from the semi-leptonic channels is  $m_W = 80.102 \pm 0.153(stat) \pm 0.063(syst) \pm 0.017(LEP) \text{ GeV}/c^2$ . From the fully-hadronic channel the value  $m_W = 80.467 \pm 0.110(stat) \pm 0.035(syst) \pm 0.054(fsi) \pm 0.017(LEP) \text{ GeV}/c^2$  is obtained, where the systematic error denoted by 'fsi' is an estimate of the possible effects from final state interactions (Bose-Einstein correlations and Colour Reconnection) that could lead to an apparent  $W$  mass shift in the fully-hadronic channel. Combining the above results with our previous measurements of the  $W$  mass yields  $m_W = 80.316 \pm 0.076(stat) \pm 0.047(syst) \pm 0.017(LEP) \text{ GeV}/c^2$ . The observed mass difference from the fully-hadronic and semi-leptonic final states is compatible with zero.

A lot of effort is going on to obtain a better understanding of the possible systematic errors from final state interactions, but also from fragmentation and detector effects. For the latter two, a new technique has been developed, the Mixed Lorentz Boosted  $Z$  (MLBZ) method. In this method one makes use of the relatively large statistics of  $Z^0$  events that are taken as calibra-

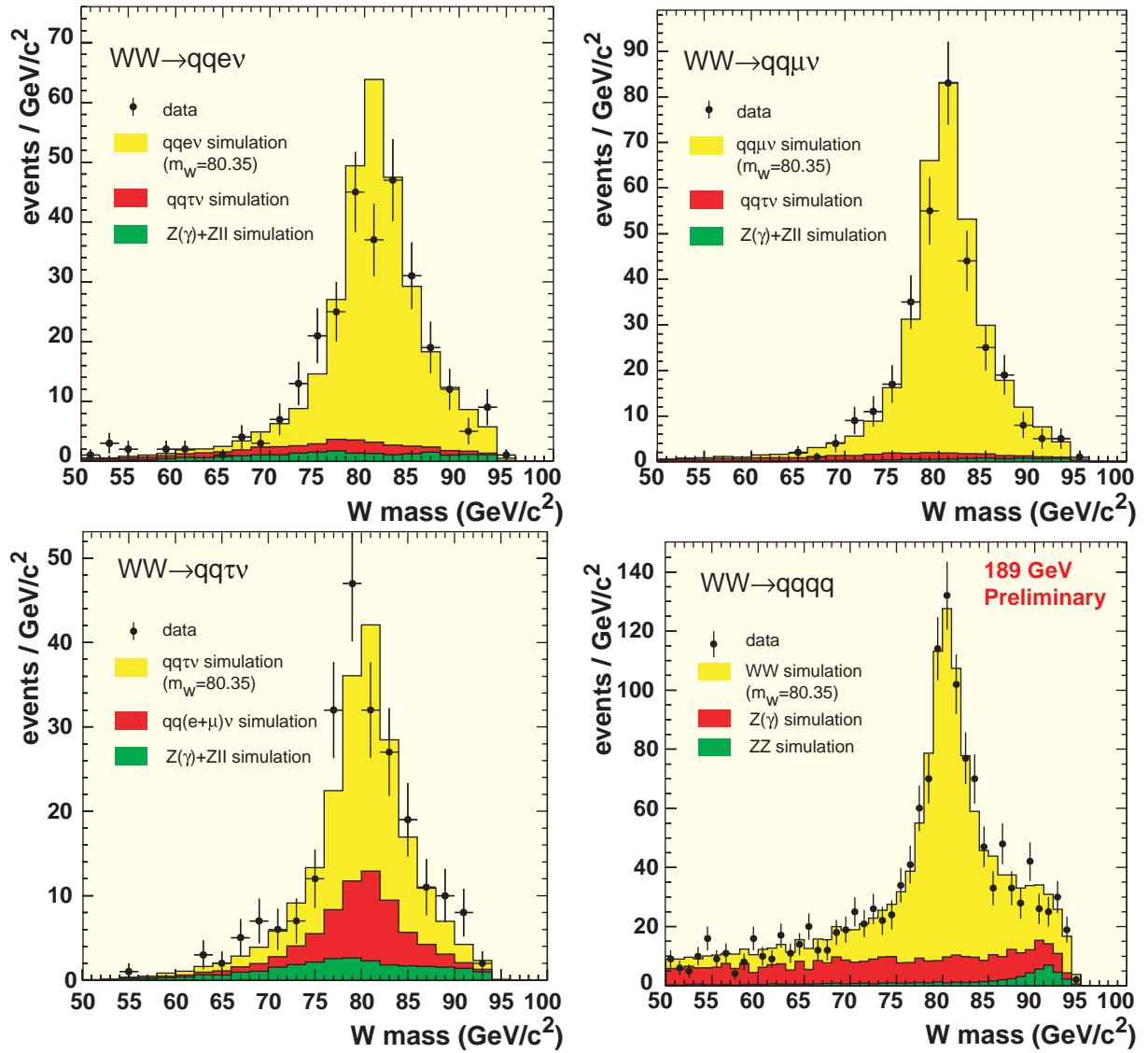


Figure 5.5: The distributions of the reconstructed masses for the electron, muon, tau and fully-hadronic channels.

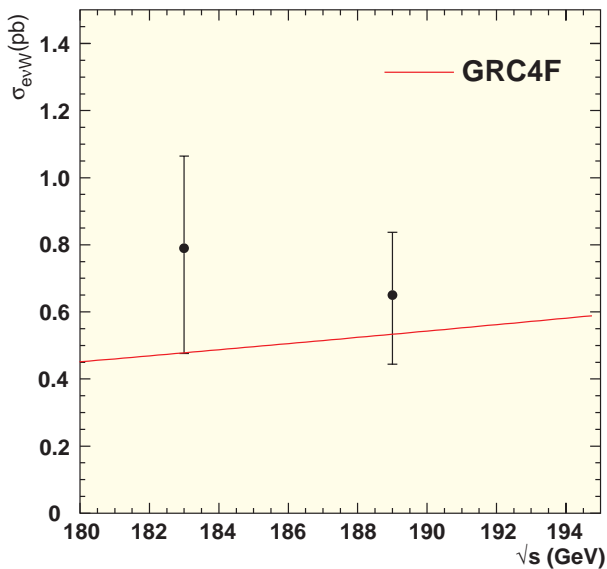


Figure 5.6: Measured cross section for single-W production, compared with the Standard Model prediction of the GRC4F Monte Carlo.

tion data at the beginning of each data taking year and during one or more shorter periods throughout the year. Two different  $Z^0$  events are each Lorentz boosted with a boost factor corresponding to that of the W bosons produced at the high-energy running of that same year. The two boosted  $Z^0$  events are then combined to mimic a W pair. In this way samples of mixed  $Z^0$  events are formed, both for real data and simulated events.

From the difference between results for the real data mixed events and those for MC mixed events, an estimate of the systematic error on the W mass from fragmentation and detector effects can be obtained of less than  $10 \text{ MeV}/c^2$ .

The combination of the W mass measurements of the four LEP experiments, based on the data collected up to and including 1998 was presented at the Tampere Conference as  $m_W = 80.350 \pm 0.056 \text{ GeV}/c^2$ . This value is now slightly more precise than and in good agreement with the value obtained by the CDF and D0 experiments at the Tevatron  $p\bar{p}$  Collider of Fermilab, Chicago. The overall combined value  $m_W = 80.394 \pm 0.042 \text{ GeV}/c^2$  is in good agreement with the Standard Model prediction  $m_W = 80.381 \pm 0.026 \text{ GeV}/c^2$  obtained from a fit to the high precision measurements performed at the  $Z^0$  (LEP and the SLD experiment at SLAC, Stanford) and to the results from  $\nu N$  scattering experiments.

This Standard Model fit also predicts the mass of the top quark, which is in agreement with the direct measurement done at Fermilab. The results of this fit are

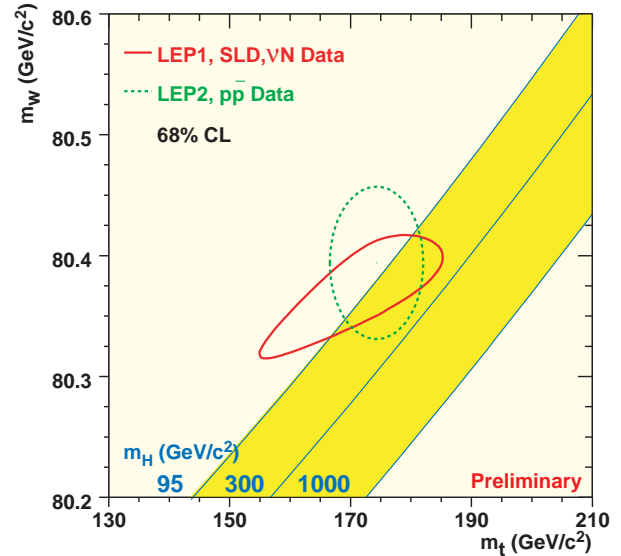


Figure 5.7: Comparison of the indirect measurements of  $m_W$  and  $m_t$  (solid contour) and the direct measurements (dashed contour). Also shown is the Standard Model relation between  $m_W$  and  $m_t$  for different values of the Higgs boson mass.

shown as a 68% confidence level contour in Figure 5.7 together with the contour of the direct measurements of  $m_W$  and  $m_t$ . Also shown are the predictions of the relation between the W mass and the top quark mass for three different values of the Higgs boson mass. It can be clearly seen that the precise measurement of the W mass starts to constrain the Higgs boson mass to relatively low values of around  $100 \text{ GeV}/c^2$ . If the measured values of the W mass and top quark mass are also taken into account in the Standard Model fit, a 'best' value for the Higgs mass is found to be around  $90 \text{ GeV}/c^2$  with a 95% confidence level upper limit of  $220 \text{ GeV}/c^2$ .

So far however, no direct signal for the production of the Higgs boson has been observed. During the September LEPC meeting an update of the combined lower limit for the Standard Model Higgs boson mass of  $102.6 \text{ GeV}/c^2$  was presented, based on the data from all four LEP experiments taken up to 196 GeV. Shortly after the end of the 1999 LEP run, DELPHI (as well as the other LEP experiments) presented a new preliminary lower limit of  $106.2 \text{ GeV}/c^2$ , based on all the 1999 data up to 102 GeV. It is expected that the combined limit from the four experiments will be around  $109 \text{ GeV}/c^2$ .

It is hoped that in 2000, the last year of LEP running, still large amounts of data can be collected at energies of 204 GeV and maybe even at 206 GeV. These new data will give the LEP experiments still a last chance to finally discover the Higgs boson so long searched for.

## 6 L3

### 6.1 Introduction

During the 1999 LEP run, the L3 experiment accumulated  $3.9 \text{ pb}^{-1}$  of luminosity at the Z peak for detector calibration. At high energy the following luminosities were recorded:  $29.4 \text{ pb}^{-1}$  at  $\sqrt{s}=192 \text{ GeV}$ ,  $81.6 \text{ pb}^{-1}$  at  $\sqrt{s}=196 \text{ GeV}$ ,  $79.9 \text{ pb}^{-1}$  at  $\sqrt{s}=200 \text{ GeV}$ , and  $26.9 \text{ pb}^{-1}$  at  $\sqrt{s}=202 \text{ GeV}$ . This was the largest amount of luminosity collected by L3 in any single year. The detector operation was relatively smooth, the averaged data taking efficiency reached 91.5%.

In May and September two central tracker sectors were damaged, forcing us to run with a reduced voltage on each of these sectors.

During 1999, 29 refereed papers were published by the collaboration. Within NIKHEF, the universities of Amsterdam, Nijmegen and Utrecht participate in L3. The latter has concluded its work in the course of 1999.

### 6.2 W and $\tau$ Physics

The analysis activities in 1999 were concentrated on the study of  $e^+e^- \rightarrow W^+W^-$  with three Ph.D. students working on this subject out of a total of six. This effort is one of the main goals of the LEP II program. From the data taken in the 1999 LEP run, approximately 3500  $e^+e^- \rightarrow W^+W^-$  candidate events have been selected, bringing the size of the total sample to some 7000 events. The measured cross sections as a function of  $\sqrt{s}$  are shown in Fig. 6.1, and are in good agreement with the Standard Model predictions.

The events selected in the various W decay topologies are used to determine the W branching fractions. The data are consistent with lepton universality, and the leptonic branching fraction  $\text{Br}(W \rightarrow \ell\nu)$  is measured to be  $10.51 \pm 0.16 \text{ (stat.)} \pm 0.11 \text{ (syst.)} \%$ .

The differential production and decay cross sections of W bosons, as well as their total production cross section, are used in fits to determine the WWZ and WW $\gamma$  couplings. These results are combined with information on W couplings obtained from analyses of single W production and single photon production. The results are in good agreement with the Standard Model predictions.

Information on the polarisation of the produced W bosons is gained by analysing the polar angle of the W decay products in the W rest frame. A fit to the angular distributions shows that  $25.9 \pm 3.5 \%$  of the W

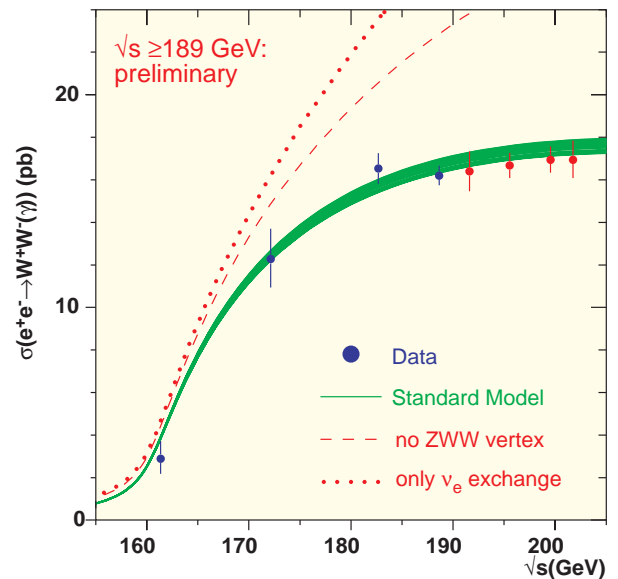


Figure 6.1: The measured WW production cross section at  $\sqrt{s} = 161$  and  $172 \text{ GeV}$  (1996),  $183 \text{ GeV}$  (1997),  $189 \text{ GeV}$  (1998), and  $192\text{--}202 \text{ GeV}$  (1999). Also shown are the Standard Model prediction (using the GENTLE program) and the predictions of two models with different W couplings. Results at  $\sqrt{s} \geq 189 \text{ GeV}$  are preliminary.

bosons are longitudinally polarised, again as expected in the Standard Model (24.8%).

Above the WW production threshold, the W mass is most accurately measured from a fit to the invariant mass spectrum of W decay products. Events are reconstructed into four jets ( $qqqq$  events), or two jets, a lepton (or lepton “jet”) and a missing momentum vector identified with an undetected neutrino ( $qq\ell\nu$  events). A kinematic fit is applied demanding energy and momentum conservation and, optionally, equal jet-jet (c.q.  $\ell-\nu$ ) masses. The W mass is extracted in an unbinned maximum likelihood fit by reweighing a fully reconstructed Monte Carlo sample. Combining the results at threshold and at  $\sqrt{s} = 172 \text{ GeV}$ ,  $183 \text{ GeV}$ ,  $189 \text{ GeV}$  and  $192\text{--}202 \text{ GeV}$ , the preliminary W mass is measured to be  $M_W = 80.353 \pm 0.058 \text{ (stat.)} \pm 0.066 \text{ (syst.)} \text{ GeV}$ .

From the width of the invariant mass spectrum of W decay products, the W width  $\Gamma_W$  is measured to be  $2.19 \pm 0.21 \text{ GeV}$ .

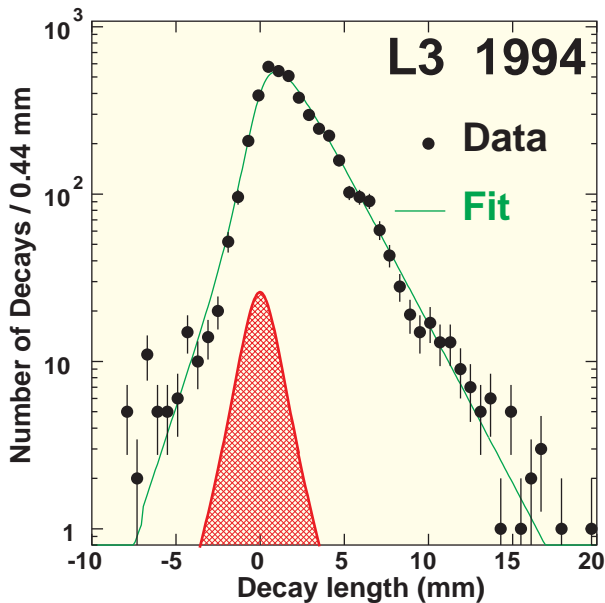


Figure 6.2: Decay length distribution of tau leptons.

The  $\tau$  lepton lifetime measurement using the silicon microvertex detector and the time expansion chamber was finalised and resulted in a thesis and a publication. About 50,000 tau pair events recorded at  $\sqrt{s} \approx 91$  GeV in 1994 and 1995 are used for this analysis. In Fig.6.2 the decay length distribution for three prong taus of the 1994 Z run is shown, with superimposed the result of the lifetime fit. The final result is found to be  $\tau_\tau = 293.2 \pm 2.0(\text{stat}) \pm 1.5(\text{syst})$  fs.

The study of tau-pairs in  $e^+e^-$  annihilation at the highest centre-of-mass energies was continued. This investigation is part of the general study of hadron and lepton-pair production cross sections and leptonic forward-backward asymmetries by L3 and led to the publication of the results up to centre-of-mass energies of 189 GeV. The results are in good agreement with the Standard Model predictions. In Fig.6.3 the highest tau jet energy normalised to the beam energy is shown for the selection of  $e^+e^- \rightarrow \tau^+\tau^-(\gamma)$  events before the final cut on this quantity is made.

Preliminary results on these processes were obtained for the 1999 data.

In collaboration with the University of Leiden a Monte Carlo generator for the production of charmonium and bottomonium resonances in two photon collisions has been written. The data has been searched, using a missing

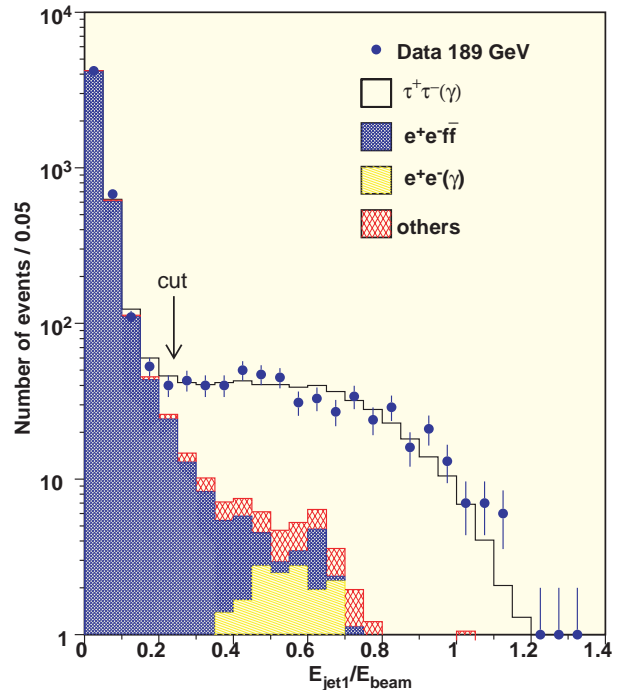


Figure 6.3: The highest tau jet energy normalised to the beam energy for  $e^+e^- \rightarrow \tau^+\tau^-(\gamma)$  events with the cut position as indicated.

mass technique, for the appearance of heavy narrow width particles. At the moment upper limits on the two-photon widths of these resonances have been obtained.

### 6.3 Particle Correlations and Cosmics

A measurement of the elongation of the pion source in Z decays was one of the contributions of the Nijmegen group to the L3 publications. It is part of the Bose-Einstein correlation studies in Z and W-decays using charged and neutral pions. In particular one investigates the possible existence of correlations between particles coming from different W's, which may influence the W mass measurements in the fully-hadronic channel  $e^+e^- \rightarrow W^+W^- \rightarrow q_1\bar{q}_2q_3\bar{q}_4$ . In Fig. 6.4 the Bose-Einstein correlation function  $R_2$  for the semi-hadronic WW events is shown. The corresponding correlation is found to agree well with that for the light-quark Z-decay sample. Clear Bose-Einstein effects are also seen in the fully-hadronic channel, but it can be shown that no evidence is found for inter-W Bose-Einstein correlations.

The analysis of the charged-track multiplicity distribution of Z events in terms of the ratio of cumulant moments to factorial moments was extended to study

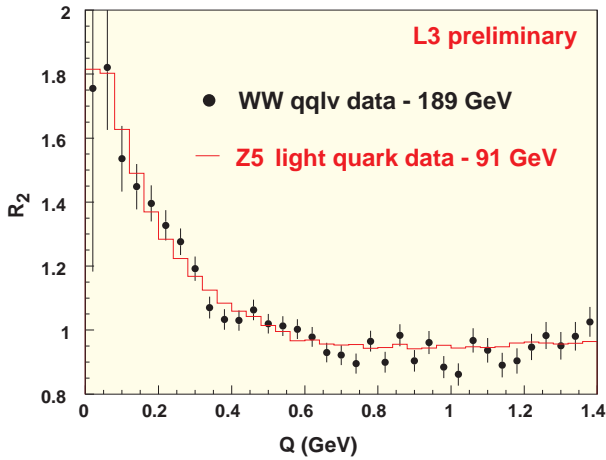


Figure 6.4: The Bose-Einstein correlation function  $R_2$  for the semi-hadronic  $WW$  events. It is compared with the result for the decay of the  $Z$  to light quarks.

heavy and light quark decays of the  $Z$  separately. Preliminary results were presented at several conferences. In addition a Ph.D. thesis has been completed in Nijmegen on the measurement of the spectroscopy of orbitally excited  $B$  mesons at LEP (W.C. van Hoek).

The group has continued the simulation of  $e^+e^-$  interactions in the L3 detector. Thanks to the addition of 19 PCs at the end of 1998, the Monte Carlo farm simulated, in total, more than 75 million events in 1999. The new PCs accounted for most of the production, nearly 60 million events, of which 31 million were cosmic muon events for the L3+C(osmics) experiment and 29 million were  $e^+e^-$  events.

The “running-in” phase of the L3+C was completed at the end of 1998 and data taking started in the spring of 1999. The specially designed trigger and DAQ system worked - after initial difficulties - in 1998 according to the specifications. An event rate of 500 Hz could be handled and consequently a huge amount of data was collected ( $5 \cdot 10^9$  events). The DAQ system is a NIKHEF production. The set-up is shown in Fig.6.6. The effort to search for high multiplicity muon events in coincidence with gamma bursts as observed by satellites or ground based observatories is a recent addition to this programme. In Fig.6.5 a first result of the measured cosmic ray muon spectrum is shown.

## 6.4 Two-photon Physics

In two-photon collisions mesons with quantum numbers  $C = +1$  and  $J = 0$  or  $2$  may be formed and the

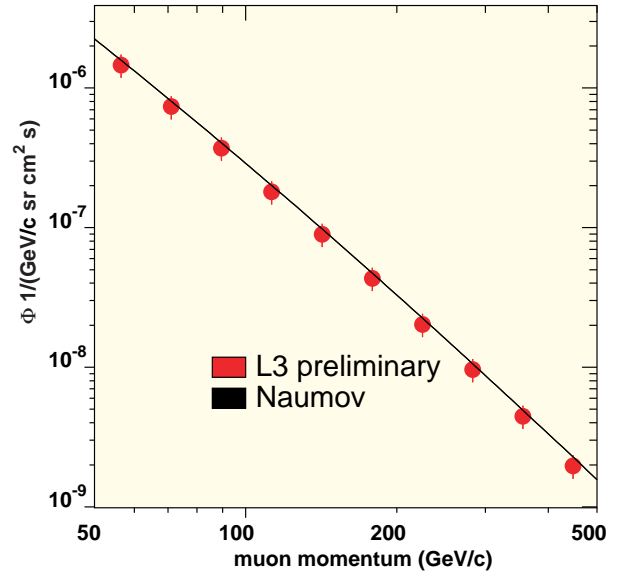


Figure 6.5: The measured momentum spectrum for cosmic ray muons (dots) compared with the prediction (line).

study of their form factors is one of the more interesting aspects of resonance formation in these reactions. The light mesons  $\pi^0$ ,  $\eta$ , and  $\eta'$ , are predicted to have a  $\rho$ -pole form factor, and this has been confirmed by experiment. We have concentrated on the study of the charmonium mesons,  $\eta_c$ ,  $\chi_{c0}$ , and  $\chi_{c2}$  and they are predicted to have a  $J/\psi$ -pole form factor. In order to test this prediction,  $\eta_c$  events have been selected by reconstruction of their decay products in the L3 detector, at  $e^+e^-$  centre-of-mass energies of 91 GeV and 183 GeV. The value of  $Q^2$  is derived from the measurement of one of the scattered beam particles, the tag. With the two tagging devices on each side of L3, the  $Q^2$  range between 0.2 and 8.5  $\text{GeV}^2$  was covered. The invariant mass spectrum (obtained from the decay products of the final state) of the selected events is shown in Fig.6.7.

The line is an unbinned likelihood fit to the data with an exponential background and a Gaussian for the signal, with the mass and the width of the Gaussian fixed at the values predicted by the  $\eta_c$  Monte Carlo. The accuracy of the Monte Carlo has first been tested by comparing it to untagged  $\eta_c$  events, where the scattered beam particles stay undetected. There, the number of events is much higher.

The number of tagged  $\eta_c$  events can be compared to



Figure 6.6: *The L3 detector with the cosmic ray counters on top.*

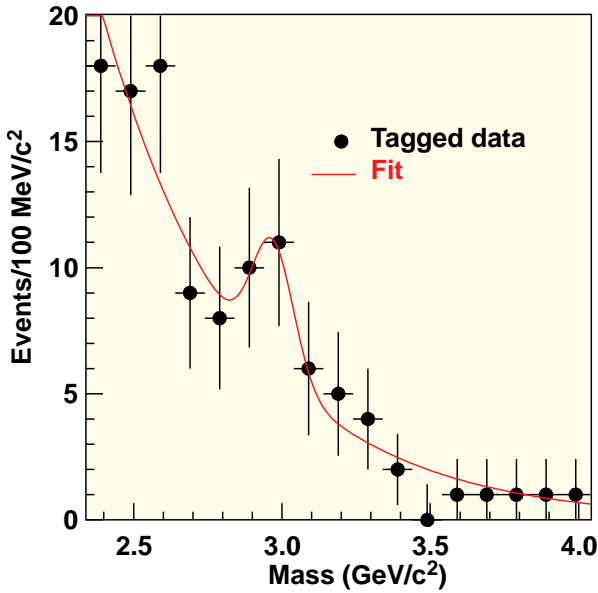


Figure 6.7: Invariant mass distribution of tagged  $\eta_c$  candidates.

the number of expected events if the  $\eta_c$  form factor were a  $\rho$ -pole, or a  $J/\psi$ -pole. Since the  $\rho$ -pole form factor decreases much faster with  $Q^2$  than the  $J/\psi$ -pole form factor, much fewer events would be expected in the first case than in the latter. The observed tagged  $\eta_c$  signal is found to be in much better agreement with a  $J/\psi$ -pole form factor than with a  $\rho$ -pole form factor. This constitutes the first measurement of the form factor of a charmonium state.

## 6.5 Some additional highlights

The main results on the measurements of the W boson properties were summarised above. The energy dependence of the cross section of single W production  $e^+e^- \rightarrow e^+\nu_e W^-$  is shown in Fig.6.8 and is fairly well described by the Standard Model prediction.

The energies reached allow also to study the pair production of the neutral Z boson. The dependence of the ZZ cross section with energy was studied using also the data at centre-of-mass energies up to 202 GeV. Good agreement with the Standard Model prediction is found as shown in Fig.6.9.

The possible existence of anomalous couplings ZZZ or ZZ $\gamma$  is also investigated; no evidence is found and limits for the anomalous couplings parameters are set.

Effects of extra dimensions in new theories of quantum

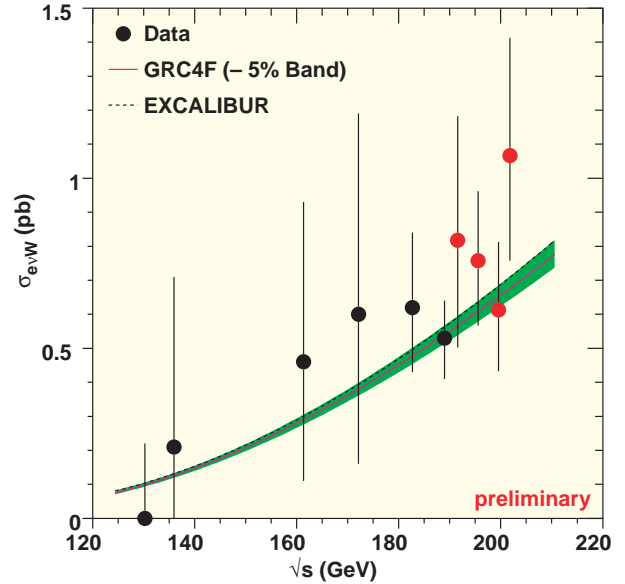


Figure 6.8: The cross section for single W production as a function of  $\sqrt{s}$ .

gravity were searched for in boson and fermion pair production. No deviations are found and lower limits on the gravity scale in excess of 1 TeV are set.

Two photon processes at LEP have the highest cross section and a small background, which allow to study the complex nature of the photon. Total hadronic cross section, double tagged cross section, photon structure function and resonances production measurements were performed. Perturbative and non-perturbative QCD models were tested. For the first time in  $\gamma\gamma$  collisions, we have measured the cross section of  $b\bar{b}$  production. Fig.6.10 shows the cross sections of heavy flavours ( $b\bar{b}, c\bar{c}$ ) production measured as a function of the LEP centre-of-mass energies.

A search for the glueball candidate  $\xi(2230)$  has been performed in the  $K_s^0 K_s^0$  decay channel as shown in Fig.6.11. Non observation of  $\xi(2230)$  in  $\gamma\gamma$  collisions gives an upper limit for  $\Gamma_{\gamma\gamma}(\xi(2230)) \times \text{Br}(\xi(2230) \rightarrow K_s^0 K_s^0) < 1.5$  eV at 95% CL under the hypothesis it is a pure spin 2, helicity two state.

As in earlier years, searches for new phenomena played an important role in the analysis of L3 data. The Higgs particles as predicted by the Standard Model and its supersymmetric extensions were searched for; no significant signal was observed. With the large increase

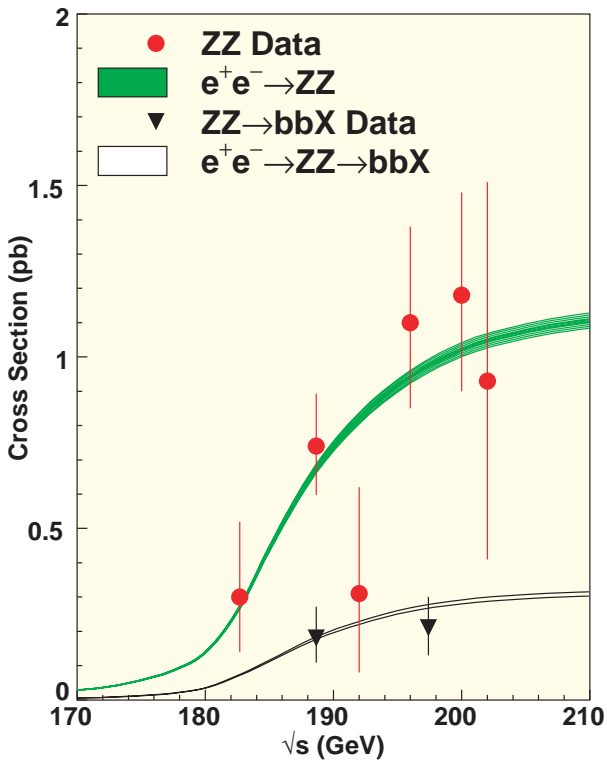


Figure 6.9: The cross section for ZZ production as a function of  $\sqrt{s}$ .

in statistics, coupled with the increase in the centre-of-mass energy, the preliminary mass limit for the Standard Model Higgs boson was improved to 106 GeV.

The spectrum of particles as predicted by Supersymmetry has been searched for in R parity conserving and R parity violating scenarios and for different symmetry breaking mechanisms. No significant excess was observed, and in many cases the resulting mass limits are close to the kinematic limit of 101 GeV. Within the framework of supergravity inspired MSSM, these limits can be expressed as an indirect limit on the lightest neutralino mass.

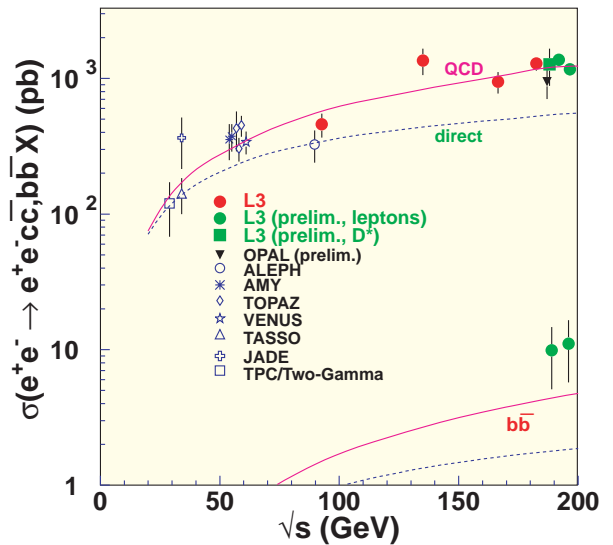


Figure 6.10: Cross-section for heavy quarks production in two-photon processes as a function of  $\sqrt{s}$

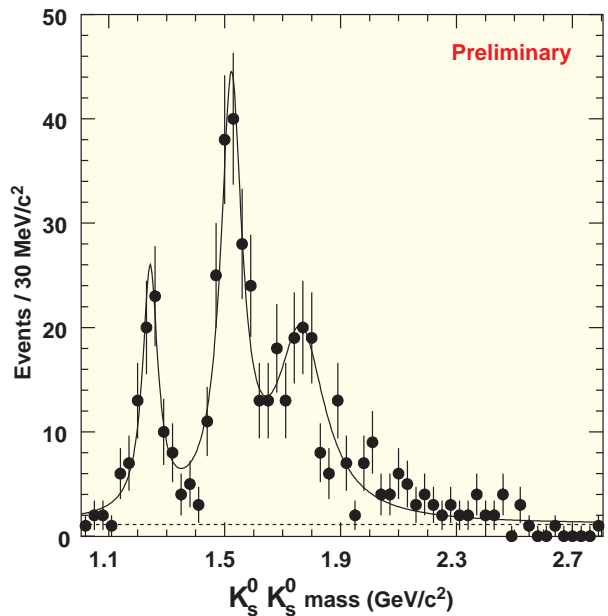


Figure 6.11: The  $K_s^0 K_s^0$  mass spectrum.

## 7 Heavy Ion Physics

### 7.1 Introduction

The use of highly relativistic heavy-ion beams is well suited for studying nuclear matter under extreme conditions. Based on a statistical treatment of quantum chromodynamics (QCD, see page 45) it is expected that a de-confined state of quarks and gluons, the so-called quark gluon plasma (QGP), will be created in violent collisions of heavy nuclei. The formation, detection and systematic study of such a QGP state would yield new information on strong interaction dynamics.

The various stages of the interaction process of two colliding heavy nuclei can be investigated by means of different probes. The hot early stage of the created system is probed by studying the thermal radiation of the system, by means of prompt photons. These prompt photons will provide information about the temperature evolution of the expanding system. Investigation of the production rates of particles containing heavy quarks will probe the composition of the early phase as well as the final particle production process (hadronisation). The dynamical evolution of the expanding system at the last stage is probed by investigation of the momentum spectra of the produced particles which eventually leave the system (freeze-out).

We investigated collisions of lead ions with thin lead targets at the CERN-SPS accelerator complex at centre-of-mass energies of 158 GeV/nucleon (A GeV). Within the WA98 collaboration the prompt photon production and neutral meson spectra were studied, whereas the strange-quark production was investigated within the NA57 experiment. A new effort was started to investigate the production of charm quarks in the context of the NA49 experiment. This is an opportunity to verify the enhancement of charm-quark production observed by the NA50 experiment. Since NIKHEF joined the NA49 effort only in November 1999, no progress can be reported here, yet.

In the future all probes will be simultaneously investigated in Pb+Pb collisions within the ALICE experiment at the CERN-LHC collider facility. The centre-of-mass energy in these collisions will be 5 ATeV. The preparations for this experiment are described in the ALICE section starting on page 45.

### 7.2 WA98

Within the WA98 experiments, the conditions at the freeze-out stage of the interaction process were investigated by means of the transverse mass spectra

of neutral pions ( $m_T^2 = p_T^2/c^2 + m_\pi^2$ ). The experiment contains a large, highly segmented array of lead-glass calorimeter modules for photon detection through Cherenkov radiation. The calorimeter is located close to mid-rapidity. To determine the impact parameter (centrality) of the collisions, calorimeters at mid-rapidity (MIRAC) and at beam rapidity (ZDC) measure the transverse and longitudinal energy flow respectively. Interpretation of these energy flows in view of a geometrical model of the collision directly yields the centrality of the event. Fig. 7.1 shows the lay-out of the experiment.

The WA98 experiment has ceased to take data. The data collected during the running periods 1996 to 1997 are currently being analysed and first results have been published. Two analyses are mentioned here: the study of freeze-out parameters in central collisions using the  $\pi^0$ -spectra (see also the PhD-thesis of F. Geurts [1]) and the study of direct photons.

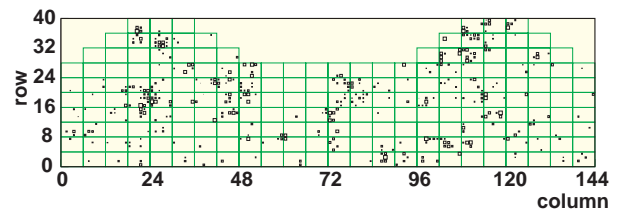


Figure 7.2: Display of a typical event in the lower lead glass detector.

Figure 7.2 shows a typical display of signals in the lower segment of the lead glass calorimeter. Each square corresponds to a signal, its surface is proportional to the amplitude.

The  $\pi^0$  signal can be extracted reliably for transverse masses above about  $0.4 \text{ GeV}/c^2$ . The resulting  $\pi^0$  yield is corrected for geometrical acceptance and reconstruction efficiency of the photon detector. The  $m_T$  range between  $0.5$  and  $3 \text{ GeV}/c^2$  was divided in bins. In each bin, a fit to the data has been performed using a (thermal) Boltzmann distribution for a static source. In this way, local inverse slopes of the  $m_T$  distribution were obtained. If we allow for part of the collision energy to be converted into collective motion (flow) of the produced particles, we expect the  $m_T$  spectra to level out.

The experimental results, shown in fig. 7.3, confirm this behaviour. We see that they are in agreement with a

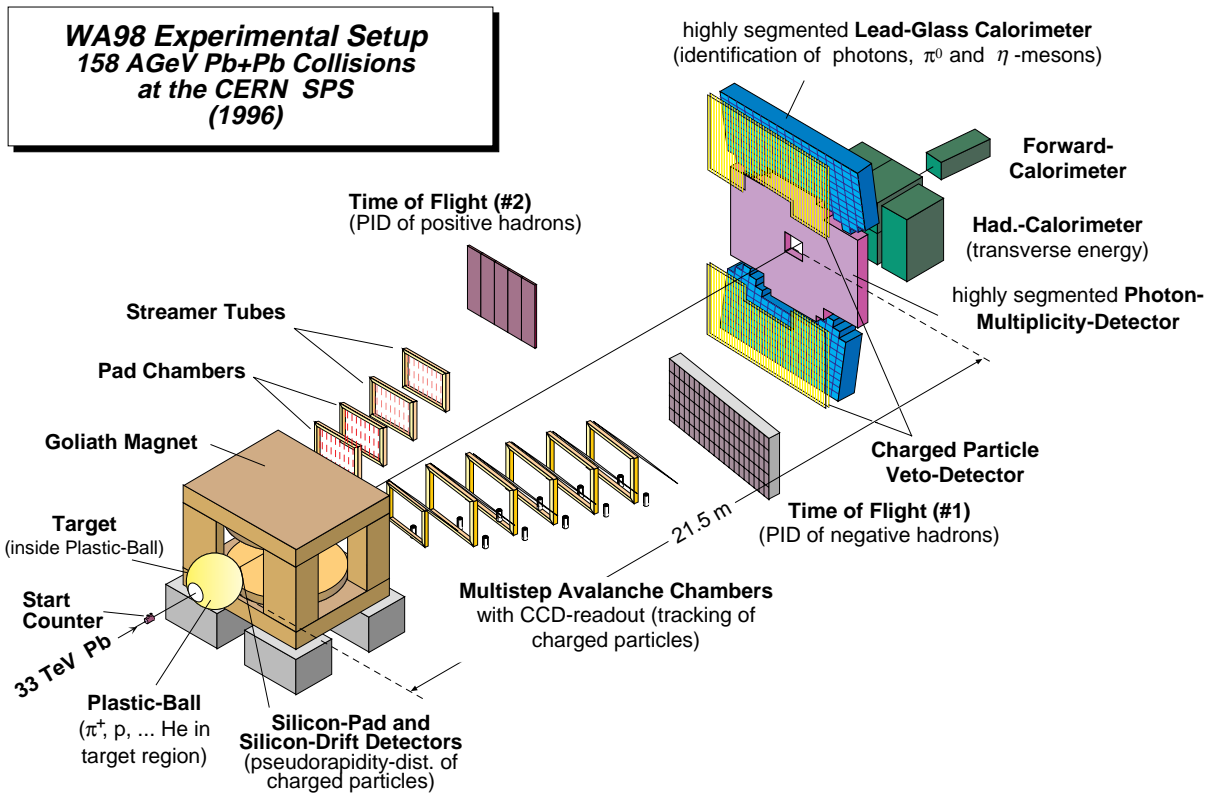


Figure 7.1: Schematic lay-out of the WA98 experiment.

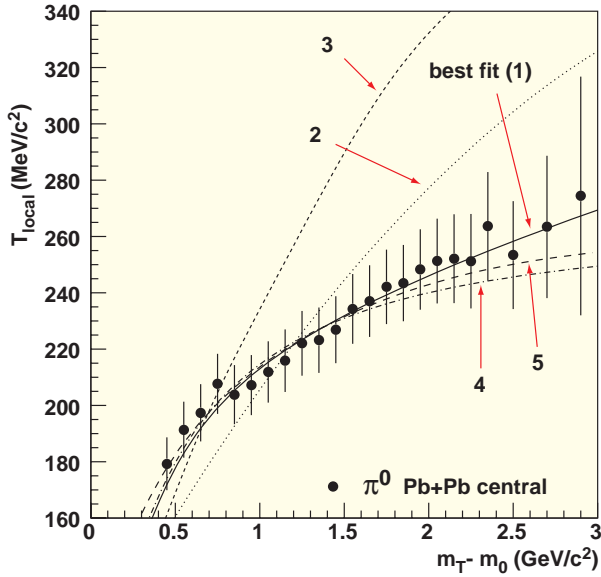


Figure 7.3: The local inverse slope of the transverse mass spectrum of neutral pions in central collisions of 158 AGeV Pb+Pb. The measured results (solid points) are compared to the best fit of the hydrodynamical model (solid line, see text). Other models are indicated, too.

hydrodynamical model which assumes a thermal source with Gaussian density distribution (curve 1) and with a transverse expansion that introduces the effects of radial flow in the resulting particle spectra [2]. The above implies that the derived freeze-out temperature  $T$  is (strongly) correlated with the flow velocity divided by the speed of light  $\langle\beta_T\rangle$ . The best fit is obtained with  $T = 185$  MeV and  $\langle\beta_T\rangle = 0.21$ . The fits represented by lines 2 and 3 correspond to much larger values of  $\langle\beta_T\rangle$ : 0.47 and 0.53, respectively. Curves 4 and 5 have a uniform density profile and a Woods-Saxon profile, respectively. Also they give good fits, with  $T$  and  $\langle\beta_T\rangle$  similar to those of curve 1.

The *direct photon*, i.e. a photon which does not originate from a meson decay is a useful probe of the state produced in heavy-ion collisions. In a QGP direct photons come, to first order, from gluon Compton scattering, bremsstrahlung, and  $q\bar{q}$ -annihilation. A major advantage of direct photons as a probe is that, once created, they have no more interaction with the surrounding quarks, gluons or hadrons and can be observed directly.

Consider a QGP with temperature  $T$ , in thermal equi-

librium and zero baryo-chemical potential. Then  $N$ , the number of photons with energy  $E_\gamma$  in phase space volume element  $d^3k$  is given by [3]:

$$E_\gamma \frac{dN}{d^3k d^4x} = \frac{5}{18\pi^2} \alpha \alpha_s T^2 e^{-E_\gamma/T} \ln \frac{0.23 E_\gamma}{\alpha_s \text{ GeV}}.$$

This expression was derived from the perturbative evaluation of the Feynmann diagrams for the production processes mentioned above, using a Boltzmann distribution at temperature  $T$  for the momenta of the quarks and gluons. It means that the direct photon spectrum gives information about the size of the state (through the number of photons) and about its temperature (through its energy dependence which is peaked somewhat above  $T$ ).

Direct photons are produced in a hadron gas as well. Important processes here are  $\pi^\pm \rho^0 \rightarrow \pi^\pm \gamma$  and  $\pi^+ \pi^- \rightarrow \rho^0 \gamma$ . A similar energy spectrum as for the QGP is obtained for a hadron gas. Note that one cannot distinguish the QGP from a hadron gas by the direct photon probe alone.

A third source of direct photons is the so-called hard scattering of the initial partons in the projectile from those in the target nucleus. Its energy spectrum can be calculated perturbatively (under certain assumptions regarding the initial parton momentum distributions) in next to leading order QCD [4]. Experimentally, hard scattering is visible at large values of  $E_\gamma$  ( $p_t$ ) in the photon spectrum.

The measurement itself appears to be very simple: one measures all the photons and subtracts (statistically) those originating from decays. However, the effect one wants to measure is small, and systematic effects need to be well understood. The measurement uses the lead glass detector of WA98, which is covered by a charged particle veto (CPV) counter, consisting of larocci tubes, which will signal the passage of a charged particle.

The efficiency for photon reconstruction was established by adding one simulated photon with known momentum to each event from the real data. This is done at the module level in terms of ADC counts. From the raw module data, one reconstructs the photons and calculates the changes in momenta or even the loss of hits to extract a  $p_t$ -dependent efficiency, which also includes effects of dead modules and edge cuts.

The decay of  $\pi^0$  mesons to two photons constitutes most of the background to be subtracted from the photon signal. Other mesons contribute, too:  $\eta$  mesons are the next biggest source and contribute about 10%

to the signal. The abundance of  $\eta$ 's was measured by WA80. The abundances of the other mesons,  $\omega$ ,  $\eta'$ , and  $K_S$ , of which the latter contribute due to the weak decays  $K_S \rightarrow \pi^0\pi^0$ , were obtained from literature and implemented in the Monte Carlo simulation. They contribute less than 1% to the photon signal.

The sum of all contributions, corrected for acceptances and efficiencies, gives the calculated background. The difference between the measured yield and this calculated background due to resonances gives the excess of photons which we identify as the direct photon signal. This preliminary study indicates that there are more photons than expected from hadronic decays in central events. No such excess is observed in peripheral events. The measurement is very sensitive to systematic effects, some of which still need to be checked before the final results can be published.

### 7.3 NA57

Earlier experiments (WA85, WA94 and WA97) have shown that the strange hyperon abundances increase faster than the number of participants in the collision when going from proton-nucleus to nucleus-nucleus interactions. The principle aim of the NA57 experiment is to investigate the existence of an onset for the strangeness enhancement as the energy and the centrality of the reactions are varied. At the core of the NA57 experiment is a silicon telescope consisting of silicon pixel detectors and four planes of silicon microstrip detectors which are located approximately 1.4 m from the target. The modules used in NA57 can be regarded as prototypes for the ALICE experiment, except that different readout chips are used.

In 1999, data were taken with proton beams at 40 GeV and with lead beams at 40 and 158 GeV. The data are currently being processed. Preliminary study of a fraction of the data shows a clear signal of  $\Lambda$ -hyperons in the invariant mass spectrum, calculated from track pairs which do not originate from the primary interaction. The spectrum is shown in fig. 7.4. The results which were obtained with regards to the prototype detectors are described on page 46 of this report.

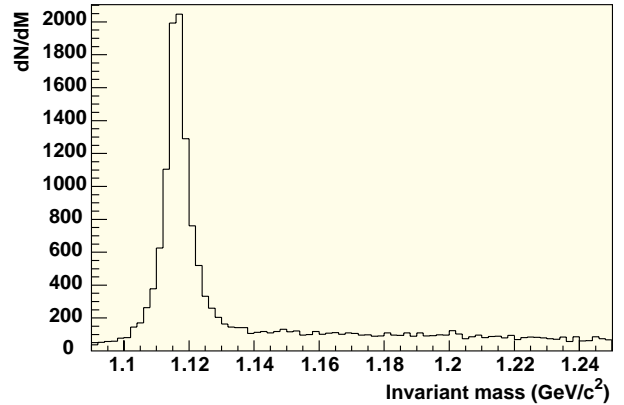


Figure 7.4: Number of two-track combinations versus the invariant mass of the combination. The  $\Lambda$ -peak is clearly visible.

### References

- [1] F.J.M. Geurts, PhD thesis, Utrecht (1998).
- [2] U.A. Wiedemann and U. Heinz, Phys. Rev. **C56** (1997) 3265.
- [3] J. Kapusta et al., Phys. Rev. **D44** (1991) 2774; R. Baier et al., Z. Phys. **C53** (1992) 433.
- [4] C.-Y. Wong and H. Wang, Phys. Rev. **C58** (1998) 376.

## B MEA/AmPS facility

### 1 MEA/AmPS decommissioning

#### 1.1 Introduction

In the course of the last quarter of 1998 final decisions were made concerning redeployment of parts of the MEA/AmPS facility following the final shut down scheduled to take place at the end of 1998. Far most important element in this procedure was removal of the MEA accelerator, the AmPS ring and related beam transfer lines to JINR (Joint Institute for Nuclear Research) at Dubna, Russia. The aim of JINR is conversion of MEA/AmPS into a synchrotron light facility called DELSY (Dubna ELectron SYNchrotron light facility) at their premises. With this in mind JINR and NIKHEF made a transfer agreement. JINR obtained the machine at no cost. JINR accepted all systems at the condition as they were at the moment of final shut-down and became fully responsible for dismantling the machine, providing all necessary manpower and covering all expenses such as transportation of the equipment to Dubna. The actual dismantling should be monitored and advised by specialized NIKHEF personnel.



Figure 1.1: Arrival first shipment at JINR (photo courtesy JINR, Dubna, Russia)

Additional agreements were made with several other institutions for redeployment of remaining parts of the facility. In this way it was possible to find a destination for almost all equipment except for the two big magneticspectrometers of the electron scattering facility Emin. Although some laboratories were interested it appeared to be impossible to redeploy this instrumentation mainly due to the extreme removal, transportation

and reconstruction costs. Computer and Internet related companies showed great interest in renting parts of the released facility buildings. Early 1999, by means of a tender procedure, an English company was selected to rent the first parts of the buildings. This company, Telecity, is a Facility Management company dedicated to providing services to Internet and Telecom business. They are operating several facility management centres all over Europe.

#### 1.2 Preparations

Following recommendations of the Scientific Advisory Committee it was decided at the end of 1998 to keep the facility operational during the first three months of 1999 to finish remaining scientific work. However, due to a serious failure in a 10-KVolt-power distribution system at Christmas 1998, causing considerable damage to various equipment and a power supply building, it was decided to terminate facility operations at January 1st, 1999. Repair was started immediately in the beginning of January, because it was necessary to have the accelerator and ring operational to educate JINR personnel and to demonstrate the relevant MEA/AmPS machine performance after repair. It took roughly six weeks to repair the equipment, the power distribution system including a temporarily repair of the AmPS power supply building. Some more weeks were spent to start up machine systems. Then hands on training of the JINR machine physicists began. NIKHEF specialists trained them in specific operating issues and in tuning the accelerator and the ring in storage mode.

This training period was completed by the end of March. Finally a particle energy of more than 900 MeV and a circulating beam current of 270 mA was obtained. In this condition the machine was formally accepted by JINR. The official hand over took place in March in a ceremonial meeting in which our director Ger van Middelkoop offered Igor Meshkov, member of the JINR board of directors, a symbolic main key of MEA/AmPS. Preparing the facility for dismantling was performed in April. This consisted mainly of a complete electrical shut down of all systems to make it safe for dismantling activities and conservation of all vacuum systems by inflation of extra dry nitrogen. The first quarter of 1999 was also used for preparing licenses for export from The Netherlands and import into The

Russian Federation. In particular the weak radioactive machine components needed attention. Research into several modes of transport was carried out. Trucking turned out to be most attractive with respect to cost, logistical flexibility and applicability related to mechanical shock resistance of the very valuable RF accelerator sections. Administrative procedures like design of a database system for registration of all machine components to be transferred were prepared and a well-documented library of all related machine documents, reports and articles important for future reconstruction and operation of MEA/AmPS at JINR was set up. For documentation purposes a high quality digital photo library of all machine components, as they were in situ at the time of dismantling, was composed.

### 1.3 JINR dismantling

April 28th a dismantling team of 10 JINR employees arrived at NIKHEF to start the activities. First aim was to collect all spare material scattered through the facility buildings and to send it to JINR. By doing so space was cleared to solve logistic problems related to machine dismantling. In the course of this activity it became clear what kind of packaging material was needed. For instance it appeared possible to pack a great deal of the equipment into standard wooden potato crates as used in agriculture, very well designed to fit on a standard truck and to transport delicate but also heavy material.



Figure 1.2: *Dismantling AmPS power supply room (photo Han Singels, Amsterdam)*

June 10th the first truckload was shipped to Dubna, which served as a pilot transportation to test all procedures underway and to test the chosen route (Amsterdam, Kiel, ferryboat, St. Petersburg, Dubna) and truck

behaviour related to mechanical shock on the cargo floor. Shock registration equipment on board of the air suspended combi truck proved that it was possible to transport the RF accelerator sections in containers with suitable shock absorbing mechanisms. These measures in combination with adapted driver behaviour guaranteed mechanical shocks to stay below 5 G. These containers arrived in Amsterdam as return freight some weeks after departure of the first shipping. After improvement of the container shock absorbing system we started in the beginning of July a fourteen days interleaved monitored transportation cycle of all twenty-four-accelerator sections.



Figure 1.3: *Loading the accelerator section in their containers (photo Han Singels, Amsterdam)*

The MEA service building was already delivered on July 1st and handed over to the selected tenant. Dismantling of all auxiliary equipment of the AmPS-ring, packaging, shipment and delivery of the AmPS power supply building was completed at the beginning of October. At the end of the year all MEA modulators and related equipment, the MEA compressed air station, the Haimson electron gun and all accelerator sections except four were shipped to JINR. At December 20th the downstream half of the MEA modulator hall was delivered for lease. At the end of 1999 in the accelerator vault and upstream half of the modulator hall minor parts and remaining infrastructure still had to be dismantled Also, all AmPS ring components were dismantled, packed and awaiting their shipment. Early 2000 the remaining part of the infrastructure and cabling will be completed. All beam lines as they were present in the beam switchyard are roughly dismantled, packed and awaiting their shipment in 2000. Heavy parts like magnets have been kept in place until the moment of transportation. Also here the remaining infrastructure has to be removed

early 2000 as well as the related cooling system, power supply room and vacuum control equipment situated in the Emin front hall. Due to regulations in countries present in the transportation route (Germany, Poland, Bela Russia and Russia) it has not yet been possible to ship stored ring and beam switchyard materials because in a certain amount of this equipment residual low-level radioactivity is present. Until transport licenses in Bela Russia and Russia are granted all equipment concerned will be stored at NIKHEF.

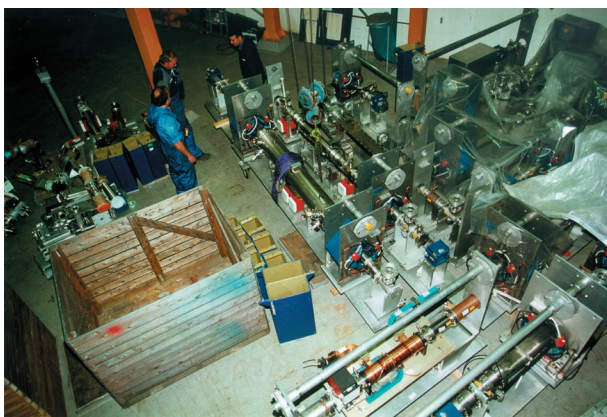


Figure 1.4: *Packaging ring components (photo Han Singels, Amsterdam)*

At the end of 1999 35 truckloads had been shipped to Dubna which corresponds to 70% of all the equipment involved with a total weight of approximately 500 tons. The amount of JINR personnel present in NIKHEF varied through the year from 10 to 16 employees. The JINR team performed very efficiently and collaboration with NIKHEF staff members showed to be very effective. It is expected that all remaining dismantling activities will be completed by the end of the first quarter of 2000.

#### **1.4 Other dismantling activities**

The Paul Scherrer Institute, Villigen, Switzerland, obtained 12 pieces of our 71-mm bore quadrupole magnets, which were in stock as spares. The Nuclear Physics Accelerator Institute, Groningen, The Netherlands, obtained all dipole magnets from the AmPS extraction line and related power supplies, the  $^3\text{He}$  cryogenic target system formerly used in the electron scattering hall (Emin) and various types of radiation measuring instruments. At the end of 1999 delivery to KVI was still in progress. The so called "Siberian Snake" and all its related equipment used as a spin rotator

in the AmPS ring and various components of the Polarised Electron Source (PES) used as polarised injector at MEA have been transferred to MIT Bates Linear Accelerator Centre in the United States of America. In an earlier stage of the project the Polarised Internal Target experimental set-up, formerly situated in the Internal Target Hall, had already been transferred to MIT. All remaining parts of PES were given to Budker Institute of Nuclear Physics, manufacturer of Snake and PES, at Novosibirsk, Russia and will be shipped with the JINR goods. The so-called Big Bite spectrometer used at the Internal Target experimental set-up and a couple of high power magnet power supplies, which were still available, were received by Thomas Jefferson National Accelerator Facility, Virginia USA. Considerable time was spent finding a destination for redeployment of the two big spectrometers of NIKHEF's Electron Scattering Facility. Finally, due to extreme removal and transport costs and high cost for reconstruction this has proven not to be an attainable option. Therefore a contract with a recycling company, HKS (Hoogovens Klöckner Scrap Metals B.V.) was made in which dismantling and recycling in the first two months of 2000 was agreed. The scattering chamber, part of this system, was already transferred to the National Accelerator Centre at Faure in South Africa, in an earlier stage of the project.

## C Experiments in preparation

### 1 ALICE

Ours is a world of broken symmetries, that is to say a world which does not adhere to the symmetries of the Lagrangians describing the underlying interactions. The best-known example is the spontaneous symmetry breaking of the electro-weak interaction, the so-called Higgs mechanism, which gives masses to particles. The strong interaction is described by Quantumchromodynamics (QCD). Its Lagrangian is invariant under chiral transformation. This implies that a left-handed particle cannot convert into a right-handed one, something which does occur in our normal world. This means that in QCD the chiral symmetry is spontaneously broken.

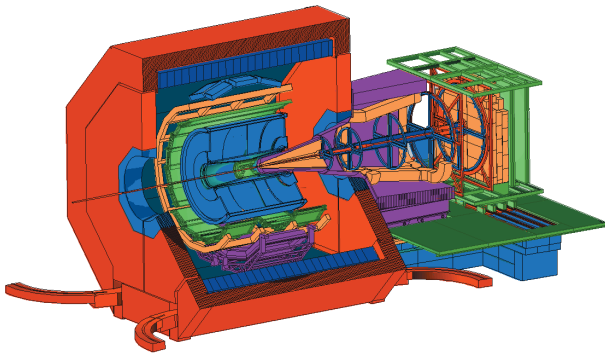


Figure 1.1: An artist's view of the ALICE detector.

Lattice gauge calculations of QCD show that in nuclear matter, when it reaches a temperature of 150 MeV ( $\approx 10^{12}$  K), chiral symmetry will be restored. This temperature seems to coincide with the one needed to make nuclear matter undergo a phase transition to a new state, the *quark gluon plasma* (QGP). In this state, the hadrons are broken up into their constituents, the quarks and gluons. The conceptual connection between the hadron-QGP transition and the chiral symmetry restoration is not clear yet. It is clear that both phenomena must have taken place in the early universe.

Nuclear matter with temperatures above 150 MeV can be formed in the collisions of heavy ions at very high energies. ALICE is a challenging research programme, in which 75 groups from 45 countries participate. Its intention is to study the processes mentioned above at the LHC collider of CERN. Fig. 1.1 shows an exploded view of the experiment. ALICE will make use of the existing magnet of the L3 experiment.

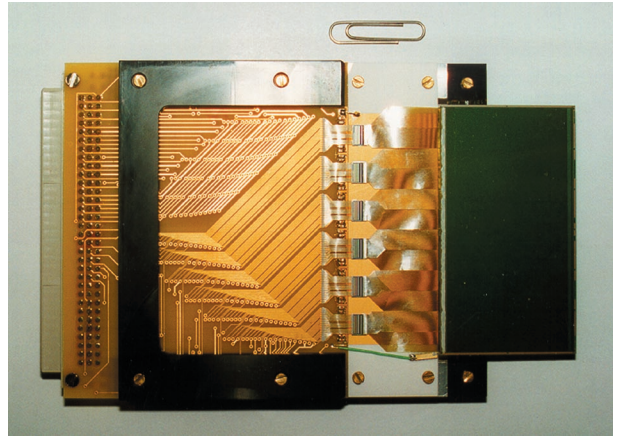


Figure 1.2: A silicon strip detector module of NA57. The sensor is connected to the readout via micro-cables. The detectors shown is a prototype for the ALICE Inner Tracking System.

The Dutch participation in ALICE, which is concentrated in the FOM-programme *QCD thermodynamics* and performed in the context of NIKHEF, focuses its efforts on the development and construction of the inner tracking system (ITS) of ALICE. The purpose of the ITS is the reconstruction of primary and secondary vertices. It will also improve the momentum resolution of tracks observed in the TPC, and it will contribute to particle identification through the measurement of energy loss.

NIKHEF carries responsibility for the fifth and sixth layers of the ITS, which are silicon strip detectors. This detector, which comprises about 1700 silicon strip sensors plus the necessary read-out electronics is built together with groups from Turin, Strasbourg, Nantes, St. Petersburg, Kharkov and Kiev (Ukraine). In the past years, the detector has been designed and its components tested in test beams or otherwise. The silicon sensors have been used successfully in the NA57 experiment (Fig. 1.2). It was shown, see fig. 1.3, that charge matching between two sides of the detector can be used to reject incorrect pairing of multiple hits, so-called *ghost hits*.

An important issue was the cooling of the detectors and the electronics. A test-setup was made to investigate the cooling properties of the design. It was shown that

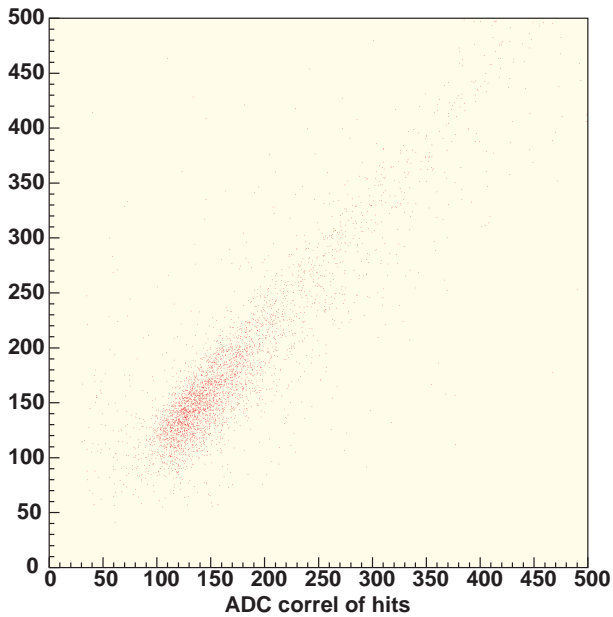


Figure 1.3: The charge collected on one side of the silicon strip sensor versus the charge collected on the other side. There is a clear correlation visible, which will allow for rejection of ghost hits in the track reconstruction.

no heat will be lost to the environment if the coolant is 4 K colder than the ambient air (see fig. 1.4). A careful design was made for the support of the detector modules, involving carbon fibre structures. The sag of the ladder was shown to be less than  $20 \mu\text{m}$  under full load.

The design and testing activities described above led to the completion of the technical design report, an important stage in the development of an experiment at CERN. The report was submitted in June and approved in September of 1999 by the LHC Committee. In October 1999, the progress of the NIKHEF contribution to ALICE was evaluated by an ad-hoc committee. The committee advised positively to FOM, which consequently approved the continuation of the ALICE programme.

The major challenge for the coming year is to develop tools for assembling the ITS ladders. The  $7 \times 4 \text{ cm}^2$  sensors will be mounted in such a way as to leave no gaps between them at all. This means that the sensors and their hybrids and read-out cables are mounted in a very complex pattern. A special tool has been fabricated by the instrumental group in Utrecht (IGF), see fig. 1.5, which allows all the sensors to be placed in position be-

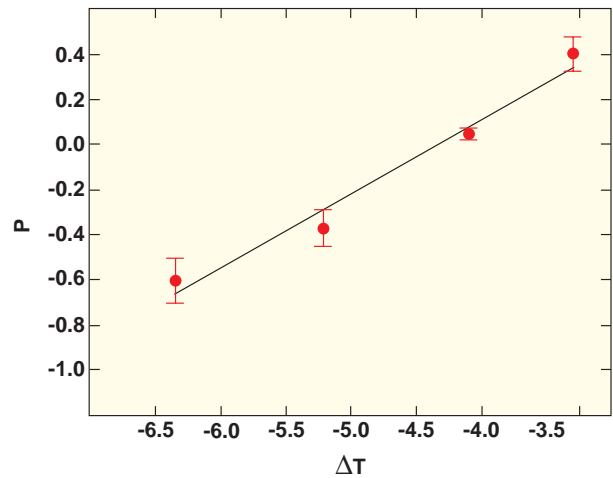


Figure 1.4: Heat loss to the environment as a function of the temperature difference between the environment and the cooling water. If the water is 4 K colder than the ambient air, no heat is transferred to the surroundings of the ladder.



Figure 1.5: The assembly tool for the prototype ALICE ITS ladder, with the carbon fibre ladder mounted. The sensors are positioned and locked in place by suction (red valves). The carbon fibre ladder rests on micro machined plegs, three per sensor.

fore they are glued to the ladder simultaneously. Funds have been requested and obtained for fabrication of a robot arm, which will perform these delicate manipulations automatically. Similar robots will then be used to measure the detector positions in various orientations and to verify the response of the detector, including electronics to laser light or particles from a radioactive source.

## 2 Antares: A cosmic neutrino telescope

The Antares project will open a new field of scientific exploration of the universe. Neutrino detection provides a novel tool to explore high-energy phenomena in astrophysical objects and in the cosmos. The neutrinos escape without interaction from the sources and travel to the earth undeviated by inter-galactic magnetic fields. Hence it is possible to obtain unique information on the nature of those sources and perhaps to observe new objects. More speculative, 'cosmological' neutrinos can originate from the decay of topological defects left over from the early phase of the universe.

The Antares collaboration was founded in 1996 with the objective to build a neutrino telescope in the Mediterranean sea. The first phase of the project has been used to learn the technology and to acquire the experience necessary to construct such a detector. With the successful completion of the first phase, the collaboration has moved on to the construction of a detector with a size sufficient to observe neutrinos from outer space.

In the framework of the Antares project, a "NWO groot" proposal has been submitted in September 1999 (see Figure 2.1 and <http://www.nikhef.nl/antares>).

The main NIKHEF contributions focus on the DAQ system, consisting of a large processor farm on shore, and an off shore time calibration system necessary for a good angular resolution of the muons produced in charged current interactions of cosmic neutrinos. In order to maximise the discovery potential, unfiltered data will be sent to shore where fast processors are used to select the physics events of different origins.

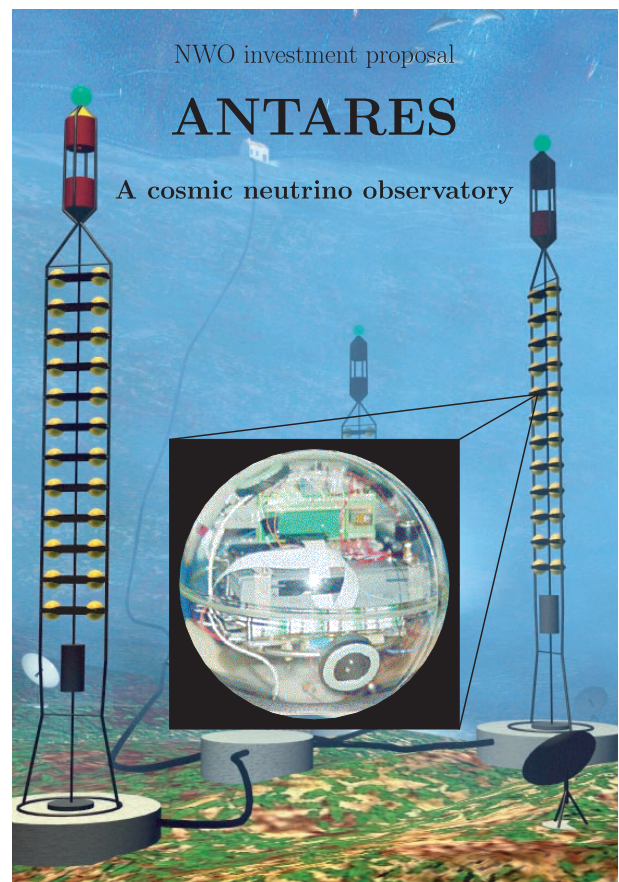


Figure 2.1: Cover of the Antares "NWO groot" proposal submitted September 1999.

## 3 ATLAS

### 3.1 Introduction

In 1999 a substantial number of staff members joined the Dutch ATLAS/D0 group. The start-up of the D0 experiment has certainly added to the appeal. In addition detector R&D projects like MediPix were merged into the ATLAS/D0 program.

### 3.2 ATLAS Experiment

The Physics Performance Technical Design Report was published containing detailed simulations of the exciting LHC physics processes (Higgs, gauge bosons, top, etc.). For example, Fig. 3.1 shows a simulated  $H \rightarrow ZZ \rightarrow e^+e^-\mu^+\mu^-$  decay as seen by the ATLAS experiment.

#### 3.2.1 End Cap Toroids

The largest Dutch contribution to the ATLAS experiment is the construction by Dutch industries of the End Cap Toroids (ECTs; part is schematically drawn in Fig. 3.1). Their basic design was made by the Rutherford Appleton Laboratory (RAL). The project comprises two major parts:

1. *Two large aluminium vacuum vessels*

These vessels measure about 10.7 m in diameter and about 5 m in length. Each vessel has a service turret on top and weighs about 40 tons.

Already in 1998 a 1:5 scale model of a vacuum vessel has been constructed by Schelde Exotech in Flushing, the Netherlands; it was delivered mid 1998 to RAL. Its main purpose was to verify the finite element calculations by measurements of deflection at various locations as a function of vacuum, overpressure and loading. The tests confirmed the validity of the design.

The final vessels will also be constructed by Schelde Exotech. The green light for manufacturing was given after a successful Production Release Review in July 1999. The manufacturing drawings are completed and the required aluminium has been delivered. The production is well under way: all 40 mm thick shell plates have been welded and bent, all 70 mm thick end plates have been welded and stay tubes, including their flanges, have been completed. All parts still need final machining. Near the end of 2000 the first vessel should be shipped to CERN/Geneva.

2. *Two cold masses*

Each cold mass consists of eight superconducting coils of  $4 \times 4.5$  m<sup>2</sup> and eight keystone boxes. The keystone boxes are used to reinforce the whole structure and form a major part of the cold "buffer". The coils are indirectly cooled. The weight of a cold mass is about 160 tons.

HMA Power Systems at Ridderkerk, the Netherlands, manufactures the cold masses. The Production Release Review, held in October 1999, was successful. Before the start of the manufacturing of the 16 double pancake coils, a dummy coil will be made during the first half of 2000. The winding machines for the winding street were ordered in Switzerland and are ready for commissioning. The aluminium for the first coil formers has been delivered. One of the two suppliers of the superconducting conductor encounters severe manufacturing problems resulting in broken strands within the cable. The second supplier has no problems. The ordered conductor will require additional cleaning prior to impregnation. This was not foreseen. A bead blasting method will be used, most likely in an in-line set-up in the winding street. Shipment of the first cold mass is scheduled for end 2001.

#### 3.2.2 Muon Spectrometer

The procurement of the components of the Muon spectrometer started in 1999. After the successful completion of the Production Readiness Review, the basic components for the individual drift tubes (aluminium tubes, endplugs and 50  $\mu$ m tungsten wire) have been ordered and first batches have been delivered. The aluminium extrusions required for the support systems have arrived. Pre-series of the RasNik alignment system components (CCDs, lenses and masks) are at NIKHEF (see Fig. 3.2) and prototypes of the RasNik readout chain are being tested.

At NIKHEF the infrastructure required for the construction of the 96 large BOL (Barrel Outer Layer) chambers has basically been completed: the large clean room meets the specifications, the precision jiggling has been mounted on the  $5.5 \times 2.5$  m<sup>2</sup> granite table and the automated drift tube wiring line awaits transport from CERN to NIKHEF. The first BOL chamber is expected to be ready by spring 2000 and serial production should start in the summer of the year 2000.

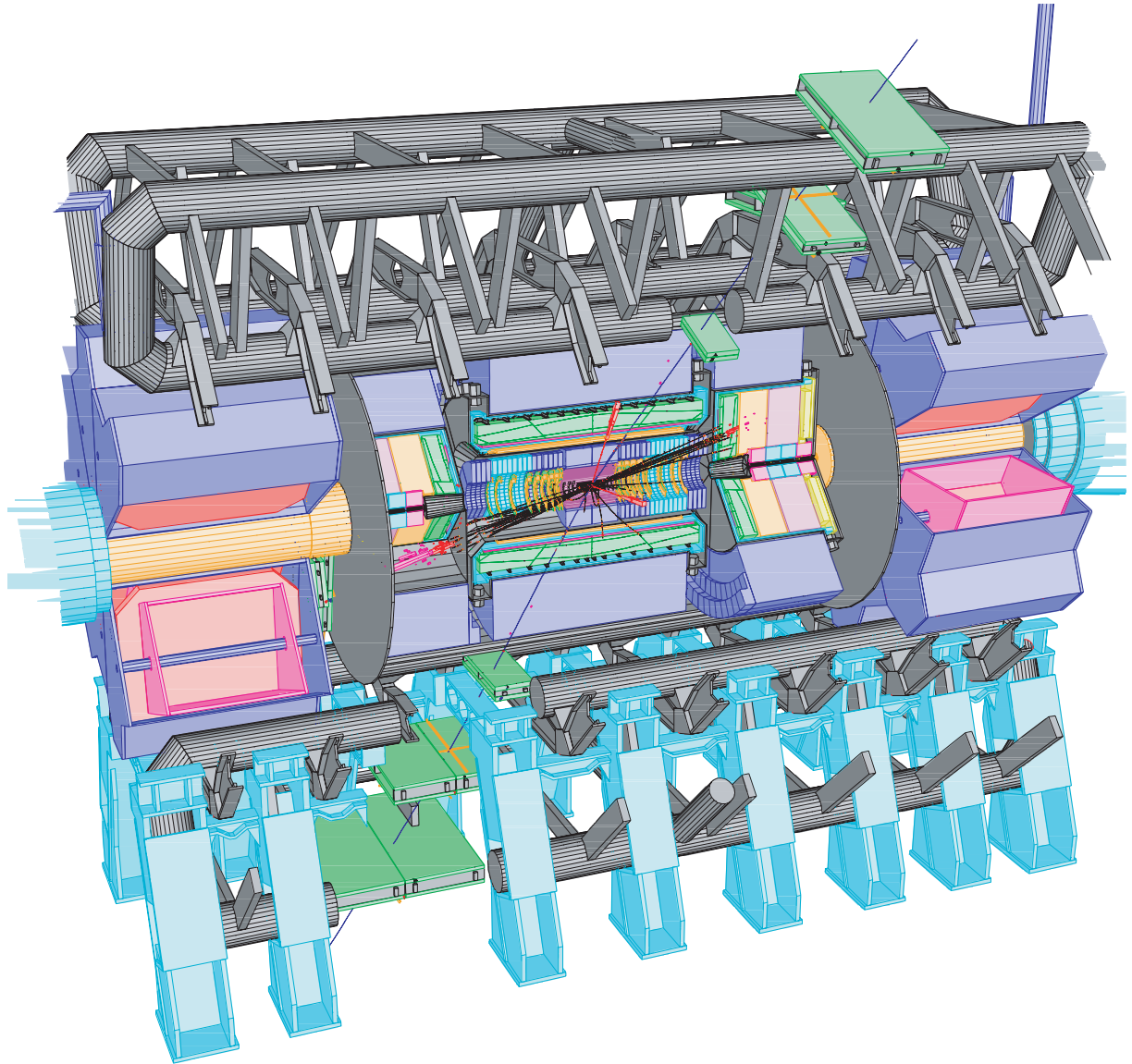


Figure 3.1: Monte Carlo simulation of a  $H \rightarrow e^+e^-\mu^+\mu^-$  decay as recorded by the future ATLAS experiment. The detector dimensions correspond to a 45 m long cylinder with a diameter of 23 m. The muon tracks are indicated in blue (bottom left and top right corners) whereas the electron energy depositions are visible in red. Some of the eight coils as well as the vacuum vessels of the toroids (barrel and endcaps) are indicated schematically.

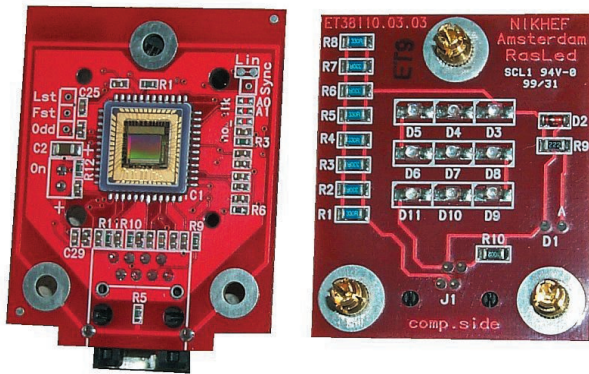


Figure 3.2: The CCD and the mask for the RasNik system.

Preparations have started to convert part of one of the experimental halls of the AmPS accelerator into a cosmic ray test area for BOL chambers. In addition, this stand will serve as a testbed for the readout electronics still under development for the muon drift chambers as well as a playground for the simulation and reconstruction software for the ATLAS muon spectrometer.

### 3.2.3 Semi Conductor Tracker

Charged particle tracking in the ATLAS detector plays an important role at both low luminosity and high luminosity phases of the LHC machine. The design of the ATLAS experiment - particle tracking close to the interaction point using a combination of a limited number of precision space points in combination with a larger set of "less precisely" determined positions - requires the application of semiconductor trackers. Several physics processes demand space point determination with a resolution better than  $20 \mu\text{m}$  in a cylindrical volume of approximately 7 m long and 1.2 m in diameter. To allow for a precise determination of production and decay vertices of particles, which is needed for bottom quark physics, it is required that multiple scattering in the detector support structure and the sensors themselves remains at a minimum. In addition, the detector should survive 10 years of LHC operation. The total integrated flux of charged and neutral particles becomes large enough to destroy semiconductor sensors and electronics completely, unless special precautions are taken. This year has shown tremendous progress on improving the radiation tolerance of silicon sensors and their readout electronics. Operating the sensors at temperatures

below  $-7^\circ \text{C}$  guarantees proper signal-to-noise ratio over the full lifetime of the experiment for all silicon strip and pixel layers except for the one located very close to the primary interaction vertex.

NIKHEF is particularly involved in the design and construction of large parts of the mechanical support to hold the detectors in the end-caps. Special attention is paid to guarantee long term spatial stability under mechanical stress and varying temperatures. Low mass constructions based on carbon fibre composites have been prototyped, while a mock-up of half an end-cap is being build to study service routing (cooling pipes, cables etc.) and assembly issues. High spatial resolution can only be achieved when the sensors are combined and mounted with high precision. Special highly automatized assembly tools are being build to glue the delicate silicon layers to local supports and to connect with readout electronics into modules. These modules are subsequently mounted on a mechanical substructure, the disk. Completed disks require testing and environmentally controlled storage facilities before they can be mounted in their final cylindrical support. NIKHEF is preparing a complete assembly line to assemble nine disks (with about 1000 modules, of which a large fraction will be delivered by collaborating institutes) to form a complete (and tested) SCT end-cap. Delivery to CERN is foreseen in 2003.

### 3.2.4 Data Acquisition, Trigger System and Detector Control System

A module (called SHASLINK, see Figure 3.3) with a SHARC processor, PCI interface and a S-link source interface was developed. In combination with the already existing CRUSH modules (each with a SHARC, an FPGA (field programmable gate array) and an S-link destination interface) a prototype Read Out Buffer (ROB) complex was built. The performance of the CRUSH itself and of the prototype ROBcomplex was determined. The measurement results were found to surpass the requirements.

The CRUSH and SHASLINK modules are also used for a study of the design of the Read Out Drivers (RODs) for the muon precision chambers. One ROD has to build event fragments from the data of six muon chambers and pass the fragments to a ROB. For this purpose the FPGA of the CRUSH module has been reprogrammed, taking into account all possible error conditions which could arise from corrupted input data. The FPGA design functions as specified. The proto-

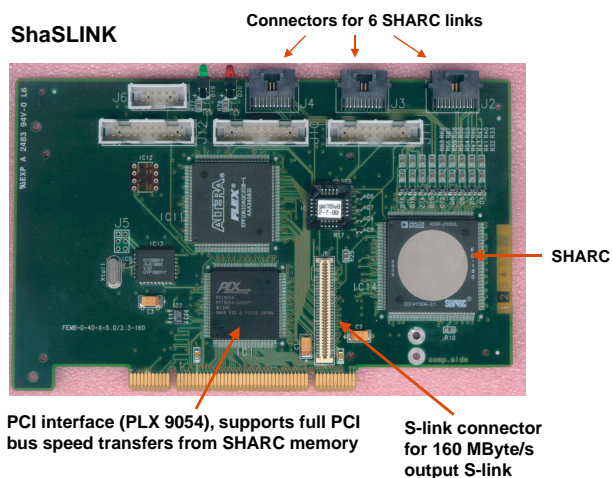


Figure 3.3: *The SHASLINK module.*

type ROD will be tested further with respect to performance and error handling using a SHASLINK module as programmable data generator. Another SHASLINK module is used as output part of the ROD.

The modelling of the Level-2 trigger system was continued with the further development of the spreadsheet and computer models. The full Level-2 system with the pilot project architecture and using sequential processing is modelled. The network bandwidths, message rates, number of farm processors needed, the buffer memory required and the Level-2 decision time distributions were studied.

The results of the spreadsheet and computer models for average bandwidths, rates and processor occupancies are in excellent agreement.

Software for CAN bus controllers, to be used for local detector control, has been developed. A contribution has been made to the specification of the requirements of the supervisory control part of the Detector Control System.

### 3.3 D0 Experiment

In 1999 the Dutch hardware contributions to the D0 detector upgrade for the forward proton detector mechanics was completed and shipped to Brazil for assembly. The magnetic field monitoring equipment is ready (see Figure E 2.4) and presently at CERN for calibration. Procurement of the radiation monitoring system is well underway.

Four NIKHEF PhD students went to Fermilab

(Chicago). The emphasis of their work is on the software for physics data analysis starting in 2001. In addition, one of our students became a key player in the characterization of the silicon detector modules and another one is in charge of the magnetic field monitoring system.

The muon reconstruction software advanced well and became a standard part of the D0 reconstruction program. The algorithms for track finding and parameter fitting are still the old ones, but the interface to the general track finding and fitting classes is underway. A new code was developed to describe the materials in the D0 detector as well as their influence on particle trajectories. This to better account for energy loss and multiple scattering in the reconstruction software. A special graphics tool has been developed and integrated into the D0 code to visualize (parts of) the detector and tracks. A paper summarizing this work will be submitted to the next Computing conference for High Energy Physics (CHEP).

In the Netherlands we also started Monte Carlo event simulation using the Pythia and Isajet event generators and specific D0 software to simulate the effects energy loss, multiple scattering etc. in the D0 detector elements. For these CPU demanding calculations the parallel computer of the academic computer centre SARA is used. By now the production amounts already to 25% of the total required. In parallel we started with the reconstruction and analysis of these Monte Carlo simulations. The emphasis is on track reconstruction in the silicon, scintillating fibre trackers and muon chambers. Algorithms are developed to find displaced vertices, which are important for bottom quark physics.

### 3.4 R&D activities: MediPix

MediPix is a collaboration between 13 European universities and research institutes, some of which are high-energy physics institutes like NIKHEF, and others are involved in medical physics or imaging. The goal of the collaboration is to transfer the technology, developed for semiconductor pixel detectors within high-energy physics, to other applications such as medical and analytical X-ray imaging.

A pixel detector for high-energy charged particle tracking consists of a sandwich of two silicon chips, one chip containing a matrix of reverse-biased diodes implanted in a high-resistivity silicon material, the other containing a matching matrix of CMOS readout electronic circuits. Due to the small pixel size and correspondingly

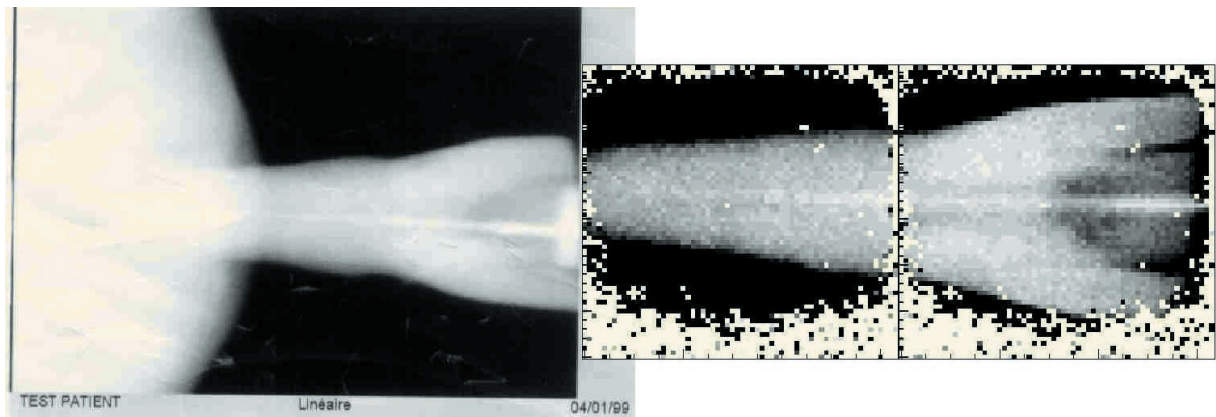


Figure 3.4: Comparison between X-ray images (B.Mikulec) of a molar recorded on standard dental film (left) and the MediPix-1 chip (right).

low input capacitance, an extremely low noise figure, in the order of 100 electrons r.m.s. on the input, can be reached at room temperature. To use this technology for X-ray imaging, the sensor material is replaced with higher Z materials like GaAs or Cd(Zn)Te. These materials have a better conversion efficiency than silicon for X-rays in the energy range used for medical imaging (20-100 keV). Also the complicated event-by-event readout circuitry is replaced by a simple 15-bits counter in each pixel-readout circuit.

The result is a unique device, performing single-photon counting with low noise and dark-current, at room temperature. First results with the MediPix-1 chip have shown that a reduction in X-ray dose of 30 times is attainable, with respect to current methods using fluorescence and integrating CCD-readout (see Figure 3.4). The remaining disadvantage with respect to CCDs is the limited resolution (pixel size  $170 \times 170 \mu\text{m}^2$ ). However, the MediPix-1 chip was designed several years ago in a SACMOS process with  $1 \mu\text{m}$  minimum gatelength, while  $0.25 \mu\text{m}$  is now available and  $0.18 \mu\text{m}$  is expected later this year.

NIKHEF is contributing to the design of a new chip in sub- $0.25 \mu\text{m}$  technology, which will have a pixel size of  $55 \times 55 \mu\text{m}^2$ . This in close interdisciplinary collaboration with the IC-design group of Twente university and the micro-electronics group at CERN. The production of this MediPix-2 chip is planned around May 2000.

Another NIKHEF effort is the development of a PCIbus interface for the readout of MediPix chips. This small multilayer printed-circuit board replaces a cumbersome, costly and complicated VME-based system. The new

interface will be used by all participants in the collaboration for imaging as well as for wafer-testing the new chips.

## 4 B Physics

### 4.1 Introduction

The B physics group of NIKHEF participates in the LHCb experiment at CERN and the forerunner experiment HERA-B at DESY. Both experiments will study the breaking of charge-parity (CP) symmetry in the decays of B mesons. After a very tight construction schedule, the HERA-B detector has been essentially completed in the course of 1999 and will be ready for its first physics run in the spring of 2000. HERA-B and its competitor experiments BaBar at SLAC and Belle in Japan are expected to demonstrate unambiguously that CP violation in B meson decays does indeed occur. However, these experiments can not measure all relevant parameters with sufficient precision to pinpoint the origin of CP violation. That task will fall to the LHCb experiment at the LHC collider of CERN, which is planned to come into operation in 2005. The development of detector components for LHCb is generally proceeding on schedule. The same is true for software development and the study of data analysis methods.

### 4.2 HERA-B

At the end of 1999, about 90 % of the detector hardware was installed. More specifically, the Outer Tracker to which NIKHEF has contributed is near completion, in spite of an earlier interruption of mass production when damage to the cathode foils of the honeycomb cells was observed in prototypes exposed to hadron beams. It was found that the cathode aging can be avoided by coating the inner surface with a thin gold layer and by use of the mixture  $Ar/CF_4/CO_2$  as drift gas. Analysis of test data taken with the installed detector modules shows that individual cell efficiencies are around 95%.

Link boards for data transport from the Outer Tracker and from the Muon Chambers to the first-level trigger electronics have all been delivered to DESY. First tests indicate that the boards work according to specifications. However, it is some cause for worry that the key element of the boards, the so-called 'Autobahn chip', is no longer produced. Many of the chips already had to be replaced because of malfunctioning. The performance of the first-level trigger hinges on the correct identification of interesting track candidates. Checking against off-line analysis of minimum bias events indicates that the trigger indeed functions properly.

Installation of 'superlayer 8' of the vertex detector, which is a responsibility of the Utrecht group, has been delayed till February 2000 because of a delay in module

production elsewhere. Some redesign of the mechanics of the superlayer, with improvements in cooling and ease of mounting, has been undertaken.

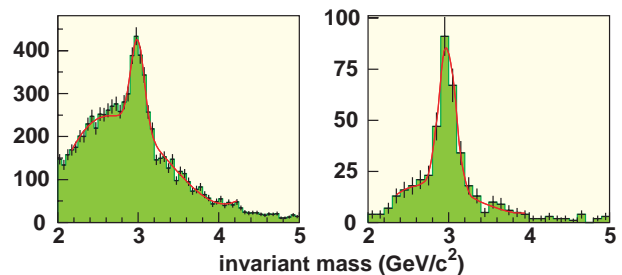


Figure 4.1:  $J/\Psi$  mass peak in the  $e^+e^-$  decay channel as observed in a HERA-B test run.

In the fall of 1999 some test runs were already performed with the partially completed HERA-B detector. Figure 4.1 shows the  $J/\Psi$  signal observed in the  $e^+e^-$  decay channel. The encouraging test results have contributed to the decision of the DESY directorate to defer the long shut-down of HERA. This will allow HERA-B to collect data during several months in 2000.

### 4.3 LHCb

NIKHEF is the principal partner in the Outer Tracker system of LHCb, which will consist of ten tracking stations distributed along the length of the spectrometer and subtending 98 % of the acceptance of the experiment. Each station contains several layers of straw tubes. The total number of readout channels is about 130,000. Because of this hardware commitment, software development and simulation studies are centred on optimization and performance studies of the tracking system of LHCb.

The NIKHEF group in LHCb also participates in the realization of the vertex detector. A total of 17 silicon stations will be placed on two moveable frames inside a vacuum tank. During data taking the detectors will be positioned at 8 mm from the LHC beams. The entire assembly will be retracted when the collider is refilled with proton bunches. NIKHEF takes care of the system design of the vacuum tank, is responsible for the 'pile-up trigger' which serves to reject events with more than one primary interaction per bunch crossing, and participates in the development of a front-end chip for readout of the vertex detector.

## Outer Tracker

Given the fact that the proton beams in LHC may interact every 25 ns, it is important to restrict drift times to a narrow window: time overlap of signals from many bunch crossings would render pattern recognition unfeasible. Tests of prototype arrays of straw tubes have been carried out with pion beams from the CERN Proton Synchrotron. Drift time spectra were measured for various drift gas mixtures, in magnetic fields up to 1.4 T. It has been shown that with a drift gas mixture of  $Ar/CF_4/CO_2$  (68/27/5), all drift signals from straws of 5 mm diameter can be collected within  $2 \times 25$  ns, even allowing for the fact that the magnetic field will in some regions of some stations rise to 1.6 T. With this same gas mixture, two staggered layers of straw tubes provide a comfortably wide plateau of stable operation at essentially full detection efficiency. The efficiency per individual cell starts to drop significantly below 100 % when the track segment lies within 0.4 mm from the cathode (See Figure 4.2.) A separate programme of aging tests has so far shown that straws made of Kapton foil with a volume-doping of carbon are not susceptible to aging due to dissociation products of the  $CF_4$  component in the drift gas, in contrast to many other materials. With these results, the basic design of the detection elements is considered to be settled, unless further aging tests would still show otherwise. The next development step consists of optimization of the straw tube assembly: studies of signal amplitude, signal rise time, cross talk and noise pick-up as a function of the placement or absence of common shielding foils, aluminium wrapping around each straw tube, distance between tube layers, etc. This work towards optimization of the electrical behaviour was started in the middle of 1999 and will continue into the year 2000.

The design of the LHCb magnet has been quite radically changed with respect to the layout foreseen in the Technical Proposal, with important consequences for the Outer Tracker stations in and near the magnet. The space available for support frames, front-end electronics and cabling has been much reduced and shielding against heat produced in the magnet coils has become an important issue. Therefore, it has been necessary to already start detailed studies of the mechanics of the magnet stations, of the lay-out of their front-end electronics and of the cabling, in order to make sure that the proposed magnet geometry is not incompatible with the required acceptance of the track detectors.

A full-size model of the station directly behind the magnet is shown in Figure 4.3.

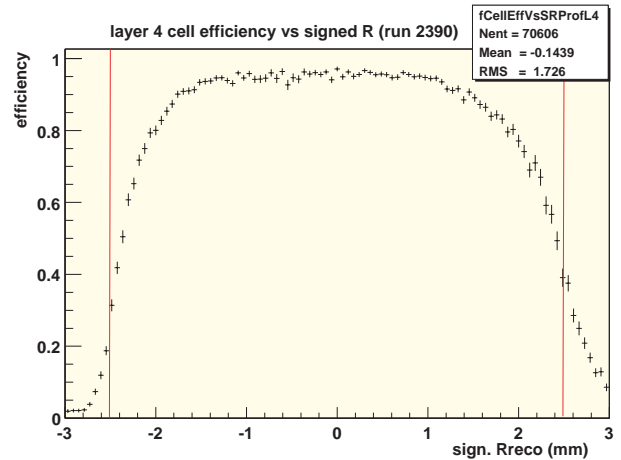


Figure 4.2: Efficiency scan over a straw tube of 5 mm diameter operated with an  $Ar/CF_4/CO_2$  gas mixture.

Much progress was achieved in the development of the read-out chain of the Outer Tracker. Extensive tests have shown that the ASD-BLR preamplifier-discriminator developed in the ATLAS community is entirely suited for our purposes. A candidate TDC chip has been identified, and read-out logic which is compatible with the characteristics of that chip is under development. Next to this default solution, an alternative TDC design is under study.

## Vertex Detector

Optimization studies of the detector design continued throughout the year. The detectors must be encapsulated in a low-mass foil to ensure maintenance of the ultra-high vacuum in the LHC beam line, while minimizing multiple scattering. The presently favoured option foresees the use of  $100 \mu\text{m}$  thick aluminium foil. In addition, the detectors must be shielded against the wake fields of the bunched LHC beams.

First designs of the differential vacuum system and the cooling system have been worked out. Some critical issues have been identified. For instance, the thin enclosures and wake field suppressors will be subject to an intense bombardment of ions and electrons accelerated in the electromagnetic fields of the proton bunches, which in turn leads to desorption of molecules. The result may be a run-away increase of pressure or space charge density. Careful studies of the optimal configuration in the neighbourhood of the beams are thus necessary, both with further simulations and with test measurements. It may be necessary to apply special coatings with low ion



Figure 4.3: *Model of a medium-sized outer tracker station.*

desorption and low secondary electron yields. Several design options for the low-mass encapsulation of the silicon planes are under study. Three-dimensional wake field calculations were performed to address specifically the issue of the RF properties of the assembly with the two detector halves in the closed and retracted positions. Effects of multiple scattering on the detector performance were studied with GEANT simulations. A prototype of the vertex detector system will be constructed and tested in the year 2000.

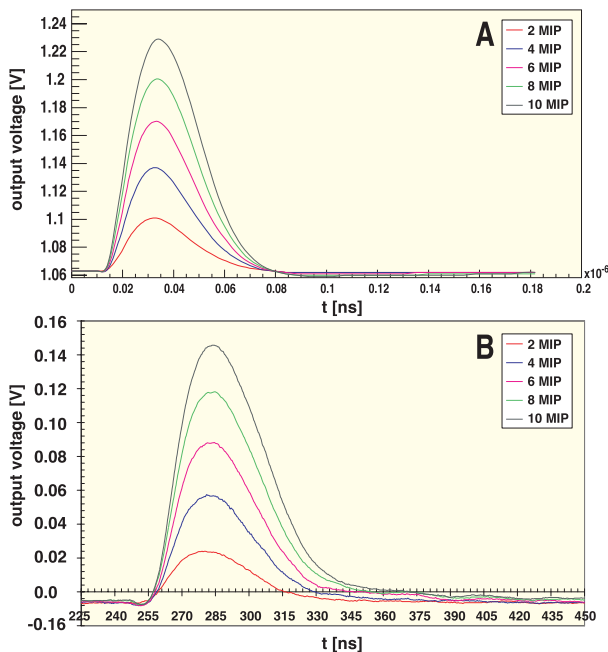


Figure 4.4: *Simulated (A) and measured (B) pulse shapes of the Beetle read-out chip.*

One of the most critical items in the read-out electronics is the front-end chip. A serious candidate is the ‘Beetle’ chip, designed in the  $0.25 \mu\text{m}$  deep-submicron technology. Together with the ASIC-lab in Heidelberg, NIKHEF is responsible for the design of the preamplifier and pulse shaper stages of the chip. Extensive simulations have resulted in a first design, which was submitted for a test production. The chips were received late in 1999. The first test bench measurements show good agreement with the calculated properties. Figure 4.4 shows simulated and measured pulse shapes after the shaper stage. Shape parameters, gain and linearity are all in good agreement with expectation. Design parameters will now be fine-tuned to optimize the chip performance.

The vacuum tank of the vertex detector will also house two silicon detector planes that are dedicated to the measurement of the number of primary interactions within a single bunch crossing. This provides a determination of the luminosity and allows a veto trigger against multiple interactions. The veto trigger is formed by collecting hits registered in the two detection planes into a correlation matrix and determining the number of primary vertices that can be formed. Design of the required dedicated electronics has been started.

### Tracking software and physics performance studies

Part of the tracking studies specifically addressed the performance of the Outer Tracker: simulations of drift cell response at various combinations of magnetic field strength and drift gas mixture; development of alignment and drift map calibration procedures for test beam data. Of course, for the track reconstruction studies proper, the full set of tracking devices (Outer Tracker, Inner Tracker near the beam pipe and Vertex Detector near the interaction region) is being used. An object oriented simulation package for track reconstruction was developed. The pattern recognition routines use the tracking stations towards the end of the LHCb spectrometer, where only a small stray magnetic field is felt, to find straight track segments. These track seeds are then followed through the magnet towards the vertex detector. Final track parameters are determined by a procedure of detailed refitting. In the context of the re-design of the LHCb magnet, the tracking performance was studied with several magnetic field maps, from the points of view of momentum resolution, occupancies and track finding efficiency.

Physics performance studies remained focused on decays of the  $B_s$  meson: decay into  $D_s\pi$ , which allows measurement of the  $B_s$  oscillation frequency; decay into  $D_sK$ , which is sensitive to the angle  $\gamma$  in one of the unitarity triangles that can be formed from the CKM matrix; decay into  $J/\Psi\phi$ , which allows access to the angle  $\delta\gamma$  in another unitarity triangle. Decay time resolutions and event selection efficiencies have been studied as a function of background rates. Emphasis has been on the decay  $B_s \rightarrow J/\Psi\phi$ , where the sensitivity to effects of CP violation has been parametrized and fitted.

More information on HERA-B, LHCb and the NIKHEF participation in the two experiments can be found at <http://www-hera-b.desy.de>, <http://lhcb.cern.ch> and <http://www.nikhef.nl/pub/experiments/bfys>.

## D Theoretical Physics

### 1 Theoretical Physics Group

#### 1.1 Particles, fields and symmetries

Theoretical physics provides the mathematical description of the properties and interactions of subatomic particles. These include quarks and leptons (e.g. electrons and neutrinos), as well as field quanta like photons for the electro-magnetic field, and gluons for the colour field of the strong interactions. Whilst the electric forces bind electrons to nuclei, the colour forces are responsible for keeping together the quarks inside the nucleon. Furthermore the weak forces, mediated by heavy field quanta known as massive vector bosons ( $W$  and  $Z$ ), induce radioactive transmutations, notably the  $\beta$ -decay of the neutron and the muon.

The general framework for the description of the subatomic particles and their interactions is quantum field theory. The universal character of this framework for the description of all observed phenomena has become clear in particular since the work of 't Hooft and Veltman in the early '70's. In recognition of this they have been awarded the 1999 Nobel prize.

Present developments in quantum field theory take place in the area of model building, aimed to explain the observed regularities in the properties of particles; furthermore the dynamical aspects of quantum field theories need further elucidation, not only to explain scattering and transmutation phenomena, but also to understand the formation of bound states, colour confinement and the question of existence of new forms of charge, like single magnetic charges (monopoles).

Three families of quarks and leptons are known. The quantum field theory describing them and their interactions is called the standard model. This name is justified by the large number of experimental tests which it has successfully passed. However, the peculiarities of this model generate new questions. For example, the standard model explains the masses of particles by their interaction with a set of scalar fields; the quanta of one of these fields should be observable as massive electrically neutral particles, the Higgs particles, produced in very energetic collisions of electrons or nucleons. So far they have not been identified. Other investigations include attempts to relate the properties of matter particles, i.e. fermions like quarks and leptons, with those of the force-carrying bosonic fields: photons, gluons and heavy Higgs particles. Such a relation could be

enforced by supersymmetry, a symmetry relating the properties of bosons with integer spin, and fermions with half-integer spin. Supersymmetry is attractive as it helps to construct viable models of unified interactions. In unified theories the electro-magnetic, weak and strong forces are different manifestations of a single set of force fields, the full effects of which are observable only at very tiny distance scales of  $10^{-30}$  cm and less. If unification occurs, all known subatomic forces must become equally strong at this very small scale. In the simplest scenario's this happens only if supersymmetry is included.

Finally, attempts at unification also include the gravitational field; supergravity and superstring theory are presently the most important and promising lines of investigation in this area.

#### 1.2 Research program

The research program of the NIKHEF Theory Group covers several aspects of quantum field theory, string theory and their applications to the physics of subatomic particles.

##### *QCD*

The strong forces acting on particles with colour-charges, notably quarks and gluons, determine the structure of hadrons. All of their interactions, including the electro-weak interactions, are affected by the hadronic environment in which they live. To estimate reliably the cross sections for production of particles like top quarks or Higgs scalars in proton-proton collisions, a good understanding of this hadronic structure is a prerequisite. The precision of the experimental data requires QCD-effects to be evaluated to a very high accuracy. Powerful techniques for computing QCD-effects to 3rd order in the coupling constant  $\alpha_s$  have been developed at NIKHEF by Jos Vermaseren and co-workers. Estimating the cross sections and rates for the production of top-quarks and Higgs particles is part of the research program of Eric Laenen. These studies include analytic methods, like the resummation of large logarithmic contributions, as well as numerical simulations of certain types of events using Monte Carlo methods.

##### *Quarks and gluons at finite temperature*

In the collisions of heavy ions, such as lead on lead,

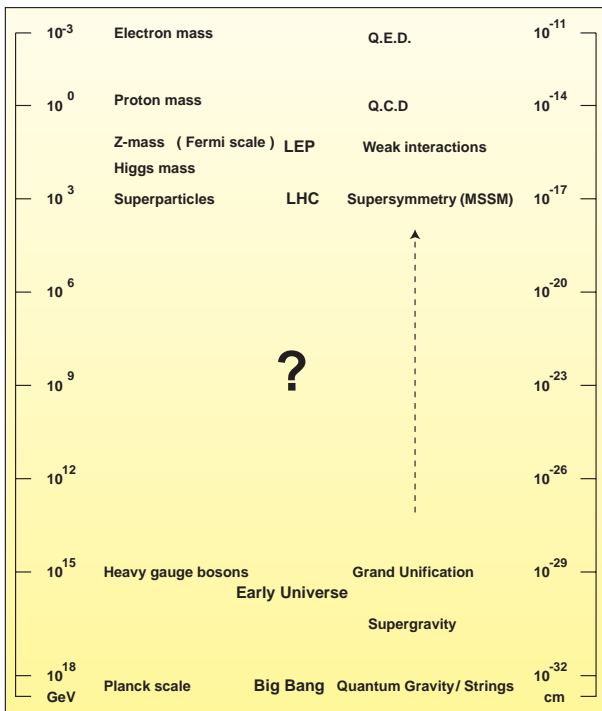


Figure 1.1: Scales in subatomic physics

at very high energies, the large number of particles involved in the process allow for a thermodynamic treatment. There is good reason to believe that the energy distribution over the different particles involved is of a thermal nature. The reaction times are very short compared to the duration of the ion-collision itself, allowing equilibrium to be established. Therefore one can assign a well-defined temperature to the gas of hadrons, or the plasma of quarks and gluons, which is formed in the collision. Justus Koch and his collaborators have taken up the study of the effects of finite temperatures on the structure of hadrons. As a first step they have undertaken to determine the temperature dependence of the pion form factor. As also input from lattice gauge theory is required, they have initiated a collaboration with the university of Bielefeld (BRD), where the necessary expertise is available.

### Supersymmetry

Supersymmetry relates the properties of bosons with those of fermions. In field theories with an exact supersymmetry the masses and charges of bosons and fermions are equal. If supersymmetry is broken in a self-consistent way, the masses of these particles may become different although their charges remain the same.

Supersymmetric versions of the standard model have been developed, but contain a very large number of free parameters. The number of free parameters can be greatly reduced in the context of unification of the electro-weak and strong interactions. Supersymmetry at the level of grand-unification is an attractive scenario for two reasons:

- with supersymmetry broken at the electro-weak scale, it can be matched smoothly to the standard model;
- with supersymmetry elevated to a local supersymmetry, the theory automatically includes long-range quantum gravity effects. In such theories it is quite natural for the unification scale to be close to the Planck scale.

Non-standard scenarios for superunification are developed at NIKHEF by Jan Willem van Holten and co-workers. Consistency conditions from quantum field theory have been incorporated, and allow for models with interesting phenomenological properties, including an explanation of charge quantization.

### Superstring theory

Consistent supergravity models are believed to be low-energy effective models for supersymmetric string theory. In string theory the point-like nature of elementary objects and field quanta is abandoned in favour of an extended object of finite length in one dimension. Point particles may be associated with such strings as viewed on scales much larger than the string length. However, more recently it has also become clear that one may associate point particles in a  $D$ -dimensional space with the endpoints of strings living in additional dimensions. These dimensions are not visible from the restricted  $D$ -dimensional space-time in which the end point of the string can move, although they may be probed by gravitational effects. In a similar way, strings themselves can be viewed as the intersection between higher-dimensional objects, e.g. membranes. This development has resulted in a theory of  $D$ -branes,  $D$ -dimensional objects in which the end points of open strings can live. The notion of  $D$ -branes has become an important tool in elucidating non-perturbative effects in string theories. At NIKHEF Bert Schellekens studies the interplay between such non-perturbative string dynamics and the perturbative dynamical behaviour of strings described by conformal field theories on their two-dimensional world surface.

## 2 CHEAF

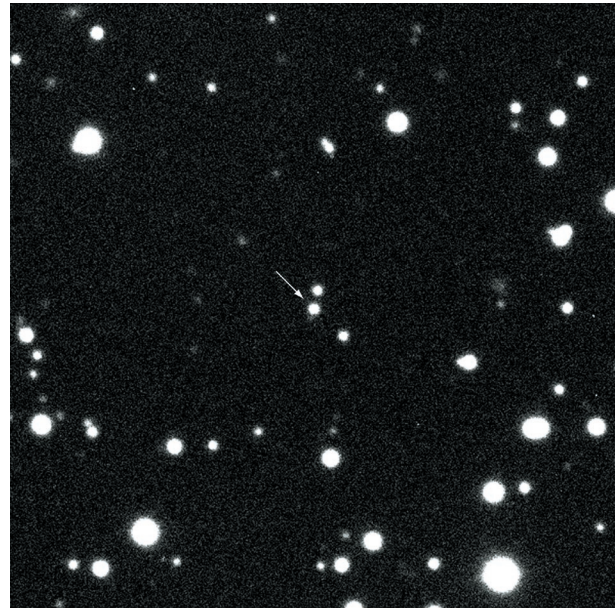
### 2.1 Introduction

Just as 1998 the year 1999 was an extremely fruitful year for the research of CHEAF (Centre for High Energy Astrophysics), with several major discoveries, one of which was ranked by the journal *Science* among the top ten scientific breakthroughs of the year 1999. On the other hand, CHEAF's research received a severe blow by the illness and death of one of its major research leaders and founding Board member of CHEAF, professor Jan van Paradijs, who died on November 2. The research highlights were:

### 2.2 Connection between Gamma ray Bursts and Supernovae: birth events of black holes?

When CHEAF graduate student Titus Galama in 1998 discovered an extremely bright and peculiar supernova, SN1998bw, which coincided in position and explosion time with the Gamma Ray Burst GRB980425, detected on 25 April 1998 by the Italian-Dutch BeppoSAX satellite, this at first seemed perhaps like a random coincidence, even though the probability for such a coincidence by chance was less than one in a million [1]. The peculiar characteristics of this rare type of supernova indicated that here one had, for the first time, witnessed the final collapse of the core of a massive star to a black hole (see the 1998 Annual Report). This was deduced from the fact that the spectrum and luminosity of the supernova showed that here at least 0.7 solar masses of Nickel-56 had been ejected –ten times more than in other supernovae– and that the exploding star consisted of Carbon and Oxygen and had a mass of around 10 solar masses. In 1999, however, it was discovered that this supernova-GRB coincidence was not a rare phenomenon. Looking back in detail at all 12 optical afterglows of GRBs discovered until then, it was found that the late lightcurves of two more bursts showed evidence for the presence of a supernova, similar to SN1998bw. Due to the extreme brightness of the early optical afterglows of the GRBs (hundreds of times brighter than a supernova), the underlying supernova lightcurves had not been noticed earlier. These supernovae were discovered by C. Bloom of Caltech for GRB980326 and by CHEAF graduate student T. Galama and D. Reichart of the University of Chicago for GRB970228, which have redshifts of about 1.0 and 0.69, respectively, corresponding to distances of about 10 and 7 billion lightyears [2].

The fact that a sizeable fraction of the GRBs (about



Afterglow of GRB 990510 (VLT ANTU + FORS1)

ESO PR Photo 22d/99 ( 18 May 1999 )

© European Southern Observatory



Figure 2.1: *Optical afterglow of the Gamma Ray Burst GRB990510 recorded on May 10, 1999 with the Very Large Telescope (VLT) of the European Southern Observatory (ESO) in Chile.*

25 per cent) now has been recognized to coincide with black hole producing supernovae established for the first time a clear connection between GRBs, supernovae and the birth events of black holes (van Paradijs 1999). Because of the unusual brightness of the supernovae that produce black holes, these GRB-supernovae received a new name: “hypernovae”. The collapsing stellar core most probably, because of its angular momentum, forms temporarily a rapidly spinning disk of nuclear matter, with a mass larger than 3 solar masses (i.e. above the upper mass limit for stable neutron stars). This differentially rotating disk rapidly loses angular momentum by gravitational waves and other –probably electromagnetic– mechanisms, leading to the formation of relativistic jets of baryonic matter ejected in directions perpendicularly to the disk. After a few thousand revolutions (a few seconds) the disk then has lost sufficient angular momentum to collapse to a black hole. The conditions for producing a GRB require that several tens to hundreds of Earth masses of baryons are accelerated in bulk to Lorentz factors between 100 and

1000. When this matter hits the surrounding interstellar matter the optical and X-ray afterglows of the burst are produced. Now that we know that "hypernovae" are involved, it seems plausible that this ejection and acceleration takes place in the form of collimated jets that are a side-product of the collapse process of the stellar core to a black hole.

The discovery of the connection between Gamma Ray Bursts and Supernovae was ranked by the journal *Science* among the top ten scientific breakthroughs of the year 1999 (*Science*, 17 December 1999).

### 2.3 First redshifts and polarisation of Gamma Ray Bursts measured with ESO's Very Large Telescope

Graduate students T.Galama, P.Vreeswijk and E.Rol led a European team which in May 1999 determined for the first time a redshift of a GRB (GRB990510) with the 8.2-meter Very Large Telescope (VLT) of the European Southern Observatory in Chile. The spectrum of the optical afterglow of this burst has a redshift of 1.6, corresponding to a distance of 11.5 billion lightyears. With this redshift measurement they broke the monopoly that until then the American 10-meter Keck-Telescope on Hawaii had held in these redshift determinations. After this, two more redshifts of GRBs were measured in 1999 by our team with the VLT. Figure 2.1 and fig 2.2 show the light and the spectrum, respectively, of the optical afterglow of the Gamma Ray Burst of May 10, 1999 (GRB990510), as recorded by Galama et al. with ESO's Very Large Telescope in Chile. The measurement of the polarisation of the light of the afterglow of the 10 May burst was a primer, which for the first time provided direct evidence that one is dealing here with a jet of matter, as expected from the "hypernova" models.

### 2.4 Record number of CHEAF Ph.D. degrees awarded

In 1999 six Ph.D. theses were defended by CHEAF graduate students and accordingly six doctor degrees were awarded. On 16 February Rudy Wijnands, who discovered the first millisecond X-ray binary pulsar, received his doctorate. He was awarded a 3-year Chandra-fellowship by NASA, with which he chose to start working at MIT at Cambridge, Massachusetts. On 14 and 23 September Mario van den Ancker and Jacco van Loon received their doctor degrees and left for 3-year postdoctoral positions at Harvard University and the University of Cambridge (UK), respectively. On 16 November Coen Schrijvers received his doctor degree; he took up

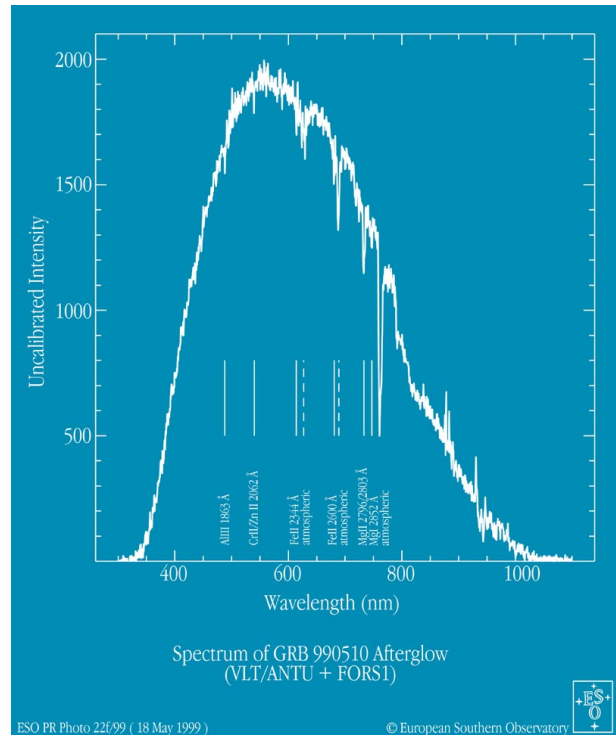


Figure 2.2: *Spectrum of GRB990510 recorded with ESO's VLT shows a redshift of 1.61, indicating a distance of some 11.5 billion lightyears.*

a position at TNO-TPD. Finally, on 7 and 8 December Paul Groot and Titus Galama defended their theses and were awarded their doctorates, in both cases with the special distinction *Cum Laude*, because of their breakthrough discoveries in the field of Gamma Ray Burst research. They left for prestigious 3-year postdoctoral positions at Harvard University and the California Institute of Technology, respectively. Both this number of doctorates awarded and the number of *Cum Laude* distinctions were a record in the history of CHEAF since its foundation in 1986.

## References

- [1] T.Galama et al. 1998, *Nature*, **395**, 670.
- [2] T.Galama et al. 1999, *Astrophysical Journal* (in press) and: Ph.D. thesis, Univ. of Amsterdam, Chapter 16, J. van Paradijs 1999; *Science*, **286**, 694-695.

# E Technical Departments

## 1 Computer Technology

### 1.1 Computer- and network infrastructure

No major changes of the infrastructure have been implemented in the year 1999.

General services on the enterprise level are running either on Solaris servers from Sun Microsystems or on Windows NT servers from DELL. Miscellaneous services, such as e-mail, web and ftp, have been moved from the good old Sun 690 servers *paramount* and *nikhef* to a set of new, relatively small Solaris servers. In the fourth quarter of 1999 the *paramount* server had its final shutdown, while for historical reasons the other server *nikhef* will continue its operation in the new millennium. The Windows-NT file server has been extended with a 200 Gbyte RAID array, to accommodate the increasing demands of the Windows-NT user groups for more home and project disk capacity.

Commodity PC's with Pentium processors replace traditional RISC-based systems from Sun Microsystems, Hewlett-Packard and SGI and Apple Macintoshes. Compared to last year, relatively more Linux systems and less Windows-NT systems were installed. In Table. 1.1 the numbers of installed systems by the end of 1999 is given.

platform	operating system	1998	1999
Sun Microsystems	Solaris/SunOS	70	50
Hewlett-Packard	HP-UX	25	20
Silicon Graphics	IRIX	20	19
X-terminals	-	50	45
DELL PC	Linux	30	65
DELL PC	Windows 95	65	54
DELL PC	Windows NT	75	110
Apple Macintosh	MacOS	40	35
PC	NextStep	12	12
Total		387	421

Table 1.1: *The installed systems by the end of 1999*

At NIKHEF both SUSE and Red Hat Linux distributions are being supported now. The SUSE Linux is required by the users who are involved in experiments at DESY. CERN and Fermilab selected Red Hat as their preferred distribution for the experiments and related activities. Although supporting two different Linux distributions is not the optimal situation in terms of manpower effort needed for installation and support, it has to be consid-

ered as an unavoidable consequence of participating in collaborations which define their own computing platforms.

Many upgrades of software and hardware systems were performed for various user groups at NIKHEF. Just to mention a few of the more important ones:

1. An upgrade of the SGI and Windows-NT workstations of the mechanical design department, including a reconfiguration of data file locations and the installation of a Solaris file server.
2. An upgrade of the HP workstations of the electronic design department.
3. Extension of disk capacity of various workgroup servers.
4. Replacement of Apple printers by HP4000 printers.
5. Installation of a second Tektronix colour printer.

The network connection to the outside world, in our case the connection to the SURFnet router at SARA, has been upgraded. Before the upgrade this connection had a capacity of only 10 Mb/s, which was even shared with other institutes on the WCW campus. The new connection is based on the SONET/SDH technology and offers a 155 Mb/s bandwidth to the outside world exclusively for NIKHEF. This upgrade has been implemented in the second quarter of the year and at that time NIKHEF was the first SURFnet client connected with 155 Mb/s. Fig. 1.1 represents the situation in June 1999, when the bandwidth from NIKHEF to SURFnet became superior compared to the capacity of the connections to CERN and DESY.

Remote access service via telephone lines for users at home has been upgraded by making available 16 ISDN channels in addition to the existing analogue modem pool.

### 1.2 SARA

In 1999 more NIKHEF users than in the past have benefited from the services offered by SARA:

1. Most of the back-up for all home and project devices have been accomplished by the ADSM back

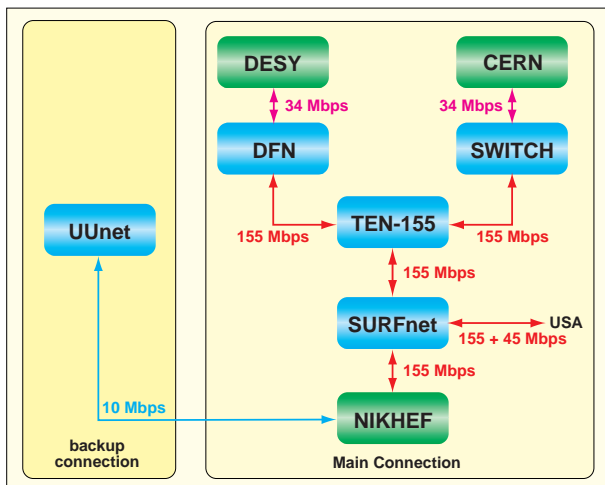


Figure 1.1: The NIKHEF connections with the World

up service offered by SARA. The total amount of file size stored at the tape robot from SARA is over 300 Gbyte by the end of the year. Files are saved for a period of 100 days after the last modification date.

2. A VRML data file of the ZEUS vertex detector has been extracted from the SDRC design software by the mechanical department at NIKHEF and has been imported into the computers of the CAVE. By doing this, one could have a spectacular virtual reality view inside the 3D model of the detector.
3. The CRAY C90 supercomputer has been used for calculations on the data generated by the AmPS Emin/ITH experiments.
4. By the end of the year a pilot project was started to experience the SGI Origin 2000 supercomputer for Monte-Carlo simulations for the D0 experiment.

### 1.3 AMS-IX

The numbers of participants of the Amsterdam Internet-Exchange increased significantly. In order to adapt to the corresponding increasing demand for floor space for 19-inch racks, it had been decided to allocate room H140 (Fig. 1.2) completely for the AMS-IX housing facility. Therefore, almost all of the NIKHEF central services, with the exception of the network patch panels, must be moved to the adjacent room. This operation was started in the second half of 1999 and will be continued in 2000. The cooling capacity has been significantly increased.

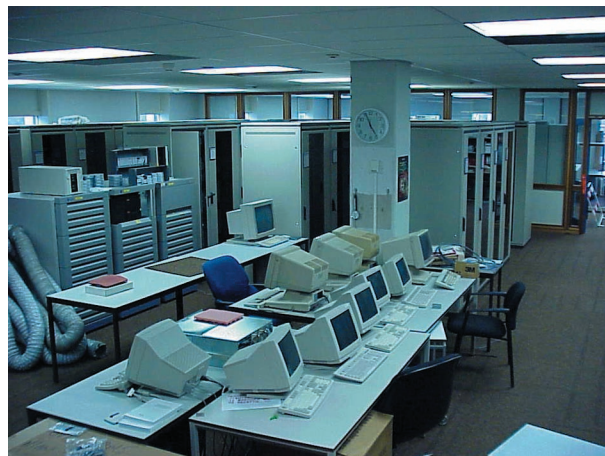


Figure 1.2: Room H140, home of the AMS-IX

### 1.4 Computer strategy 2000-2001

In last quarter of 1999 a survey was made of the computer and network requirements for the period 2000-2001. The input for the definition of these requirements came from the various user groups at NIKHEF and from the experts in the computer group. After discussions with representatives of the users groups and with the NIKHEF management, an investment plan has been defined.

The major conclusions of the survey are listed here:

1. improve the quality and reliability of central services
2. increase the network bandwidth between desk top and central services as well as between NIKHEF and external sources
3. increase the capacity of enterprise and workgroup file servers
4. start setting up computing services (Linux farms)
5. implement a general replacement scheme for desk top systems.

### 1.5 Software for experiments

The CT participates in a number of instrumentation projects for high-energy physics detectors. Most of the effort had been put into the research and development for the ATLAS detector. Minor, but significant, contributions were provided to the DESY experiments ZEUS

and HERMES and to the L3 Cosmics and LHCb experiments at CERN. The reader is referred to the corresponding chapters for more general information on these experiments.

### ATLAS MDT

- A. A database has been designed for the storage of all parameters relevant to the (future) production of 96 large muon (MDT) chambers. For this purpose the Microsoft ACCESS database has been integrated with LabView applications, to store data autonomously during production and quality control procedures.
- B. In close collaboration with the central ATLAS controls group, CANopen software has been developed for MDT chamber control functions. Other parts of the ATLAS detector will profit from these developments based on industry standards, since this software will be applied ATLAS wide.
- C. LabView applications have been developed to control the tooling for the production phase of the project. Amongst these are the continuous temperature monitoring devices and a device, called coffin, to test the MDT tubes with respect to gas leakage.

### ATLAS Level-2 DAQ

Test software has been developed for miscellaneous electronic boards, such as ShasLink, (M)CRUSH, which are equipped with digital signal processors (SHARC) and which are designed and produced by the electronic department of NIKHEF. Performance measurements were done on down-scaled configurations of the ATLAS level-2 ROB-in complex (Fig. 1.3), producing valuable data to be used as input in a future decision on the implementation of the final system.

### ATLAS Back-end DAQ

The software process of the design and implementation of the back-end DAQ system with complex interfaces to other systems can be considered an excellent example of the production by a large team with many members at different locations. The CT participates in this project by taking responsibility for the 'testmanager', one of the components of the back-end DAQ software. By the end of 1999, the software is ready to be used for real applications in the test beam environment.

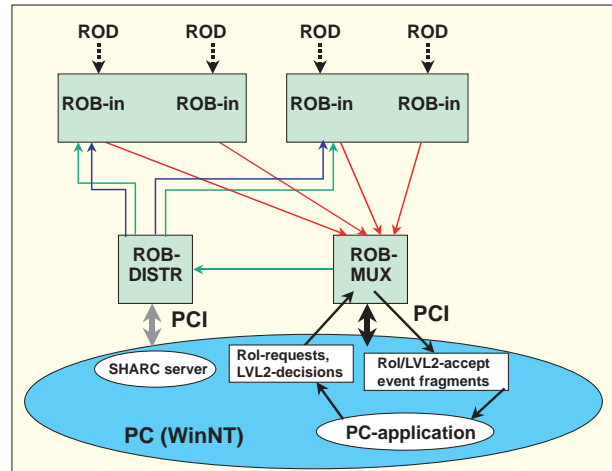


Figure 1.3: The structure of the ROB-in complex

### L3 Cosmics DAQ/LHCb outertracker DAQ

Both experiments run the software for the DAQ system in a real-time UNIX environment (LynxOS) in VME. The L3 experiment became operational during 1999 and is running smoothly now from the software point of view. The LHCb system has been used for limited periods in the test beam at CERN.

### ZEUS Vertex/HERMES

As a spin-off from the developments for the MDT chambers of ATLAS, CAN fieldbus systems are being installed for various control functions in the ZEUS Vertex and the HERMES detectors. In both cases the very same embedded CANopen software modules have been implemented as in the ATLAS control system.

## 2 Electronic Department

### 2.1 Introduction

Design and engineering activities are considered to be the main assignment of the Electronic Technology Group. The majority of the production is contracted out to specialized firms.

Development of the required skills is an item of continuous attention. New expertise-fields have to be mastered such as  $.25\mu\text{m}$  VLSI technology, fibre-optics technology, digital signal processors and still higher data rates. There is a permanent high claim on manpower and expertise (Fig. 2.1.)

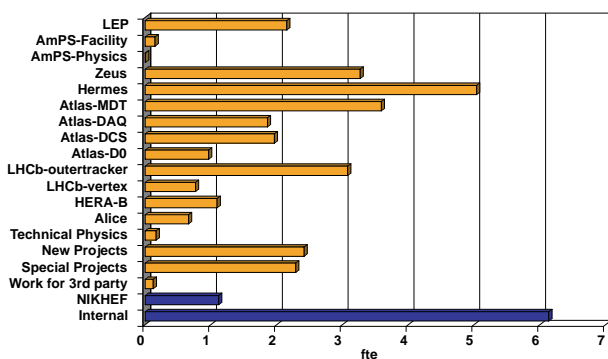


Figure 2.1: ET manpower distribution in 1999.

### 2.2 Projects

Information on the following projects can be found on the NIKHEF website <http://www.nikhef.nl/pub/departments/et/>

#### LEP/L3 Cosmics

For the upgrade of the L3 Cosmics-experiment to the full eighth octants of L3, a large amount of additional hardware has been produced. This production effort included 200 Cosmic Personality Cards [CPCv3] and 16 Nikhef Muon ReadOut Drivers [NIMROD] complete with Fanout-Cards and Patch-panels. The existing CPCv1's were modified to comply with the new CPCv3 versions. The upgrade and modifications were aiming mainly at clock stabilization and jitter reduction, as the internal delay-locked loop of the Time-to-Digital Converter (TDC32) proved to be extremely sensitive to the slightest clock jitter.

The Cosmic Timing and Trigger module (CTTv2) with enhanced trigger algorithms and Event/Trigger FIFO

for the trigger proved to work fine after initial tuning of various complicated and overlapping trigger settings.

Although the NIMROD still had minor problems after the spring 1999 installation, stable operation was reached in summer. To further enhance the data-rate handling capability of the NIMROD, the original memory chip on the NIMROD was replaced with a very high speed Zero Bus Turn-around (ZBT) type, now making the VME readout the data-rate limiting device in the electronics chain.

#### ZEUS Micro Vertex Detector

##### *The cooling system*

The detector consists of ladders with silicon detectors. The readout electronics produces about 650 W of heat. In order to keep the temperature of the detector and electronics stable at a value between  $13^\circ$  and  $15^\circ\text{C}$ , a cooling system had to be designed. The mechanical- and electronic departments have constructed a cooling system for this detector. A temperature measurement ((Fig. 2.2) system is capable of reading out about 60 NTC temperature sensors. The system connects the ZEUS MVD controls via a CANbus.

The controls of the cooling system have been done with a Siemens PLC. This PLC is also connected via a CANbus with the overall detector control system. The PLC is used to control and readout a number of valves, a water pump and a number of pressure and temperature sensors.

The silicon detectors consist of bare silicon chips. These chips are extremely sensitive to moisture, hence a number of humidity and water sensors have been used to detect water leaks.

##### *Analogue Link*

In the detector the HELIX chip is used as front-end chip. To minimize the dissipation, signals from the HELIX must be brought outside of the barrel and outside of the entire detector, before any signal processing can be done. It is decided to bring the signals to the cryotower area, where a patchbox is to be installed. From there the cable routing to the veto-wall area, where the data acquisition set-up is planned, is more relaxed. For reasons of accessibility, the patchbox should contain as little active components as possible.

The HELIX chip's unbalanced output signals are "analogue" and "dummy". These two signals are connected

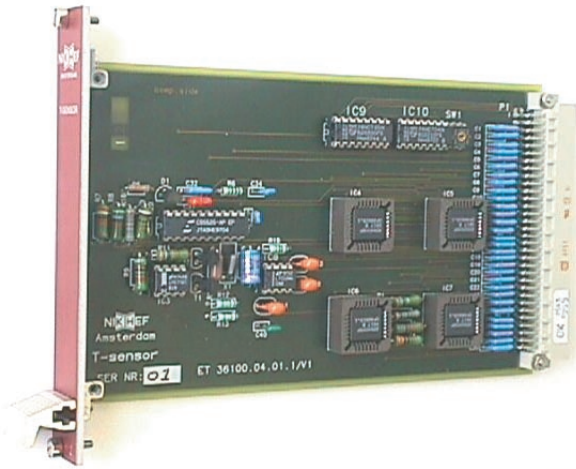


Figure 2.2: *Temperature measurement system without the sensors.*

to the two wires of a shielded twisted pair cable. Between the hybrids and the patchbox a very thin STP cable from Habia is used; between the box and the veto-wall area a Cat.5 cable is used. The main problem in signal transport lies in the properties of the cable and in the unusual way of using a STP cable for transporting two non-differential signals. Due to the very thin conductors, the resistive losses are high, and the skin effect is dominant for the used clock frequency and cable length. Symmetry of the cable is another point of concern. The nature of the production process causes the conductors to be of unequal diameter, length, resistance and impedance. As the “analogue” and “dummy” signals have to be subtracted at the end of the cable, all of these properties must be taken into account, and must be compensated for.

The termination of the cables should be correct between the two twisted wires, but also between each wire and shield. An analogue link module was developed. The module contains 16 channels. In total 206 channels are required; 15 modules will be produced in the year 2000. Each channel provides subtraction of the signals, thus forming the representation of the event in the silicon strip. From the ‘dummy’ signal a datastrobe for the ADC is generated. In the analogue part of the channel, amplification and compensation for the cable properties is performed. The output voltage is between 0 and 2 Volts into 50 Ohms, for an input signal between 0 and 10 MIPS. The overall performance of the cables and link module should be within 1% of the full-scale

range. Interpulse crosstalk will be within 1% of the stepsize. With a readout frequency of 10 MHz, the sample moment should be between 70 and 90 ns after the leading edge of the analogue signal on the link-modules input. The output noise level is less than 0.025 MIPS.

The above described way of signal handling is susceptible to noise. Therefore great care has been taken in designing the grounding and shielding scheme for the entire set-up. EMC and ESD safety have been taken into account from the beginning for mechanical parts as well as electronic circuits and cable routings.

### **HERMES Lambda Wheels**

The design of the electronics for the lambda wheels has been finalized. The production of the front-end hybrids, adc-modules and power supplies was contracted out to industry. In the shutdown period of May and June the first complete silicon detector module has been installed in the experiment setup. The module did not function at the nominal value of the beam current. This was due to the large electromagnetic fields leaking through the wakefield suppressor (WFS) that acts as a shield for the electron beam. Investigation of the problem was complicated by the fact that only once a month it was possible to access the module. Therefore a test setup was made to simulate the beam environment at NIKHEF.

With this setup it was possible to select the circuit configuration that is least sensitive to the rf-noise. The problem was finally tackled in December by three changes to the system. The sensitivity of the control signals was reduced, the contact of the spring-fingers of the WFS was improved to reduce the rf-leak at that point and an extra rf-screen was put in between the WFS contacts and the lambda wheels.

### **ATLAS**

#### *RASNIK*

RASNIK is used for the alignment of the large muon (MDT) chambers in ATLAS. A mask is projected on an image sensor and from the projected mask the adjustment parameters are determined. The basic electronics components of this system are an image sensor called RasCaM (Fig. 2.3) and a light source called RasLeD. The RasNiK system for the MDT Barrel chambers will need close to 5000 RasCaMs and 6000 RasLeDs.

Handling this large amount of basic components within the confined space of the MDT chambers is done with progressive layers of multiplexers. The first level

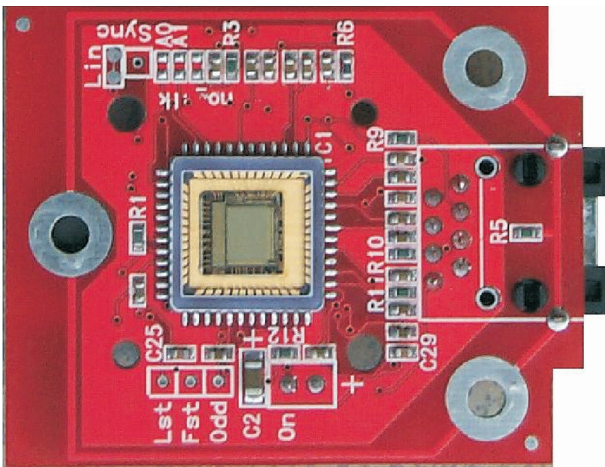


Figure 2.3: RASCAM ca. 4 x 5cm.

of multiplexing is the RasMuX (RasNiK Multiplexer). This RasMuX combines the limited number of RasNiK components (8 RasCaMs and 12 RasLeDs) of just one chamber. The second level of multiplexing is the MasterMuX, which combines the signals of 16 RasMuXs. The MasterMuX connects to USA15, the location where more multiplexers will finally deliver their signals to the PC-Based Video Digitizers.

This tree-like RasNiK structure distributes power and control from USA15 upwards in the system to the RasCaMs and RasLeDs and collects RasCaM signals from the chambers downwards to USA15 over single cable connections to/from the various RasNiK sub-components. The image sensor RasCaM design is centred around a commercial CMOS videocamera-IC, the VVL5430, with I2C controls for exposure-time and video-gain. It provides differential standard CCIR video output for a pixel array of 384 x 287 pixels and a LVDS pixel clock output. Therefore the image capture can be pixel synchronous for improved and more stable video digitization and enhanced spatial resolution. The RasCaM I/O uses a standard lowcost CAT5-SFTP network cable.

The light source RasLed uses nine special AlGaAs-LEDs which are proven to be tolerant for a long-term neutron radiation, expected in our application. These special LEDs are transparent substrate types. All other standard commercial Ir-LEDs failed the radiation tests.

For the various assembly stations of MDT chambers in Europe we have produced a number of prototype series of each of the above RasNiK components.

Distribution of complete RasMuX sets with RasCaMs, RasLeDs, cables and control and analyses software (Icaras) started in December 1999. The RasNiK prototype components have found alternative uses at the MDT assembly stations, i.e. the MDT Sphere Monitor and in the 'Wokkel' monitor, where the RasCaM is used with a standard lens.

## Dzero

The Dzero detector is one of the two general-purpose detectors at the Tevatron accelerator and storage ring, in which protons and anti-protons are accelerated and collided.

A magnetic field measurement system has been designed for the 2T solenoidal superconducting magnet. This system is constructed by the electronic department as a pilot project for the field measurement system of the ATLAS detector. The height of the magnetic field sensor for the Dzero detector has to be kept within 4 mm (Fig. 2.4). In order to measure not only the strength but also the direction of the magnetic field, each magnetic field probe consists of three hall sensors placed perpendicularly to each other. Because of the strong temperature dependency of the Hall effect, the temperature of the magnetic field probe is measured with a NTC temperature sensor (negative temperature coefficient).

Since the electric signals of the hall sensors are very small, a signal conditioner is placed close to the magnetic field probe. The signal-conditioner digitizes the analogue signals from the hall sensors and the temperature sensor. The digital information is read out via a CAN field bus, a solution pioneered by NIKHEF for the ATLAS MDT detector. Each signal conditioner can read out three magnetic field probes.

The probes are designed in cooperation with the Magnet Lab of CERN and will also be calibrated there.

## Data Acquisition and Triggering

### ROB Complex

The front-end electronics of the various detector parts will send their data via a Read-Out Driver (ROD) over a 1 Gbit/s optical Read-Out Link (ROL) to a Read-Out Buffer (ROB). A total of 1500 - 2000 ROLs are foreseen. After a Level-1 trigger decision, the front-end electronics will send its data via a ROD to a ROB. The ROB must buffer the data during the time the Level-2 trigger system is processing the data. When accepted, the data will be requested by the Event Filter for further processing. When rejected, the data is deleted.

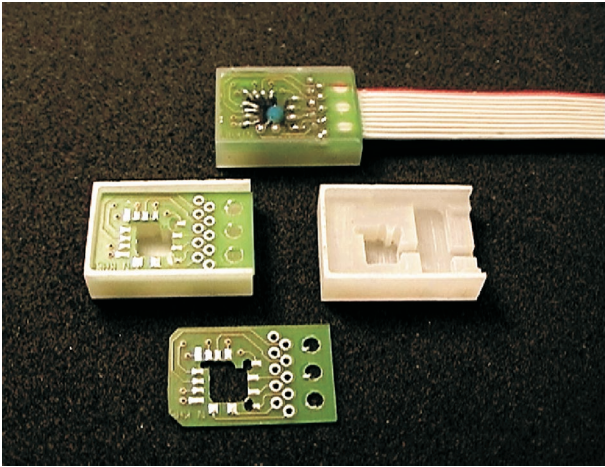


Figure 2.4: *The Hall probes to be installed within the central solenoid of the D0 experiment for magnetic field strength monitoring. (15 × 10 × 4 mm)*

The ROB Complex module contains multiple ROB-in parts, a ROB controller part and a ROB-out part. Each ROB-in is connected to a ROL and performs the actual buffering of the data. The ROB controller manages the ROB-Complex and handles requests for data or monitoring information. The ROB-out sends data over a network interface to the Level-2 trigger-system or the Event Filter.

After the design and successful test of a NIKHEF prototype ROB-in (the CRUSH module), a combined ROB-controller/ROB-out prototype was defined; the ShaSLINK module.

#### *ShaSLINK*

ShaSLINK, an acronym for SHARC S-LINK, consists of an S-LINK output-interface, a PCI-bus interface (implemented with the PLX-9054) and a 40 MHz SHARC processor. From the SHARC processor the data rate to the S-LINK is 160 MByte/s which is the maximum rate for the S-LINK. For data exchange between SHARC and PCI-bus the maximum 132 Mbytes/s data rate of the PCI-bus is possible by using the DMA controllers of the SHARC.

The ShaSLINK is used as a prototype S-LINK output-module for the MDT Read-Out Driver (MROD) of the muon-chambers.

The design was finished and 5 modules have been build and tested successfully.

#### *MROD-0/MCRUSH*

The MROD has to build event fragments from the data of 6 muon-chambers and send the results to the ROB. On each chamber the data of at maximum 18 TDCs will be multiplexed on one S-LINK by a Chamber Service Module (CSM). So the MROD will have 6 S-LINK inputs and one S-LINK output to the ROB.

A first prototype MROD-0 has been designed. This module consists of 6 MCRUSH modules and one ShaSLINK module. The MCRUSH module is a modified CRUSH module. The field programmable gate array (FPGA) on the CRUSH is reprogrammed with a totally different functionality.

Via its S-LINK input the MCRUSH handles the data produced by the TDCs on a muon-chamber, to do event building, signal various error conditions and potentially recover from errors. Output data from 6 MCRUSH modules must be fed through S-Links to the ShaSLINK module of the MROD-0, where further event building is performed and the resulting event fragments are send via the S-LINK output to the ROB.

The redesign of the functionality of the FPGA on the MCRUSH is finished and good first test results have been obtained.

### **B-Physics**

#### *HERA-B Outer tracker*

The production of the First Level Trigger-LinkBoard is finished. After installation some boards need fine-tuning or have problems with a chip. Twenty boards needed a timing modification for the muon pixel detector.

#### *LHCb Outer tracker*

A new set of chamber prototypes has been prepared, one with Kapton straws and one foam plate type. Using the existing 512 channel DAQ-system we helped testing these chambers in CERN in May. There was still some trouble with the DAQ-system, but the data has proven to be useful to check primary characteristics of the chambers.

Work is done on a pre-design for the future TDC-board, with Level-0 and Level-1 buffers. The chip will be a successor of the TDC32-chip, presently used in the beam tests.

A proposal is worked out for the electronics in the LHCb magnet, where the total space allowed for electronics, cabling and the gas system is only 10 cm high. This

space has large consequences for the maximum power consumption.

As the newly tested Kapton straws give good results, an investigation of the electrical properties was performed, also using straws with an aluminium layer in the hope to reduce cross talk even further. This work will result in the final choice for the best sensor-straw for the outer-tracker.

In collaboration with the electronics department of the Beijing Institute for High Energy Physics we developed some testers. With the Krakow Institute of Nuclear Physics we just started to develop new front-end coupling boards to compress the data going to the readout units.

#### LHCb Vertex

The BEETLE chip, a design programme of the ASIC Labor of Heidelberg, is a front-end chip for the LHCb Vertex detector. The design is done in deep sub-micron technology to achieve a better radiation hardness. It exists of an amplifier, comparator, analogue memory and an analogue multiplexer to the output (Fig. 2.5). For these functional blocks a number of control blocks are implemented for control and communication purposes.

Several institutes, included NIKHEF participate in the design.

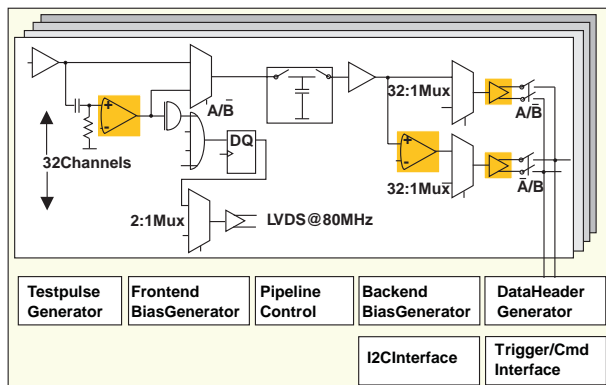


Figure 2.5: Principle of the BEETLE-chip.

NIKHEF takes care of the comparator and buffering of the analogue signals from multiplexer to output. Several prototype chips have been developed to test the individual functional blocks.

#### Alice

The electronics department has been involved in the project since 1999. She will design a part of the control

and interface electronics for the Silicon Strip Detector (SSD) layer in the Alice Inner Tracker in coordination with NIKHEF-Utrecht. The SSD has been built of low mass ladder structures with detector and front-end electronics on it. On both ends will be placed an 'EndCap' module, which is the interface with the detector electronics. The module provides the following functions; prevention of single event latchup burnout of the front-end chips, buffering of the control signal inputs and the analogue outputs, multiplexing of signals and regulated power supply.

There are stringent power- and mass budgets to fulfil in a narrow space.

## 2.3 New Projects

### Antares

In the initial phase of the Antares-project research is done on some system issues as data transmission and master timing distribution. Our attention focuses on the offshore trigger limitations due to the very high 40K and biological background environment. As a result the so called All Data To Shore concept was presented in the Antares collaboration meeting. In this concept the need of having offshore hardware and firmware for a trigger selection mechanism is replaced by a more flexible processor farm on shore. In addition anticipation of now unforeseeable trigger selection requirements can then more easily be implemented on shore. These ideas are reflected in the Conceptual Design Report, produced by the collaboration in the fall of '99. From then on a process of testing two concepts was started in the electronics department. Both are based on fibre optics techniques. The first one tests the principle of using a passive data-concentrator with help of multiple wave length multiplexers. The second one consists of a feasibility study of measuring the propagation delay properties in the offshore clock signal distribution system.

In the prologue to a Technical Design Report both concepts have to be completed in spring 2000.

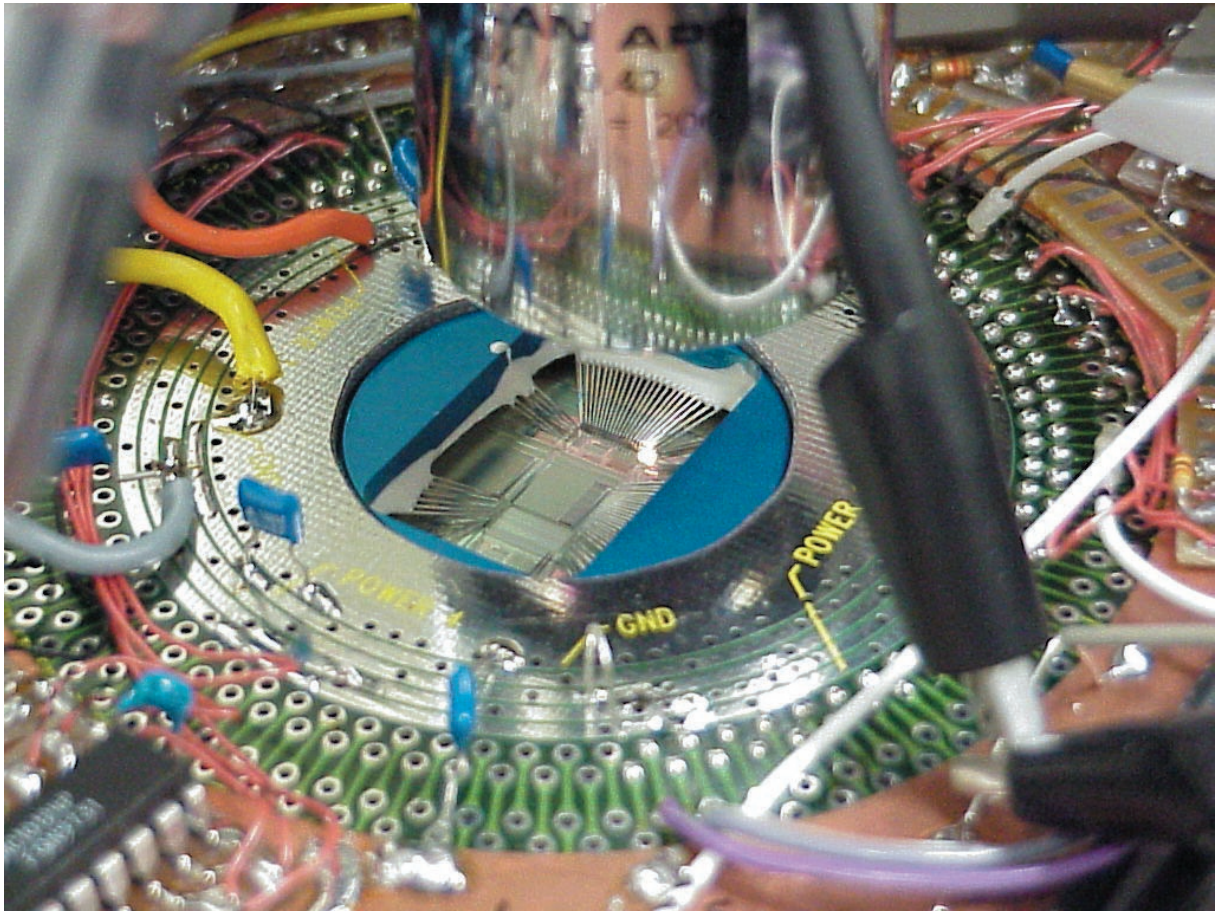


Figure 2.6: *Impression of the probestation.*

## 2.4 Special projects

### MEAmPS decommissioning

In cooperation with the customers there has been intensive expertise and documentation transfer. JINR technicians have been helped to dismantle the facility in such a way that transport and reconstruction is possible.

### Infra-structure

#### *Electronic Design Automation*

The newly acquired Leonardo logic synthesis software was successfully used within the Hermes lambdawheel and the ATLAS data acquisition project. Also a remotely accessible fast PC with a large amount of memory was bought to meet the needs for the FPGA software.

The large number of gates in the FPGA (now 1 - 2 million) requires multiple designers working on the implementation of a design. To integrate the design environment, we evaluated Mentor Graphics Electronic Design Automation flow and the use of revision control tools such as RCS and CLEARCASE.

#### *VLSI (Very Large Scale Integration)*

There is a growing expertise on VLSI available in the electronics department major due to the commitment in three projects. The first project is already mentioned in the section of LHCb Vertex. The other projects are partly generic developments. The Helix front-end IC's are produced by Austria Micro Systems for the Hermes and the ZEUS detector. The wafers have been tested at NIKHEF. The dicing has been contracted out. For wafer testing a semi-automatic probestation has been purchased (Fig. 2.6.) The wafers are changed manually and the probestation automatically steps from chip to chip. Test equipment has been developed with input/output generation under computer control.

Another development is the design of a Low Noise Amplifier to amplify signals from a silicon-strip detector for vertex detectors. Two kinds of amplifiers have been designed to test the behaviour due to radiation, since it changes the properties of a circuit. Special layout structures, i.e. 'gate-around' and extra isolation (guard rings, (Fig. 2.7) between the transistors, reduce the disadvantageous effects.

#### *PCB layout system*

The use of the Ultimate Printed Circuit Board software is extended. A more low-end system has been installed such that more people, even trainees are able to design

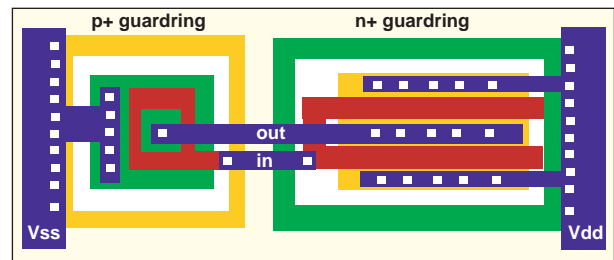


Figure 2.7: Guard rings in chip design.

a PCB-layout in a short time. Some work has been contracted out. Due to the necessary interaction between designer and layouter this is only efficient if the communication between layout firm and layouter uses a platform such as Mentor Graphic.

## 3 Mechanical Technology

### 3.1 Introduction

Numerous instrumentation projects demanded in 1999 manpower and specific expertise from the Mechanical Technology department. In fig. 3.1 the projects are listed that consumed  $\geq 0.5$  FTE. In general ATLAS is the main absorber of the resources among the various projects.

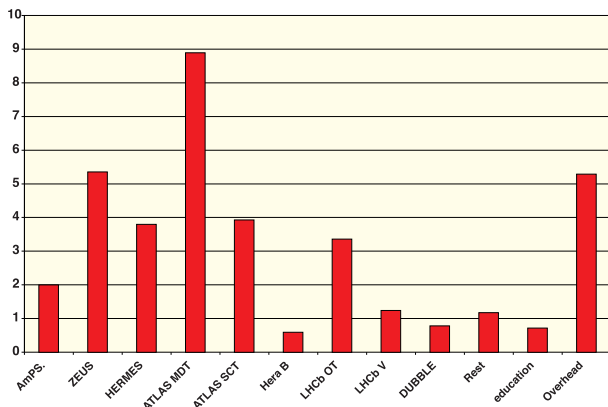


Figure 3.1: Distribution of manpower of MT in 1999 over the most important projects.

### 3.2 Projects in exploitation

#### L3

The L3 muon chambers had, like in previous years, to be repaired due to aging effects.

#### MEA/AmPS

Specialized expertise has been invested in dismantling MEA/AmPS, while installation experts assisted in the preparation of equipment for transportation to Dubna.

#### Hermes

The Hermes Vertex detector at DESY, consisting of Micro Strip Gas Counters, was dismantled and transported to NIKHEF in order to replace chips that were malfunctioning due to aging.

#### FWI, WINS

Approximately one man-year was invested in robot technology.

#### ATLAS Muon chambers

In order to optimize the production site for the precision



Figure 3.2: A view of the production site of the muon precision chambers.

muon chambers in the cleanroom many tools have been designed and manufactured. Quality control of the jigs was realized by precision measurements with the 3-D survey machine. Extensive tests have also been done on this apparatus in order to determine a reliable way of positioning the jigs on the granite table (Fig. 3.2). This recipe was successfully used for the assembly in the cleanroom. Subsequently the positioning of the space-frame has been checked. At the end of 1999 we were ready for the assembly of the first layer of tubes. All auxiliary equipment for the assembly is being prepared, while at CERN the wiring machine is being finalized.

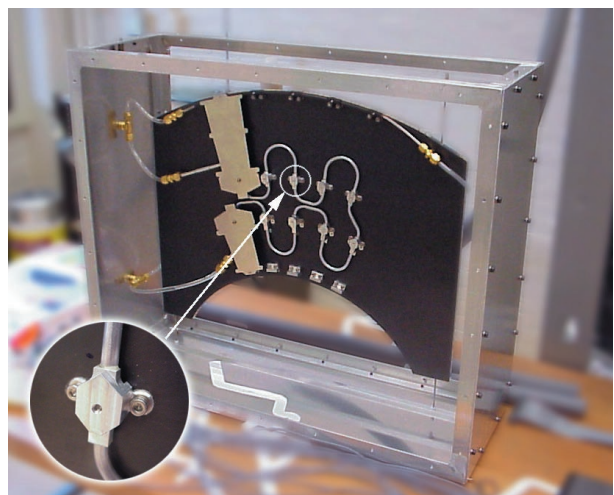


Figure 3.3: A test setup for the wiggly pipe on the disc for the inner detector of ATLAS.

Many assembly tools such as the vacuum system, the high-pressure supply for the crimping tool, the glueing equipment and the quality control setup were designed and partly manufactured. A machine has been constructed with which the wire position within the tube can be determined. Two systems for the control of the leak tightness have been manufactured and tested.

## ATLAS SCT

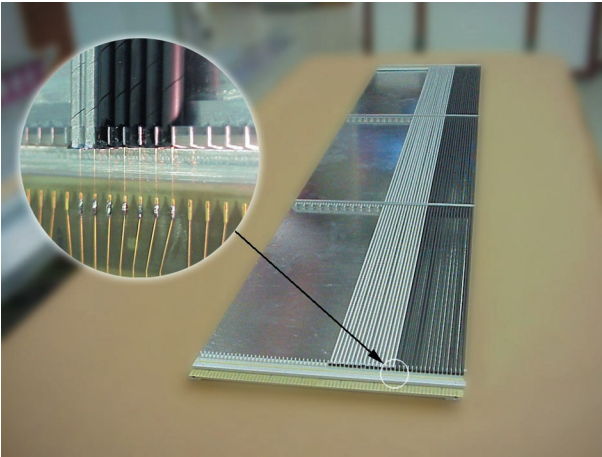


Figure 3.4: An impression of the straw tube chambers for the outer tracker. The inset shows the way the wires are led from the straw to the electronics.

Many aspects such as cooling, frequency behaviour, minimum mass and stability have influence on the construction of the discs. Investigations of heat flow patterns and mounting devices have been performed. Carbon fibre prototype constructions have been build in order to measure stiffness and eigen frequencies. By building a mock up (see Fig. 3.3) the fixation and positioning of a prototype disc into a support cylinder have been studied. A number of decisions concerning the cooling have to be made within the collaboration, in order to be able to continue with the design.

## D0

Twenty Roman Pot constructions have been build following our accepted design. Also the stands for the Forward Proton Detector have been manufactured and sent to FERMI lab.

## LHCb Outer tracker

As one of the baseline solutions kapton straws have been chosen (Fig. 3.4). Several prototypes have been constructed and tested in the beam at CERN. Some problems still have to be solved such as moisture influ-

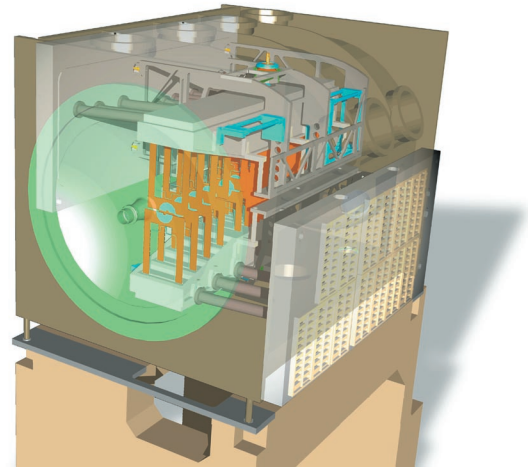


Figure 3.5: A simulation of the LHCb vertex detection chamber. In the center the movable upper and lower halves, containing the silicon detectors, are visible.

ences, stiffness and space, especially for the chambers that will be positioned inside the magnet. Solutions for the electromagnetic effects are also under investigation. Some of the prototypes have proven to withstand the aging tests and are accepted.

## LHCb Microvertex

The design for the vertex detector has made considerable progress. Its vacuum aspects have been presented to the collaboration and at the European Vacuum Conference. Still some vacuum, high frequency, cooling and mechanical problems have to be solved and accepted by the CERN experts. The fact that the silicon detectors have to be retracted during injection forms a major design complication. A prototype of the vacuum tank and its detectors is being designed in order to test vacuum characteristics of the full-scale model. (see Fig. 3.5).

## HERMES

The Lambda wheels have been installed in the HERMES experiment with one of the detector modules present (Fig. 3.6). This served as a test module in particular for the noise generated by the beam. Several beam runs were necessary to find the solution concerning the optimal screening of the detector. Production of the final module assembly is started.

## ZEUS Microvertex

Building the carbon support structures appeared to be a very complicated and therefore time consuming activity.

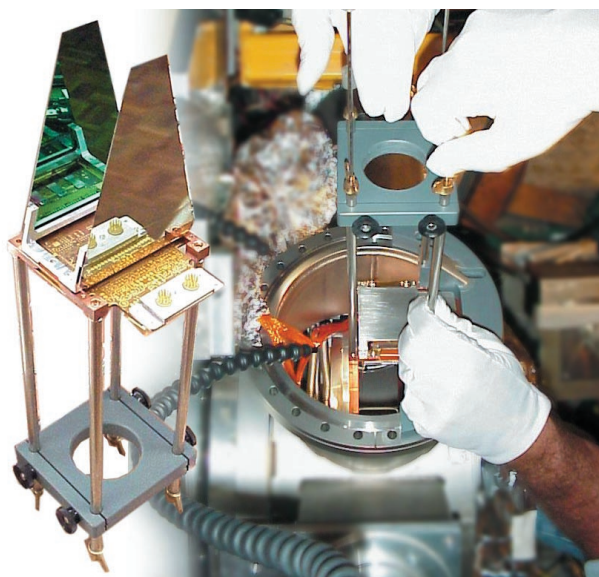


Figure 3.6: *Mounting of the silicon modules in the lambda wheels of HERMES.*

The automated positioning machine for the modules on the ladder was constructed and calibrated and is ready for production. The support frames are ready (Fig. 3.7) The production of the ladders will start as soon as the modules arrive. The protection tube for the modules during installation is in production.

### ALICE

In collaboration with the University of Utrecht we contribute to the ALICE detector. General engineering support will be delivered as well as the design of the assembly tooling. A preliminary study has been performed and resulted in accepted ideas for an automated positioning of the silicon detectors.

### 3.3 Projects for third parties

#### ATLAS end cap

The MT department contributed to the optimization of the vacuum chamber design made by Rutherford Laboratory. With Dutch manufacturers the manufacturing aspects of the vessel and the cold mass are discussed.

#### DUBBLE

Various constructions for the beam line have not only been designed but also manufactured and tested in our department (the EXAFS sample and detection station, see Fig. 3.8) The assembly of the mirrorboxes and the monochromator is finalized and the installation and

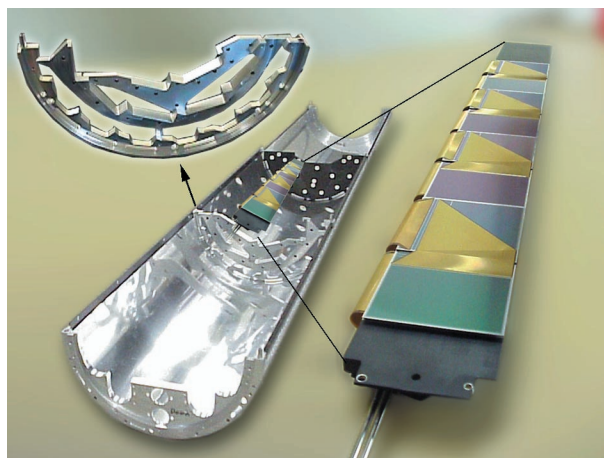


Figure 3.7: *The support frame for the ZEUS microvertex.*

alignment is prepared. A study of the mirror bending mechanism is finished and resulted in a report with recommendations. Design work on the experimental setup in Grenoble at ESRF is still ongoing.

#### VISIR

The tasks between NIKHEF and ASTRON were divided in such a way that NIKHEF was contributing the expertise for the temperature and mechanical stability of a detector module in an environment of 40K. The cryogenic aspects were formulated in a model with which modifications in the setup quickly can be evaluated. On the basis of the mechanical model the dimensions and

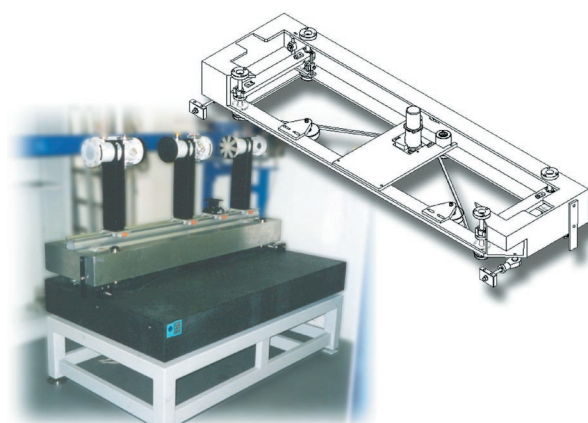


Figure 3.8: *The sample stage for the DUBBLE beam-line.*

the material were chosen. A Project Readiness Review was held in Saclay, ASTRON and NIKHEF and resulted in the go signal for the production.

### AMS

We joined several progress meetings of the AMS collaboration in order to select a topic to which NIKHEF could contribute. Prospects for becoming a collaborator are promising.

## 3.4 Developments within the Mechanical Technology group

### Wire relaxation

Fundamental mechanical research was done by studying the wire tension in a detector over a long period. The required sensitivity and stability in time is on the, challenging, sub micron level (see Fig. 3.9)

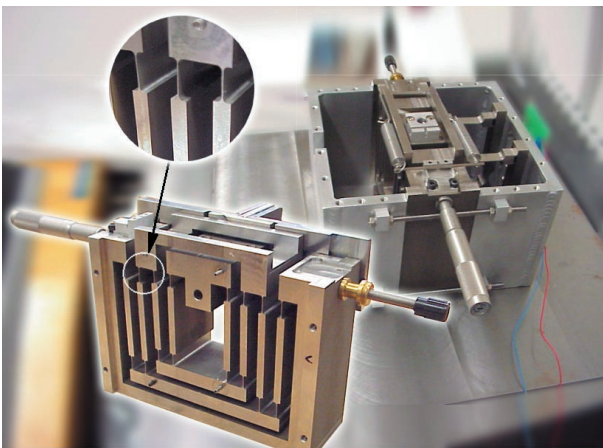


Figure 3.9: *The construction for the measurement of the wire relaxation.*

### Desorption measurements for vertex detectors

Vertex detector technologies are evolving gradually in the direction of measuring impact positions very close to the interaction point. This implies that electronics is present inside the vacuum system. We developed an apparatus with which one is able to determine desorption levels in the order of  $10^{-9}$  mbarl/sec/cm<sup>2</sup>.

### Bonding expertise

As a consequence of the involvement in chip technology we developed knowledge on bonding techniques for the connections of the electronics to the silicon stripdetectors (Fig. 3.10)

### Education program

In our group we substantially increased the knowledge level on thermal modelling, design and manufacturing of carbon structures, management and computer aided manufacturing.



Figure 3.10: *The connection of the silicon to the electronics. The inset shows the ultrasonic process of connecting the 17 micron thick wires.*

# F Publications, Theses and Seminars

## 1 Publications

- [1] P. Abreu, *et al.*, H.M. Blom, E. Boudinov, D. Holthuisen, N. Kjaer, P. Kluit, M. Mulders, J. Timmermans, D.Z. Toet, G.W. van Apeldoorn, P. van Dam, J. van Eldik, I. van Vulpen, DELPHI Collaboration  
*Search for composite and exotic fermions at LEP 2*  
Eur. Phys. J. **C8** (1999) 41-58
- [2] P. Abreu, *et al.*, H.M. Blom, E. Boudinov, N. Kjaer, P. Kluit, M. Mulders, D. Reid, J. Timmermans, G.W. van Apeldoorn, P. van Dam, J. van Eldik, I. van Vulpen, DELPHI Collaboration  
*W pair production cross-section and W branching fractions in  $e^+e^-$  interactions at 183 GeV*  
Phys. Lett. **B456** (1999) 310-321
- [3] P. Abreu, *et al.*, H.M. Blom, E. Boudinov, N. Kjaer, P. Kluit, M. Mulders, D. Reid, J. Timmermans, G.W. van Apeldoorn, P. van Dam, J. van Eldik, I. van Vulpen, DELPHI Collaboration  
*Energy dependence of event shapes and of  $\alpha_s$  at LEP 2*  
Phys. Lett. **B456** (1999) 322-340
- [4] P. Abreu, *et al.*, H.M. Blom, E. Boudinov, N. Kjaer, P. Kluit, M. Mulders, D. Reid, J. Timmermans, G.W. van Apeldoorn, P. van Dam, J. van Eldik, I. van Vulpen, DELPHI Collaboration  
*Multiplicity fluctuations in one- and two-dimensional angular intervals compared with analytic QCD calculations*  
Phys. Lett. **B457** (1999) 368-382
- [5] P. Abreu, *et al.*, H.M. Blom, E. Boudinov, N. Kjaer, P. Kluit, M. Mulders, D. Reid, J. Timmermans, G.W. van Apeldoorn, P. van Dam, J. van Eldik, I. van Vulpen, DELPHI Collaboration  
*Search for the Higgs boson in events with isolated photons at LEP2*  
Phys. Lett. **B458** (1999) 431-446
- [6] P. Abreu, *et al.*, H.M. Blom, E. Boudinov, D. Holthuisen, N. Kjaer, P. Kluit, M. Mulders, J. Timmermans, D.Z. Toet, G.W. van Apeldoorn, P. van Dam, J. van Eldik, I. van Vulpen, DELPHI Collaboration  
*Measurement of  $A_{FB}^{b\bar{b}}$  in hadronic Z decays using a jet charge technique*  
Eur. Phys. J. **C9** (1999) 367-381
- [7] P. Abreu, *et al.*, H.M. Blom, E. Boudinov, N. Kjaer, P. Kluit, M. Mulders, D. Reid, J. Timmermans, G.W. van Apeldoorn, P. van Dam, J. van Eldik, I. van Vulpen, DELPHI Collaboration  
*A search for invisible Higgs bosons produced in  $e^+e^-$  interactions at LEP 2 energies*  
Phys. Lett. **B459** (1999) 367-381
- [8] P. Abreu, *et al.*, H.M. Blom, E. Boudinov, N. Kjaer, P. Kluit, M. Mulders, D. Reid, J. Timmermans, G.W. van Apeldoorn, P. van Dam, J. van Eldik, I. van Vulpen, DELPHI Collaboration  
*Measurements of the Trilinear Gauge Boson Couplings  $WWV$  ( $V \equiv \gamma, Z$ ) in  $e^+e^-$  Collisions at 183 GeV*  
Phys. Lett. **B459** (1999) 382-396
- [9] P. Abreu, *et al.*, H.M. Blom, E. Boudinov, N. Kjaer, P. Kluit, M. Mulders, D. Reid, J. Timmermans, G.W. van Apeldoorn, P. van Dam, J. van Eldik, I. van Vulpen, DELPHI Collaboration  
*Energy Dependence of Inclusive Spectra in  $e^+e^-$  Annihilation*  
Phys. Lett. **B459** (1999) 397-411
- [10] P. Abreu, *et al.*, H.M. Blom, E. Boudinov, N. Kjaer, P. Kluit, M. Mulders, D. Reid, J. Timmermans, G.W. van Apeldoorn, P. van Dam, J. van Eldik, I. van Vulpen, DELPHI Collaboration  
*Search for charged Higgs bosons at LEP 2*  
Phys. Lett. **B460** (1999) 484-497
- [11] P. Abreu, *et al.*, H.M. Blom, E. Boudinov, N. Kjaer, P. Kluit, M. Mulders, D. Reid, J. Timmermans, G.W. van Apeldoorn, P. van Dam, J. van Eldik, I. van Vulpen, DELPHI Collaboration  
*Measurement of the mass of the W boson using direct reconstruction at  $\sqrt{s} = 183$  GeV*  
Phys. Lett. **B462** (1999) 410-424
- [12] P. Abreu, *et al.*, H.M. Blom, E. Boudinov, N. Kjaer, P. Kluit, M. Mulders, D. Reid, J. Timmermans, G.W. van Apeldoorn, P. van Dam, J. van Eldik, I. van Vulpen, DELPHI Collaboration  
*Measurement of the rate of  $b\bar{b}b\bar{b}$  events in hadronic Z decays and the extraction of the gluon splitting into  $b\bar{b}$*   
Phys. Lett. **B462** (1999) 425-439
- [13] P. Abreu, *et al.*, H.M. Blom, E. Boudinov, N. Kjaer, P. Kluit, M. Mulders, D. Reid, J. Timmermans, G.W. van Apeldoorn, P. van Dam, J. van Eldik, I. van Vulpen, DELPHI Collaboration  
*A precise measurement of the partial decay width ratio  $R_b^0 = \Gamma_{b\bar{b}}/\Gamma_{had}$*   
Eur. Phys. J. **C10** (1999) 415-442
- [14] P. Abreu, *et al.*, H.M. Blom, E. Boudinov, N. Kjaer, P. Kluit, M. Mulders, D. Reid, J. Timmermans, G.W. van Apeldoorn, P. van Dam, J. van Eldik, I. van Vulpen, DELPHI Collaboration  
*Measurement of the lifetime of b-baryons*  
Eur. Phys. J. **C10** (1999) 185-199
- [15] P. Abreu, *et al.*, H.M. Blom, E. Boudinov, N. Kjaer, P. Kluit, M. Mulders, D. Reid, J. Timmermans, G.W. van Apeldoorn, P. van Dam, J. van Eldik, I. van Vulpen, DELPHI Collaboration  
*Measurements of the leptonic branching fractions of the tau*  
Eur. Phys. J. **C10** (1999) 201-218
- [16] P. Abreu, *et al.*, H.M. Blom, E. Boudinov, N. Kjaer, P. Kluit, M. Mulders, D. Reid, J. Timmermans, G.W. van Apeldoorn, P. van Dam, J. van Eldik, I. van Vulpen, DELPHI Collaboration  
*Measurement of the forward backward asymmetry of c and b quarks at the Z pole using reconstructed D mesons*  
Eur. Phys. J. **C10** (1999) 219-237
- [17] P. Abreu, *et al.*, H.M. Blom, E. Boudinov, N. Kjaer, P. Kluit, M. Mulders, D. Reid, J. Timmermans, G.W. van Apeldoorn, P. van Dam, J. van Eldik, I. van Vulpen, DELPHI Collaboration  
*Search for neutral Higgs bosons in  $e^+e^-$  collisions at  $\sqrt{s} = 183$  GeV*  
Eur. Phys. J. **C10** (1999) 563-604
- [18] P. Abreu, *et al.*, H.M. Blom, E. Boudinov, N. Kjaer, P. Kluit, M. Mulders, D. Reid, J. Timmermans, G.W. van Apeldoorn, P. van Dam, J. van Eldik, I. van Vulpen, DELPHI Collaboration  
*Search for charginos nearly mass-degenerate with the lightest neutralino*  
Eur. Phys. J. **C11** (1999) 1-17
- [19] P. Abreu, *et al.*, H.M. Blom, E. Boudinov, N. Kjaer, P. Kluit, M. Mulders, D. Reid, J. Timmermans, G.W. van Apeldoorn, P. van Dam, J. van Eldik, I. van Vulpen, DELPHI Collaboration  
*Search for chargino pair production in scenarios with gravitino LSP and stau NLSP at  $\sqrt{s} \sim 183$  GeV at LEP*  
Phys. Lett. **B466** (1999) 61-70
- [20] P. Abreu, *et al.*, H.M. Blom, E. Boudinov, N. Kjaer, P. Kluit, M. Mulders, D. Reid, J. Timmermans, G.W. van Apeldoorn, P. van Dam, J. van Eldik, I. van Vulpen, DELPHI Collaboration  
*Measurement and interpretation of fermion-pair production at LEP energies from 130 to 172 GeV*  
Eur. Phys. J. **C11** (1999) 383-407
- [21] P. Abreu, *et al.*, A. Augustinus, E. Boudinov, D. Holthuisen, N. Kjaer, P. Kluit, M. Mulders, M. Nieuwenhuizen, J. Timmermans, D.Z. Toet, G.W. van Apeldoorn, P. van Dam, J. van Eldik, DELPHI Collaboration  
*Measurement of the quark and gluon fragmentation functions in  $Z^0$  hadronic decay*  
Eur. Phys. J. **C6** (1999) 19-33
- [22] P. Abreu, *et al.*, H.M. Blom, E. Boudinov, N. Kjaer, P. Kluit, M. Mulders, D. Reid, J. Timmermans, G.W. van Apeldoorn, P. van Dam, J. van Eldik, I. van Vulpen, DELPHI Collaboration

- The Scale Dependence of the Hadron Multiplicity in Quark and Gluon Jets and a Precise Determination of  $C_A/C_F$*   
Phys. Lett. **B449** (1999) 383-400
- [23] P. Abreu, et al., H.M. Blom, E. Boudinov, D. Holthuisen, N. Kjaer, P. Kluit, M. Mulders, J. Timmermans, D.Z. Toet, G.W. van Apeldoorn, P. van Dam, J. van Eldik, I. van Vulpen, DELPHI Collaboration  
*Search for lightest neutralino and stau pair production in light gravitino scenarios with stau NLSP*  
Eur. Phys. J. **C7** (1999) 595-607
- [24] P. Abreu, et al., H.M. Blom, E. Boudinov, D. Holthuisen, N. Kjaer, P. Kluit, M. Mulders, J. Timmermans, D.Z. Toet, G.W. van Apeldoorn, P. van Dam, J. van Eldik, I. van Vulpen, DELPHI Collaboration  
*Search for pair-produced neutralinos in events with photons and missing energy from  $e^+e^-$  collisions at  $\sqrt{s}=130$ -183 GeV*  
Eur. Phys. J. **C6** (1999) 371-384
- [25] P. Abreu, et al., H.M. Blom, E. Boudinov, D. Holthuisen, N. Kjaer, P. Kluit, M. Mulders, J. Timmermans, D.Z. Toet, G.W. van Apeldoorn, P. van Dam, J. van Eldik, I. van Vulpen, DELPHI Collaboration  
*Search for scalar fermions and long-lived scalar leptons at centre-of-mass energies of 130 GeV to 172 GeV*  
Eur. Phys. J. **C6** (1999) 385-401
- [26] P. Abreu, et al., H.M. Blom, E. Boudinov, D. Holthuisen, N. Kjaer, P. Kluit, M. Mulders, J. Timmermans, D.Z. Toet, G.W. van Apeldoorn, P. van Dam, J. van Eldik, I. van Vulpen, DELPHI Collaboration  
*Search for Leptoquarks and FCNC in  $e^+e^-$  annihilations at  $\sqrt{s}=183$  GeV*  
Phys. Lett. **B446** (1999) 62-74
- [27] P. Abreu, et al., H.M. Blom, E. Boudinov, D. Holthuisen, N. Kjaer, P. Kluit, M. Mulders, J. Timmermans, D.Z. Toet, G.W. van Apeldoorn, P. van Dam, J. van Eldik, I. van Vulpen, DELPHI Collaboration  
*Search for charginos, neutralinos and gravitinos in  $e^+e^-$  interactions at  $\sqrt{s}=183$  GeV*  
Phys. Lett. **B446** (1999) 75-91 erratum Phys. Lett. **B451** (1999) 447-449
- [28] P. Abreu, et al., H.M. Blom, E. Boudinov, N. Kjaer, P. Kluit, M. Mulders, D. Reid, J. Timmermans, G.W. van Apeldoorn, P. van Dam, J. van Eldik, I. van Vulpen, DELPHI Collaboration  
*Study of the four-jet anomaly observed at LEP centre-of-mass energies of 130 and 136 GeV*  
Phys. Lett. **B448** (1999) 311-319
- [29] P. Abreu, et al., H.M. Blom, E. Boudinov, N. Kjaer, P. Kluit, M. Mulders, D. Reid, J. Timmermans, G.W. van Apeldoorn, P. van Dam, J. van Eldik, I. van Vulpen, DELPHI Collaboration  
*Measurement of Inclusive  $p^0$ ,  $f_0(980)$ ,  $f_2(1270)$ ,  $K_2^{*0}(1430)$  and  $f_2'(1525)$  Production in  $Z^0$  Decays*  
Phys. Lett. **B449** (1999) 364-382
- [30] P. Abreu, et al., N. Kjaer, M. Mulders  
*The Estimation of the Effective Centre of Mass Energy in  $q\bar{q}\gamma$  Events from DELPHI*  
Nucl. Instr. Meth. **A427** (1999) 487-494
- [31] P. Abreu, et al., H.M. Blom, E. Boudinov, P. Kluit, M. Mulders, D. Reid, J. Timmermans, P. van Dam, J. van Eldik, I. van Vulpen, DELPHI Collaboration  
*Two-dimensional Analysis of the Bose-Einstein Correlations in  $e^+e^-$  Annihilations at the  $Z^0$  Peak*  
Phys. Lett. **B471** (1999) 460-470
- [32] M. Acciarri, et al., G.J. Bobbink, A. Buijs, A.P. Colijn, J.A. van Dalen, D. van Dierendocnk, P. Duinker, F.C. Ern , R. van Gulik, P. de Jong, W. Kittel, A.C.K. K nig, F.L. Linde, D. Mangeol, G.G.G. Massaro, W.J. Metzger, A.J.M. Muijs, B. Petersen, T. van Rhee, M.P. Sanders, D. J. Schotanus, C. Timmermans, H. Wilkens, L3 Collaboration  
*Measurement of an elongation of the pion source in Z decays*  
Phys. Lett. **B458** (1999) 517-528
- [33] M. Acciarri, et al., G.J. Bobbink, A. Buijs, A.P. Colijn, J.A. van Dalen, D. van Dierendocnk, P. Duinker, F.C. Ern , R. van Gulik, P. de Jong, W. Kittel, A.C.K. K nig, F.L. Linde, D. Mangeol, G.G.G. Massaro, W.J. Metzger, A.J.M. Muijs, B. Petersen, T. van Rhee, M.P. Sanders, D. J. Schotanus, C. Timmermans, H. Wilkens, L3 Collaboration  
*Search for R-parity Violating Chargino and Neutralino Decays in  $e^+e^-$  Collisions up to  $\sqrt{s}=183$  GeV*  
Phys. Lett. **B456** (1999) 354-366
- [34] M. Acciarri, et al., G.J. Bobbink, A. Buijs, A.P. Colijn, J.A. van Dalen, D. van Dierendocnk, P. Duinker, F.C. Ern , R. van Gulik, P. de Jong, W. Kittel, A.C.K. K nig, F.L. Linde, D. Mangeol, G.G.G. Massaro, W.J. Metzger, A.J.M. Muijs, B. Petersen, T. van Rhee, M.P. Sanders, D. J. Schotanus, C. Timmermans, H. Wilkens, L3 Collaboration  
*Formation of the  $\eta_c$  in Two-Photon Collisions at LEP*  
Phys. Lett. **B461** (1999) 155-166
- [35] M. Acciarri, et al., G.J. Bobbink, A. Buijs, A.P. Colijn, J.A. van Dalen, D. van Dierendocnk, P. Duinker, F.C. Ern , R. van Gulik, P. de Jong, W. Kittel, A.C.K. K nig, F.L. Linde, D. Mangeol, G.G.G. Massaro, W.J. Metzger, A.J.M. Muijs, B. Petersen, T. van Rhee, M.P. Sanders, D. J. Schotanus, C. Timmermans, H. Wilkens, L3 Collaboration  
*Search for Heavy Isosinglet Neutrinos in  $e^+e^-$  Annihilation at  $130 < \sqrt{s} < 189$  GeV*  
Phys. Lett. **B461** (1999) 397-404
- [36] M. Acciarri, et al., G.J. Bobbink, A. Buijs, A.P. Colijn, J.A. van Dalen, D. van Dierendocnk, P. Duinker, F.C. Ern , R. van Gulik, P. de Jong, W. Kittel, A.C.K. K nig, F.L. Linde, D. Mangeol, G.G.G. Massaro, W.J. Metzger, A.J.M. Muijs, B. Petersen, T. van Rhee, M.P. Sanders, D. J. Schotanus, C. Timmermans, H. Wilkens, L3 Collaboration  
*Search for the Standard Model Higgs boson in  $e^+e^-$  interactions at  $\sqrt{s}=189$  GeV*  
Phys. Lett. **B461** (1999) 376-386
- [37] M. Acciarri, et al., G.J. Bobbink, A. Buijs, A.P. Colijn, J.A. van Dalen, D. van Dierendocnk, P. Duinker, F.C. Ern , R. van Gulik, P. de Jong, W. Kittel, A.C.K. K nig, F.L. Linde, D. Mangeol, G.G.G. Massaro, W.J. Metzger, A.J.M. Muijs, B. Petersen, T. van Rhee, M.P. Sanders, D. J. Schotanus, C. Timmermans, H. Wilkens, L3 Collaboration  
*Search for Heavy Neutral and Charged Leptons in  $e^+e^-$  Annihilation at  $\sqrt{s}=183$  GeV and 189 GeV*  
Phys. Lett. **B462** (1999) 354-364
- [38] M. Acciarri, et al., G.J. Bobbink, A. Buijs, A.P. Colijn, J.A. van Dalen, D. van Dierendocnk, P. Duinker, F.C. Ern , R. van Gulik, P. de Jong, W. Kittel, A.C.K. K nig, F.L. Linde, D. Mangeol, G.G.G. Massaro, W.J. Metzger, A.J.M. Muijs, B. Petersen, T. van Rhee, M.P. Sanders, D. J. Schotanus, C. Timmermans, H. Wilkens, L3 Collaboration  
*Search for Low Scale Gravity Effects in  $e^+e^-$  Collisions at LEP*  
Phys. Lett. **B464** (1999) 135-144
- [39] M. Acciarri, et al., G.J. Bobbink, A. Buijs, A.P. Colijn, J.A. van Dalen, D. van Dierendocnk, P. Duinker, F.C. Ern , R. van Gulik, P. de Jong, W. Kittel, A.C.K. K nig, F.L. Linde, D. Mangeol, G.G.G. Massaro, W.J. Metzger, A.J.M. Muijs, B. Petersen, T. van Rhee, M.P. Sanders, D. J. Schotanus, C. Timmermans, H. Wilkens, L3 Collaboration  
*Measurement of the spectroscopy of orbitally excited B mesons at LEP*  
Phys. Lett. **B465** (1999) 323-334
- [40] M. Acciarri, et al., G.J. Bobbink, A. Buijs, A.P. Colijn, J.A. van Dalen, D. van Dierendocnk, P. Duinker, F.C. Ern , R. van Gulik, P. de Jong, W. Kittel, A.C.K. K nig, F.L. Linde, D. Mangeol, G.G.G. Massaro, W.J. Metzger, A.J.M. Muijs, B. Petersen, T. van Rhee, M.P. Sanders, D. J. Schotanus, C. Timmermans, H. Wilkens, L3 Collaboration  
*Study of Z Boson Pair Production in  $e^+e^-$  Collisions at LEP at  $\sqrt{s}=189$  GeV*  
Phys. Lett. **B465** (1999) 363-375

- [41] M. Acciarri, *et al.*, G.J. Bobbink, A. Buijs, A.P. Colijn, J.A. van Dalen, D. van Dierendonck, P. Duinker, F.C. Ern , R. van Gulik, P. de Jong, W. Kittel, A.C.K. K nig, F.L. Linde, D. Mangeol, G.G.G. Massaro, W.J. Metzger, A.J.M. Muijs, B. Petersen, T. van Rhee, M.P. Sanders, D. J. Schotanus, C. Timmermans, H. Wilkens, L3 Collaboration  
*Search for Charged Higgs Bosons in  $e^+e^-$  Collisions at  $\sqrt{s} = 189$  GeV*  
Phys. Lett. **B466** (1999) 71-78
- [42] M. Acciarri, *et al.*, G.J. Bobbink, A. Buijs, A.P. Colijn, J.A. van Dalen, D. van Dierendonck, P. Duinker, F.C. Ern , R. van Gulik, P. de Jong, W. Kittel, A.C.K. K nig, F.L. Linde, D. Mangeol, G.G.G. Massaro, W.J. Metzger, A.J.M. Muijs, B. Petersen, T. van Rhee, M.P. Sanders, D. J. Schotanus, C. Timmermans, H. Wilkens, L3 Collaboration  
*Measurement of inclusive  $D^{*\pm}$  production in two-photon collisions at LEP*  
Phys. Lett. **B467** (1999) 137-146
- [43] M. Acciarri, *et al.*, G.J. Bobbink, P. Colijn, D. van Dierendonck, P. Duinker, F.C. Ern , R. van Gulik, P. de Jong, F.L. Linde, G.G.G. Massaro, A.J.M. Muijs, J.A. van Dalen, W. Kittel, A.C.K. K nig, D. Mangeol, W.J. Metzger, B. Petersen, M.P. Sanders, D. J. Schotanus, C. Timmermans, H. Wilkens, A. Buijs, T. van Rhee, L3 collaboration  
*Measurement of triple-gauge-boson couplings of the W boson at LEP*  
Phys. Lett. **B467** (1999) 171-184
- [44] M. Acciarri, *et al.*, G.J. Bobbink, A. Buijs, A.P. Colijn, D. van Dierendonck, P. Duinker, F.C. Ern , R. van Gulik, W. Kittel, A.C.K. K nig, F.L. Linde, D. Mangeol, G.G.G. Massaro, W.J. Metzger, A.J.M. Muijs, B. Petersen, T. van Rhee, M.P. Sanders, D. J. Schotanus, C. Timmermans, H. Wilkens, L3 Collaboration  
*Study of Neutral-Current Four-Fermion and ZZ Production in  $e^+e^-$  Collisions at  $\sqrt{s} = 183$  GeV*  
Phys. Lett. **B450** (1999) 281-293
- [45] M. Acciarri, *et al.*, G.J. Bobbink, A. Buijs, A.P. Colijn, D. van Dierendonck, P. Duinker, F.C. Ern , W.C. van Hoek, W. Kittel, A.C.K. K nig, F.L. Linde, D. Mangeol, G.G.G. Massaro, W.J. Metzger, A.J.W. van Mil, A.J.M. Muijs, B. Petersen, T. van Rhee, M.P. Sanders, D.J. Schotanus, C. Timmermans, L3 Collaboration  
*Searches for scalar top and scalar bottom quarks in  $e^+e^-$  interactions at 161 GeV  $\leq \sqrt{s} \leq 183$  GeV*  
Phys. Lett. **B445** (1999) 428-438
- [46] M. Acciarri, *et al.*, G.J. Bobbink, A. Buijs, A.P. Colijn, J.A. van Dalen, D. van Dierendonck, P. Duinker, F.C. Ern , R. van Gulik, W. Kittel, A.C.K. K nig, F.L. Linde, D. Mangeol, G.G.G. Massaro, W.J. Metzger, A.J.M. Muijs, B. Petersen, T. van Rhee, M.P. Sanders, D. J. Schotanus, C. Timmermans, H. Wilkens, L3 Collaboration  
 *$\chi_{c2}$  formation in two-photon collisions at LEP*  
Phys. Lett. **B453** (1999) 73-82
- [47] M. Acciarri, *et al.*, G.J. Bobbink, A. Buijs, A.P. Colijn, J.A. van Dalen, D. van Dierendonck, P. Duinker, F.C. Ern , R. van Gulik, W. Kittel, A.C.K. K nig, F.L. Linde, D. Mangeol, G.G.G. Massaro, W.J. Metzger, A.J.M. Muijs, B. Petersen, T. van Rhee, M.P. Sanders, D. J. Schotanus, C. Timmermans, H. Wilkens, L3 Collaboration  
*Inclusive charm production in two-photon collision at LEP*  
Phys. Lett. **B453** (1999) 83-93
- [48] M. Acciarri, *et al.*, G.J. Bobbink, A. Buijs, A.P. Colijn, J.A. van Dalen, D. van Dierendonck, P. Duinker, F.C. Ern , R. van Gulik, W. Kittel, A.C.K. K nig, F.L. Linde, D. Mangeol, G.G.G. Massaro, W.J. Metzger, A.J.M. Muijs, B. Petersen, T. van Rhee, M.P. Sanders, D. J. Schotanus, C. Timmermans, H. Wilkens, L3 Collaboration  
*Heavy quarkonium production in Z decays*  
Phys. Lett. **B453** (1999) 94-106
- [49] M. Acciarri, *et al.*, G.J. Bobbink, A. Buijs, A.P. Colijn, J.A. van Dalen, D. van Dierendonck, P. Duinker, F.C. Ern , R. van Gulik, W. Kittel, A.C.K. K nig, F.L. Linde, D. Mangeol, G.G.G. Massaro, W.J. Metzger, A.J.M. Muijs, B. Petersen, T. van Rhee, M.P. Sanders, D. J. Schotanus, C. Timmermans, H. Wilkens, L3 Collaboration  
*Measurement of the cross-section for the process  $\gamma^* \gamma^* \rightarrow$  hadrons at LEP*  
Phys. Lett. **B453** (1999) 333-342
- [50] M. Acciarri, *et al.*, G.J. Bobbink, A. Buijs, A.P. Colijn, J.A. van Dalen, D. van Dierendonck, P. Duinker, F.C. Ern , R. van Gulik, W. Kittel, A.C.K. K nig, F.L. Linde, D. Mangeol, G.G.G. Massaro, W.J. Metzger, A.J.M. Muijs, B. Petersen, T. van Rhee, M.P. Sanders, D. J. Schotanus, C. Timmermans, H. Wilkens, L3 Collaboration  
*Measurement of mass and width of the W boson at LEP*  
Phys. Lett. **B454** (1999) 386-398
- [51] M. Acciarri, *et al.*, G.J. Bobbink, A. Buijs, A.P. Colijn, J.A. van Dalen, D. van Dierendonck, P. Duinker, F.C. Ern , R. van Gulik, W. Kittel, A.C.K. K nig, F.L. Linde, D. Mangeol, G.G.G. Massaro, W.J. Metzger, A.J.M. Muijs, B. Petersen, T. van Rhee, M.P. Sanders, D. J. Schotanus, C. Timmermans, H. Wilkens, L3 Collaboration  
*Search for Scalar Leptons in  $e^+e^-$  collisions at  $\sqrt{s} = 183$  GeV*  
Phys. Lett. **B456** (1999) 283-296
- [52] M. Acciarri, *et al.*, G.J. Bobbink, A. Buijs, A.P. Colijn, D. van Dierendonck, P. Duinker, F.C. Ern , R. van Gulik, W.C. van Hoek, W. Kittel, A.C.K. K nig, F.L. Linde, D. Mangeol, G.G.G. Massaro, W.J. Metzger, A.J.W. van Mil, A.J.M. Muijs, B. Petersen, T. van Rhee, M.P. Sanders, D.J. Schotanus, C. Timmermans, L3 Collaboration  
*Search for charged Higgs bosons in  $e^+e^-$  collisions at centre-of-mass energies between 130 and 183 GeV*  
Phys. Lett. **B446** (1999) 368-377
- [53] M. Acciarri, *et al.*, G.J. Bobbink, A. Buijs, A.P. Colijn, D. van Dierendonck, P. Duinker, F.C. Ern , R. van Gulik, W.C. van Hoek, W. Kittel, A.C.K. K nig, F.L. Linde, D. Mangeol, G.G.G. Massaro, W.J. Metzger, A.J.W. van Mil, A.J.M. Muijs, B. Petersen, T. van Rhee, M.P. Sanders, D.J. Schotanus, C. Timmermans, L3 Collaboration  
*The  $Q^2$  evolution of the Hadronic Photon Structure Function  $F_2^{\gamma}$  at LEP*  
Phys. Lett. **B447** (1999) 147-156
- [54] M. Acciarri, *et al.*, G.J. Bobbink, A. Buijs, A.P. Colijn, J.A. van Dalen, D. van Dierendonck, P. Duinker, F.C. Ern , R. van Gulik, W. Kittel, A.C.K. K nig, F.L. Linde, D. Mangeol, G.G.G. Massaro, W.J. Metzger, A.J.M. Muijs, B. Petersen, T. Rhee, M.P. Sanders, D.J. Schotanus, C. Timmermans, L3 Collaboration  
*Measurement of the  $e^+e^- \rightarrow Z \rightarrow b\bar{b}$  forward-backward asymmetry and the  $B^0\bar{B}^0$  mixing parameter using prompt leptons*  
Phys. Lett. **B448** (1999) 152-162
- [55] M. Acciarri, *et al.*, G.J. Bobbink, A. Buijs, A.P. Colijn, J.A. van Dalen, D. van Dierendonck, P. Duinker, F.C. Ern , R. van Gulik, P. de Jong, W. Kittel, A.C.K. K nig, F.L. Linde, D. Mangeol, G.G.G. Massaro, W.J. Metzger, A.J.M. Muijs, B. Petersen, T. van Rhee, M.P. Sanders, D. J. Schotanus, C. Timmermans, H. Wilkens, L3 Collaboration  
*Searches for Scalar Quarks in  $e^+e^-$  Interactions at  $\sqrt{s} = 189$  GeV*  
Phys. Lett. **B471** (1999) 308-320
- [56] M. Acciarri, *et al.*, G.J. Bobbink, A. Buijs, A.P. Colijn, J.A. van Dalen, D. van Dierendonck, P. Duinker, F.C. Ern , R. van Gulik, P. de Jong, W. Kittel, A.C.K. K nig, F.L. Linde, D. Mangeol, G.G.G. Massaro, W.J. Metzger, A.J.M. Muijs, B. Petersen, T. van Rhee, M.P. Sanders, D. J. Schotanus, C. Timmermans, H. Wilkens, L3 Collaboration  
*Search for Neutral Higgs Bosons of the Minimal Supersymmetric Standard Model in  $e^+e^-$  Interactions at  $\sqrt{s} = 189$  GeV*  
Phys. Lett. **B471** (1999) 321-331
- [57] M. Acciarri, *et al.*, G.J. Bobbink, A. Buijs, A.P. Colijn, J.A. van Dalen, D. van Dierendonck, P. Duinker, F.C. Ern , R. van Gulik, P. de Jong, W. Kittel, A.C.K. K nig, F.L. Linde, D. Mangeol, G.G.G. Massaro, W.J. Metzger, A.J.M. Muijs, B. Petersen, T. van Rhee, M.P. Sanders, D. J. Schotanus, C. Timmermans, H. Wilkens, L3 Collaboration  
*Search for Extra Dimensions in boson and Fermion Pair Production in  $e^+e^-$  Interactions at LEP*  
Phys. Lett. **B470** (1999) 281-288

- [58] M. Acciarri, *et al.*, G.J. Bobbink, A. Buijs, A.P. Colijn, J.A. van Dalen, D. van Dierendocnk, P. Duinker, F.C. Ern , R. van Gulik, P. de Jong, W. Kittel, A.C.K. K nig, F.L. Linde, D. Mangeol, G.G.G. Massaro, W.J. Metzger, A.J.M. Muijs, B. Petersen, T. van Rhee, M.P. Sanders, D. J. Schotanus, C. Timmermans, H. Wilkens, L3 Collaboration  
*Search for Scalar Leptons in  $e^+e^-$  collisions at  $\sqrt{s}=189$  GeV*  
Phys. Lett. **B471** (1999) 280-292
- [59] M. Acciarri, *et al.*, G.J. Bobbink, A. Buijs, A.P. Colijn, J.A. van Dalen, D. van Dierendocnk, P. Duinker, F.C. Ern , R. van Gulik, P. de Jong, W. Kittel, A.C.K. K nig, F.L. Linde, D. Mangeol, G.G.G. Massaro, W.J. Metzger, A.J.M. Muijs, B. Petersen, T. van Rhee, M.P. Sanders, D. J. Schotanus, C. Timmermans, H. Wilkens, L3 Collaboration  
*Single and Multi-Photon Events with Missing Energy in  $e^+e^-$  Collisions at  $\sqrt{s}=189$  GeV*  
Phys. Lett. **B470** (1999) 268-280
- [60] K. Ackerstaff, *et al.*, M. Amarian, E.C. Aschenauer, J. Blouw, H.J. Bulten, P.K.A. de Witt Huberts, M.G. Guidal, T. Henkes, H. Ihssen, M. Kolstein, H.R. Poolman, J.F.J. van den Brand, G. van der Steenhoven, J.J. van Hunen, J. Visser, HERMES collaboration  
*Observation of a Coherence Length Effect in Exclusive  $\rho^0$  Electroproduction*  
Phys. Rev. Lett. **82** (1999) 3025-3029
- [61] K. Ackerstaff, *et al.*, M. Amarian, E.C. Aschenauer, J. Blouw, H.J. Bulten, P.K.A. de Witt Huberts, M.G. Guidal, T. Henkes, H. Ihssen, M. Kolstein, H.R. Poolman, J.F.J. van den Brand, G. van der Steenhoven, J.J. van Hunen, J. Visser, HERMES collaboration  
*Flavor Decomposition of the Polarized Quark Distributions in the Nucleon from Inclusive and Semi-inclusive Deep-inelastic Scattering*  
Phys. Lett. **B464** (1999) 123-134
- [62] K. Ackerstaff, *et al.*, J. Blouw, H.J. Bulten, P.K.A. de Witt Huberts, M.G. Guidal, T. Henkes, H. Ihssen, M. Kolstein, J.F.J. van den Brand, G. van der Steenhoven, J.J. van Hunen, HERMES collaboration  
*Beam-induced nuclear depolarization in a gaseous polarized-hydrogen target*  
Phys. Rev. Lett. **82** (1999) 1164-1168
- [63] W. Adam, *et al.*, B. van Eijk, F. Hartjes, RD42 collaboration  
*Recent results with CVD diamond trackers*  
Nucl. Phys. B (Proc. Suppl.) **78** (1999) 329-334
- [64] W. Adam, *et al.*, B. van Eijk, F. Hartjes, RD42 collaboration  
Nucl. Instr. Meth. **A434** (1999) 131-145
- [65] W. Adam, *et al.*, B. van Eijk, F. Hartjes, RD42 collaboration  
*The first bump-bonded pixel detectors on CVD diamond*  
Nucl. Instr. Meth. **A436** (1999) 326-335
- [66] D. Adams, *et al.*, T. Cuhadar, R. van Dantzig, N. de Groot, T.J. Ketel, M. Litmaath, G. van Middelkoop, J.E.J. Oberski, H. Postma, E.P. Sichtermann, Spin Muon Collaboration  
*A large streamer chamber muon tracking detector in a high-flux fixed-target application*  
Nucl. Instr. Meth. **A435** (1999) 354-374
- [67] B. Adeva, *et al.*, M.K. Ballintijn, T. Cuhadar, R. van Dantzig, N. de Groot, T.J. Ketel, L. Klostermann, M. Litmaath, G. van Middelkoop, J.E.J. Oberski, H. Postma, E.P. Sichtermann, Spin Muon Collaboration  
*The polarized double cell target of the SMC*  
Nucl. Instr. Meth. **A437** (1999) 23-67
- [68] B. Adeva, *et al.*, T. Cuhadar, R. van Dantzig, N. de Groot, T.J. Ketel, M. Litmaath, G. van Middelkoop, J.E.J. Oberski, H. Postma, E.P. Sichtermann, Spin Muon Collaboration  
*Spin asymmetries  $A(1)$  of the proton and the deuteron in the low  $x$  and low  $Q(2)$  region from polarized high energy muon scattering*  
Phys. Rev. **D60** (1999) 72004
- [69] M.M. Aggarwal, *et al.*, A. Buijs, N.J.A.M. Eijndhoven, F.J.M. Geurts, R. Kamermans, C.J.W. Twenhoefel, WA98 Collaboration  
*Systematics of inclusive photon production in 158 dot A GeV Pb induced reactions on Ni, Nb, and Pb targets*  
Phys. Lett. **B458** (1999) 422-430
- [70] M.M. Aggarwal, *et al.*, A. Buijs, N.J.A.M. Eijndhoven, F.J.M. Geurts, R. Kamermans, B. Raeven, E. van de Pijl WA98 Collaboration  
*Freeze-Out Parameters in Central 158A GeV 208Pb + Pb Collisions*  
Phys. Rev. Lett. **83** (1999) 926-930
- [71] M.M. Aggarwal, *et al.*, A. Buijs, N.J.A.M. Eijndhoven, F.J.M. Geurts, R. Kamermans, C.J.W. Twenhoefel, WA98 Collaboration  
*Elliptic emission of  $K^+$  and  $\pi^+$  in 158 GeV Pb+Pb collisions*  
Phys. Lett. **B469** (1999) 30
- [72] G. Albrecht, *et al.*, E. Boudinov, N. Kjaer, P. Kluit, G.W. van Apeldoorn, I. van Vulpen  
*Operation, optimisation, and performance of the DELPHI RICH detectors*  
Nucl. Instr. Meth. **A433** (1999) 47-58
- [73] P. Amran, *et al.*, J. Charles, J. Engelen, D. Huss, G.J. Nooren, ANTARES collaboration  
*The ANTARES project*  
Nucl. Phys. B (Proc. Suppl.) **75A** (1999) 415-417
- [74] M. Anselmino, M. Boggione, F. Murgia  
*Predictions for single spin asymmetries in  $1 + p^\uparrow \rightarrow \pi + X$  and  $\gamma^* + p^\uparrow \rightarrow \pi + X$*   
Proceedings 7th International Workshop on Deep Inelastic Scattering and QCD (DI99), DESY  
Nucl. Phys. Proc. Suppl. **B79** (1999) 632-634
- [75] M. Anselmino, M. Boggione, F. Murgia  
*Phenomenology of single spin asymmetries in  $p^\uparrow p \rightarrow \pi X$*   
Phys. Rev. **D60** (1999) 054027
- [76] N. van Bakel, *et al.*, J. van den Brand  
*Design of a prototype frontend and bias generator for a new readout chip for LHCb*  
Proceedings 5th Conference on Electronics for LHC Experiments, Snowmass, CO, USA, 20-24 Sep. 1999, 167-171
- [77] U. Bassler, *et al.*, E. Laenen  
*Summary of the structure function working group at DIS'99*  
Nucl. Phys. B (Proc. Suppl.) **79** (1999) 701-722
- [78] M. Battaglia, P.M. Kluit  
*Particle identification using the DELPHI RICH detectors*  
Nucl. Instr. Meth. **A433** (1999) 252-256
- [79] C. Bauer, *et al.*, R. Kluit  
*Performance and radiation tolerance of the helix128-2.2 and 3.0 readout chips for the HERA-B microstrip detectors*  
Proceedings 5th Conference on Electronics for LHC Experiments, Snowmass, CO, USA, 20-24 Sep. 1999, 508-512
- [80] M.G. van Beuzekom, *et al.*, J.C. Boes, E.A. van den Born, M.J.F. Jaspers, J. Konijn, R.G.C. Oldeman, C.A.F.J. van der Poel, T. van Reen, J. Stolte, J.W.E. Uiterwijk  
*The trigger system of the CHORUS experiment*  
Nucl. Instr. Meth. **A427** (1999) 587-606
- [81] J. Blouw, *et al.*, J.F.J. van den Brand, H.J. Bulten, M. Doets, F.G. Hartjes, Th. Henkes, J.J. van Hunen, E. Kok, M. Kolstein, M.J. Kraan, F. Udo, J. Visser  
*Design and performance of a large microstrip gas tracker for HERMES*  
Nucl. Instr. Meth. **A434** (1999) 227-243
- [82] F.W.N. de Boer, *et al.*, R. van Dantzig  
*Search for a short-lived neutral boson with a mass around 9 MeV/c<sup>2</sup>*  
Nucl. Phys. B (Proc. Suppl.) **72** (1999) 189-194

- [83] M. Boglione, P.J. Mulders  
*Time-reversal od fragmentation and distribution functions in pp and ep single spin asymmetries*  
Phys. Rev. **D60** (1999) 054007
- [84] M. Boglione, M.R. Pennington  
*Determination of Radiative Widths of Scalar Mesons from Experimental Results on  $\gamma\gamma \rightarrow \pi\pi$*   
Eur. Phys. J. **C9** (1999) 11-29
- [85] M. Boglione, P.J. Mulders  
*Estimates of T-odd distribution and fragmentation functions*  
Proceedings 7th international Workshop on Deep Inelastic Scattering and QCD (DIS99), DESY  
Nucl. Phys. (Proc. Suppl.) **B79** (1999) 635-637
- [86] M. Botje  
*A QCD analysis of HERA and fixed target structure function data*  
Nucl. Phys. B (Proc. Suppl.) **79** (1999) 111-114
- [87] M. Bouwhuis, et al., T. Botto, J.F.J. van den Brand, H.J. Bulten, M. Ferro-Luzzi, D.W. Higinbotham, C.W. de Jager, D.D.J. de Lange, N. Papadakis, I. Passchier, H.R. Poolman, E. Six, J.J.M. Steijger, N. Vodinas, H. de Vries  
*Measurement of T20 in Elastic Electron-Deuterium Scattering*  
Phys. Rev. Lett. **82** (1999) 3755-3758
- [88] G.C. Branco, M.N. Rebelo, J.I. Silva-Marcos  
*Degenerate and quasidegenerate majorana neutrinos*  
Phys. Rev. Lett. **82** (1999) 683-686
- [89] J.F.J. van den Brand  
*Spin observables of the nucleon*  
Studies of few-body systems with high duty factor electron beams: Proceedings 10th Amsterdam mini-conference, Amsterdam, 6-7 Jan. 1999, 1-7
- [90] J.F.J. van den Brand  
*Spin Correlations in Medium Energy Electron Scattering at NIKHEF*  
Proceedings of the Second Workshop on Electronuclear Physics with Internal Targets and the BLAST Detector, Ed. R. Alarcon & R. Milner, World Scientific 1999
- [91] J. Breitweg, et al., C. Bokel, M. Botje, N. Bruemmer, J. Engelen, E. Koffeman, P. Kooijman, A. van Sighem, H. Tiecke, W. Tuning, M. Verkerke, J. Vossebeld, L. Wiggers, E. de Wolf, ZEUS Collaboration  
*Forward jet production in deep inelastic scattering at HERA*  
Eur. Phys. J. **C6** (1999) 239-252
- [92] J. Breitweg, et al., C. Bokel, M. Botje, N. Bruemmer, J. Engelen, E. Koffeman, P. Kooijman, A. van Sighem, H. Tiecke, W. Tuning, M. Verkerke, J. Vossebeld, L. Wiggers, E. de Wolf, ZEUS Collaboration  
*ZEUS results on the measurement and phenomenology of  $F_2$  at low x and low  $Q^2$*   
Eur. Phys. J. **C7** (1999) 609-630
- [93] J. Breitweg, et al., C. Bokel, M. Botje, N. Bruemmer, J. Engelen, E. Koffeman, P. Kooijman, A. van Sighem, H. Tiecke, W. Tuning, M. Verkerke, J. Vossebeld, L. Wiggers, E. de Wolf, ZEUS Collaboration  
*Measurement of jet shapes in high- $Q^2$  deep inelastic scattering at HERA*  
Eur. Phys. J. **C8** (1999) 367-380
- [94] J. Breitweg, et al., C. Bokel, M. Botje, N. Bruemmer, J. Engelen, E. Koffeman, P. Kooijman, A. van Sighem, H. Tiecke, W. Tuning, M. Verkerke, J. Vossebeld, L. Wiggers, E. de Wolf, ZEUS Collaboration  
*Measurement of the diffractive cross section in deep inelastic scattering using ZEUS 1994 data*  
Eur. Phys. J. **C6** (1999) 43-66
- [95] J. Breitweg, et al., C. Bokel, M. Botje, N. Bruemmer, J. Engelen, E. Koffeman, P. Kooijman, A. van Sighem, H. Tiecke, W. Tuning, M. Verkerke, J. Vossebeld, L. Wiggers, E. de Wolf, ZEUS Collaboration  
*Measurement of dijet photoproduction at high transverse energies at HERA*  
Eur. Phys. J. **C11** (1999) 35-50
- [96] J. Breitweg, et al., C. Bokel, M. Botje, N. Bruemmer, J. Engelen, E. Koffeman, P. Kooijman, A. van Sighem, H. Tiecke, W. Tuning, J.J. Velthuis M. Verkerke, J. Vossebeld, L. Wiggers, E. de Wolf, ZEUS Collaboration  
*Measurement of multiplicity and momentum spectra in the current and target regions of the Breit frame in Deep Inelastic Scattering at HERA*  
Eur. Phys. J. **C11** (1999) 251-270
- [97] J. Breitweg, et al., C. Bokel, M. Botje, N. Bruemmer, J. Engelen, E. Koffeman, P. Kooijman, A. van Sighem, H. Tiecke, W. Tuning, M. Verkerke, J. Vossebeld, L. Wiggers, E. de Wolf, ZEUS Collaboration  
*Measurement of high- $Q^2$  neutral-current  $e^+p$  deep inelastic scattering cross-sections at HERA*  
Eur. Phys. J. **C11** (1999) 447-471
- [98] J. Breitweg, et al., C. Bokel, M. Botje, N. Bruemmer, J. Engelen, E. Koffeman, P. Kooijman, A. van Sighem, H. Tiecke, W. Tuning, M. Verkerke, J. Vossebeld, L. Wiggers, E. de Wolf, ZEUS Collaboration  
*Measurement of inclusive  $D^{*\pm}$  and associated dijet cross sections in photoproduction at HERA*  
Eur. Phys. J. **C6** (1999) 67-83
- [99] J. Breitweg, et al., C. Bokel, M. Botje, N. Bruemmer, J. Engelen, E. Koffeman, P. Kooijman, A. van Sighem, H. Tiecke, W. Tuning, M. Verkerke, J. Vossebeld, L. Wiggers, E. de Wolf, ZEUS Collaboration  
*Exclusive electroproduction of  $p^0$  and  $J/\psi$  mesons at HERA*  
Eur. Phys. J. **C6** (1999) 603-627
- [100] M. Burns, M. Campbell, E. Cantatore, V. Cencelli, R. Dinapoli, F. Formenti, T. Grassi, E. Heijne, P. Jarron, K. Kloukinas, P. Lamanna, M. Morel, V. O'Shea, V. Quiquempoix, D. San Segundo Bello, W. Snoeys, K. Wyllie  
*A pixel readout chip for tracking at ALICE and particle identification at LHCb*  
Snowmass CO, USA: proceedings 5th Conference on Electronics for LHC Experiments, USA, 20-24 Sept. 1999, 93-97
- [101] A. Buijs  
*The study of heavy-ion collisions with the ALICE detector at the LHC*  
Nucl. Phys. B (Proc. Suppl.) **75A** (1999) 200-202
- [102] S.V. Chekanov, W. Kittel, W.J. Metzger  
*Local properties of local multiplicity distributions in hadronic Z decay*  
Nucl. Phys. B (Proc. Suppl.) **71** (1999) 146-151
- [103] S.V. Chekanov, E.A. de Wolf, W. Kittel  
*Bose-Einstein correlations and color reconnection in W-pair production*  
Eur. Phys. J. **C6** (1999) 403-411
- [104] A.P. Colijn  
*L3 measurement of the tau lepton lifetime*  
Nucl. Phys. B (Proc. Suppl.) **76** (1999) 101-106
- [105] A.E.L. Dieperink, S.I. Nagorny  
*Photodisintegration of the deuteron in the few GeV region using asymptotic amplitudes*  
Phys. Lett. **B456** (1999) 9-15
- [106] M. Doerrzapf, B. Gato-Rivera  
*Transmutations between Singular and Subsingular Vectors of the  $N=2$  Superconformal Algebras*  
Nucl. Phys. **B557** (1999) 517-534
- [107] M. Doerrzapf, B. Gato-Rivera  
*Determinant formulae for the topological  $N=2$  Superconformal Algebra*  
Nucl. Phys. **B558** (1999) 503-544
- [108] M. Doerrzapf, B. Gato-Rivera  
*Singular dimensions of the  $N=2$  superconformal algebras. 1*  
Communications in Mathematical Physics **206** (1999) 493-531
- [109] B. Erzen, et al., N. Kjaer, P. Kluit, I. van Vulpen  
*Analysis of the DELPHI RICH data at LEP II*  
Nucl. Instr. Meth. **A433** (1999) 247-251

- [110] M. Friedl, *et al.*, B. van Eijk, F. Hartjes  
*CVD diamond detectors for ionizing radiation*  
Nucl. Instr. Meth. **A435** (1999) 194-201
- [111] D.L. Groep, *et al.*, M.F. van Batenburg, Th.S. Bauer, H.P. Blok, D. Boersma, P.C. Heimberg, W.H.A. Hesselink, E. Jans, L. Lapikás, R. Starink, M.F.M. Steenbakkers, H. de Vries  
*Investigation of the exclusive  $^3\text{He}(e,e'pp)n$  reaction*  
Phys. Rev. Lett. **83** (1999) 5443-5446
- [112] D.L. Groep, *et al.*, M.F. van Batenburg, Th.S. Bauer, H.P. Blok, D. Boersma, P.C. Heimberg, W.H.A. Hesselink, E. Jans, L. Lapikás, R. Starink, M.F.M. Steenbakkers, H. de Vries  
*Electron-induced two-proton knockout reaction on  $^3\text{He}$*   
Proceedings Few Body Conference, 1998  
Few-Body Systems, Suppl. **10** (1999) 351-354
- [113] D.L. Groep, *et al.*, M.F. van Batenburg, Th.S. Bauer, H.P. Blok, D.J. Boersma, P. Heimberg, W.H.A. Hesselink, E. Jans, L. Lapikás, R. Starink, M.F.M. Steenbakkers, H. de Vries  
*Electron-induced two-proton knockout reaction from  $^3\text{He}$*   
Nuclear Physics **A654** (1999) 509c
- [114] A.P. de Haas, *et al.*, A. van den Brink, P. Kuijjer, C.J. Oskamp  
*Very low mass microcables for the ALICE silicon strip detector*  
Proceedings 5th Conference on Electronics for LHC Experiments, Snowmass, CO, USA, 20-24 Sep. 1999, 143-146
- [115] F. Hartjes, *et al.*, B. van Eijk, RD42 collaboration  
*Parameterisation of radiation effects on CVD diamond for proton irradiation*  
Nucl. Phys. B (Proc. Suppl.) **78** (1999) 675-682
- [116] R. Helling, J. Plefka, M. Serone, A. Waldron  
*Three Graviton Scattering in M-Theory*  
Nucl. Phys. B **559** (1999) 184-204
- [117] W.H.A. Hesselink, D.L. Groep, E. Jans, R. Starink  
*Probing short range correlations in  $^3\text{He}$  and  $^{16}\text{O}$  using the reaction  $(e,e'pp)$*   
Studies of few-body systems with high duty factor electron beams: proceedings 10th Amsterdam mini-conference, Amsterdam, 6-7 Jan. 1999, 80-94
- [118] D.W. Higinbotham  
*Results from Recoil Detection with Polarized Nuclei*  
Proceedings of the Second Workshop on Electronuclear Physics with Internal Targets and the BLAST Detector, Ed. R. Alarcon & R. Milner, World Scientific 1999.
- [119] J.-W. van Holten, A. Waldron, K. Peeters  
*An index theorem for nonstandard Dirac operators*  
Class. Quantum Grav. **16** (1999) 2537-2544
- [120] L.R. Huiszoon, A.N. Schellekens, N. Sousa  
*Klein Bottles and simple currents*  
Phys. Lett. **B470** (1999) 95
- [121] J.J. van Hunen  
*Semi-inclusive hadron production on  $^{14}\text{N}$*   
Studies of few-body systems with high duty factor electron beams: Proceedings 10th Amsterdam mini-conference, Amsterdam, 6-7 Jan. 1999, 68-71
- [122] H. Ihssen, *et al.*, M. Amarian, E.C. Aschenauer, J. Blouw, H.J. Bulten, P.K.A. de Witt Huberts, M.G. Guidal, T. Henkes, H. Ihssen, M. Kolstein, H.R. Poolman, J.F.J. van den Brand, G. van der Steenhoven, J.J. van Hunen, J. Visser, HERMES collaboration  
*Nucleon spin structure measurements at DESY*  
Nucl. Phys. B (Proc. Suppl.) **74** (1999) 133-137
- [123] H. Ihssen  
*Flavour Asymmetry of the Light Quark Sea*  
Proceedings of the XXXIIIth Rencontres de Moriond, France (1999)
- [124] S. Keller, E. Laenen  
*Next-to-leading order cross sections for tagged reactions*  
Phys. Rev. **D59** (1999) 114004
- [125] A. Khodjamirian, R. Rueckl, S. Weinzierl, O. Yakovlev  
*Perturbative QCD corrections to the light-cone sum rule for  $B^*B\pi$  and  $D^*D\pi$  couplings*  
Phys. Lett. **B457** (1999) 245
- [126] W. Kittel, S.V. Chekanov, D.J. Mangeol, W.J. Metzger  
*Multiplicities, fluctuations and QCD: Interplay between soft and hard physics?*  
Nucl. Phys. B (Proc. Suppl.) **71** (1999) 90-99
- [127] J. Konijn  
*The solar neutrino problem*  
Eur. J. Phys. **20** (1999) 399-407
- [128] I. Koop, *et al.*, R. Maas, I. Passchier  
*Polarized electrons in AmPS*  
Nucl. Instr. Meth. **A427** (1999) 36-40
- [129] B.V. Krippa  
*Chiral symmetry and properties of hadron correlators in nuclear matter*  
Proceedings 8th International Conference (BARYON98), Germany (1999)
- [130] E. Laenen, S.-O. Moch  
*Soft gluon resummation for heavy quark electroproduction*  
Phys. Rev. **D59** (1999) 034027
- [131] L. Lapikás, J. Wesseling, R.B. Wiringa  
*Nuclear structure studies with the  $^7\text{Li}(e,e'p)$  reaction*  
Phys. Rev. Lett. **82** (1999) 4404-4407
- [132] L. Lapikás, M.F. van Batenburg, D.L. Groep, W.H.A. Hesselink, E. Jans, R. Starink  
*Nucleons and nucleon pairs in nuclei*  
Proceedings Workshop on electron nucleus scattering, Elba, 1998  
Eds. O. Benhar, A. Fabrocini, R. Schiavilla  
Edizione ETS (1999) 275, Pisa
- [133] D.J. Mangeol  
*QCD studies with the L3 detector*  
Nucl. Phys. B (Proc. Suppl.) **74** (1999) 24-33
- [134] V. Manzani, *et al.*, M. Botje, A.P. de Haas, R. Kamermans, P. Kuijjer, A. van den Brink, P. van de Ven, N. van Eijndhoven, NA57 collaboration  
*Experiment NA57 at the CERN SPS*  
J. Phys. **G25** (1999) 473-479
- [135] D. Meier, *et al.*, B. van Eijk, F. Hartjes, RD42 collaboration  
*Proton irradiation of CVD diamond detectors for high-luminosity experiments at the LHC*  
Nucl. Instr. Meth. **A426** (1999) 173-180
- [136] O. Melzer, CHORUS collaboration  
*Neutrino induced charm production in the CHORUS experiment*  
Nucl. Phys. B (Proc. Suppl.) **75B** (1999) 112-116
- [137] B.L. Milityn, P.W. van Amersfoort, G. Luijckx  
*Beam optical system of the polarized electron source of the Amsterdam pulse stretcher AmPS*  
Nucl. Instr. Meth. **A427** (1999) 46-50
- [138] P.J. Mulders, J.J. Engelen  
*Het vonkende vacuum*  
Nederl. Tijdschr. voor Natuurk. **65** (1999) 142-145
- [139] S.I. Nagorny, A.E.L. Dieperink  
*Gauge constraints and electromagnetic properties of off-shell particles*  
Eur. Phys. J. **A5** (1999) 417-428
- [140] J. Noomen  
*Emittance increase due to transient beam loading*  
Nucl. Instr. Meth. **A427** (1999) 51-57
- [141] R.G.C. Oldeman, CHORUS collaboration  
*Status of the CHORUS structure function measurement*  
Nucl. Phys. B (Proc. Suppl.) **79** (1999) 96-98

- [142] V. Pascalutsa, J.A. Tjon  
*Relativistic quasipotential equations with u-channel exchange interactions*  
Phys. Rev. **C60** (1999) 34005
- [143] V. Pascalutsa, R.G.E. Timmermans  
*Field theory of nucleon to higher-spin baryon transitions*  
Phys. Rev. **C60** (1999) 042201
- [144] I. Passchier, Th.S. Bauer, D. Boersma, J.F.J. van den Brand, H.J. Bulten, L.D. van Buuren, M. Ferro-Luzzi, P. Heimberg, D.W. Higinbotham, C.W. de Jager, S. Klous, H. Kolster, B.L. Milityn, G.J.L. Nooren, H.R. Poolman, M.C. Simani, L.E. Six, D. Szczerba, H. de Vries  
*Charge Form Factor of the Neutron from the Reaction  $^2\vec{H}(\vec{e}, e'n)p$*   
Phys. Rev. Lett. **82** (1999) 4988-4991
- [145] K. Peeters, A. Waldron  
*Spinors on manifolds with boundary: APS index theorems with torsion*  
Journal High Energy Physics **02** (1999) 024
- [146] A. Pellegrino, et al., M.G. van Beuzekom, E.E. van den Born, D.L. Groep, W.H.A. Hesselink, E. Jans, W.-J. Kasdorp, J. Kos, M.N. Kruszynska, E. Kwakkel, J.J. van Leeuwe, F.A. Mul, C.J.G. Onderwater, H.Z. Peek, T. Ploegmakers, A. Poelman, R. Starink, J.J.M. Steijger, H.J. Sturris, J.A. Templon, J.L. Visschers, R.F. van Wijk, A.N.M. Zwart  
*Proton detection with large-acceptance scintillator detection systems in electron-scattering environments*  
Nucl. Instr. Meth. **A437** (1999) 188-205
- [147] T. van Ritbergen, A.N. Schellekens, J.A.M. Vermaseren  
*Group theory factors for Feynman diagrams*  
Int. J. Mod. Phys. **A14** (1999) 41-96
- [148] M.J.M. van Sambeek, et al., M.G. van Beuzekom, T. Botto, P.P.M. Jansweijer, D.J.J. de Lange, J.J.M. Steijger, J.C. Verkooijen  
*A Recoil Detector for electron scattering experiments with internal targets*  
Nucl. Instr. Meth. **A434** (1999) 279-296
- [149] A.N. Schellekens  
*Cloning  $SO(N)$  level 2*  
Int. J. Mod. Phys. **A14** (1999) 1283-1292
- [150] A.N. Schellekens  
*Fixed point resolution in extended WZW-models*  
Nucl. Phys. **B558** (1999) 484-502
- [151] S. Schnetzer, et al., B. van Eijk, F. Hartjes, RD42 collaboration  
*Tracking with CVD diamond radiation sensors at high luminosity colliders*  
IEEE Trans. Nucl. Sci. **46** (1999) 193-200
- [152] C. Schwarz, et al., G. Meddeler  
*X-ray imaging using a hybrid photon counting GaAs pixel detector*  
Nucl. Phys. B (Proc. Suppl.) **78** (1999) 491-496
- [153] J.I. Silva-Marcos  
*Alternative to the seesaw mechanism*  
Phys. Rev. **D59** (1999) 091301
- [154] C.M. Spaltro, H.P. Blok, E. Jans, L. Lapikás, S.I. Nagorny  
*Study of the  $^4\text{He}(e, e'd)pn$  reaction*  
Few-Body Systems **26** (1999) 271-283
- [155] G. van der Steenhoven  
*AmPS: charges inside the neutron*  
Nucl. Phys. News Int. **9** No. 1 (1999) 30  
*HERMES: the nucleus as a femtometer probe*  
Nucl. Phys. News Int. **9** No. 1 (1999) 31
- [156] M.A. van Uden, R.L.J. van der Meer, Th.S. Bauer, M. Bron, R. Buis, P.J.M. de Groen, Y. Lefevre, G.J.L. Nooren, H. Postma, G. van der Steenhoven, H.W. Willering  
*The HARP liquid hydrogen system*  
Nucl. Instr. Meth. **A424** (1999) 580-593
- [157] J.A.M. Vermaseren  
*Harmonic sums, Mellin transforms and integrals*  
Int. J. Mod. Phys. **A14** (1999) 2037-2076
- [158] E. Voutier, et al., Th.S. Bauer, H.W. Willering  
*Analytical method for polarimeter design optimization*  
Nucl. Instr. Meth. **A430** (1999) 110-126
- [159] A.H. Wapstra  
*Russische en Amerikaanse atoomlaboratoria ontdekken nieuw element*  
Nederl. Tijdschr. voor Natuurk. **65** (1999) 192-193
- [160] R. Wedenig, et al., B. van Eijk, F. Hartjes, RD42 collaboration  
*CVD diamond pixel detectors for LHC experiments*  
Nucl. Phys. B (Proc. Suppl.) **78** (1999) 497-504
- [161] S. Weinzierl  
*Reduction of multi-leg loop integrals*  
Phys. Lett. **B450** (1999) 234-240
- [162] S. Weinzierl, D.A. Kosower  
*QCD corrections to four-jet production and three-jet structure in  $e(+)e(-)$  annihilation*  
Phys. Rev. **D60** (1999) 054028
- [163] P.K.A. de Witt Huberts  
*Correlated nucleon motion and fractional occupation of orbitals in  $^{208}\text{Pb}$*   
Nucl. Phys. **A649** (1999) 3c-13c
- [164] K. Wyllie, et al., D. San Segundo Bello  
*A pixel readout chip for tracking at ALICE and particle identification at LHCb*  
Proceedings 5th Conference on Electronics for LHC Experiments, Snowmass, CO, USA, 20-24 Sep. 1999, 93-97
- [165] Z.L. Zhou, et al., M. Bouwuis, M. Ferro-Luzzi, R. van Bommel, T. Botto, J.F.J. van den Brand, H.J. Bulten, D.W. Higinbotham, C.W. de Jager, D.D.J. de Lange, N. Papadakis, E. Passchier, I. Passchier, H.R. Poolman, E. Six, J.J.M. Steijger, N. Vodinas, H. de Vries  
*Tensor analyzing powers for quasielastic electron scattering from deuterium*  
Phys. Rev. Lett. **82** (1999) 687-690

## 1.1 Ph.D. Theses

- [1] Hans Roeland Poolman  
*'Quasifree spin-dependent electron scattering from a polarized  $^3\text{He}$  internal target'*  
Vrije Universiteit Amsterdam, January 1999
- [2] Andres Kruse  
*'Charged current interactions at HERA'*  
Universiteit van Amsterdam, February 1999
- [3] Edward Paul Prendergast  
*'Dynamic processes in heavy ion collisions at intermediate energies'*  
Universiteit Utrecht, March 1999
- [4] Rosella Medaglia  
*'Mesure des facteurs spectroscopiques des cinq premiers niveaux en énergie du noyau de plomb-208 à l'aide de la réaction  $^{208}\text{Pb}(e, e'p)^{207}\text{Tl}^*$  à grande impulsion transférée'*  
Université Paris XI Orsay, April 1999
- [5] Ronald Starink  
*'Short-range correlations studied with the reaction  $^{16}\text{O}(e, e'pp)^{14}\text{C}$ '*  
Vrije Universiteit Amsterdam, May 1999
- [6] Auke Pieter Colijn  
*'Measurement of the tau lepton lifetime'*  
Universiteit van Amsterdam, June 1999

- [7] Joost Herman Vosseveld  
*'Dijet photoproduction at high tranverse energies'*  
Universteit van Amsterdam, September 1999
- [8] Cornelis Andreas Franciscus Johannes van der Poel  
*'Neutrino induced charm production in the CHORUS calorimeter'*  
Katholieke Universiteit Nijmegen, September 1999
- [9] Tancredi Enrico Giusto Botto  
*'Coherent  $\pi^0$  electroproduction on  $^4\text{He}$  in the Delta region'*  
Vrije Universiteit Amsterdam, November 1999
- [10] Douglas W. Higinbotham  
*'Spitfire - Spin Physics with Internal Targets For International RE-search'*  
University of Virginia, Charlottesville, USA, November 1999
- [11] Edward Six  
*'Spin correlations in quasi-elastic electron scattering from a  $^3\text{He}$  internal target'*  
Arizona State University, Tempe, USA, December 1999

## 1.2 Invited Talks

- [1] A. Bacchetta  
*Semi-inclusive rho-leptoproduction*  
University of Wuppertal (Germany), December 7, 1999
- [2] H.P. Blok  
*The pion form factor*  
Nuclear Physics Lab, University of Colorado, Boulder, CO (USA), October 21, 1999  
Physics Department, George Washington University, Washington, DC (USA), November 1, 1999
- [3] H.P. Blok  
*Form factor of the nucleon and the pion*  
Conference on Electromagnetic Interactions with Nucleons and Nuclei, Santorini (Greece), October 6, 1999
- [4] H.P. Blok  
*Polarized and unpolarized ( $e,e'x$ ) studies of few nuclon systems at NIKHEF*  
Symposium Current Topics in the field of light nuclei, Cracow (Poland), June 22, 1999
- [5] G.J. Bobbink  
*Tests of QCD at LEP*  
9<sup>th</sup> Lomonosov Conference on Elementary Particle Physics, Moscow (Russia), September 20-25, 1999
- [6] G.J. Bobbink  
*L3 Results from the 189 GeV run*  
LEPC CERN, Geneva (Switzerland), March 24, 1999
- [7] G.J. Bobbink  
*L3 Status report*  
LEPC CERN, Geneva (Switzerland), September 7, 1999
- [8] D. Boersma  
*The neutron electric form factor at  $Q^2=0.2\text{ GeV}^2$  extracted from polarised  $^3\text{He}(e, e' n)$  scattering*  
Particles And Nuclei International Conference 'PANIC99', Uppsala (Sweden), June 1999
- [9] M. Boglione  
*Estimates of T-odd distribution and fragmentation functions*  
7<sup>th</sup> International Workshop on Deep Inelastic Scattering and QCD (DIS99), DESY, Zeuthen (Germany), April 1999
- [10] M. Boglione  
*From hadrons to quarks and viceversa: phenomenology of distribution and fragmentation functions*  
TMR-meeting, Erlangen (Germany), February 11-13, 1999
- [11] M. Boglione  
*The proton spin - history and new results*  
Asian Pacific Centre of Theoretical Physics, Seoul (Korea), November 4-7, 1999
- [12] M. Botje  
*A QCD analysis of HERA and fixed target structure functions*  
7<sup>th</sup> Int. Workshop on Deep Inelastic Scattering and QCD (DIS99), Zeuthen (Germany), April 20, 1999
- [13] E. Boudinov  
*Measurement of the strange quark forward-backward asymmetry around the Z0 peak with DELPHI detector*  
University of Victoria, Victoria (Canada), December 3, 1999  
SLAC, Stanford, California (USA), December 9, 1999  
PASCOS99, 7th International Symposium on Particles, Strings and Cosmology, Granlibakken, Lake Tahoe CA (USA), December 10-16, 1999
- [14] J.F.J. van den Brand  
*Recent results from Spin Dependent Electron Scattering in Amsterdam*  
Second International Conference on Perspectives in Hadronic Physics, ICTP, Trieste (Italy) 10-14 May 1999
- [15] J.F.J. van den Brand  
*Spin Dependent Electron Scattering in Amsterdam*  
The First Asia-Pacific Conference on Few-Body Problems in Physics (APFB99), Noda/Kashiwa (Japan), August 23-28, 1999
- [16] J.F.J. Van den Brand  
*Electromagnetic Studies of the Nucleon and Few-Body Systems*  
Int. Workshop on Polarized Sources and Targets 'PST99', Erlangen (Germany), September 1999
- [17] J.F.J. van den Brand  
*Recent Results on Spin-Dependent Scattering in Amsterdam*  
Conference on Electromagnetic Interactions with Nucleons and Nuclei, Santorini (Greece), October 8, 1999
- [18] J.F.J. van den Brand  
*Recent Results on Spin Dependent Scattering from Few-Body Systems obtained in Amsterdam*  
25 years of MIT-Bates Celebration, MIT, Cambridge MA (USA), November 1999
- [19] N. Brummer  
*Search for Exotic Physics at HERA*  
EPS-HEP99, Tampere (Finland), July 15-21, 1999
- [20] L.D. van Buuren  
*High Density Polarized Hydrogen/Deuterium Internal Target*  
Particles And Nuclei International Conference 'PANIC99', Uppsala (Sweden), June 1999
- [21] L.D. van Buuren  
*Electron Scattering Experiments with Polarized Hydrogen/Deuterium Internal Targets*  
4<sup>th</sup> Int. Conf. on Nucl. Phys. at Storage Rings 'STORI99', Bloomington IN (USA), September 1999
- [22] A. Buijs  
*The formation of charmonium states in photon-photon collisions at LEP*  
PHOTON '99, Freiburg (Germany), May 23-27, 1999
- [23] J.A. van Dalen  
*Bose-Einstein Correlations in W-Pair Production at  $\sqrt{s} = 189\text{ GeV}$  at LEP*  
QCD conference, Montpellier (France) July 7-13, 1999
- [24] J.A. van Dalen  
*Bose-Einstein Correlations (BEC) between Like-Sign Particles*  
International Summerschool Nijmegen99, Nijmegen (The Netherlands), August 8-20, 1999
- [25] J.J. Engelen  
*Calorimeters in the LHC experimental programme*  
CALOR99 Conference, Lisbon (Portugal), June 1999

- [26] J.J. Engelen  
*Over Tijd*  
Nationale Wetenschapsdag, Amsterdam (The Netherlands), October 10, 1999
- [27] J.J. Engelen  
*Probing the proton down to  $10^{-19}$  m, what do we see?*  
Universiteit Twente (The Netherlands), April 7, 1999
- [28] F.C.ERNÉ  
*Measurements of the Photon Structure Function at L3*  
PHOTON '99, Freiburg (Germany), May 23-27, 1999
- [29] B. van Eijk  
*ATLAS tracking: The interplay between frontier physics and frontier technology*  
Rijks Universiteit Utrecht, Utrecht (The Netherlands), November 11, 1999
- [30] B. van Eijk  
*Charged particle tracking in ATLAS*  
University Valencia (Spain), November 18, 1999
- [31] M. Ferro-Luzzi  
*Electromagnetic Studies of the Nucleon and Few-body System with Polarized Electrons and Polarized Internal Targets*  
Int. Workshop on Polarized Sources and Targets 'PST99', Erlangen (Germany), September 1999
- [32] M. Ferro-Luzzi  
*Recent  $G_E^p$  results from Amsterdam*  
International Conference on the Structure of the Nucleon 'Nucleon 99', Frascati (Italy), June 1999
- [33] B. Gato-Rivera  
*Recent Results on  $N=2$  Superconformal Algebras*  
'Conformal Field Theory and Integrable Models', Landau Institute for Theoretical Physics (Russia), 1999  
6<sup>th</sup> International Wigner Symposium, Bogazici University, Istanbul (Turkey), 1999
- [34] D. Groep  
*Investigation of the exclusive  $^3\text{He}(e,e'pp)n$  reaction* Electromagnetically Induced Two-Hadron Emission, Granada (Spain), May 26-29, 1999.
- [35] S. Groot Nibbelink  
*Consistent supersymmetric sigma models*  
Imperial College, London, (UK), July 1999
- [36] S. Groot Nibbelink  
*Kähler inflates? - supersymmetry and inflation*  
Les Houches Summerschool on Astrophysics and the Primordial Universe, August 1999
- [37] R. van Gulik  
*GaGaRes: a Monte Carlo generator for resonance production in weak photon physics*  
PHOTON '99, Freiburg (Germany), May 23-27, 1999
- [38] F. Hartjes  
*Amplitude Distribution and Radiation Damage on CVD Diamond*  
Vertex99, Texel (The Netherlands)
- [39] M. Harvey  
*Measurement of the Transverse Asymmetry in the Inclusive Quasielastic Scattering of Polarized Electrons from Polarized Helium 3*  
American Physical Society Centennial Meeting, Atlanta GA (USA), March 1999
- [40] W.H.A. Hesselink  
*Probing Short-Range Correlations in  $^3\text{He}$ ,  $^{16}\text{O}$  Using the Reaction  $(e, e'pp)$*   
10<sup>th</sup> Mini-Conference on Studies of Few-Body Systems with High Duty-Factor Electron Beams, Amsterdam (The Netherlands), January 6-7, 1999
- [41] W.H.A. Hesselink  
*Probing Short-Range Correlations in  $^{16}\text{O}$  Using the Reaction  $^{16}\text{O}(e, e'pp)^{14}\text{C}$*   
Electromagnetically Induced Two-Hadron Emission, Granada (Spain), May 26-29, 1999.
- [42] W.H.A. Hesselink  
*Electron Induced Two-Nucleon Knockout and Short-Range Correlations*  
16<sup>th</sup> Students' Workshop on Electromagnetic Interactions, Bosen (Germany), September 5-10, 1999
- [43] W.H.A. Hesselink  
*Probing Short-Range Correlations in  $^3\text{He}$  and  $^{16}\text{O}$  Using the Reaction  $(e, e'pp)$*   
International School on Nuclear Physics, Erice (Italy), September 17-27, 1999
- [44] J.W. van Holten  
*Gravitational waves and massless particle fields*  
Karpacz Winterschool of Theoretical Physics (Poland), February 2, 1999
- [45] J.W. van Holten  
*Gravitationgolven*  
Gastcollege TUE, Eindhoven (The Netherlands), April 22, 1999
- [46] J.W. van Holten  
*4 Lectures on Gravitational Waves*  
FANTOM zomerschool; Dourdan (France), May 17-21, 1999
- [47] J.W. van Holten  
*Physics of gravitational waves*  
Thinkshop on gravitational waves, CERN, Geneva (Switzerland), June 18, 1999
- [48] J.W. van Holten  
*Gravitational waves*  
DESY theoretical physics colloquium, Hamburg (Germany), June 10, 1999
- [49] J.W. van Holten  
*Killing-Yano tensors, non-standard supersymmetry and an index theorem on manifolds with torsion*  
Journées relativistes; Weimar (Germany), September 13, 1999
- [50] J.W. van Holten  
Interview TELEAC, Nobelprijs fysica 1999, October 16, 1999
- [51] J.W. van Holten  
*2 Lectures on Cosmology*  
Topical lectures, NIKHEF, Amsterdam (The Netherlands), November 18-19, 1999
- [52] J.J. van Hunen  
*Semi-inclusive hadron production from  $^{14}\text{N}$*   
10<sup>th</sup> Mini-Conference on Studies of Few-Body Systems with high-duty factor electron beams, NIKHEF, Amsterdam (The Netherlands), January 6-7, 1999  
Rijks Universiteit Utrecht, Department of subatomic Physics, Utrecht (The Netherlands), March 15, 1999
- [53] J.J. van Hunen  
*Deep-inelastic scattering off  $^{14}\text{N}$*   
Workshop on Perspectives in Hadronic Physics, Trieste (Italy), May 10-14, 1999
- [54] J.J. van Hunen  
*A-dependence of  $R = \sigma_L/\sigma_T$  in Deep-Inelastic Scattering*  
Workshop on the Role of the Nuclear Medium in Deep Inelastic Scattering, European Center for Theory (ECT\*), Trento (Italy), October 11-15, 1999
- [55] E. Jans  
*Investigation of the exclusive  $^3\text{He}(e,e')$  reaction*  
Workshop on Nucleon and Quark correlations, Santorini (Greece), October 4-5, 1999

- [56] M. de Jong  
*Neutrinos: masses, mixing and oscillations*  
Seminar at the Institute for Atomic and Molecular Physics (AMOLF), Amsterdam (The Netherlands), January 11, 1999  
Colloquium Ehrenfestii, Leiden (The Netherlands), May 12, 1999  
Seminar Rijks Universiteit Utrecht, Utrecht (The Netherlands), May 12, 1999
- [57] P. de Jong  
*Some Observations on Final State Interactions in  $WW \rightarrow qq\bar{q}\bar{q}$*   
Final State Interaction sessions at WW99, the LEP workshop on W physics, Kolymbari-Chania, Crete (Greece), October 23 1999
- [58] P. de Jong  
*Experimental Studies of the Electroweak Interaction at CERN*  
Algemeen Natuurkundig Colloquium, Rijksuniversiteit Groningen (The Netherlands), April 15, 1999
- [59] W. Kittel  
*Review of Bose-Einstein Correlations and Colour Reconnection*  
Rencontre de Moriond, Les Arcs (France), March 20-27, 1999
- [60] W. Kittel  
*Correlations and Fluctuations in High-Energy Collisions*  
Int. Summer School on Particle Production Spanning MeV and TeV Energies, Nijmegen (The Netherlands), August 8-20, 1999
- [61] W. Kittel  
*Bose-Einstein Correlations in  $WW$  Decay in  $L3$*   
Crete WW99 Workshop, Kolymbari (Greece), October 20-23, 1999
- [62] W. Kittel  
*Bose-Einstein Correlations and Color Reconnection*  
Inst. f. Hochenergiephysik, Vienna (Austria), March 11, 1999
- [63] W. Kittel  
*Color Reconnection and Bose-Einstein Correlation in  $WW$  Decay*  
First Meeting of Final-State-Interaction Group, CERN, Geneva (Switzerland), June 4, 1999
- [64] N. Kjaer  
*Electroweak studies at LEP2*  
Cracow Epiphany Conference, Cracow (Poland), January 5-10, 1999
- [65] P. Kluit  
*A Search for Heavy Stable Particles at LEP2*  
Helsinki Institute of Physics, Helsinki (Finland), March 12, 1999
- [66] E. Koffeman  
*The ZEUS Microvertex Detector*  
7<sup>th</sup> International Conference on Instrumentation for Colliding Beam Physics, Hamamatsu, Shizuoka (Japan), November 15-19, 1999
- [67] H. Kolster  
*Polarized Gas Targets for Storage Rings - The HERMES Internal Target*  
Institute Seminar, RCNP Osaka Univ., Osaka (Japan), July 15, 1999  
Bates Linear Accelerator Center - MIT, Cambridge MA (USA), September 21, 1999
- [68] H. Kolster  
*Recombination of H and D atoms on Surfaces and Polarization of the Molecules*  
IUCF, Bloomington IN (USA), September 17, 1999
- [69] H. Kolster  
*The Measurement of the Polarization in the HERMES Internal Target*  
Workshop on Polarized Sources and Targets (PST99), Erlangen Univ., Erlangen (Germany), October 1, 1999
- [70] H. Kolster  
*A Polarized Atomic Jet Target for RHIC Polarimetry*  
RHIC Spin Workshop, BNL, Upton NY (USA), October 8, 1999
- [71] H. Kolster  
*Measurements of Recombination in the HERMES Internal Target*  
Marburg University, Marburg (Germany), December 7, 1999
- [72] P. Kooijman  
*Deep inelastic  $e^\pm p$  scattering at high  $Q^2$*   
EPS-HEP99, Tampere (Finland), July 15-21, 1999
- [73] B.V. Krippa  
*On Chiral theory of NN interactions in nuclear matter*  
International workshop on hadron physics; effective theories of low-energy QCD, Coimbra (Portugal), September 10 - 15, 1999
- [74] E. Laenen  
*Soft Gluon Resummation in QCD Cross Sections*  
Rijks Universiteit Utrecht, Utrecht (The Netherlands), October 6, 1999  
Universiteit van Amsterdam, Amsterdam (The Netherlands), December 2, 1999
- [75] E. Laenen  
*Summary Talk of Structure Function Working Group*  
7<sup>th</sup> International Workshop on Deep Inelastic Scattering and QCD (DIS 99), Zeuthen (Germany), April 23, 1999
- [76] E. Laenen  
*Sudakov Effects in QCD*  
Jyvaskyla University (Finland), July 13, 1999
- [77] E. Laenen  
*Topics in Heavy Flavor Physics at Colliders*  
UK Phenomenology Workshop on Collider Physics, Durham (UK), September 24, 1999
- [78] E. Laenen  
*Status of NLO calculations for charm production in DIS*  
UK Phenomenology Workshop on Collider Physics, Durham (UK), September 20, 1999
- [79] E. Laenen  
*Heavy Quark Fragmentation*  
Fermilab B-physics Workshop, Batavia IL (USA), November 11, 1999
- [80] E. Laermann  
*Finite temperature QCD on the lattice*  
Workshop Understanding Deconfinement in QCD, Trento (Italy)
- [81] L. Lapikás  
*Electron scattering in Amsterdam - an historical overview*  
10<sup>th</sup> Mini-Conference on Studies of Few-Body Systems with High Duty-Factor Electron Beams, Amsterdam (The Netherlands), January 7, 1999
- [82] L. Lapikás  
*Correlations in the ground-state wave function of  $^7\text{Li}$*   
15<sup>th</sup> Particles and Nuclei International Conference (PANIC 99), Uppsala (Sweden), June 12, 1999
- [83] L. Lapikás  
*Complex nuclei and the  $(e, e'p)$  reaction*  
Conference on Electromagnetic Interactions with Nucleons and Nuclei, Santorini (Greece), October 8, 1999
- [84] F. Linde  
*Cornering the elusive Higgs*  
Universiteit van Amsterdam, Amsterdam (The Netherlands), June 15, 1999
- [85] D.J. Mangeol  
*Analysis of the Charged Particle Multiplicity Distribution using the  $H_q$  Moments at 91.2 GeV with the L3 Detector*  
International Summerschool Nijmegen99, Nijmegen (The Netherlands), August 8-20, 1999
- [86] O. Melzer  
*Data handling in the CHORUS emulsion experiment at CERN*  
International Europhysics Conference on High Energy Physics (HEP99) Tampere (Finland), July 15-21, 1999

- [87] W.J. Metzger  
*Oscillating  $H_q$ , Event Shapes and QCD*  
Int. Symp. on Multiparticle Dynamics (IMSD99), Providence RI (USA), August 11, 1999
- [88] W.J. Metzger  
*Bose-Einstein Results from L3*  
Int. Symp. on Multiparticle Dynamics (IMSD99), Providence RI (USA), August 11, 1999
- [89] W.J. Metzger  
*Analysis of  $e^+e^- \rightarrow q\bar{q}$  Data from L3 at CERN*  
Inst. of Particle Physics, Central China Normal University, Wuhan (China), April 23 and May 7, 1999
- [90] W.J. Metzger  
*QCD (Experimental) (mostly  $e^+e^-$ )*  
Inst. of Particle Physics, Central China Normal University, Wuhan (China), April 26 - May 5, 1999
- [91] W.J. Metzger  
*A Short Course on Statistics*  
Inst. of Particle Physics, Central China Normal University, Wuhan (China), April 27 - May 6, 1999
- [92] W.J. Metzger  
*CERN and the L3 Experiment*  
Jingzhou Normal University, Jingzhou (China), April 30, 1999
- [93] W.J. Metzger  
*Elongation of the Pion Source in  $Z \rightarrow$  Hadrons from L3 at CERN*  
Inst. of Particle Physics, Central China Normal University, Wuhan (China), May 12, 1999  
Inst. of High Energy Physics, Beijing (China), May 18, 1999
- [94] S. Moch  
*Soft gluon resummation for heavy quark production* 11<sup>th</sup> Workshop on Theory beyond the Standard Model, Bad Honnef (Germany), March 3, 1999  
International workshop QCDNET99, Firenze (Italy), September 17, 1999
- [95] S. Moch  
*Mellin moments of deep inelastic structure functions at two loop*  
International Euroconference on Quantumchromodynamics - QCD 99, Montpellier (France), July 7, 1999
- [96] S. Moch  
*Heavy quark production in deep inelastic scattering at HERA*  
Workshop on Monte Carlo Generators for HERA Physics, Hamburg (Germany), April 27-30, 1999
- [97] M. Mulders  
*W mass and cross sections at LEP2*  
11<sup>th</sup> Rencontres de Blois, Blois (France), June 28 - July 3, 1999
- [98] M. Mulders  
*Emulation of WW events using Mixed Lorentz Boosted Z0s in DELPHI*  
WW99 Workshop on WW physics at LEP200, Crete (Greece), October 20-23, 1999
- [99] M. Mulders  
*Treatment of non-Gaussian resolution effects with ideograms*  
WW99 Workshop on WW physics at LEP200, Crete (Greece), October 20-23, 1999
- [100] M. Mulders  
*Summary of W mass systematics*  
WW99 Workshop on WW physics at LEP200, Crete (Greece), October 20-23, 1999
- [101] P.J. Mulders  
*Perspectives in Polarized Leptoproduction*  
Workshop on the Structure of the Nucleon (NUCLEON99), Frascati (Italy), June 7 - 9, 1999
- [102] P.J. Mulders  
*Parton correlations in the proton; going beyond collinearity*  
Workshop on Physics with Polarized Electron Ion Collider (EPIC99), Bloomington, April 8 - 11, 1999
- [103] P.J. Mulders  
*Structure of hadrons measured in hard processes*  
International workshop on hadron physics; effective theories of low-energy QCD, Coimbra (Portugal), September 10 - 15, 1999
- [104] P.J. Mulders  
*Structure of hadrons in hard scattering processes*  
International Summer School on Particle Production Spanning MeV and TeV Energies, Nijmegen (The Netherlands), 1999
- [105] P.J. Mulders  
*New possibilities in leptoproduction*  
Bosen99, Bosen (Germany), September 6 - 10, 1999
- [106] P.J. Mulders  
*The many faces of the nucleon*  
Fall Meeting of the Nuclear and Particle Physics sections of the Dutch Physical Society (NNV), Petten (The Netherlands), October 29, 1999
- [107] A.J.M. Muijs  
*Measurement of fermion pair production at LEP2 energies with the L3 detector*  
DPF conference, Los Angeles CA (USA), January 6-9, 1999
- [108] V. Pascalutsa  
*Delta isobar as explicit d.o.f. in field theory*  
ECT\* Workshop on The Nuclear Interaction: Modern Developments, Trento (Italy), July 3, 1999
- [109] V. Pascalutsa  
*Spin-3/2 fields in models of pion scattering and photoproduction*  
Institut für Kernphysik, Forschungszentrum Jülich, Jülich (Germany), August 5, 1999
- [110] I. Passchier  
*The Charge Form Factor of the Neutron from  $^2H(e, e'n)p$*   
Particles And Nuclei International Conference 'PANIC99', Uppsala (Sweden), June 1999
- [111] I. Passchier  
*Longitudinally Polarized Electrons in a Storage Ring at 1 GeV*  
4<sup>th</sup> Int. Conf. on Nucl. Phys. at Storage Rings 'STOR199', Bloomington IN (USA), September 1999
- [112] D. Reid  
*A Study of the Higgs decay to gamma-gamma*  
ECFA/DESY Linear Collider Workshop, Oxford (UK), March 20-23, 1999
- [113] D. Reid  
*Measurement of Branching Ratio fo Higgs to two photons*  
International Workshop on Linear Colliders, Sitges, Barcelona (Spain), April 28 - May 5, 1999
- [114] D. Reid  
*DELPHI results at LEP-2*  
Ecole Polytechnique, Palaiseau (France), December 13, 1999
- [115] M.P. Sanders  
*Neutral Pion Interferometry or Bose-Einstein Correlations with Neutral Pions*  
International Summerschool Nijmegen99, Nijmegen (The Netherlands), August 8-20, 1999
- [116] K. Schalm  
*Quantization of the  $SL(2,Z)$  covariant superstring*  
Spinoza Inst., Utrecht (The Netherlands), September 22, 1999
- [117] A.N. Schellekens  
*Meromorphic  $c=24$  conformal field theories*  
Technische Universiteit Eindhoven, Eindhoven (The Netherlands), January 1999

- [118] A.N. Schellekens  
*Recent developments in String theory*  
Universiteit Nijmegen (The Netherlands), April 1999
- [119] A.N. Schellekens  
*Open Strings, Simple Currents and Fixed Points*  
Wigner Symposium, Istanbul (Turkey), August 1999
- [120] A. van Sighem  
*Deep inelastic  $e^\pm p$  scattering at the highest  $Q^2$*   
14<sup>th</sup> Intern. Workshop on High Energy Physics and Quantum Field Theory (QFTHEP 99), Moscow (Russia), May 17 - June 2, 1999
- [121] G. van der Steenhoven  
*Quarks, gluonen en de rest*  
Afdeling Natuurkunde, Technische Universiteit Eindhoven, Eindhoven (The Netherlands), 28 April 1999
- [122] G. van der Steenhoven  
*The HERMES Silicon Detector Project*  
Institut für Kernphysik, Forschungszentrum Jülich, Jülich (Germany), March 19, 1999
- [123] G. van der Steenhoven  
*The HERMES Silicon Detector Project*  
15<sup>th</sup> International Conference on Particles and Nuclei (PANIC XV), Uppsala (Sweden), June 11, 1999
- [124] G. van der Steenhoven  
*Deep-Inelastic Scattering and vector-meson production at HERMES*  
Service de Physique Nucleaire (CEA-DAPNIA), Centre d'Etudes de Saclay (France), September 3, 1999
- [125] G. van der Steenhoven  
*Nuclear Effects on  $R = \sigma_L/\sigma_T$  in Deep-Inelastic Scattering*  
Workshop on Structure Functions and Higher Twist Effects, MIT, Cambridge MA (USA), October 1, 1999
- [126] O. Steinkamp  
*The LHCb and HERA-B experiments*  
Workshop on B physics at the Tevatron, Fermilab, Batavia IL (USA), September 23-25, 1999
- [127] J.J.M. Steijger  
*The HERMES silicon project*  
8<sup>th</sup> International workshop on vertex detectors (Vertex99), Texel (The Netherlands), June 20-25, 1999
- [128] J.J.M. Steijger  
*The Lambda Wheels, a silicon vertex detector for HERMES*  
7<sup>th</sup> International conference on instrumentation for colliding beam physics (Instr99), Hamamatsu (Japan), November 15-19, 1999
- [129] E. Tassi  
*Measurement of Differential Cross Sections for Dijet Production in Neutral Current DIS at High  $Q^2$  and Determination of  $\alpha_s$*   
7<sup>th</sup> Int. Workshop on Deep Inelastic Scattering and QCD (DIS99), Zeuthen (Germany), April 20, 1999
- [130] J. Timmermans  
*Precision measurements of the W boson mass*  
University Roma III, Rome (Italy), May 21, 1999
- [131] C. Timmermans  
*Status of the L3+C Experiment and its First Data Set*  
26<sup>th</sup> International Cosmic Ray Conference (ICRC 99), Salt Lake City, Utah (USA), August 17-25, 1999
- [132] J. Vermaseren  
*Group theory factors for Feynman diagrams*  
Technische Universiteit Eindhoven, Eindhoven (The Netherlands), February 1999
- [133] J. Vermaseren  
*The calculation of the 4-loop beta function in QCD*  
Hiroshima (Japan), March 15, 1999
- [134] J. Vermaseren  
*New functions for loop diagrams*  
Osaka (Japan), March 17, 1999
- [135] J. Vermaseren  
*New features of FORM*  
Kogakuin Univ., Shinjuku/Tokyo (Japan), March 25, 1999
- [136] J. Vermaseren  
*New Methods for computing Feynman diagrams in QCD*  
Lissabon (Portugal), October 2, 1999
- [137] J. Visser  
*Recoil detection at HERMES*  
Workshop on the Role of the Nuclear Medium in Deep Inelastic Scattering, European Center for Theory (ECT\*), Trento (Italy), October 11-15, 1999
- [138] J. Vossebelt  
*The Partonic Structure of Quasi-Real Photons*  
EPS-HEP99, Tampere (Finland), July 15-21, 1999
- [139] J. Vossebelt  
*The Partonic Structure of the Photon at HERA*  
Rijks Universiteit Utrecht (The Netherlands), September 27, 1999
- [140] H. de Vries  
*Longitudinally Polarized Electrons in a Storage Ring at 1 GeV*  
Int. Workshop on Polarized Sources and Targets 'PST99', Erlangen (Germany), September 1999
- [141] I. van Vulpen  
*DELPHI's Higgs analysis in the 4-jet channel*  
European School of High-Energy Physics, Casta-Papiernicka (Slovak Republic), August 22 - September 4, 1999
- [142] S. Weinzierl  
*QCD corrections to  $e^+ e^- \rightarrow 4$  jets*  
Durham Collider Workshop, Durham (UK), September 19-24, 1999
- [143] S. Weinzierl  
*QCD sum rules on the light-cone and  $B \rightarrow \pi$  form factors*  
Durham Collider Workshop, Durham (UK), September 19-24, 1999
- [144] H. Wilkens  
*Status and Prospects of L3+Cosmics*  
First Arctic Workshop on Cosmic Ray Physics, Sodankyla (Finland), April 24-29, 1999
- [145] P.K.A. de Witt Huberts  
*The spin structure of the nucleon: flavour, sea and glue*  
Workshop on Perspectives in Hadronic Physics, Trieste (Italy), May 10-14, 1999
- [146] P.K.A. de Witt Huberts  
*Multi-GeV electron accelerators in Europe*  
15<sup>th</sup> International Conference on Particles and Nuclei (PANIC XV), Uppsala (Sweden), June 10-19, 1999
- [147] N. Zaitsev  
*The LHCb pile-up detector*  
8<sup>th</sup> International Workshop on vertex detectors, Texel (The Netherlands), June 20-25, 1999

### 1.3 Seminars at NIKHEF

- [1] January 15, 1999, Amsterdam  
F. Hartjes (NIKHEF)  
*Performance and radiation hardness modelling of diamond detectors*
- [2] January 21, 1999, Amsterdam  
Igor Meshkov (JINR)  
*The Dubna Synchrotron facility*

- [3] January 29, 1999, Amsterdam  
R. Wigmans (Texas Tech. University)  
*On Big Bang relics, the neutrino mass and the spectrum of cosmic rays*
- [4] February 5, 1999, Amsterdam  
M. Campbell (CERN/RD49)  
*Pixel detector electronics for high energy physics and X-ray imaging applications*
- [5] February 12, 1999, Amsterdam  
Dr. J.P. van der Weele (Universiteit Twente)  
*The motion of animals explained by a set of oscillators*
- [6] February 24, 1999, Amsterdam  
P.J.T. Bruinsma (NIKHEF)  
*Signalen en Storingen bij Silicium Detectors*
- [7] February 24, 1999, Amsterdam  
G.J van Oldenborgh (KNMI)  
*El Nino*
- [8] February 26, 1999, Amsterdam  
J. Stachel (Heidelberg)  
*Towards the Quark-Gluon Plasma*
- [9] March 4, 1999, Amsterdam  
C.P. Datema (Astrophysics Group, University of Southampton, UK)  
*The Hybrid Photodiode and its applications*
- [10] March 5, 1999, Amsterdam  
B. Nauta (U-Twente/MESA)  
*Trends and Challenges in deepsubmicron CMOS design*
- [11] March 8, 1999, Amsterdam  
A. Brandt (Fermilab)  
*Hard Diffraction and the D0 Forward Proton Detector*
- [12] March 16, 1999, Amsterdam  
G. Watts (Brown University)  
*DZERO and its Triggers*
- [13] March 19, 1999, Amsterdam  
A.P. Colijn (NIKHEF)  
*Measurement of the taulifetime*
- [14] April 9, 1999, Amsterdam  
N. Obers (Nordita)  
*Non-perturbative aspects of string theory*
- [15] April 16, 1999, Amsterdam  
J. Lang (ETH Zuerich)  
*Time Reversal Invariance in Weak Interactions*
- [16] April 23, 1999, Amsterdam  
D. Broadhurst (Open University)  
*The number content of the standard model*
- [17] May 7, 1999, Amsterdam  
M. Strikman (Penn State/DESY)  
*The HERA e-A collider project*
- [18] June 11, 1999, Amsterdam  
J. de Boer (Leiden)  
*What information does string theory give us?*
- [19] June 24, 1999, Amsterdam  
H. van der Graaf & J.W. van Holten (NIKHEF)  
*GRAPPA: A Precision Measurement of Newtons Gravitational Constant and the Verification of the  $R^{-2}$  Law at mm Scale*
- [20] June 25, 1999, Amsterdam  
E. Boudinov (NIKHEF)  
*Measurement of the strange quark forward-backward asymmetry around the  $Z^0$  peak with the Delphi Detector*
- [21] July 2, 1999, Amsterdam  
A. Kusenko (UCLA)  
*The highest energy cosmic rays and neutrinos*
- [22] July 7, 1999, Amsterdam  
D. Galtsov (Moskou/Jussieu, Parijs)  
*Gravitational lumps*
- [23] July 9, 1999, Amsterdam  
A. Sill (Texas)  
*W-mass measurement at CDF*
- [24] August 14, 1999, Amsterdam  
J. Smith (Stony Brook)  
*Variable Flavor Number Schemes in Heavy Quark Production*
- [25] August 27, 1999, Amsterdam  
E. Levin (Tel Aviv/DESY)  
*High parton density QCD*
- [26] September 3, 1999, Amsterdam  
J. Vosseveld (NIKHEF)  
*Partonic structure of the photon at HERA*
- [27] September 8, 1999, Amsterdam  
E. Tassi (DESY)  
 $\alpha_s$  measurement from dijet production at HERA
- [28] September 9, 1999, Amsterdam  
G. Mancinelli (SLAC)  
*Direct measurements of  $A_b$  and  $A_c$  at the  $Z^0$  pole at SLD*
- [29] September 10, 1999, Amsterdam  
P. Kooijman & H. Tiecke (NIKHEF)  
*Summary talk on EPS-HEP99 (Tampere) and Lepton Photon (Stanford)*
- [30] October 1, 1999, Amsterdam  
P.K.A. de Witt Huberts and M. de Jong (NIKHEF)  
*Summary talk on PANIC XV and muon-collider workshop*
- [31] October 5, 1999, Amsterdam  
Y. Igarashi (Niigata University, Japan)  
*Electric-Magnetic duality*
- [32] October 8, 1999, Amsterdam  
E. Leader (Birnbeck College-U.London/VU)  
*How well do we know the polarized densities of the proton?*
- [33] October 15, 1999, Amsterdam  
J. Butterworth (UC London)  
*Photon Structure*
- [34] October 22, 1999, Amsterdam  
T. van Rhee (NIKHEF/L3)  
*Charmonium formation in two-photon collisions*
- [35] November 5, 1999, Amsterdam  
S. Hofmann (GSI)  
*The search for superheavy elements*
- [36] November 12, 1999, Amsterdam  
D. Calvet (CPPM)  
*Status of the readout architecture of the ATLAS pixel detector*
- [37] November 26, 1999, Amsterdam  
M. Spira (University of Hamburg)  
*Higgs Production and Decay at Hadron Colliders*
- [38] December 10, 1999, Amsterdam  
G. Raven (Stanford)  
*The BaBar experiment at SLAC*

## 1.4 NIKHEF Annual Scientific Meeting, December 16-17, 1999, Utrecht

- [1] P. de Jong  
*LEP overview and W's at LEP*
- [2] Ivo van Vulpen  
*Higgs search and  $e^+e^- \rightarrow Z^0Z^0$  at DELPHI*
- [3] S. Muijs  
*Fermion pair production with the L3 detector*
- [4] J. Volmer  
*The pion form factor*
- [5] M. Ferro-Luzzi  
*Electronuclear Spin Observables at AmPS*
- [6] M. Steenbakkens  
*Pion production on  $^4\text{He}$  with AmPS*
- [7] E. Koffeman  
*ZEUS status and microvertex detector project*
- [8] N. Tuning  
*New proton structure function results from HERA*
- [9] G. van der Steenhoven  
*HERMES overview*
- [10] J.J. van Hunen  
*Deep-inelastic scattering of  $^{14}\text{N}$*
- [11] J. Uiterwijk  
*Status report*
- [12] S. Weinzierl  
*Standard model and QCD aspects*
- [13] S. Groot Nibbelink  
*Supersymmetry and unification*
- [14] F. Linde  
*ATLAS overview*
- [15] N. Hessey  
*The ATLAS silicon tracker*
- [16] P. Hendriks  
*ATLAS muon reconstruction from a C++ perspective*
- [17] K. Bos  
*D0 overview*
- [18] B. Wijngaarden  
*The D0 silicon tracker*
- [19] A. Buijs  
*Status report*
- [20] D. Muigg  
*The ALICE silicon detectors*
- [21] M. Botje  
*NA49 and charm detection*
- [22] O. Steinkamp  
*HERA-B: Status and perspectives*
- [23] M. Merk  
*LHCb: Tracking and physics-performance*
- [24] N. van Bakel  
*The LHCb silicon vertex detector*
- [25] M. de Jong  
*The ANTARES project*
- [26] J. Timmermans  
*Linear collider activities*
- [27] G. van Middelkoop  
*NIKHEF in the 21st century*

# G Resources and Personnel

## 1 Resources

In 1999 NIKHEF received a budget for exploitation (including salaries) of some MHfl 36 (Fig. 1.1). The budget figures of the NIKHEF partners were: FOM-institute (SAF/NIKHEF) MHfl 25.3, universities MHfl 9.2 of which FOM supplied MHfl 3.4 through the Community for Subatomic Physics (SAF). Third parties (EU-funding, other scientific institutions, commercial activities) contributed MHfl 1.5 to the NIKHEF income.

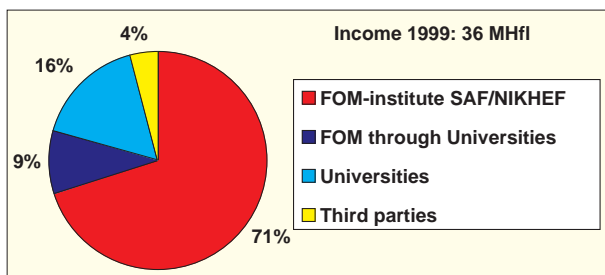


Figure 1.1: NIKHEF funding.

Roughly a quarter of the total exploitation budget has been spent (Fig. 1.2) on the largest NIKHEF activity, ATLAS (24%). LEP-activities (Delphi and L3/Cosmics) and B-physics (at HERA and LHC) each took up about 13% of the budget. About 14% of the budget went to Theory and new activities such as ANTARES and general R&D not related to a specific experiment (transition programme).

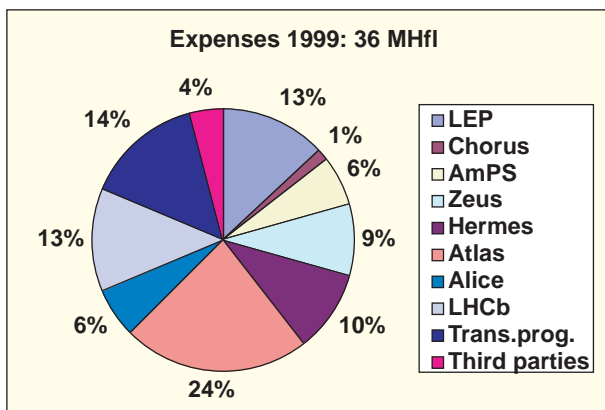


Figure 1.2: Exploitation budget.

been allocated: MHfl 3.2 to ATLAS, MHfl 3.9 to LHCb, MHfl 0.9 to general infrastructure (buildings, workshops, computing).

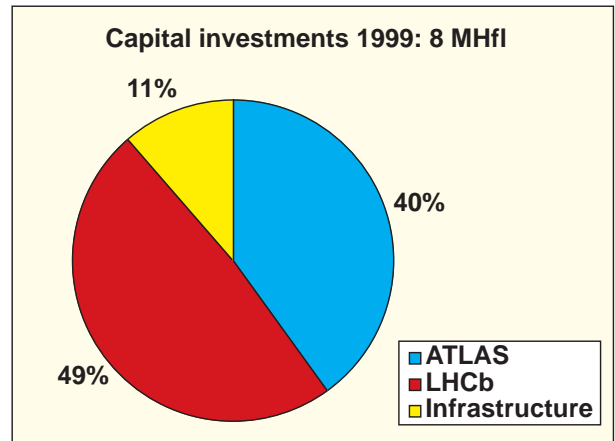


Figure 1.3: Capital investments.

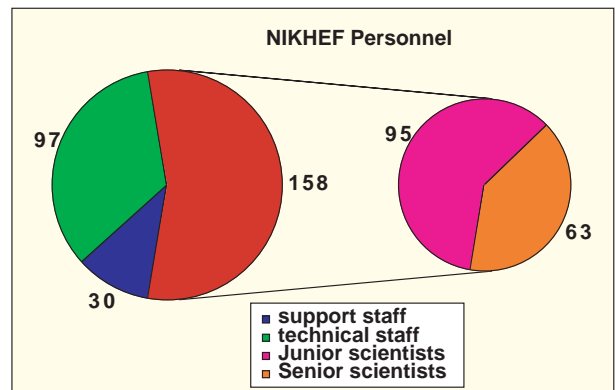


Figure 1.4: Personnel. Subdivision of personnel: the scientists are divided into senior and junior scientists (right plot).

In 1999 MHfl 8 of capital investments (Fig. 1.3) has

## 2 Membership of Councils and Committees during 1999

### **NIKHEF Board**

A.R. de Monchy (FOM, Chairman)  
K.H. Chang (FOM)  
J.J.M. Franse (UvA)  
G.W. Noomen (VU)  
Th.H.J. Stoelinga (KUN)  
J.G.F. Veldhuis (UU)  
H.M. van Pinxteren (secretary, FOM)

### **Scientific Advisory Committee NIKHEF**

P. Darrulat (CERN, Chairman)  
B. Frois (CEA Saclay)  
D. von Harrach (Univ. Mainz)  
G. Ross (Univ. Oxford)  
P. Söding (DESY)  
J. Stachel (Univ. Heidelberg)

### **NIKHEF Works Council**

L.W. Wiggers (Chairman)  
R.G.K. Hart (1st secretary)  
J.J. Hogenbirk (2nd secretary)  
H. Boer Rookhuizen  
J.H.G. Dokter  
W.D. Hulsbergen  
F.B. Kroes

### **FOM Board**

J.J. Engelen

### **Fund for Scientific Research, Flanders, Belgium**

G. van Middelkoop

### **Schwerpunktprogramm, Advisory Commission DFG, Bonn**

J.H. Koch

### **SPC-CERN**

J.J. Engelen  
K.J.F. Gaemers

### **LHCC-CERN**

J.J. Engelen (Chairman)

### **SPSC-CERN**

B. Koene

### **Extended Scientific Council, DESY**

K.J.F. Gaemers

### **ECFA**

J.J. Engelen, K.J.F. Gaemers, R. Kamermans, E.W. Kittel,  
G. van Middelkoop (also in Restricted ECFA)

### **NuPECC**

G. van Middelkoop

### **HEP Board EPS**

J.J. Engelen

### **EPAC**

P.W. van Amersfoort  
G. Luijckx

### **Scientific Advisory Committee, Physique Nucleaire, Orsay**

P.K.A. de Witt Huberts

### **Scientific Advisory Committee, DFG 'Hadronen Physik'**

P.K.A. de Witt Huberts

### **Program Advisory Committee, ELSA (Bonn) / MAMI (Mainz)**

H.P. Blok

### **Other committees**

**ASP Board** W. Hoogland

**EPCS** W. Heubers

**ESRF** G. Luijckx

**HTASK** K. Bos

**IRI** J.H. Koch

**IUPAP, C11 committee** W. Hoogland

**OECD Megascience Forum Working Groups** W. Hoogland,  
G. van Middelkoop

**SURF** W. Hoogland

**RIPE** R. Blokzijl

**SCTF** W. van Amersfoort

**WCW Board** A.J. van Rijn

### 3 Personnel as of December 31, 1999

FOM, and the universities UVA, VU, KUN and UU are partners in NIKHEF (See colofon). UL and UT denote the universities of Leiden and Twente. TE stands for temporary employee, GST for guest. Other abbreviations refer to the experiments, projects and departments.

#### 1. Experimental Physicists:

Agasi, Drs. E.E.	GST	DELPHI	FOM	ATLAS
Amersfoort, Dr.Ir. P.W. van	FOM	B Phys	FOM-VU	B Phys
Apeldoorn, Dr. G.W. van	UVA	B Phys	FOM	B Phys
Bakel, Drs. N.A. van	FOM	B Phys	UVA	B Phys
Baldew, Drs. S.V.	UVA	L3	FOM-KUN	L3
Balm, Drs. P.W.	FOM	ATLAS	FOM	B Phys
Barneo González, Drs. P.J.	FOM	AmPS Phys	FOM	HERMES
Batenburg, Drs. M.F. van	FOM	AmPS Phys	FOM	AmPS Phys
Bauer, Dr. T.S.	FOM-UU	B Phys	FOM	ANTARES
Blok, Dr. H.P.	VU	AmPS Phys	FOM	ATLAS
Blom, Drs. H.M.	FOM	DELPHI	FOM-VU	B Phys
Bobbink, Dr. G.J.	FOM	L3	KUN	L3
Boer, Dr. F.W.N. de	GST		FOM-KUN	ATLAS
Boersma, Drs. D.J.	GST	AmPS Phys	FOM	ATLAS
Bokeel, Drs. C.H.	FOM	ZEUS	FOM	B Phys
Bos, Dr. K.	FOM	ATLAS	FOM	ATLAS
Botje, Dr. M.A.J.	FOM	ALICE	FOM	HERMES
Boudinov, Drs. E.	FOM	DELPHI	FOM	CHORUS
Brand, Prof.Dr. J.F.J. van den	FOM	AmPS Phys	KUN	ATLAS
Bruinsma, Drs. M.	FOM	B Phys	UVA	ZEUS
Bruinsma, Ir. P.J.T.	GST	ANTARES	FOM	ALICE
Brummer, Dr. N.C.	FOM	ZEUS	FOM	Other Projects
Buis, Drs. E.J.	FOM	ATLAS	FOM	AmPS Phys
Buijs, Prof.Dr. A.	UU	ALICE	FOM-KUN	ATLAS
Bulten, Dr. H.J.	FOM-VU	HERMES	FOM-VU	HERMES
Buuren, Drs. L.D. van	FOM	AmPS Phys	FOM	ATLAS
Colijn, Drs. A.P.	FOM	ZEUS	FOM	CHORUS
Crijns, Dipl.Phys. F.J.G.H.	FOM-KUN	ATLAS	UU	DELPHI
Dalen, Drs. J. van	FOM-KUN	L3	KUN	L3
Dam, Dr. P.H.A. van	UVA	DELPHI	FOM-UU	B Phys
Dantzig, Dr. R. van	FOM	CHORUS	VU	DIR
Daum, Prof.Dr. C.	GST	ATLAS	KUN	L3
Diddens, Prof.Dr. A.N.	GST	DELPHI	FOM	L3
Dierendonck, Drs. D.N. van	FOM	L3	Mulders, Ir. M.P.	FOM-BR
Dierckxsens, Drs. M.E.T.	FOM	L3	Needham, Dr. M.D.	FOM
Duensing, Drs. Mw. S.	KUN	ATLAS	Noomen, Ir. J.G.	FOM
Duinker, Prof.Dr. P.	FOM	L3	Nooren, Dr.Ir. G.J.L.	FOM
Eijk, Prof.Dr. B. van	FOM	ATLAS	Oberski, Dr. J.E.J.	FOM
Eijk, Ir. R.M. van der	FOM	B Phys	Oldeman, Ir. R.G.C.	GST
Eldik, Drs. J.E. van	GST	DELPHI	Passchier, Drs. I.	GST
Engelen, Prof.Dr. J.J.	UVA	ZEUS	Payre, Dr. P.D.P.D.	GST
Erné, Prof.Dr.Ir F.C.	GST	L3	Peeters, Ir. S.J.M.	FOM
Ferreira Montenegro, Drs. Mw. J.	FOM	DELPHI	Peters, Drs. O.	UVA
Ferro-Luzzi, Dr. M.M.E.	FOM-VU	B Phys	Petersen, Drs. B.	KUN
Garutti, Drs. Mw. E.	FOM	HERMES	Phaf, Drs. L.K.	FOM
Graaf, Dr.Ir. H. van der	FOM	ATLAS	Pijl, Drs. E.C. van der	FOM-UU
Grijpink, Drs. S.J.L.A.	FOM	ZEUS	Poel, Drs. C.A.F.J. van der	GST
Groep, Drs. D.L.	FOM	AmPS Phys	Reid, Dr. D.W.	FOM
Gulik, Drs. R.C.W.	UL	L3	Rhee, Drs. Mw. T. van	GST
Hartjes, Dr. F.G.	FOM	ATLAS		
Heesbeen, Drs. D.	FOM	HERMES		
Heijboer, Drs. A.J.	UVA	ANTARES		
Heijne, Dr. H.M.	GST			
Hendriks, Drs. P.J.	FOM	ATLAS		
Hesselink, Dr. W.H.A.	VU	HERMES		
Hessey, Dr. N.P.	FOM			
Hierck, Drs. R.H.	FOM-VU			
Hommels, Ir. L.B.A.	FOM			
Hoogland, Prof.Dr. W.	UVA			
Hu, Drs. Y.	FOM-KUN			
Hulsbergen, Drs. W.D.	FOM			
Hunen, Ir. J.J. van	FOM			
Jans, Dr. E.	FOM			
Jong, Dr. M. de	FOM			
Jong, Dr. P.J.	FOM			
Jong, Prof.Dr. S.J.	KUN			
Kamermans, Prof.Dr. R.	FOM-UU			
Ketel, Dr. T.J.	FOM-VU			
Kittel, Prof.Dr. E.W.	KUN			
Klok, Drs. P.F.	FOM-KUN			
Kluit, Dr. P.M.	FOM			
Koene, Dr. B.K.S.	FOM			
Koffeman, Dr.Ir. Mw. E.N.	FOM			
Kolster, Dr. H.	FOM			
Konijn, Dr.Ir. J.	GST			
König, Dr. A.C.	KUN			
Kooijman, Dr. P.M.	UVA			
Kuijjer, Dr. P.G.	FOM			
Laan, Dr. J.B. van der	FOM			
Lapikás, Dr. L.	FOM			
Lavrijsen, Drs. W.T.L.P.	FOM-KUN			
Laziev, Drs. A.E.	FOM-VU			
Leeuwen, Drs. M. van	FOM			
Linde, Prof.Dr. F.L.	UVA			
Luijckx, Ir. G.	FOM			
Lutterot, Drs. M.	FOM			
Maas, Dr. R.	FOM			
Mangeol, Drs. D	FOM			
Massaro, Dr. G.G.G.	FOM			
Melzer, Dipl.Phys. O.	FOM			
Merk, Dr. M.H.M.	UU			
Metzger, Dr. W.J.	KUN			
Mevius, Drs. Mw. M.	FOM-UU			
Middelkoop, Prof.Dr. G. van	VU			
Mil, Drs. A. van	KUN			
Muijs, Drs. Mw. A.J.M.	FOM			
Mulders, Ir. M.P.	FOM-BR			
Needham, Dr. M.D.	FOM			
Noomen, Ir. J.G.	FOM			
Nooren, Dr.Ir. G.J.L.	FOM			
Oberski, Dr. J.E.J.	FOM			
Oldeman, Ir. R.G.C.	GST			
Passchier, Drs. I.	GST			
Payre, Dr. P.D.P.D.	GST			
Peeters, Ir. S.J.M.	FOM			
Peters, Drs. O.	UVA			
Petersen, Drs. B.	KUN			
Phaf, Drs. L.K.	FOM			
Pijl, Drs. E.C. van der	FOM-UU			
Poel, Drs. C.A.F.J. van der	GST			
Reid, Dr. D.W.	FOM			
Rhee, Drs. Mw. T. van	GST			

San Segundo Bello, Drs. D.	FOM-HCM	Other Projects
Sanders, Drs. M.	KUN	L3
Schagen, Drs. S.E.S.	FOM	ZEUS
Schillings, Drs. E.	FOM-UU	ALICE
Scholte, Ir. R.C.	UT	ATLAS
Schotanus, Dr. D. J.	KUN	L3
Sichteremann, Drs. E.P.	GST	SMC
Sighem, Drs. A.I. van	GST	ZEUS
Simani Drs. Mw. M.C.	FOM-VU	HERMES
Steenbakkers, Drs. M.F.M.	FOM-VU	AmPS Phys
Steenhoven, Dr. G. van der	FOM	HERMES
Steijger, Dr. J.J.M.	FOM	HERMES
Tassi, Dr. E.	FOM	ZEUS
Tiecke, Dr. H.G.J.M.	FOM	ZEUS
Timmermans, Dr. J.J.M.	FOM	DELPHI
Tuning, Drs. N.	UVA	ZEUS
Uiterwijk, Ir. J.W.E.	GST	CHORUS
Velthuis, Ir. J.J.	FOM	ZEUS
Ven, Drs. P.A.G. van de	FOM-UU	WA93/98
Vermeulen, Dr.Ir. J.C.	UVA	ATLAS
Visschers, Dr. J.L.	FOM	ATLAS
Visser, Drs. E.	KUN	ATLAS
Visser, Drs. J.	FOM	HERMES
Volmer, Dipl.Phys. J.	GST	AmPS Phys
Vreeswijk, Dr. M.	FOM	ATLAS
Vries, Dr. H. de	FOM	AmPS Phys
Vulpen, Drs. I.B. van	FOM	DELPHI
Wiggers, Dr. L.W.	FOM	ZEUS
Wilkins, Drs. H.	FOM-KUN	L3
Witt Huberts, Prof.Dr. P.K.A.	FOM	HERMES
Wijngaarden, Drs. D.A.	KUN	ATLAS
Wolf, Dr. Mw. E. de	UVA	ZEUS
Woudstra, Ir. M.J.	FOM	ATLAS
Zaitsev, Drs. N.U.	UVA	B Phys

## 2. Theoretical Physicists:

Bachetta, Drs. A.	FOM-VUA
Eynck, Dipl.Phys. T.O.	FOM
Gaemers, Prof.Dr. K.J.F.	UVA
Gato-Rivera, Dr. Mw. B.	GST
Groot Nibbelink, Drs. S.	FOM
Henneman, Drs. A.	VU
Holten, Dr. J.W. van	FOM
Huiszoon, Drs. L.R.	FOM
Iersel, Drs. M. van	FOM-VUA
Kleiss, Prof.Dr. R.H.P.	KUN
Koch, Prof.Dr. J.H.	FOM
Laenen, Dr. E.	FOM
Marques de Sousa, Drs. N.M.	GST
Moch, Dr. S.O.	FOM
Mulders, Prof.Dr. P.J.G.	VU
Nyawelo, B.Sc. T.S.	GST
Schalm, Dr. K.E.	FOM
Schellekens, Prof.Dr. A.N.J.J.	FOM
Vermaseren, Dr. J.A.M.	FOM
Weinzierl, Dr. S.D.	FOM
Wit, Prof.Dr. B.Q.P.J. de	GST

## 3. Computer Technology Group:

Akker, T.G.M. van den	FOM
Blokzijl, Dr. R.	FOM
Boontje, Ing. R.	FOM
Boterenbrood, Ir. H.	FOM
Damen, Ing. A.C.M.	FOM
Hart, Ing. R.G.K.	FOM
Heubers, Ing. W.P.J.	FOM
Huysen, K.	FOM
Kruszynska, Drs. Mw. M.N.	FOM
Kuipers, Drs. P.	FOM
Leeuwen, Drs. W.M. van	FOM
Oudolf, J.D.	TE
Schimmel, Ing. A.	FOM
Tierie, Mw. J.J.E.	FOM
Wassenaar, Drs. E.	FOM
Wijk, R.F. van	FOM

## 4. Electronics Technology Group:

Berkien, A.W.M.	FOM
Beuzekom, Ing. M.G. van	FOM
Boer, J. de	FOM
Boerkamp, A.L.J.	FOM
Born, E.A. van den	FOM
Es, J.T. van	FOM
Evers, G.J.	FOM
Gotink, G.W.	FOM
Groen, P.J.M. de	FOM
Groenstege, Ing. H.L.	FOM
Gromov, Drs. V.	FOM
Haas, Ing. A.P. de	FOM
Harmsen, C.J.	FOM
Heine, Ing. E.	FOM
Heutenik, B.	FOM
Hogenbirk, Ing. J.J.	FOM
Jansen, L.W.A.	FOM
Jansweijer, Ing. P.P.M.	FOM
Kieft, Ing. G.N.M.	FOM
Kluit, Ing. R.	FOM
Kok, Ing. E.	FOM
Koopstra, J.	UVA
Kroes, Ir. F.B.	FOM
Kruijjer, A.H.	FOM
Kuijt, Ing. J.J.	FOM
Mos, Ing. S.	FOM
Peek, Ing. H.Z.	FOM
Reen, A.T.H. van	FOM
Rewiersma, Ing. P.A.M.	FOM
Schipper, Ing. J.D.	FOM
Sluijk, Ing. T.G.B.W.	FOM
Stolte, J.	FOM
Timmer, P.F.	FOM
Trigt, J.H. van	FOM
Verkooijen, Ing. J.C.	FOM
Vink, Ing. W.E.W.	FOM
Wieten, P.	FOM
Zwart, Ing. A.N.M.	FOM
Zwart, F. de	FOM

## 5. Mechanical Technology Group:

Arink, R.P.J.	FOM
Band, H.A.	FOM
Beumer, H.	FOM
Boer, R.P. de	FOM
Boer Rookhuizen, H.	FOM
Boomgaard-Hilferink, Mw. J.G.	FOM
Boucher, A.	FOM
Bron, M.	FOM
Brouwer, G.R.	FOM
Buis, R.	FOM
Buskens, J.P.M.	UVA
Buskop, Ir. J.J.F.	FOM
Ceelie, L.	UVA
Doets, M.	FOM
Homma, J.	FOM
IJzermans, P.A.	TE
Jacobs, J.	TE
Jaspers, M.J.F.	UVA
Kaan, Ir. A.P.	FOM
Kok, J.W.	FOM
Korporaal, A.	FOM
Kraan, Ing. M.J.	FOM
Kuilman, W.C.	FOM
Langedijk, J.S.	FOM
Lassing, P.	FOM
Lefévere, Y.	FOM
Leguyt, R.	FOM
Mul, F.A.	FOM-VU
Munneke, Ing. B.	FOM
Overbeek, M.G. van	FOM
Petten, O.R. van	FOM
Postma, Ing. O.	FOM
Rietmeijer, A.A.	FOM
Roeland, E.	FOM
Rövekamp, J.C.D.F.	UVA
Schuijlenburg, Ing. H.W.A.	FOM
Thobe, P.H.	FOM
Veen, J. van	FOM
Verlaat, Ing. B.A.	FOM
Werneke, Ing. P.J.M.	FOM
Zegers, Ing. A.J.M.	FOM

## 6. AmPS Management Project:

Kuijjer, L.H.	FOM
La Rooij, Mw. T.J.	TE
Spelt, Ing. J.B.	FOM
Spruit, Drs. A.	FOM
Steman, W.A.	FOM
Stoffelen, A.C.	FOM

## 8. Management and Administration

Bakker, C.N.M.	FOM
Berg, A. van den	FOM
Buitenhuis, W.E.J.	FOM
Bulten, F.	FOM

Dokter, J.H.G.	FOM
Dulmen, Mw. A.C.M. van	FOM
Echtelt, Ing. H.J.B. van	FOM
Egdom, T. van	FOM
Geerinck, Ir. J.	FOM
Gerritsen-Visser, Mw. J.	FOM
Greven-v.Beusekom, Mw. E.C.L.	FOM
Heuvel, Mw. G.A. van den	FOM
Kerkhoff, Mw. E.H.M. van	FOM
Kesgin-Boonstra, Drs. Mw. M.J.	FOM
Kolkman, J.	FOM
Kwakkel, Ir. E.	FOM
Laan, Mw. F.M.	FOM
Langelaar, Dr. J.	UVA
Langenhorst, A.	FOM
Lemaire-Vonk, Mw. M.C.	FOM
Louwrier, Dr. P.W.F.	FOM
Mors, A.G.S.	UVA
Mur, Drs. Mw. L.	FOM
Ploeg, F.	FOM
Post, Mw. E.C.	FOM
Post, Dr. J.C.	GST
Rijn, Drs. A.J. van	FOM
Schäfer-v.d.Weijden, Mw. W.	FOM
Schoemaker - Weltevreden, Mw. S.	FOM
Visser, J.	FOM
Vries, W. de	FOM

## Apprentices in 1999:

Baakman, Y.	MT
Belkasmı, M.	ET
Bello, O.S.F.	ANTARES
Blekman, F.	B Phys
Buis, C.J.P.	THD
Burg, B.J.F. van der	MT
Dalhuizen, J.M. van	ZEUS
Donders, R.	ANTARES
Ejere, D.	HERMES
Enthoven, J.	MT
Everaars, J.S.	ET
Feki, N.	MT
Floor, J.P.	ET
Francke, J.	MT
Grijpink, S.J.L.A.	ZEUS
Haan, M.	MT
Haddaoui, R. El	ET
Heida, M.S.	MT
Heide, J. van der	Theory
Hoogstraten, V.G. van	MT
Hulsman, M.	ATLAS
Köper, D.H.	ZEUS
Krijnen, J.P.	ET
Maddox, E.	ZEUS
Mahfouz, A.M.Y.	MT
Mirani, R.	ANTARES
Mos, S.	ET
Mosch, M.	ZEUS
Mus, P.	MT

Oudshoorn, J.	MT	Moch, S.O.	Theory
Overbeek, M.G. van	MT	Morrow, S	AmPS Phys
Pels, S.	ATLAS	Nieuwenhuysse, O.P.	Administration
Pinto, Y.	ZEUS	Nikanorov, A.	HERMES
Pronk, M.	ET	Pascalutsa, V.V.	Theory
Renner, C.A.	B Phys	Poel, C.A.J.F. van der	CHORUS
Rens, B.A.P. van	ATLAS	Pols, C.L.A.	ATLAS
Roeland, E.	MT	Pronk, M.	ET
Rooth, M.	MT	Ruckstuhl, W. † 3/7/99	B Phys
Schenk, B.	CT	Schenk, B.	CT
Schimmel, E.C.	B Phys	Schenkelaars, E.M.	Personnel Department
Slopsema, R.L.	ATLAS	Schwebke, H.	AmPS Management Project
Vago, N.	ATLAS	Sijpheer, N.C.	MT
Vogelvang, M.	ATLAS	Silva Marcos, J.T. da	Theory
Vries, D.J. de	THD	Spallici, M.	Theory
Windt, D.N. de	ET	Starink, R.	AmPS Phys
Wong, W.Y.	ET	Steinkamp, O.	B Phys
Zand, J.A. van 't	CT	Townsend Swart, G.	AmPS Phys
		Udias, J.	Theory
<b>They left us in 1999:</b>		Vassiliev, A.	HERMES
		Vos, R.A.	Reception
Arlaud, R.E.	THD	Vosseveld, J.H.	ZEUS
Backerra, F.E.H.M.	Management assistance	Waldron, A.K.	Theory
Bardelloni, G.	TF	Weijers, F.H.J.	Purchasing
Birke, L.	Theory	Wielenga, M.	Management assistance
Boersma, D.J.	AmPS Phys	Wolters, G.F.	Theory
Boglione, M.	Theory	Woudstra, M.J.	ATLAS
Botto, T.	AmPS Phys	Zelst, W. van	THD
Bruinsma, P.J.T.	Directie-staf		
Brummer, N.C.	ZEUS		
Bytchkov, A.	MT		
Cara, E.D.	Administration		
Carpentier, M.H.B.R. de	Reception		
Colijn, A.P.	L3		
Dabrowski, B.J.	MT		
Dernison, P.J.H.	MT		
Feki, N.	MT		
Franklin, W.	AmPS Phys		
Gao, Cui Shan	B Phys		
Groep, D.L.	AmPS Phys		
Groot, J.I. de	MT		
Harred, R.	MT		
Harvey, M.	AmPS Phys		
Haster, S.M.A.	MT		
Heyselaar - Van 't Hof, M.J.	Reception		
Higinbotham, D.W.	AmPS Phys		
Hoek, M.	L3		
Hoffmann - Rothe, P.	HERMES		
Holthaus, D.	AmPS Management Project		
Ihssen, H.	HERMES		
Kan, R.P.	MT		
Kjaer, N.J.	DELPHI		
Klous, S.	MT		
Koten, T.I. van	Administration		
Kozlov, S.	HERMES		
Kranenburg, M.E.L.	Management assistance		
Kuur, J. van der	B Phys		
Laermann, E.	ALICE		
Larin, S.	Theory		